REGULATION OF THE METALLOPROTEASE OF *LISTERIA MONOCYTOGENES* DURING INTRACELLULAR INFECTION

A Dissertation

Presented to the Faculty of the Graduate School

of Cornell University

In Partial Fulfillment of the Requirements for the Degree of

Doctor of Philosophy

by

Brian Michael Forster

August 2011

REGULATION OF THE METALLOPROTEASE OF *LISTERIA MONOCYTOGENES* DURING INTRACELLULAR INFECTION

Brian Michael Forster, Ph.D.

Cornell University 2011

Listeria monocytogenes is a Gram-positive, facultative intracellular bacterial pathogen that multiplies in the cytosol of host cells and relies on an actin-based mechanism of motility to spread from cell-to-cell without exiting the intracellular milieu. Virulence of *L. monocytogenes* is related to its ability to escape from vacuoles formed upon initial entry into a host cell and during cell-to-cell spread. One factor contributing to escape from vacuoles is a broad-range phospholipase C (PC-PLC). PC-PLC is translocated across the bacterial membrane as an inactive proenzyme and accumulates in the periplasmic space. PC-PLC maturation is dependent upon a decrease in pH and on the metalloprotease of *L. monocytogenes* (Mpl). Mpl, a thermolysin-like protease, is produced as a zymogen and matures via intramolecular autocatalysis. In this study, we wished to investigate the regulation of Mpl during intracellular infection. Our results show that at physiological pH, the zymogen remains bacterium-associated, presumably in the periplasm. Mpl produced in absence of its propeptide is aberrantly secreted suggesting that the propeptide regulates compartmentalization. Upon a decrease in pH, the bacterium-associated zymogen undergoes autocatalysis and mediates the proteolytic activation of PC-PLC. Mature Mpl and PC-PLC are then rapidly secreted across the cell wall. Two amino acids in the catalytic domain of Mpl, H226 and H241, influence mature Mpl secretion and its ability to process PC-PLC. The compartmentalization of the zymogen is also influenced by PrsA2, a peptidyl prolyl *cis-trans*

isomerase that is anchored by an acyl chain to the *trans* side of the membrane. In absence of PrsA2, the proforms of Mpl and PC-PLC are aberrantly secreted across the cell wall and no longer undergo maturation upon a decrease in pH. Taken together, these results indicate that PrsA2 and the propeptide of Mpl serve to maintain the association of Mpl with bacteria and that this compartmentalization is required for Mpl to undergo autocatalysis at acidic pH and to mediate the proteolytic activation of PC-PLC.

BIOGRAPHICAL SKETCH

Brian Michael Forster received his Bachelors of Science in Cell/Molecular Biology from the State University of New York at Binghamton, with a minor in Mathematical Sciences in 2006. From 2004 to 2006, he worked at the Tottenville High School JCC After School and Saturday Academy as a math instructor. In 2006, Brian was accepted into the field of Microbiology Ph.D. program at Cornell University. While at Cornell, Brian worked in the laboratory of Hélène Marquis in the Department of Microbiology and Immunology in the College of Veterinary Medicine. Additionally, Brian taught several courses for the Cornell Microbiology Department in the College of Agriculture and Life Sciences. Following the completion of his degree, Brian hopes to obtain a position in academia.

To my family and friends

ACKNOWLEDGMENTS

I would first like to thank my Ph.D. advisor, Hélène Marquis. Hélène graciously accepted me into her lab and has been an invaluable resource to me during my Ph.D. studies here at Cornell. She was always willing to assist me with any problem and helped me greatly in designing the study and collecting the data presented here. I would also like to thank my committee members, Marci Scidmore and David Wilson, for all of their advice, reagents and equipment that were used for this work. Additionally, I would also like to thank Daniel Portnoy, Jason Zemansky and members of the Portnoy lab at the University of California, Berkeley, for their assistance on part of the work presented in this dissertation.

I thank all the current and past members of the Marquis lab that assisted me with completing this work, especially Heather O'Neil and Alan Bitar. These two individuals helped me enormously in the lab, from teaching me techniques I commonly use in the lab, to assisting me in experiments when needed.

Finally, and most importantly, I would like to thank my parents, Mary and Arthur, and all my friends throughout my years here at Cornell, most especially Rachel Pfuntner. All of these individuals gave me the advice, support and inspiration I needed as I progressed through the Ph.D. program.

TABLE OF CONTENTS

LIST OF FIGURES

LIST OF TABLES

CHAPTER 1

INTRODUCTION

With the exception of Figures 1.1, 1.6A and 1.7, all figures presented in this chapter are previously published images. Acknowledgements are listed underneath each figure.

Part I. The Gram-positive cell envelope

This work focuses on the Gram-positive, facultative intracellular bacterial pathogen *Listeria monocytogenes*. The cell envelope of a Gram-positive bacterium includes the cytoplasmic membrane and a cell wall primarily composed of a thick layer of peptidoglycan, teichoic acids and proteins (Figure 1.1) (155). The cell wall is approximately 40 nm thick (101). In between the cell membrane and cell wall is a 20 nm thick space referred to as the membrane-cell wall interface or periplasm. This space is visible by cryo-electron microscopy (65, 101).

Peptidoglycan withstands the turgor pressure of the cell, thus providing rigidity and shape to the bacterium. Peptidoglycan consists of glycan chains crosslinked by small peptide chains. The glycan chain consists of a repeating disaccharide composed of N-acetylglucosamine (NAG) and N-acetylmuramic acid (NAM) (58-60). Covalently attached to NAM is a peptide chain consisting of amino acids L-alanine, D-glutamine, L-lysine and D-alanine. *L. monocytogenes* and other Gram-positive bacteria replace L-lysine with *meso*-diaminopimelic acid (145).

Synthesis of peptidoglycan begins in the cytoplasm where NAM is covalently attached to the peptide chain and undecaprenyl diphospho-sugar (UDP) (114). This intermediate is referred to as lipid I. NAG is attached to NAM through a β(1,4) glycosidic bond, generating a second intermediate known as lipid II. Lipid II is then translocated across the bacterial cell membrane. Surface proteins can then be covalently attached to lipid II.

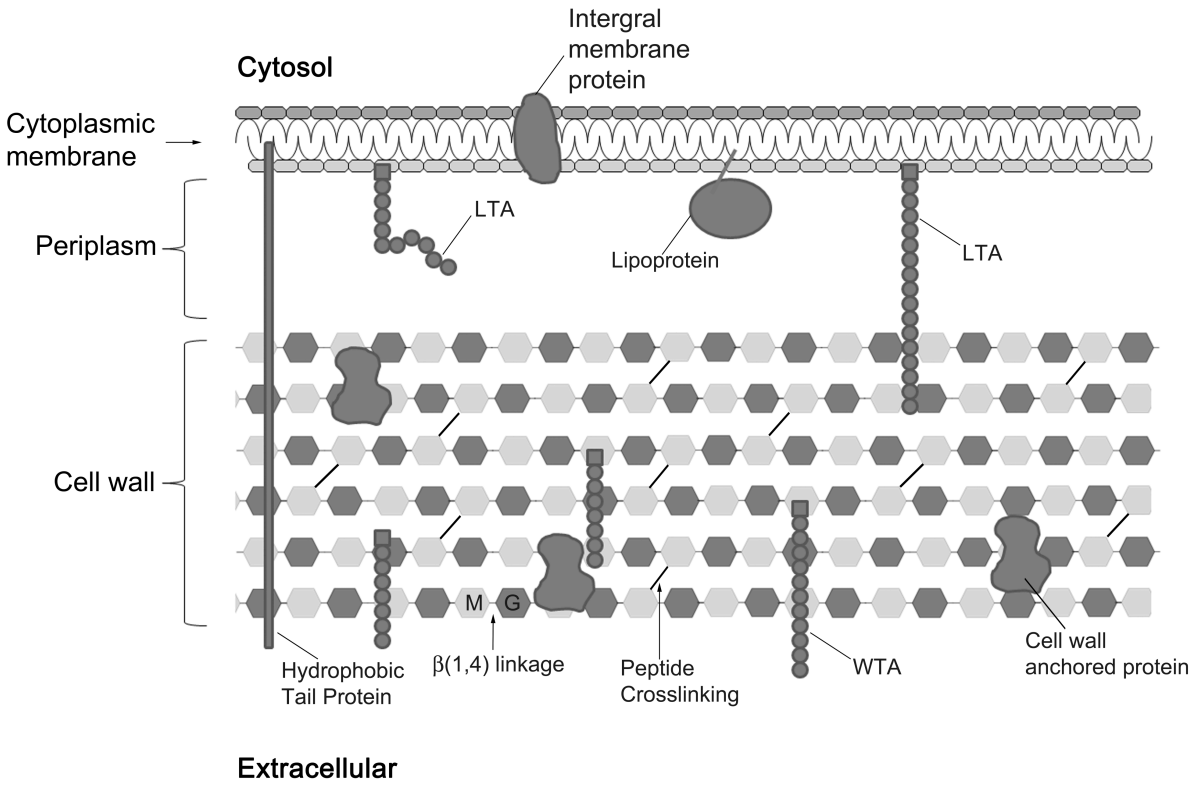

Figure 1.1. The Gram-positive cell envelope. Hexagons labeled M and G refer to N-acetylmuramic acid and N-acetylglucosamine of peptidoglycan, respectively. WTA, wall teichoic acid; LTA, lipoteichoic acid.

UDP is removed and the peptidoglycan subunit is attached to the pre-existing peptidoglycan layer at the side closest to the cell membrane through a transglycosylase reaction. The short peptides of peptidoglycan can be crosslinked through transpeptidation reactions. This crosslinking provides additional strength for peptidoglycan. In the Gram-positive bacterium *Bacillus subtilis*, it is estimated that the glycan chain length is 100 disaccharides with approximately 20% of the peptide chains crosslinked (5, 174). Crosslinking in *Listeria* peptidoglycan occurs by the formation of an amide bond between the ε-amino acid group of *meso*-diaminopimelic acid and the C-terminus of the fourth D-alanine residue (114). Assembly of peptidoglycan requires penicillin binding proteins (PBPs) (61). There are two classes of PBPs. Class A PBPs are involved in both transglycosylation and transpeptidation. Class B PBPs are involved only in transpeptidation. *L. monocytogenes* is able to deacetlyate peptidoglycan using PgdA (17, 82). The deacetylation of peptidoglycan confers resistance to lysozyme, a muramidase.

Polysaccharides and proteins can bind to the cell wall (Figure 1.1). How proteins are linked to the cell wall is discussed in Part II. A major polysaccharide covalently attached to the cell wall is teichoic acid (136, 161). There are two classes of teichoic acids. Wall teichoic acids are covalently attached to NAM while lipoteichoic acids are anchored in the cell membrane. Lipoteichoic acids are a major component of the periplasm (101). Teichoic acids are zwitterionic linear polymers containing glycerol phosphate or ribitol phosphate groups. Teichoic acids can contain ester-linked D-alanine residues. The D-alanylation of teichoic acid decreases the negative charge of the cell wall and has been shown to be important for folding and secretion of some proteins in *B. subtilis* (75). Teichoic acids also bind divalent cations

and provide a scaffold for proteins to attach to the cell wall (Figure 1.1) (122, 155). Under phosphate limiting conditions, Gram-positive bacteria can produce teichuronic acid in place of teichoic acid. Teichuronic acid is a polymer of glucuronic acid and N-acetylgalactosamine (45). *L. monocytogenes* does not produce teichuronic acid (41).

There are numerous systems used by Gram-positive bacteria to translocate proteins out of the cytoplasm and into the cell envelope (114, 125, 141). Proteins destined for export typically contain N-terminal signal sequences. As the protein is translocated, signal peptidases cleave the signal sequence. The majority of translocated proteins pass through the Sec translocon (Figure 1.2) (40, 62). During translation, the signal sequence of a newly synthesized protein is bound to signal recognition proteins (SRPs). SRPs target the mRNA-ribosome complex to the Sec translocon where protein synthesis continues with the nascent chain passing through the translocon. ATP is required for this translocation. The SRP pathway is the only known mechanism for Sec translocation in Gram-positive bacteria (150). A SecA paralog (SecA2) has been identified in Gram-positive pathogens, including *Listeria*, *Mycobacteria* and *Streptococci* (12, 19, 92-93). Interestingly, the proteins that are found to be secreted through this pathway do not have a consensus signal sequence.

Besides the Sec translocon, there are other translocation pathways used by Gram-positive bacteria (114, 125, 141). The twin arginine transporter (TAT) allows for the translocation of folded proteins that contain a twin arginine motif in their signal sequence.

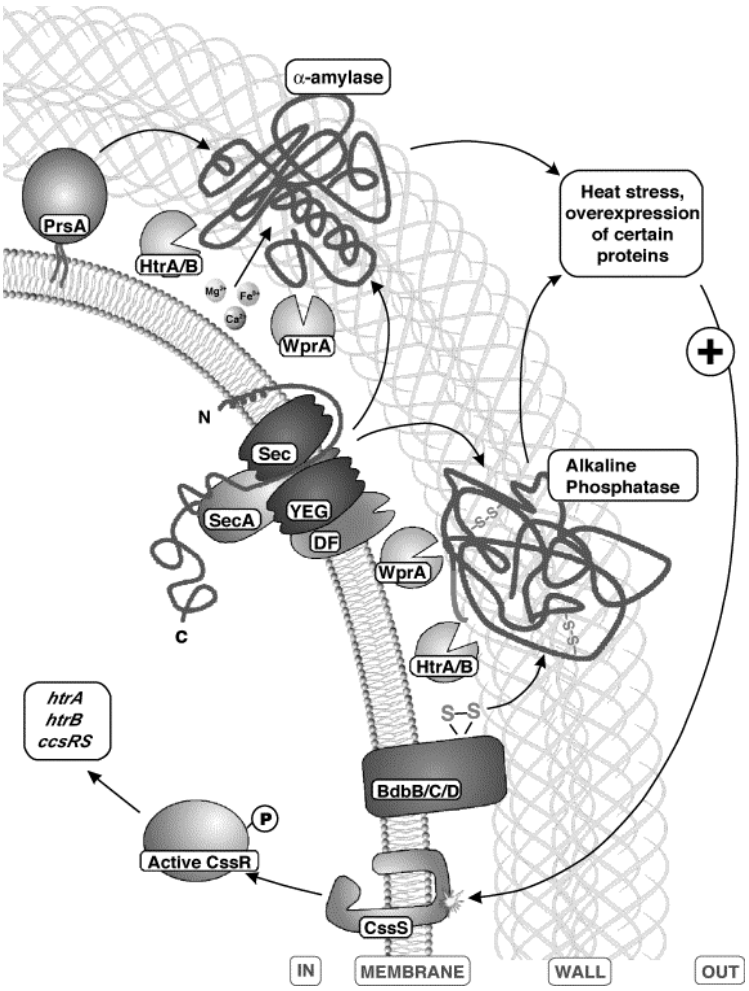

Figure 1.2. Post-translocational folding factors in the cell envelope of the Gram-positive bacterium *Bacillus subtilis*. The folding factors involved in the folding of a-amylase (from *B. subtilis*) and alkaline phosphatase (from *E. coli* being expressed in *B. subtilis*) are shown. Factors that upregulate cell envelope stress responses are also shown.

From Sarvas *et al*. 2004. Post-translocation folding of secretory proteins in Gram-positive bacteria. Biochimica et Biophysica Acta 1694: 311-327.

Additional translocation pathways Gram-positive bacteria utilize include ABC transporters (121), holins (162) and the fimbrilin-protein exporter (31). Several Gram-positive pathogens use specialized secretion systems for virulence factors. For example, *Staphylococcus aureus* and *Mycobacterium tuberculosis* have an ESAT-6/WXG100 pathway, which translocate proteins that contain a WXG motif in the middle of the protein (1, 24). While many of these secretion systems are encoded in *L. monocytogenes*, *Listeria* seems to rely only on the Sec pathway (36).

Part II. Post-Translation Events

During protein translocation, proteins are delivered to the periplasm (Figure 1.2). Due to the polymers in the cell wall, this environment is negatively charged (101). Divalent cations, including Ca^{2+}, Mg^{2+}, and Fe^{2+} are present (13). Additionally, this space is oxidizing and contains proteases. It is in the periplasm that translocated proteins fold into their native conformations. Proteins that are destined to remain within the cell envelope must be attached to either the cell membrane or the cell wall. Proteins destined to be secreted fold in periplasm before crossing the cell wall (69, 91).

Translocated proteins can also undergo post-translational modifications, including proteolytic cleavage, and chemical modification. These modifications can lead to regulation in protein compartmentalization and activity. Discussed below are some of these post-translational events.

1. Anchoring to the cell membrane

There are two ways a protein can be anchored to the cytoplasmic membrane. The first mechanism is through a C-terminal hydrophobic tail in the protein (38). As the nascent peptide chain passes through the Sec translocon, a stop-transfer sequence causes translocation arrest. The peptide is released from the translocon to the phospholipid bilayer.

Proteins that do not have a hydrophobic tail can be tethered to the *trans* side of the cell membrane by the addition of an acyl chain (54, 165, 179). These lipoproteins contain a lipobox following the signal sequence. The consensus sequence for the lipobox is LXXC where X is typically a small neutral amino acid. Diacyl glycerol transferase catalyzes the transfer of diacylglycerol from phosphatidylglycerol on the cytoplasmic membrane to the cysteine residue to produce a diglyceride-prelipoprotein. A lipoprotein signal peptidase then cleaves between X and C in the lipobox, resulting in a mature lipoprotein that is anchored to the cell membrane.

2. Anchoring to the cell wall

Proteins destined for attachment to the the cell wall have numerous sorting signals and motifs (114). A major class of proteins that is covalently attached to the cell wall contain a LPXTG motif, followed by a hydrophobic region and a tail of positively charged amino acids at the C-terminus of the protein. Following translocation and cleavage of the signal sequence, the hydrophobic/positive charged terminus prevents the secretion of the protein. The LPXTG motif is cleaved between the threonine and glycine residues by Sortase A, a cysteine protease-transpeptidase (166). Sortase A is a lipoprotein with a C-terminal hydrophobic tail.

Following cleavage, the N-terminus of the surface protein is then covalently attached to lipid II which is incoporated into the pre-exisiting peptidoglycan cell wall. *Listeria* surface proteins carrying the LPXTG motif are covalently attached to *meso*-diaminopimelic acid (14). Mutations in the LPXTG motif can result in the protein remaining in the membrane (147).

Additional Sortase A-like proteins and cell wall sorting motifs have been identified. Several cell wall proteins from *L. monocytogenes* and *S. aureus* have a NXXTX motif in their cell wall sorting signal, which is cleaved by Sortase B (15, 104). *Streptococcus pyogenes* relies on sortase SrtC2, which cleaves a QVPTGV motif (6).

Proteins may also be non-covalently attached to the cell wall (114, 150). One way is by association with the teichoic acids that are anchored to the cell wall (Figure 1.1). Proteins associate with teichoic acids through GW repeat motifs. Proteins from *Streptococcus pneumoniae* can associate with the choline residues of teichoic acids (64). Proteins containing WXL or LysM motifs can also non-covalently attach to the peptidoglycan (114, 150). LysM motifs were originally identified in bacterial lysins (22). Within the LysM motif is a carbohydrate binding motif that allows for the protein to bind to peptidoglycan.

3. Protein folding

The periplasm has numerous folding factors and chaperones to assist with protein folding following translocation across the cell membrane (Figure 1.2). The proper folding of proteins contribute to their ability to be secreted across the cell wall.

One folding factor in the periplasm is a peptidyl prolyl *cis-trans* isomerase (PPIase). PPIases also serve as chaperones in addition to their isomerase activity (11, 134). One well-studied PPIase is PrsA from *B. subtilis* (74, 76, 171). PrsA is a parvulin-like PPIase that is anchored to the *trans* side of the cell membrane. PrsA is essential for viability. PrsA contributes to the morphology of the cell as it contributes to the folding of PBPs. PrsA has been shown to act as a post-translocation chaperone for proteins destined to be secreted through the cell wall. Increasing the amount of PrsA expressed in *B. subtilis* results in an increase in levels of secreted proteins. It is hypothesized that the chaperone activity and not the PPIase activity of PrsA-like proteins is necessary for the efficient secretion and activity of secreted proteases (4, 39).

In addition to PPIases, there are other folding factors in the periplasm. Because the periplasm is oxidizing, disulfide bridge formation is favored. Disulfide bridges contribute to the stability and activity of proteins (167). However, spontaneous disulfide bridge formation is slow. Therefore, disulfide bond oxidoreductases (DBOs) are used by the cell to speed up the formation of disulfide bridges (152). Proteins that are translocated and misfolded can be targeted by cell envelope proteases. Two such proteases are WprA (95) and HtrA (also known as DegP) (118). Both are serine proteases. HtrA has also been reported to have chaperone activity as well.

When the bacterium is growing in conditions that perturb the cell envelope or when it encounters a secretion stress (Figure 1.2), an accumulation of misfolded proteins in the cell envelope can occur. This leads to the activation of cell envelope stress responses (CESRs),

which are characterized by the upregulation of the folding factors described above. CESRs are regulated by both a two component system (CssRS, Figure 1.2) or by the use of extracytoplasmic function sigma factors (79, 134).

4. Propeptides

Proteases that are to be secreted from the cell can be produced as inactive zymogens in order to regulate protease activity and prevent degradation (83). These zymogens contain propeptides of various length either at the N- and/or C-terminus of the protease domain. Propeptides are capable of folding independently of their cognate protease domain (21). Many of these propeptides serve as intramolecular chaperones (153). Much of the work showing the role of propeptide-assisted folding has come from the propeptide of the serine protease subtilisin from *Bacillus* spp. Folding of the subtilisin protease domain is slow due to the large kinetic barrier between the unfolded and folded state (42). The subtilisin propeptide serves to speed up the folding of the protease domain by serving to stabilize the protease domain as it folds into its native conformation. Once subtilisin is properly folded, the propeptide is proteolytically degraded. The propeptide must be removed in order for active subtilisin to be secreted across the cell wall (128).

Propeptides can serve other functions than protein folding. They can facilitate protein-protein interactions (30, 66) and serve as a means of controlling the proper compartmentalization of proteins (117, 182). Propeptides can be removed either by autocatalysis or by the action of cell envelope proteases. Propeptides are also found in non-proteolytic enzymes (153).

5. Chemical modifications

Proteins can be modified by the addition of chemical groups. Mass spectrometry is a method that can be used to study protein modifications (68). Chemical modifications to cell envelope and secreted proteins from *L. monocytogenes* includes glycosylated flagella (142) and the phosphorylation of ActA, a C-terminal hydrophobic tail protein (20). Other chemical modifications found in Gram-positive proteins include the formation of heterocycles on secreted virulence factors (89) and the ADP-ribosylation of membrane-bound proteins (120).

Part III. *Listeria monocytogenes* pathogenesis

1. History and basic biology

L. monocytogenes is the causative agent of the foodborne disease listeriosis. The bacterium is a saprophytic, facultative anaerobe found in diverse environments including soil, water, food, humans and animals (170). The bacterium is capable of growing under different environmental stresses. It is psychrotrophic, with the ability to grow at temperatures as low as -0.4°C up to 45°C (173). The optimum growth temperature is between 30°C and 37°C (105). Growth can also occur over a wide range of pHs (4.3 to 9.6) and high salt concentrations (10-20%) (105). The ability to cope with these and other environmental stresses is dependent upon an alternative sigma factor σ^B (9-10, 178) and the LisRK two component system (33). The fact that *L. monocytogenes* is able to grow under such conditions allows this bacterium to be a common cause of food contamination.

This bacterium was first reported in 1924, as causing mononuclear leukocytosis in rabbits and guinea pigs (113). It was also attributed to causing an epizootic outbreak of wild gerbils in South Africa in 1924 (124). The bacterium was originally reported as *Bacterium monocytogenes*. In 1940, the genus was renamed *Listeria* (123). The first human case of listeriosis was reported in Denmark in 1929 (116). During World War II, *Listeria* was identified as a cause of neonatal infection. Following World War II up through the 1980's, there was an increase in the number of reported cases of listeriosis. With the invention of immunosuppresive drugs and the outbreak of human immunodeficiency virus, higher cases of listeriosis from immunocompromised individuals were being reported (80, 160). In the 1960s, the bacterium was found to survive in macrophages (94). In 1972, a guinea pig infection model showed that *L. monocytogenes* was able to invade non-phagocytic cells (132). In 1983, Schlech et al. showed listeriosis to be a foodborne disease when an outbreak in Maritime Providence in Canada was found to be due to coleslaw that was prepared from cabbage located on a farm that had cases of ovine listeriosis (144). Tilney and Portnoy documented the intracellular lifecycle of *L. monocytogenes* through the use of electron microscopy in 1989 (164). In 2001, listeriosis was added to the list of nationally notifiable diseases.

2. Listeriosis

Consumption of food contaminated with *L. monocytogenes* can lead to the foodborne disease listeriosis. Foods commonly contaminated with *L. monocytogenes* include soft cheeses and many ready to eat food products (143). Upon ingestion of food contaminated with *L. monocytogenes*, the bacterium is able to survive the acidic environment of the stomach

(Figure 1.3). Symptoms occur approximately 20 hours after ingestion of contaminated food and resembles febrile gastroenteritis (139). Following passage through the stomach, *L. monocytogenes* can enter into the host through the intestinal mucosa. The bacterium can directly invade enterocytes or translocate across the M-cells of Peyer's patches. Bacteria then translocate to the liver, spleen or mesenteric lymph nodes through the blood or lymph. Bacterial replication occurs mainly in hepatocytes. Immunity to *L. monocytogenes* infection is cell-mediated and dependent on an effective CD8+ T-cell response (18). Individuals who are immunodeficient, including the elderly and pregnant women, are at a higher risk for infection. Uncontrolled bacterial growth will lead to microabscesses and apoptosis of hepatocytes (140). The bacterium can gain access to the bloodstream where it can migrate throughout the body. *L. monocytogenes* can cross the blood-brain barrier causing meningitis and encephalitis. In pregnant women, the bacterium can cross the blood-placental barrier, leading to neonatal septicemia or abortion (170). These symptoms present approximately two to four weeks after initial infection (139). The Center for Disease Control estimates 1,600 cases of listeriosis annually in the United States resulting in 260 deaths (28).

Treatment of listeriosis is usually unsuccessful since there is a delay in the presentation of symptoms (139, 163). Pencillins are effective against *Listeria*, especially ampicillin and amoxicillin (73). Penicillin diffuses into the host cell and targets *Listeria* PBPs. Today, the most common antibiotic therapy given is ampicillin along with gentamicin or another aminoglycoside (163). Trimethoprim-sulfamethoxazole is also used as an alternative treatment for listeriosis.

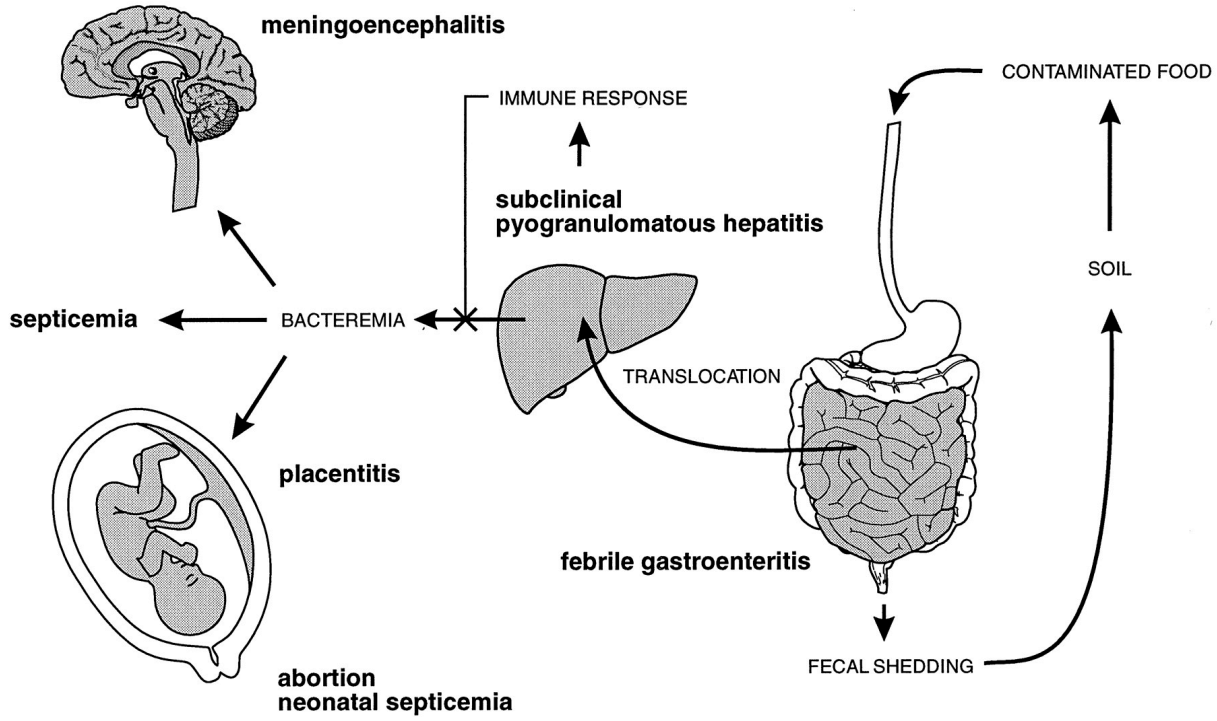

Figure 1.3. Pathophysiology of *Listeria* infection.

From Vazquez-Boland *et al*. 2001. *Listeria* pathogenesis and molecular virulence determinants. Clin. Microbiol. Rev. 14:584 - 640.

3. Intracellular lifecycle

The intracellular lifecycle of *L. monocytogenes* is shown in Figure 1.4. The bacterium is capable of entering both professionally phagocytic and non-phagocytic cells. Entry into non-phagocytic cells is facilitated by a group of surface proteins known as the internalins (49, 52). The internalins are cell wall proteins that induce actin cytoskeleton rearrangement in the host cell to allow the bacterium to enter by a zipper mechanism (148).

Upon entry into the host cell, the bacterium is enclosed in a single membrane or primary vacuole. *L. monocytogenes* is able to escape vacuoles by secreting a cholesterol-dependent, pore-forming hemolysin known as listeriolysin O (LLO) (50) and two phospholipases, a phosphatidylinositol-specific phospholipase C (PI-PLC) (26) and a broad-range phospholipase C (PC-PLC) (158).

Once the bacterium has gained access to the host cytosol, the bacterium will divide (164). The bacterium gains nutrients by upregulating a hexose phosphate transporter (Hpt) and may utilize intracellular peptides as a source of amino acids (97). ActA, a surface protein that is anchored to the bacterial cell membrane through a C-terminal hydrophobic tail and spans the cell wall (85), polymerizes filamentous actin. This allows *Listeria* to spread from cell-to-cell (84). Other intracellular bacteria that escape the phagocytic vacuole and use an actin-based mechanism of motility include *Rickettsia, Shigella, Mycobacterium marinum* and *Burkholderia* (27).

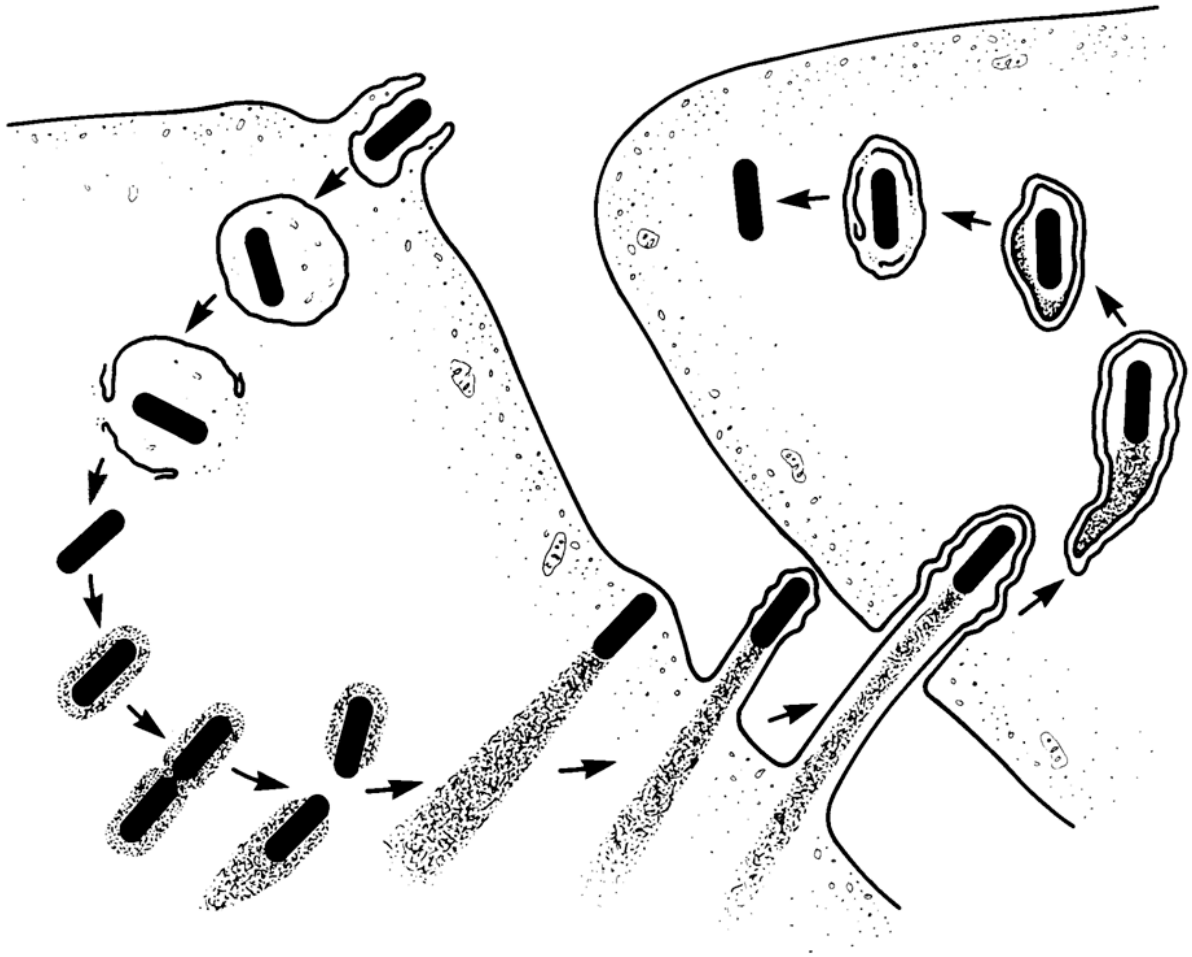

Figure 1.4. Intracellular lifecycle of *Listeria monocytogenes*. The bacterium is able to enter a host cell, escape to the host cytosol and spread from cell-to-cell using actin.

From Tilney, L.G., and D.A. Portnoy. 1989. Actin filaments and the growth, movement and spread of the intracellular bacterial parasite, *Listeria monocytogenes*. J. Cell Biol. 109:1597 - 1608.

Intracellular movement will lead to the formation of filopodia-like projections, which can be engulfed by a neighboring cell. The bacterium will then be entrapped in a double membrane or secondary vacuole. LLO and the phospholipases again mediate escape from secondary vacuoles. Once free from the vacuole, *L. monocytogenes* can resume motility and continue to infect neighboring cells. The virulence of *L. monocytogenes* is dependent on its ability to escape from vacuoles formed upon entry into a host cell and during cell-to-cell spread.

The virulence factors that promote intracellular survival are under the transcriptional regulation of positive regulatory factor A (PrfA) (Figure 1.5). PrfA is a member of the *Listeria* pathogenicity island I (LIPI-1) and is considered the switch that facilitates *L. monocytogenes*' transition from being an environmental microorganism to a pathogen (47). At temperatures below 30°C, the 5' untranslated region of the *prfA* mRNA forms a secondary structure which masks the ribosomal binding site (77, 90). At higher temperatures, the secondary structure is not stable and PrfA can be translated. Once PrfA has been produced, it dimerizes and binds to a palindrome near the promoters of the virulence factors (Figure 1.5, black boxes). There is evidence that PrfA undergoes a conformational change prior to binding to its cognate DNA sequences (44). The trigger for this conformational change is unknown.

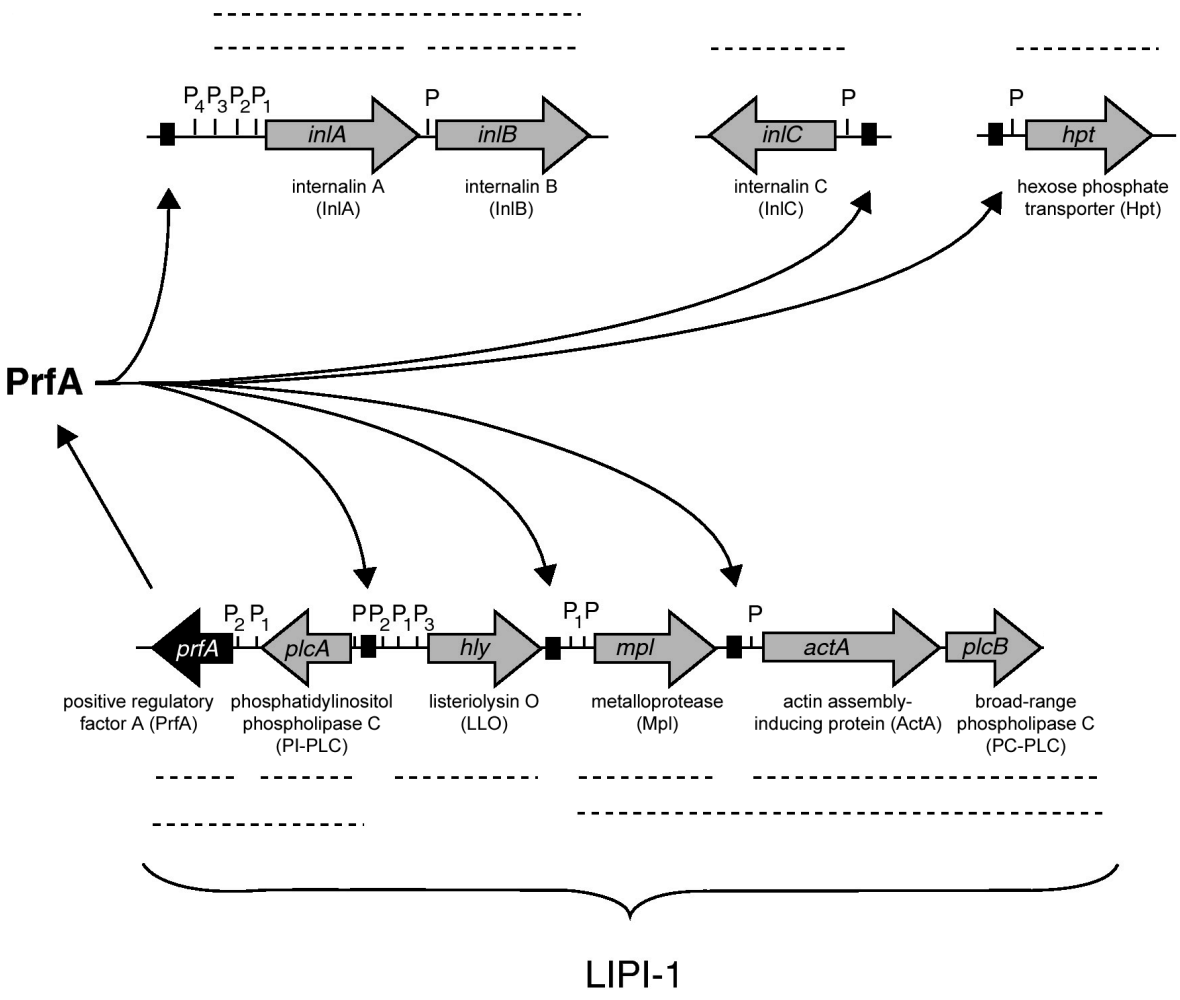

Figure 1.5. The PrfA regulon. The genes and proteins they encode for under the regulation of PrfA is shown in the diagram. *prfA*, *plcA*, *hly*, *mpl*, *actA* and *plcB* are contained in the LIPI-I pathogenicity island. Black boxes indicate PrfA binding sites. P indicate promoters. Dashed lines indicate known transcripts.

Adapted from Scortti *et al*. 2007. The PrfA regulon. Microbes and Infection. 9: 1196-1207.

4. Factors contributing to escape from vacuoles

Shortly after entering a host cell, *L. monocytogenes* manages to escape from the membrane bound vacuole. Escape is mediated by three virulence factors described below, and is dependent on acidification of the vacuole, which is mediated by the vacuolar proton pump ATPase.

a. Listeriolysin O (LLO)

LLO was first identified in a transposon screen that identified a strain of *L. monocytogenes* that was non-hemolytic and avirulent (51). LLO is important for both escape from primary and secondary vacuoles (34, 55). This hemolysin is secreted as a soluble monomer that binds to cholesterol (56). The monomers then oligomerize to form a transmembrane β-barrel pre-pore complex, which upon a decrease in pH inserts into the vacuolar membrane to form a pore. Oligomerization of LLO is influenced by chloride ion concentration, possibly due to the cystic fibrosis transmembrane conductance regulator, a chloride-ion channel recruited to vacuoles (133). Pore formation also requires the reduction of residue C485 by γ-interferon inducible lysosomal thiol reductase (GILT) (156).

The ability of LLO to form pores is optimal at acidic pH, as the protein is unstable at neutral pH (149). Three amino acids residues located in the transmembrane β-hairpin regions act as pH sensors to destabilize LLO at neutral pH. This pH-mediated mechanism of regulation is imperative to the virulence of *L. monocytogenes* as loss of regulation causes cytotoxicity (78).

b. PI-PLC (PlcA)

The phosphatidylinositol-specific phospholipase C (PI-PLC) is one of two phospholipases produced by *L. monocytogenes*. PI-PLC is encoded by *plcA* (25). A *plcA* mutant is defective in escape from the primary vacuole in tissue culture cells, and in colonization of the liver *in vivo* (158). PI-PLC promotes escape from the vacuole by generating diacylglycerol, resulting in activation of protein kinase C, release of intracellular Ca^{2+} stores and recruitment of PKCβ to early endosomes (127). It is hypothesized that the phosphorylation of proteins on early endosomes may promote vacuole permeabilization (126).

Unlike PI-PLC from *Bacillus* spp., PI-PLC from *L. monocytogenes* has low activity against GPI-anchored proteins. *Listeria* PI-PLC lacks a □-strand (Vb) in the C-terminal region of the protein (176). This region is necessary for hydrolysis of GPI-anchored proteins. When the *Bacillus cereus* PI-PLC was introduced in place of *Listeria* PI-PLC in *L. monocytogenes*, the bacterium was unable to colonize the liver or the spleen of mice. However, upon removal of the Vb □-strand, virulence was partially restored. From these results, it is suggested that these GPI-anchored host proteins are important for *L. monocytogenes* virulence and that PI-PLC has evolved as not to act on them.

c. PC-PLC (PlcB)

The phosphatidylcholine phospholipase C (PC-PLC) is the second phospholipase produced by *L. monocytogenes*. PC-PLC is encoded by *plcB* (169). It is homologous to the *B. cereus* PC-PLC. Although known as PC-PLC, this phospholipase is referred to as a broad-range phospholipase. In addition to phosphatidylcholine, PC-PLC has activity on

phosphatidylethanolamine, phosphatidylserine, sphingomyelin and phosphatidylinositol (57, 63). PC-PLC activity has a broad pH optimum, from pH 5.5 to 8.0. *plcB* is transcribed on the same operon as *actA* (Figure 1.5). PC-PLC is synthesized as a 33 kDa preproprotein containing a 24 amino acid long N-terminal propeptide and a 240 amino acid catalytic domain (Figure 1.6A) (169). It is a zinc-dependent phospholipase with nine amino acids coordinating the Zn^{2+} ion (57, 185). Activation of PC-PLC requires removal of its propeptide, which is mediated primarily by the metalloprotease of *L. monocytogenes* (Mpl) (182).

While *plcB* mutants are able to escape primary vacuoles, they have a defect in the escape of secondary vacuoles. As a result, bacteria lacking PC-PLC are defective in cell-to-cell spread (158, 169). Interestingly, the defect associated with a double *plcA* and *plcB* mutant is more than additive when compared to the single mutants, suggesting that the two phospholipases have overlapping functions. On the other hand, PC-PLC is capable of promoting escape from primary vacuoles and cell-to-cell spread from human cell lines independent of LLO (67, 72, 98). This phenomenon was associated with a defect in vacuolar maturation (23). The significance of this finding is not obvious as a LLO-minus strain has never been associated with a human infection.

The localization and maturation of PC-PLC during intracellular infection has been well documented (Figure 1.6B) (99-100, 157, 159, 182). During infection, the proform of PC-PLC is found in the cytosol and bacterium-associated. Secreted PC-PLC is rapidly degraded in a proteasome-dependent manner. Bacterium-associated proPC-PLC is detectable by immunofluorescence microscopy after digesting the cell wall (100).

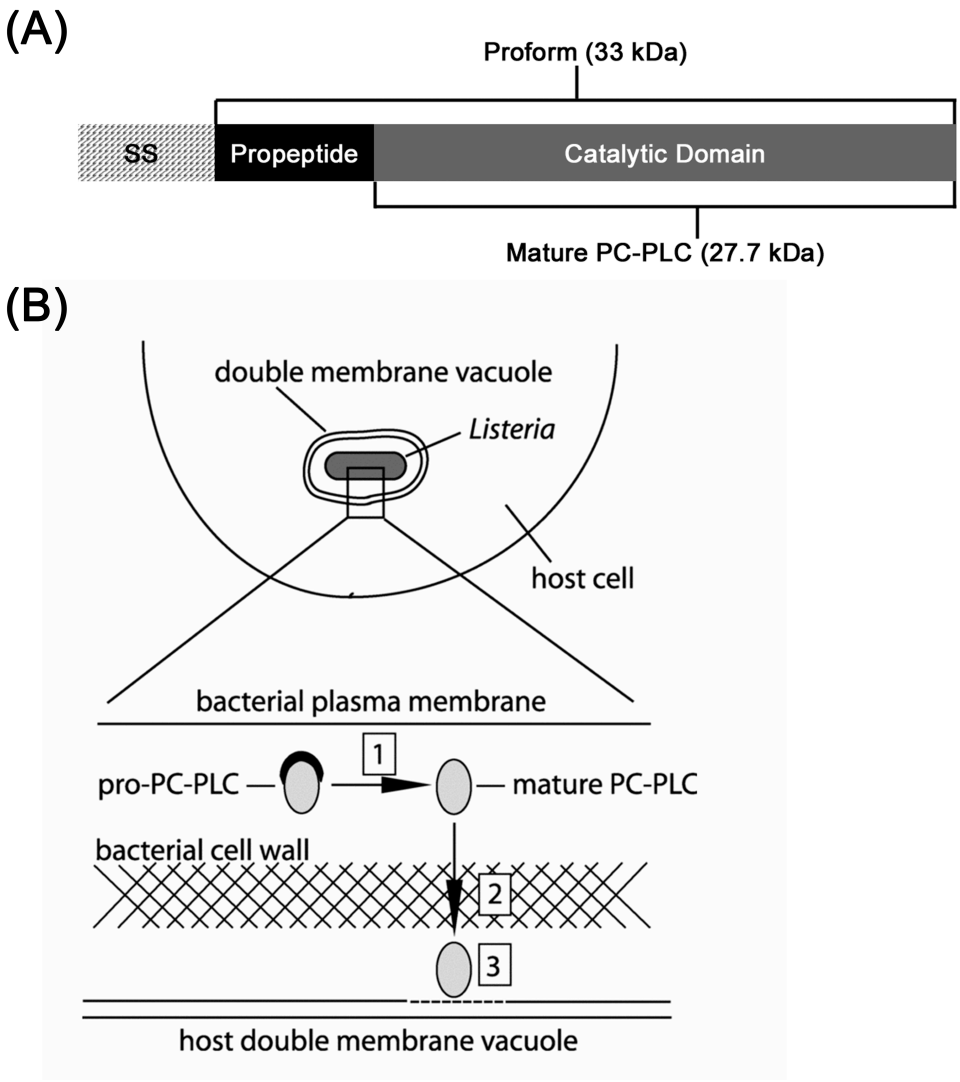

Figure 1.6. Schematic and localization of PC-PLC during intracellular infection. (A) Schematic of PC-PLC showing the relative sizes of both the pro and mature forms of the protein. SS refers to Sec-dependent signal sequence. (B) Localization of PC-PLC in the cell envelope during intracellular infection. Refer to text for details.

Figure (B) is from Slepkov *et al*. 2010. Differentiation of propeptide residues regulating the compartmentalization, maturation and activity of the broad-range phospholipase C of *Listeria monocytogenes*. Biochemical Journal. 432: 557-563.

Upon cell-to-cell spread, bacteria become confined to vacuoles that acidify, leading to the maturation of PC-PLC (Figure 1.6B, #1). Maturation of bacterium-associated PC-PLC is dependent on a decrease in pH and Mpl, and leads to the release of a bolus of active PC-PLC (Figure 1.6B, #2), whereas a vacuolar cysteine protease mediates the maturation of secreted PC-PLC (99). A decrease in pH and Mpl are sufficient for the secretion of PC-PLC (182). Secretion of PC-PLC is independent of propeptide cleavage.

The propeptide of PC-PLC is not necessary for the proper folding of the catalytic domain, but it does inhibit enzymatic activity (182). A single residue located at the P1 position prior to cleavage is sufficient to prevent phospholipase activity (157). This suggests that the first residue of the catalytic domain resides in the active site of PC-PLC. A six residue propeptide is sufficient for Mpl to mediate the processing of PC-PLC. Specifically, the N-terminus of the propeptide influences proper compartmentalization and Mpl-mediated maturation of PC-PLC. Within the N-terminus of the propeptide are hydrophobic (L33) and negatively charged (D30 and E31) residues that are important for the interaction between PC-PLC and Mpl. It is hypothesized that the spatial location of these residues is necessary for interaction with Mpl to promote PC-PLC activation. Propeptide mutants that lack these residues demonstrate maturation defects.

A PC-PLC mutant that is synthesized in absence of its propeptide (*plcB*□pro) is active (182). Secretion of this mutant is independent of pH and Mpl. The *plcB*□pro mutant affects host cell membrane integrity during cell-to-cell spread, but is not cytotoxic (181). However, the mutant is highly attenuated *in vivo*.

d. Metalloprotease (Mpl)

The metalloprotease of *Listeria monocytogenes* was first identified in a Tn1545 transposon mutant that resulted in the loss of PC-PLC activity (135). The open reading frame that was interrupted encoded a thermolysin-like zinc metalloprotease found in other Gram-positive and Gram-negative bacteria (refer to Part IV for a discussion of metalloproteases) (107). The closest ortholog to Mpl is aureolysin from *S. aureus* (46% sequence identity). It was believed that *mpl* was synthesized as part of an operon that included *plcB* (Figure 1.5) and that insertion of the transposon had polar affects. However, when *mpl* was introduced in *trans* into the transposon mutant, PC-PLC activity was restored (129).

Mpl is synthesized as a 55kDa zymogen with a 176 amino acid long N-terminal propeptide and a 310 amino acid protease domain (Figure 1.7). Removal of the propeptide occurs by intramolecular autocatalysis (16). Four species of Mpl are typically identified from the supernatants of broth-grown cultures. These species include a 55-kDa species corresponding to the zymogen, a 42 kDa species that represents mature Mpl, a degradation product of approximately 32 kDa and a 20 kDa propeptide (16, 159). In broth cultures, Mpl is also located in the periplasm (159).

What causes Mpl and PC-PLC to remain in the periplasm has not yet been identified. Neither protein has a cell wall anchor motif or lipid modification to retain the protein in the periplasm. The localization of Mpl and PC-PLC are also not dependent on Sortase A (159).

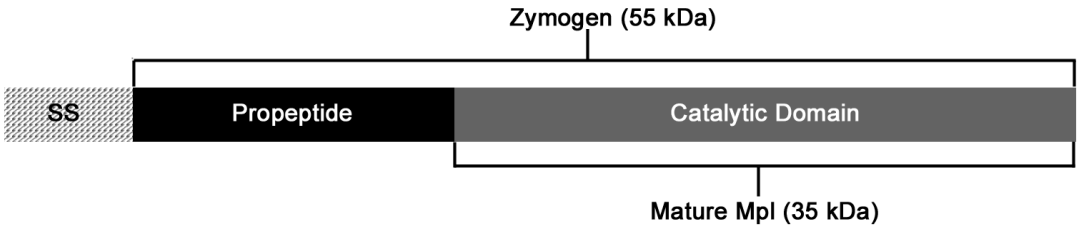

Figure 1.7. Schematic of Mpl. Relative sizes of the both the zymogen and mature Mpl are indicated. SS refers to Sec-dependent signal sequence.

Mpl performs two independent functions in the activation of PC-PLC. As previously mentioned, it is involved in the maturation of PC-PLC. Independent of its processing function, Mpl is necessary for the efficient secretion of PC-PLC across the cell wall (182). Disruption or deletion of Mpl prevents the maturation and secretion of PC-PLC. In addition, a catalytic mutant of Mpl that is not able to undergo autocatalysis does not mediate PC-PLC processing or secretion (16). The contribution of Mpl to virulence is a result of its activity on PC-PLC. *mpl* mutants do not exhibit a defect in invasion or intracellular growth in J774 mouse macrophage-like cells (135). However, they do exhibit a slight defect in cell-to-cell spread (99).

Mpl is also implicated in the pH-dependent degradation of ActA (138). This observation indicates why bacteria, upon escape from the secondary vacuole, do not generate actin tails immediately. Mpl has also been reported to degrade casein over a pH range of 5 to 10, with a pH optimum of 7 (32). Metal chelators and the metalloprotease inhibitor phosphoramidon inhibit Mpl activity.

e. Peptidyl prolyl *cis-trans* isomerase (PrsA2)

PrsA2 is one of two PPIases found in *L. monocytogenes* that contributes to pathogenesis (2-4, 184). It is an ortholog of PrsA from *B. subtilis*. Unlike PrsA, PrsA2 is not essential for growth. PrsA2 is a lipoprotein that contains three domains: the N-terminus, a PPIase domain and the C-terminus. Broth grown *prsA2* mutants secrete an aberrant amount of cytoplasmic and surface-associated proteins, and are deficient in flagella-mediated motility (2, 184).

prsA2 mutants are severely attenuated (2-4, 184). This level of attenuation is comparable to LLO-minus mutants of *L. monocytogenes*. PrsA2-deficient bacteria have limited LLO and PC-PLC activity. PrsA2 contributes to the proper folding of LLO. The PPIase activity of PrsA2 is needed for optimal LLO activity while the N-terminus of PrsA2 is necessary for PC-PLC activity.

Part IV. Metalloproteases

1. Functions

Metalloproteases are proteases that rely on one or two divalent metal ions for catalytic activity. Most metalloproteases have Zn^{2+} as the catalytic ion. The Zn^{2+} ion can be replaced with other ions, including Co^{2+} and Mn^{2+} without affecting the activity of the protease (48). Metalloproteases also bind Ca^{2+} ions, which contributes to stability of the protein by preventing major conformational changes (32, 46).

There are two types of eukaryotic metalloproteases; a secreted matrix metalloprotease (MMP) and a transmembrane protein that contains both a disintegrin and metalloprotease domain (ADAM) (29). Both MMPs and ADAMs are involved in breaking down proteins in the extracellular matrix (ECM) of the cell. This allows for the release of cytokines and protein precursors that are attached to the cell membrane.

Similarly, bacterial metalloproteases target proteins within the ECM and cause damage to host cells (110). This allows for the increased ability of a bacterial pathogen to colonize and disseminate to other cells in the host. Thermolysin from *Bacillus thermoproteolyticus,* the metalloprotease of *Vibrio vulnificus* (VVP) and a metalloprotease from *Burkholderia cepacia* (ZmpB) can cleave type IV collagen, a connective glycoprotein found in the basal surface of epithelial tissue (108). Aureolysin from *S. aureus* and VVP can activate the human fibrinolytic system by cleaving plasminogen into plasmin (7, 109). Plasmin can then degrade fibrin and activate matrix metalloproteases to degrade the ECM. Other bacterial metalloproteases can disrupt the integrity of epithelial cell layers and target tight junctions. They do so by affecting the epithelial cell cytoskeleton or targeting tight junction structures (71).

Metalloproteases from bacterial pathogens can also target the immune system of a host to promote survival. ZmpB targets components of the immune system, including neutrophil α-1 protease inhibitor and interferon-γ (86). IgA is cleaved by metalloproteases produced by *Streptococcus* (88) and *Proteus* (172). The metalloprotease of *Legionella* alters the recruitment and function of phagocytic cells (37). Aureolysin can affect the stimulation of lymphocytes *in vitro* (130), cleave the antimicrobial peptide LL-37 (154) and inhibit the alternative complement system (87).

2. Families of bacterial metalloproteases

Bacterial metalloproteases are classified into superfamilies based on the consensus sequence of their active site residues. These active site residues are involved either in catalysis or

coordinate the Zn^{2+} ion. The metalloprotease superfamilies include the DD-carboxypeptidases, carboxypeptidases, zincins and inverzincins. The consensus sequence of the zincins is HEXXH…E. The zincins can be further broken down into families based upon the location of the second glutamic acid in the consensus motif. The thermolysin family has the second glutamic acid 25 residues downstream from the start of HEXXH (HEXXH(19X)E). In this family, the histidines, the second glutamic acid in the motif, and a water molecule coordinate the Zn^{2+} ion. The model protease in this family is thermolysin from *B. thermoproteolyticus*. Other Gram-positive intracellular pathogens that produce thermolysin-like metalloproteases include *Clostridium*, *Staphylococcus*, *Streptococcus* and *Listeria* (70).

3. Regulation of metalloprotease activity

Metalloproteases are produced as inactive zymogens, containing propeptide sequences at either the N- and/or C-terminus of the protease domain. These propeptides can serve as intramolecular chaperones and assist in folding (151, 153) and/or block the protease active site (112). The propeptides of thermolysin-like metalloproteases contains two domains, a fungalysin-thermolysin propeptide (FTP) domain and a PepSY domain (35). Propeptides can facilitate folding either when covalently attached to the protease or when provided in *trans* (96, 106, 115).

The removal of the propeptide must be a highly regulated event in order to prevent premature activity. For MMPs and ADAMs, the zymogens are kept in an inactive state due to a cysteine switch, where a cysteine in the propeptide electrostatically interacts with the Zn^{2+} ion (168).

Activation of these metalloproteases requires a disruption of the thiol-Zn^{2+} interaction, which can then lead to cleavage of the propeptide (131). One mechanism to activate MMPs and ADAMs is through the serine protease furin which cleaves the metalloprotease propeptide. Additionally, the thiol-Zn^{2+} interaction could be perturbed either by thiol reduction or through protein conformational changes due to pH or reactive oxygen species. Once the interaction is removed, the MMP or ADAM can undergo intramolecular autocatalysis (146).

For thermolysin-like metalloproteases, maturation occurs by intramolecular autocatalysis. Recently, the crystal structure of vibriolysin MCP-02 from *Pseudoalteromonas* sp. SM991 was resolved and a proposed mechanism for autocatalysis was proposed (Figure 1.8) (53). In this model, the zymogen folds into its native conformation. Once autocatalysis occurs, the N-terminus of the protease domain becomes free. The propeptide, however, remains non-covalently attached to the protease domain in an autoprocessed complex. The protease then cleaves the propeptide at sites within the FTP domain (Figure 1.8, site 1 and 2). This results in degradation of the propeptide and the generation of an active protease. This model resembles the maturation of the serine protease subtilisin, where the rate determining step for the generation of an active protease is propeptide degradation (180).

The autocatalysis of aureolysin begins with an autocatalytic cleavage in the FTP domain of the propeptide (115). It is believed that this cleavage activates the chaperone function of the propeptide and is necessary for the rapid autocatalysis of aureolysin. Mature aureolysin is unstable if the cleavage site in the FTP domain is removed.

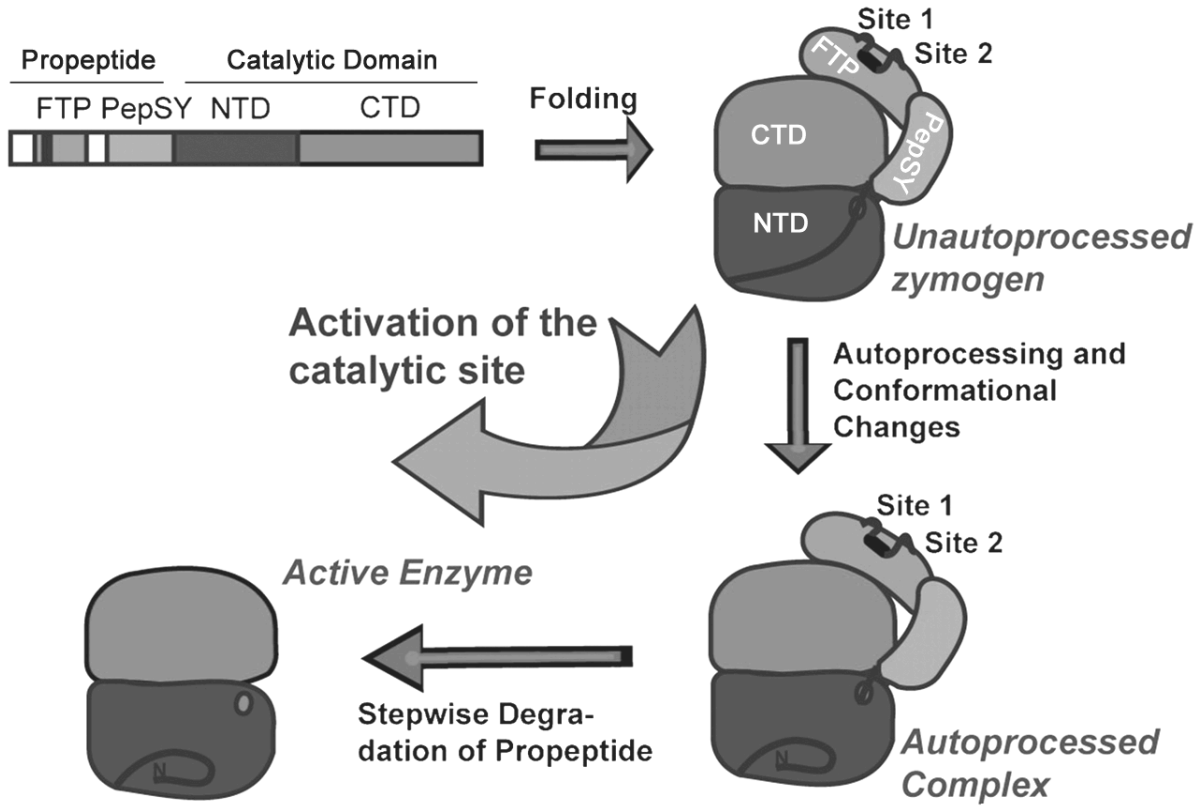

Figure 1.8. Proposed mechanism of autocatalysis for thermolysin-like metalloproteases. Metalloprotease is produced as an unautoprocessed zymogen. Upon intramolecular autocatalysis, the propeptide and catalytic domains remain in an autoprocessed complex. The propeptide is then degraded, leaving an active catalytic domain.

Adapted from Gao *et al*. 2010. Structural basis for the autoprocessing of zinc metalloproteases in the thermolysin family. PNAS 107(41): 17569-17574.

Although the Mpl propeptide contains both the FTP and PepSY domains, Mpl releases a full length propeptide following autocatalysis (16). These observations suggest that the mechanisms of autocatalysis for thermolysin-metalloproteases are varied.

Other domains within the metalloprotease can regulate autocatalysis. Toxin B of *Clostridium difficile* has an intrinsic cysteine protease domain (CPD) located near the site of autocatalysis (137). CPD-regulated autocatalysis is induced by the binding of inositol hexakisphosphate or under reducing conditions (43). The presence of cysteine protease inhibitors prevents autocatalysis from occurring. Proteases can also regulate autocatalysis. The rate of autocatalysis of the zincin astacin from the crayfish *Astacus astacus* is increased in the presence of *Astacus* trypsin (183). Trypsin cleaves the N-terminus of the zymogen, the shortest cut being between the N-terminal methionine and the second amino acid in the primary sequence. Once autocatalysis occurs, a salt bridge is generated between the N-terminal residue of the mature protease and an active site residue. The presence of the salt bridge is necessary to keep the protein properly folded.

4. Catalysis mechanism of thermolysin

In 1972, Matthews et al. resolved the crystal structure of the catalytic domain of thermolysin (103). The structure showed two domains. The N-terminal domain was composed of primarily β-strands while the C-terminal domain was composed of α-helices. In between the two domains was the active site with the HEXXH(19X)E motif. Matthews proposed that the first glutamic acid residue in the motif acts as a general base (102). When a substrate enters the active site of thermolysin, the water molecule coordinating the Zn^{2+} ion is displaced and

deprotonated by the catalytic glutamic acid. This promotes nucleophilic attack of the carbonyl carbon of the P1 residue by the water molecule. The protonated glutamic acid then transfers the proton to the amide nitrogen on the P1' residue. This results in the hydrolysis of a peptide bond. A histidine residues downstream of the motif is implicated in stabilizing the tetrahedral intermediate transition state during catalysis (8). Positions P3 and P1' are typically non-polar amino acids while P1 is usually polar (177).

There have been alternative mechanisms suggested for thermolysin catalysis. The first alternative mechanism was that the catalytic glutamic acid attacks the carbonyl directly, forming an anhydride intermediate (81). However, the crystal structure of thermolysin bound to phosphoramidon showed that the formation of the anhydride intermediate would not be ideal due to steric hindrance (175). The substrate would need to be brought 1 Å closer to the glutamic acid. Instead, the crystal structure showed that the transition state of thermolysin with a substrate formed a tetrahedral intermediate, which would be formed during nucleophilic attack by the water molecule. A second alternative mechanism that has been suggested is that the stabilizing histidine residue in Matthews' mechanism acts as the general base rather than the glutamic acid (111). However, this mechanism does not explain why mutating the first glutamic acid in the HEXXH(19X)E motif eliminates enzymatic activity. *In silico* measurements of the potential free energy of the different mechanisms show Matthews' proposed mechanism to be the most energetically favorable (119).

Part V. Brief overview of dissertation research

Escape from the vacuole is critical for *L. monocytogenes* to be a successful intracellular pathogen. The factors contributing to escape from vacuoles must be regulated in order to prevent damage to the host cell. This research focuses on the post-translational regulation of Mpl during intracellular infection. In **chapter 2**, we show that the propeptide is not required for the catalytic domain of Mpl to fold into an active enzyme. However, during intracellular infection, Mpl's ability to remain in the periplasm is dependent upon the propeptide. This compartmentalization of Mpl during intracellular infection is critical for its activity. In **chapter 3**, we show that at physiological pH, Mpl accumulates in the periplasm as a zymogen. Upon a decrease in pH, the Mpl zymogen undergoes intramolecular autocatalysis and processes PC-PLC. Both mature proteins are then rapidly secreted across the cell wall. In **chapter 4**, we show that PrsA2 is necessary to maintain Mpl and PC-PLC as proproteins in the periplasm. Proproteins that are secreted are not able to undergo maturation upon a decrease in pH. In **chapter 5**, we determine that amino acids H226 and H241 contribute to Mpl secretion and processing of PC-PLC. Finally, **chapter 6** summarizes this work and suggests future work to further understand the regulation of Mpl.

REFERENCES

1. **Abdallah, A. M., N. C. Gey van Pittius, P. A. Champion, J. Cox, J. Luirink, C. M. Vandenbroucke-Grauls, B. J. Appelmelk, and W. Bitter.** 2007. Type VII secretion--mycobacteria show the way. Nat. Rev. Microbiol. **5:**883-91.

2. **Alonzo, F., 3rd, and N. E. Freitag.** 2010. *Listeria monocytogenes* PrsA2 is required for virulence factor secretion and bacterial viability within the host cell cytosol. Infect. Immun. **78:**4944-57.

3. **Alonzo, F., 3rd, G. C. Port, M. Cao, and N. E. Freitag.** 2009. The posttranslocation chaperone PrsA2 contributes to multiple facets of *Listeria monocytogenes* pathogenesis. Infect. Immun. **77:**2612-23.

4. **Alonzo, F., 3rd, B. Xayarath, J. C. Whisstock, and N. E. Freitag.** 2011. Functional analysis of the *Listeria monocytogenes* secretion chaperone PrsA2 and its multiple contributions to bacterial virulence. Mol. Microbiol. **80:**no. doi: 10.1111/j.1365-2958.2011.07665.x.

5. **Atrih, A., P. Zollner, G. Allmaier, M. P. Williamson, and S. J. Foster.** 1998. Peptidoglycan structural dynamics during germination of *Bacillus subtilis* 168 endospores. J. Bacteriol. **180:**4603-12.

6. **Barnett, T. C., A. R. Patel, and J. R. Scott.** 2004. A novel sortase, SrtC2, from *Streptococcus pyogenes* anchors a surface protein containing a QVPTGV motif to the cell wall. J. Bacteriol. **186:**5865-75.

7. **Beaufort, N., P. Wojciechowski, C. P. Sommerhoff, G. Szmyd, G. Dubin, S. Eick, J. Kellermann, M. Schmitt, J. Potempa, and V. Magdolen.** 2008. The human

fibrinolytic system is a target for the staphylococcal metalloprotease aureolysin. Biochem. J. **410:**157-65.

8. **Beaumont, A., M. J. O'Donohue, N. Paredes, N. Rousselet, M. Assicot, C. Bohuon, M. C. Fournie-Zaluski, and B. P. Roques.** 1995. The role of histidine 231 in thermolysin-like enzymes. A site-directed mutagenesis study. J. Biol. Chem. **270:**16803-8.

9. **Becker, L. A., M. S. Cetin, R. W. Hutkins, and A. K. Benson.** 1998. Identification of the gene encoding the alternative sigma factor sigmaB from *Listeria monocytogenes* and its role in osmotolerance. J. Bacteriol. **180:**4547-4554.

10. **Becker, L. A., S. N. Evans, R. W. Hutkins, and A. K. Benson.** 2000. Role of sigma(B) in adaptation of *Listeria monocytogenes* to growth at low temperature. J. Bacteriol. **182:**7083-7.

11. **Behrens, S., R. Maier, H. de Cock, F. X. Schmid, and C. A. Gross.** 2001. The SurA periplasmic PPIase lacking its parvulin domains functions *in vivo* and has chaperone activity. Embo. J. **20:**285-94.

12. **Bensing, B. A., and P. M. Sullam.** 2002. An accessory sec locus of *Streptococcus gordonii* is required for export of the surface protein GspB and for normal levels of binding to human platelets. Mol. Microbiol. **44:**1081-94.

13. **Beveridge, T. J., and R. G. Murray.** 1980. Sites of metal deposition in the cell wall of *Bacillus subtilis*. J. Bacteriol. **141:**876-87.

14. **Bierne, H., and P. Cossart.** 2007. *Listeria monocytogenes* surface proteins: from genome predictions to function. Microbiol. Mol. Biol. Rev. **71:**377-97.

15. **Bierne, H., C. Garandeau, M. G. Pucciarelli, C. Sabet, S. Newton, F. Garcia-del Portillo, P. Cossart, and A. Charbit.** 2004. Sortase B, a new class of sortase in *Listeria monocytogenes*. J Bacteriol **186:**1972-82.

16. **Bitar, A. P., M. Cao, and H. Marquis.** 2008. The metalloprotease of *Listeria monocytogenes* is activated by intramolecular autocatalysis. J. Bacteriol. **190:**107-11.

17. **Boneca, I. G., O. Dussurget, D. Cabanes, M. A. Nahori, S. Sousa, M. Lecuit, E. Psylinakis, V. Bouriotis, J. P. Hugot, M. Giovannini, A. Coyle, J. Bertin, A. Namane, J. C. Rousselle, N. Cayet, M. C. Prevost, V. Balloy, M. Chignard, D. J. Philpott, P. Cossart, and S. E. Girardin.** 2007. A critical role for peptidoglycan N-deacetylation in *Listeria* evasion from the host innate immune system. Proc. Natl. Acad. Sci. USA **104:**997-1002.

18. **Bouwer, H. G., C. S. Nelson, B. L. Gibbins, D. A. Portnoy, and D. J. Hinrichs.** 1992. Listeriolysin O is a target of the immune response to *Listeria monocytogenes*. J. Exp. Med. **175:**1467-71.

19. **Braunstein, M., A. M. Brown, S. Kurtz, and W. R. Jacobs, Jr.** 2001. Two nonredundant SecA homologues function in mycobacteria. J. Bacteriol. **183:**6979-90.

20. **Brundage, R. A., G. A. Smith, A. Camilli, J. A. Theriot, and D. A. Portnoy.** 1993. Expression and phosphorylation of the *Listeria monocytogenes* ActA protein in mammalian cells. Proc. Natl. Acad. Sci. USA **90:**11890-4.

21. **Bryan, P. N.** 2002. Prodomains and protein folding catalysis. Chem. Rev. **102:**4805-16.

22. **Buist, G., A. Steen, J. Kok, and O. P. Kuipers.** 2008. LysM, a widely distributed protein motif for binding to (peptido)glycans. Mol. Microbiol. **68:**838-47.

23. **Burrack, L. S., J. W. Harper, and D. E. Higgins.** 2009. Perturbation of vacuolar maturation promotes listeriolysin O-independent vacuolar escape during *Listeria monocytogenes* infection of human cells. Cell Microbiol.

24. **Burts, M. L., W. A. Williams, K. DeBord, and D. M. Missiakas.** 2005. EsxA and EsxB are secreted by an ESAT-6-like system that is required for the pathogenesis of *Staphylococcus aureus* infections. Proc. Natl. Acad. Sci. USA **102:**1169-74.

25. **Camilli, A., H. Goldfine, and D. A. Portnoy.** 1991. *Listeria monocytogenes* mutants lacking phosphatidylinositol-specific phospholipase C are avirulent. J. Exp. Med. **173:**751-4.

26. **Camilli, A., L. G. Tilney, and D. A. Portnoy.** 1993. Dual roles of *plcA* in *Listeria monocytogenes* pathogenesis. Mol. Microbiol. **8:**143-57.

27. **Carlsson, F., and E. J. Brown.** 2006. Actin-based motility of intracellular bacteria, and polarized surface distribution of the bacterial effector molecules. J. Cell Physiol. **209:**288-96.

28. **Centers for Disease Control and Prevention** April 6, 2011 2011, posting date. Listeriosis. [Online.]

29. **Chang, C., and Z. Werb.** 2001. The many faces of metalloproteases: cell growth, invasion, angiogenesis and metastasis. Trends Cell Biol. **11:**S37-43.

30. **Chaudhary, P. M., M. T. Eby, A. Jasmin, and L. Hood.** 1999. Activation of the c-Jun N-terminal kinase/stress-activated protein kinase pathway by overexpression of caspase-8 and its homologs. J. Biol. Chem. **274:**19211-9.

31. **Chen, I., and D. Dubnau.** 2004. DNA uptake during bacterial transformation. Nat. Rev. Microbiol. **2:**241-9.

32. **Coffey, A., B. van den Burg, R. Veltman, and T. Abee.** 2000. Characteristics of the biologically active 35-kDa metalloprotease virulence factor from *Listeria monocytogenes*. J. Appl. Microbiol. **88:**132-41.

33. **Cotter, P. D., N. Emerson, C. G. Gahan, and C. Hill.** 1999. Identification and disruption of *lisRK*, a genetic locus encoding a two-component signal transduction system involved in stress tolerance and virulence in *Listeria monocytogenes*. J. Bacteriol. **181:**6840-3.

34. **Dancz, C. E., A. Haraga, D. A. Portnoy, and D. E. Higgins.** 2002. Inducible control of virulence gene expression in *Listeria monocytogenes*: temporal requirement of listeriolysin O during intracellular infection. J. Bacteriol. **184:**5935-5945.

35. **Demidyuk, I. V., E. V. Gasanov, D. R. Safina, and S. V. Kostrov.** 2008. Structural organization of precursors of thermolysin-like proteinases. Protein J. **27:**343-54.

36. **Desvaux, M., and M. Hebraud.** 2006. The protein secretion systems in *Listeria*: inside out bacterial virulence. FEMS Microbiol. Rev. **30:**774-805.

37. **Dowling, J. N., A. K. Saha, and R. H. Glew.** 1992. Virulence factors of the family *Legionellaceae*. Microbiol. Rev. **56:**32-60.

38. **Driessen, A. J., and N. Nouwen.** 2008. Protein translocation across the bacterial cytoplasmic membrane. Annu. Rev. Biochem. **77:**643-67.

39. **Drouault, S., J. Anba, S. Bonneau, A. Bolotin, S. D. Ehrlich, and P. Renault.** 2002. The peptidyl-prolyl isomerase motif is lacking in PmpA, the PrsA-like protein

involved in the secretion machinery of *Lactococcus lactis*. Appl. Environ. Microbiol. **68:**3932-42.

40. **du Plessis, D. J., N. Nouwen, and A. J. Driessen.** 2011. The Sec translocase. Biochim. Biophys. Acta **1808:**851-65.

41. **Dubail, I., A. Bigot, V. Lazarevic, B. Soldo, D. Euphrasie, M. Dupuis, and A. Charbit.** 2006. Identification of an essential gene of *Listeria monocytogenes* involved in teichoic acid biogenesis. J. Bacteriol. **188:**6580-91.

42. **Eder, J., M. Rheinnecker, and A. R. Fersht.** 1993. Folding of subtilisin BPN': characterization of a folding intermediate. Biochemistry **32:**18-26.

43. **Egerer, M., T. Giesemann, T. Jank, K. J. Satchell, and K. Aktories.** 2007. Auto-catalytic cleavage of *Clostridium difficile* toxins A and B depends on cysteine protease activity. J. Biol. Chem. **282:**25314-21.

44. **Eiting, M., G. Hageluken, W. D. Schubert, and D. W. Heinz.** 2005. The mutation G145S in PrfA, a key virulence regulator of *Listeria monocytogenes*, increases DNA-binding affinity by stabilizing the HTH motif. Mol. Microbiol. **56:**433-446.

45. **Ellwood, D. C., and D. W. Tempest.** 1969. Control of teichoic acid and teichuronic acid biosyntheses in chemostat cultures of *Bacillus subtilis* var. *niger*. Biochem. J. **111:**1-5.

46. **Feder, J., L. R. Garrett, and B. S. Wildi.** 1971. Studies on the role of calcium in thermolysin. Biochemistry **10:**4552-6.

47. **Freitag, N. E., G. C. Port, and M. D. Miner.** 2009. *Listeria monocytogenes* - from saprophyte to intracellular pathogen. Nat. Rev. Microbiol. **7:**623-8.

48. **Fukasawa, K. M., T. Hata, Y. Ono, and J. Hiros.** 2011. Metal Preferences of Zinc-Binding Motif on Metalloproteases. Journal of Amino Acids **2011:**doi:10.4061/2011/574816.

49. **Gaillard, J. L., P. Berche, C. Frehel, E. Gouin, and P. Cossart.** 1991. Entry of *L. monocytogenes* into cells is mediated by internalin, a repeat protein reminiscent of surface antigens from gram-positive cocci. Cell **65:**1127-1141.

50. **Gaillard, J. L., P. Berche, J. Mounier, S. Richard, and P. Sansonetti.** 1987. *In vitro* model of penetration and intracellular growth of *Listeria monocytogenes* in the human enterocyte-like cell line Caco-2. Infect. Immun. **55:**2822-2829.

51. **Gaillard, J. L., P. Berche, and P. Sansonetti.** 1986. Transposon mutagenesis as a tool to study the role of hemolysin in the virulence of *Listeria monocytogenes*. Infect. Immun. **52:**50-55.

52. **Gaillard, J. L., F. Jaubert, and P. Berche.** 1996. The *inlAB* locus mediates the entry of *Listeria monocytogenes* into hepatocytes *in vivo*. J. Exp. Med. **183:**359-369.

53. **Gao, X., J. Wang, D. Q. Yu, F. Bian, B. B. Xie, X. L. Chen, B. C. Zhou, L. H. Lai, Z. X. Wang, J. W. Wu, and Y. Z. Zhang.** 2010. Structural basis for the autoprocessing of zinc metalloproteases in the thermolysin family. Proc. Natl. Acad. Sci. USA **107:**17569-74.

54. **Garcia-del Portillo, F., and P. Cossart.** 2007. An important step in *Listeria* lipoprotein research. J. Bacteriol. **189:**294-7.

55. **Gedde, M. M., D. E. Higgins, L. G. Tilney, and D. A. Portnoy.** 2000. Role of listeriolysin O in cell-to-cell spread of *Listeria monocytogenes*. Infect. Immun. **68:**999-1003.

56. **Geoffroy, C., J. L. Gaillard, J. E. Alouf, and P. Berche.** 1987. Purification, characterization, and toxicity of the sulfhydryl-activated hemolysin listeriolysin O from *Listeria monocytogenes*. Infect. Immun. **55:**1641-1646.

57. **Geoffroy, C., J. Raveneau, J. L. Beretti, A. Lecroisey, J. A. Vazquez-Boland, J. E. Alouf, and P. Berche.** 1991. Purification and characterization of an extracellular 29-kilodalton phospholipase C from *Listeria monocytogenes*. Infect. Immun. **59:**2382-2388.

58. **Ghuysen, J. M., and J. L. Strominger.** 1963. Structure of the Cell Wall of *Staphylococcus aureus*, Strain Copenhagen. I. Preparation of Fragments by Enzymatic Hydrolysis. Biochemistry **2:**1110-9.

59. **Ghuysen, J. M., and J. L. Strominger.** 1963. Structure of the Cell Wall of *Staphylococcus aureus*, Strain Copenhagen. II. Separation and Structure of Disaccharides. Biochemistry **2:**1119-25.

60. **Ghuysen, J. M., D. J. Tipper, and J. L. Strominger.** 1965. Structure of the Cell Wall of *Staphylococcus aureus*, Strain Copenhagen. IV. The Teichoic Acid-Glycopeptide Complex. Biochemistry **4:**474-85.

61. **Goffin, C., and J. M. Ghuysen.** 1998. Multimodular penicillin-binding proteins: an enigmatic family of orthologs and paralogs. Microbiol. Mol. Biol. Rev. **62:**1079-93.

62. **Gold, V. A., F. Duong, and I. Collinson.** 2007. Structure and function of the bacterial Sec translocon. Mol. Membr. Biol. **24:**387-94.

63. **Goldfine, H., N. C. Johnston, and C. Knob.** 1993. Nonspecific phospholipase C of *Listeria monocytogenes*: activity on phospholipids in Triton X-100-mixed micelles and in biological membranes. J. Bacteriol. **175:**4298-4306.

64. **Gosink, K. K., E. R. Mann, C. Guglielmo, E. I. Tuomanen, and H. R. Masure.** 2000. Role of novel choline binding proteins in virulence of *Streptococcus pneumoniae*. Infect. Immun. **68:**5690-5.

65. **Graham, L. L., and T. J. Beveridge.** 1994. Structural differentiation of the *Bacillus subtilis* 168 cell wall. J. Bacteriol. **176:**1413-21.

66. **Gray, T. E., J. Eder, M. Bycroft, A. G. Day, and A. R. Fersht.** 1993. Refolding of barnase mutants and pro-barnase in the presence and absence of GroEL. Embo. J. **12:**4145-4150.

67. **Grundling, A., M. D. Gonzalez, and D. E. Higgins.** 2003. Requirement of the *Listeria monocytogenes* broad-range phospholipase PC-PLC during infection of human epithelial cells. J. Bacteriol. **185:**6295-6307.

68. **Gupta, N., S. Tanner, N. Jaitly, J. N. Adkins, M. Lipton, R. Edwards, M. Romine, A. Osterman, V. Bafna, R. D. Smith, and P. A. Pevzner.** 2007. Whole proteome analysis of post-translational modifications: applications of mass-spectrometry for proteogenomic annotation. Genome Res. **17:**1362-77.

69. **Haddaoui, E. A., L. Leloup, M. F. Petit-Glatron, and R. Chambert.** 1997. Characterization of a stable intermediate trapped during reversible refolding of *Bacillus subtilis* alpha-amylase. Eur. J. Biochem. **249:**505-9.

70. **Hase, C. C., and R. A. Finkelstein.** 1993. Bacterial extracellular zinc-containing metalloproteases. Microbiol. Rev. **57:**823-37.

71. **Hecht, G., C. Pothoulakis, J. T. LaMont, and J. L. Madara.** 1988. *Clostridium difficile* toxin A perturbs cytoskeletal structure and tight junction permeability of cultured human intestinal epithelial monolayers. J. Clin. Invest. **82:**1516-24.

72. **Hense, M., E. Domann, S. Krusch, P. Wachholz, K. E. Dittmar, M. Rohde, J. Wehland, T. Chakraborty, and S. Weiss.** 2001. Eukaryotic expression plasmid transfer from the intracellular bacterium *Listeria monocytogenes* to host cells. Cell Microbiol. **3:**599-609.

73. **Hof, H.** 1991. Therapeutic activities of antibiotics in listeriosis. Infection **19 Suppl 4:**S229-33.

74. **Hyyrylainen, H. L., B. C. Marciniak, K. Dahncke, M. Pietiainen, P. Courtin, M. Vitikainen, R. Seppala, A. Otto, D. Becher, M. P. Chapot-Chartier, O. P. Kuipers, and V. P. Kontinen.** 2010. Penicillin-binding protein folding is dependent on the PrsA peptidyl-prolyl *cis-trans* isomerase in *Bacillus subtilis*. Mol. Microbiol. **77:**108-27.

75. **Hyyrylainen, H. L., M. Vitikainen, J. Thwaite, H. Wu, M. Sarvas, C. R. Harwood, V. P. Kontinen, and K. Stephenson.** 2000. D-Alanine substitution of teichoic acids as a modulator of protein folding and stability at the cytoplasmic membrane/cell wall interface of *Bacillus subtilis*. J. Biol. Chem. **275:**26696-703.

76. **Jacobs, M., J. B. Andersen, V. Kontinen, and M. Sarvas.** 1993. *Bacillus subtilis* PrsA is required *in vivo* as an extracytoplasmic chaperone for secretion of active enzymes synthesized either with or without pro-sequences. Mol. Microbiol. **8:**957-66.

77. **Johansson, J., P. Mandin, A. Renzoni, C. Chiaruttini, M. Springer, and P. Cossart.** 2002. An RNA thermosensor controls expression of virulence genes in *Listeria monocytogenes*. Cell **110:**551-561.

78. **Jones, S., K. Preiter, and D. A. Portnoy.** 1996. Conversion of an extracellular cytolysin into a phagosome-specific lysin which supports the growth of an intracellular pathogen. Mol. Microbiol. **21:**1219-1225.

79. **Jordan, S., M. I. Hutchings, and T. Mascher.** 2008. Cell envelope stress response in Gram-positive bacteria. FEMS Microbiol. Rev. **32:**107-46.

80. **Jurado, R. L., M. M. Farley, E. Pereira, R. C. Harvey, A. Schuchat, J. D. Wenger, and D. S. Stephens.** 1993. Increased risk of meningitis and bacteremia due to *Listeria monocytogenes* in patients with human immunodeficiency virus infection. Clin. Infect. Dis. **17:**224-7.

81. **Kaiser, E. T., and B. L. Kaiser.** 1972. Carboxypeptidase A. Mechanistic analysis. Acc. Chem. Res. **5:**219–224.

82. **Kamisango, K., I. Saiki, Y. Tanio, H. Okumura, Y. Araki, I. Sekikawa, I. Azuma, and Y. Yamamura.** 1982. Structures and biological activities of peptidoglycans of *Listeria monocytogenes* and *Propionibacterium acnes*. J. Biochem. **92:**23-33.

83. **Khan, A. R., and M. N. James.** 1998. Molecular mechanisms for the conversion of zymogens to active proteolytic enzymes. Protein Sci. **7:**815-36.

84. **Kocks, C., E. Gouin, M. Tabouret, P. Berche, H. Ohayon, and P. Cossart.** 1992. *L. monocytogenes*-induced actin assembly requires the *actA* gene product, a surface protein. Cell **68:**521-531.

85. **Kocks, C., R. Hellio, P. Gounon, H. Ohayon, and P. Cossart.** 1993. Polarized distribution of *Listeria monocytogenes* surface protein ActA at the site of directional actin assembly. J. Cell. Sci. **105 (Pt 3):**699-710.

86. **Kooi, C., B. Subsin, R. Chen, B. Pohorelic, and P. A. Sokol.** 2006. *Burkholderia cenocepacia* ZmpB is a broad-specificity zinc metalloprotease involved in virulence. Infect. Immun. **74:**4083-93.

87. **Laarman, A. J., M. Ruyken, C. L. Malone, J. A. van Strijp, A. R. Horswill, and S. H. Rooijakkers.** 2011. *Staphylococcus aureus* metalloprotease aureolysin cleaves complement C3 to mediate immune evasion. J. Immunol. **186:**6445-53.

88. **Labib, R. S., N. J. Calvanico, and T. B. Tomasi, Jr.** 1978. Studies on extracellular proteases of *Streptococcus sanguis*. Purification and characterization of a human IgA1 specific protease. Biochim. Biophys. Acta **526:**547-59.

89. **Lee, S. W., D. A. Mitchell, A. L. Markley, M. E. Hensler, D. Gonzalez, A. Wohlrab, P. C. Dorrestein, V. Nizet, and J. E. Dixon.** 2008. Discovery of a widely distributed toxin biosynthetic gene cluster. Proc. Natl. Acad. Sci. USA **105:**5879-84.

90. **Leimeister-Wachter, M., E. Domann, and T. Chakraborty.** 1992. The expression of virulence genes in *Listeria monocytogenes* is thermoregulated. J. Bacteriol. **174:**947-952.

91. **Leloup, L., A. Haddaoui el, R. Chambert, and M. F. Petit-Glatron.** 1997. Characterization of the rate-limiting step of the secretion of *Bacillus subtilis* alpha-amylase overproduced during the exponential phase of growth. Microbiology **143 (Pt 10):**3295-303.

92. **Lenz, L. L., S. Mohammadi, A. Geissler, and D. A. Portnoy.** 2003. SecA2-dependent secretion of autolytic enzymes promotes *Listeria monocytogenes* pathogenesis. Proc. Natl. Acad. Sci. USA **100:**12432-12437.

93. **Lenz, L. L., and D. A. Portnoy.** 2002. Identification of a second *Listeria secA* gene associated with protein secretion and the rough phenotype. Mol. Microbiol. **45:**1043-1056.

94. **Mackaness, G. B.** 1962. Cellular resistance to infection. J. Exp. Med. **116:**381-406.

95. **Margot, P., and D. Karamata.** 1996. The *wprA* gene of *Bacillus subtilis* 168, expressed during exponential growth, encodes a cell-wall-associated protease. Microbiology **142 (Pt 12):**3437-44.

96. **Marie-Claire, C., E. Ruffet, A. Beaumont, and B. P. Roques.** 1999. The prosequence of thermolysin acts as an intramolecular chaperone when expressed *in trans* with the mature sequence in *Escherichia coli*. J. Mol. Biol. **285:**1911-1915.

97. **Marquis, H., H. G. Bouwer, D. J. Hinrichs, and D. A. Portnoy.** 1993. Intracytoplasmic growth and virulence of *Listeria monocytogenes* auxotrophic mutants. Infect. Immun. **61:**3756-60.

98. **Marquis, H., V. Doshi, and D. A. Portnoy.** 1995. The broad-range phospholipase C and a metalloprotease mediate listeriolysin O-independent escape of *Listeria monocytogenes* from a primary vacuole in human epithelial cells. Infect. Immun. **63:**4531-4.

99. **Marquis, H., H. Goldfine, and D. A. Portnoy.** 1997. Proteolytic pathways of activation and degradation of a bacterial phospholipase C during intracellular infection by *Listeria monocytogenes*. J. Cell Biol. **137:**1381-92.

100. **Marquis, H., and E. J. Hager.** 2000. pH-regulated activation and release of a bacteria-associated phospholipase C during intracellular infection by *Listeria monocytogenes*. Mol. Microbiol. **35:**289-98.

101. **Matias, V. R., and T. J. Beveridge.** 2008. Lipoteichoic acid is a major component of the *Bacillus subtilis* periplasm. J. Bacteriol. **190:**7414-8.

102. **Matthews, B. W.** 1988. Structual Basis of the Action of Thermolysin and Related Zinc Peptidases. Acc. Chem. Res **21:**333-340.

103. **Matthews, B. W., J. N. Jansonius, P. M. Colman, B. P. Schoenborn, and D. Dupourque.** 1972. Three-dimensional structure of thermolysin. Nat. New Biol. **238:**37-41.

104. **Mazmanian, S. K., H. Ton-That, K. Su, and O. Schneewind.** 2002. An iron-regulated sortase anchors a class of surface protein during *Staphylococcus aureus* pathogenesis. Proc. Natl. Acad. Sci. USA **99:**2293-8.

105. **McClure, P. J., T. M. Kelly, and T. A. Roberts.** 1991. The effects of temperature, pH, sodium chloride and sodium nitrite on the growth of *Listeria monocytogenes*. Int. J. Food Microbiol. **14:**77-91.

106. **McIver, K. S., E. Kessler, J. C. Olson, and D. E. Ohman.** 1995. The elastase propeptide functions as an intramolecular chaperone required for elastase activity and secretion in *Pseudomonas aeruginosa*. Mol. Microbiol. **18:**877-889.

107. **Mengaud, J., C. Geoffroy, and P. Cossart.** 1991. Identification of a new operon involved in *Listeria monocytogenes* virulence: its first gene encodes a protein homologous to bacterial metalloproteases. Infect. Immun. **59:**1043-1049.

108. **Miyoshi, S., H. Nakazawa, K. Kawata, K. Tomochika, K. Tobe, and S. Shinoda.** 1998. Characterization of the hemorrhagic reaction caused by *Vibrio vulnificus* metalloprotease, a member of the thermolysin family. Infect. Immun. **66:**4851-5.

109. **Miyoshi, S., H. Narukawa, K. Tomochika, and S. Shinoda.** 1995. Actions of *Vibrio vulnificus* metalloprotease on human plasma proteinase-proteinase inhibitor systems: a comparative study of native protease with its derivative modified by polyethylene glycol. Microbiol. Immunol. **39:**959-66.

110. **Miyoshi, S., and S. Shinoda.** 2000. Microbial metalloproteases and pathogenesis. Microbes Infect. **2:**91-8.

111. **Mock, W. L., and M. Aksamawati.** 1994. Binding to thermolysin of phenolate-containing inhibitors necessitates a revised mechanism of catalysis. Biochem. J. **302:**57-68.

112. **Morgunova, E., A. Tuuttila, U. Bergmann, M. Isupov, Y. Lindqvist, G. Schneider, and K. Tryggvason.** 1999. Structure of human pro-matrix metalloproteinase-2: activation mechanism revealed. Science **284:**1667-70.

113. **Murray, E. G. D., R. A. Webb, and M. B. R. Swann.** 1926. A disease of rabbits characterized by a large mononuclear leucocytosis, caused by a hitherto undescribed bacillus, *Bacterium monocytogenes*. J. Pathol. Biol. **29:**407-439.

114. **Navarre, W. W., and O. Schneewind.** 1999. Surface proteins of gram-positive bacteria and mechanisms of their targeting to the cell wall envelope. Microbiol. Mol. Biol. Rev. **63:**174-229.

115. **Nickerson, N. N., V. Joag, and M. J. McGavin.** 2008. Rapid autocatalytic activation of the M4 metalloprotease aureolysin is controlled by a conserved N-terminal fungalysin-thermolysin-propeptide domain. Mol. Microbiol. **69:**1530-43.

116. **Nyfelt, A.** 1929. Etiologie de la mononucléose infectieuse. C. R. Soc. Biol. **101:**590-591.

117. **Ohnishi, Y., M. Nishiyama, S. Horinouchi, and T. Beppu.** 1994. Involvement of the COOH-terminal pro-sequence of *Serratia marcescens* serine protease in the folding of the mature enzyme. J. Biol. Chem. **269:**32800-6.

118. **Pallen, M. J., and B. W. Wren.** 1997. The HtrA family of serine proteases. Mol. Microbiol. **26:**209-21.

119. **Pelmenschikov, V., M. R. Blomberg, and P. E. Siegbahn.** 2002. A theoretical study of the mechanism for peptide hydrolysis by thermolysin. J. Biol. Inorg. Chem. **7:**284-98.

120. **Penyige, A., G. Barabas, I. Szabo, and J. C. Ensign.** 1990. ADP-ribosylation of membrane proteins of *Streptomyces griseus* strain 52-1. FEMS Microbiol. Lett. **57:**293-7.

121. **Peschel, A., N. Schnell, M. Hille, K. D. Entian, and F. Gotz.** 1997. Secretion of the lantibiotics epidermin and gallidermin: sequence analysis of the genes *gdmT* and *gdmH*, their influence on epidermin production and their regulation by EpiQ. Mol. Gen. Genet. **254:**312-8.

122. **Peschel, A., C. Vuong, M. Otto, and F. Gotz.** 2000. The D-alanine residues of *Staphylococcus aureus* teichoic acids alter the susceptibility to vancomycin and the activity of autolytic enzymes. Antimicrob. Agents Chemother. **44:**2845-7.

123. **Pirie, J. H. H.** 1940. *Listeria*: change of name for a genus of bacteria. Nature **145:**264.

124. **Pirie, J. H. H.** 1927. A new disease of veld rodents, "Tiger River disease.". S. Afr. Inst. Med. Res. **3:**163-186.

125. **Pohl, S., and C. R. Harwood.** 2010. Heterologous protein secretion by *Bacillus* species from the cradle to the grave. Adv. Appl. Microbiol. **73:**1-25.

126. **Poussin, M. A., and H. Goldfine.** 2005. Involvement of *Listeria monocytogenes* phosphatidylinositol-specific phospholipase C and host protein kinase C in permeabilization of the macrophage phagosome. Infect. Immun. **73:**4410-3.

127. **Poussin, M. A., M. Leitges, and H. Goldfine.** 2009. The ability of *Listeria monocytogenes* PI-PLC to facilitate escape from the macrophage phagosome is dependent on host PKCbeta. Microb. Pathog. **46:**1-5.

128. **Power, S. D., R. M. Adams, and J. A. Wells.** 1986. Secretion and autoproteolytic maturation of subtilisin. Proc. Natl. Acad. Sci. USA **83:**3096-100.

129. **Poyart, C., E. Abachin, I. Razafimanantsoa, and P. Berche.** 1993. The zinc metalloprotease of *Listeria monocytogenes* is required for maturation of phosphatidylcholine phospholipase C: direct evidence obtained by gene complementation. Infect. Immun. **61:**1576-80.

130. **Prokesova, L., Z. Porwit-Bobr, K. Baran, J. Potempa, M. Pospisil, and C. John.** 1991. Effect of metalloproteinase from *Staphylococcus aureus* on *in vitro* stimulation of human lymphocytes. Immunol. Lett. **27:**225-30.

131. **Ra, H. J., and W. C. Parks.** 2007. Control of matrix metalloproteinase catalytic activity. Matrix Biol. **26:**587-96.

132. **Racz, P., K. Tenner, and E. Mero.** 1972. Experimental *Listeria* enteritis. I. An electron microscopic study of the epithelial phase in experimental listeria infection. Lab Invest **26:**694-700.

133. **Radtke, A. L., K. L. Anderson, M. J. Davis, M. J. DiMagno, J. A. Swanson, and M. X. O'Riordan.** 2011. *Listeria monocytogenes* exploits cystic fibrosis transmembrane conductance regulator (CFTR) to escape the phagosome. Proc. Natl. Acad. Sci. USA **108:**1633-8.

134. **Raivio, T. L., and T. J. Silhavy.** 2001. Periplasmic stress and ECF sigma factors. Annu. Rev. Microbiol. **55:**591-624.

135. **Raveneau, J., C. Geoffroy, J. L. Beretti, J. L. Gaillard, J. E. Alouf, and P. Berche.** 1992. Reduced virulence of a *Listeria monocytogenes* phospholipase-deficient mutant obtained by transposon insertion into the zinc metalloprotease gene. Infect. Immun. **60:**916-921.

136. **Reichmann, N. T., and A. Grundling.** 2011. Location, synthesis and function of glycolipids and polyglycerolphosphate lipoteichoic acid in Gram-positive bacteria of the phylum *Firmicutes*. FEMS Microbiol. Lett. **319:**97-105.

137. **Reineke, J., S. Tenzer, M. Rupnik, A. Koschinski, O. Hasselmayer, A. Schrattenholz, H. Schild, and C. von Eichel-Streiber.** 2007. Autocatalytic cleavage of *Clostridium difficile* toxin B. Nature **446:**415-9.

138. **Robbins, J. R., A. I. Barth, H. Marquis, E. L. de Hostos, W. J. Nelson, and J. A. Theriot.** 1999. *Listeria monocytogenes* exploits normal host cell processes to spread from cell to cell. J. Cell Biol. **146:**1333-50.

139. **Roberts, A. J., and M. Wiedmann.** 2003. Pathogen, host and environmental factors contributing to the pathogenesis of listeriosis. Cell Mol. Life Sci. **60:**904-918.

140. **Rogers, H. W., M. P. Callery, B. Deck, and E. R. Unanue.** 1996. *Listeria monocytogenes* induces apoptosis of infected hepatocytes. J. Immunol. **156:**679-684.

141. **Sarvas, M., C. R. Harwood, S. Bron, and J. M. van Dijl.** 2004. Post-translocational folding of secretory proteins in Gram-positive bacteria. Biochim. Biophys. Acta **1694:**311-27.

142. **Schirm, M., M. Kalmokoff, A. Aubry, P. Thibault, M. Sandoz, and S. M. Logan.** 2004. Flagellin from *Listeria monocytogenes* is glycosylated with beta-O-linked N-acetylglucosamine. J. Bacteriol. **186:**6721-7.

143. **Schlech, W. F., 3rd.** 2000. Foodborne listeriosis. Clin. Infect. Dis. **31:**770-5.

144. **Schlech, W. F., 3rd, P. M. Lavigne, R. A. Bortolussi, A. C. Allen, E. V. Haldane, A. J. Wort, A. W. Hightower, S. E. Johnson, S. H. King, E. S. Nicholls, and C. V. Broome.** 1983. Epidemic listeriosis--evidence for transmission by food. N. Engl. J. Med. **308:**203-206.

145. **Schleifer, K. H., and O. Kandler.** 1972. Peptidoglycan types of bacterial cell walls and their taxonomic implications. Bacteriol. Rev. **36:**407-77.

146. **Schlomann, U., D. Wildeboer, A. Webster, O. Antropova, D. Zeuschner, C. G. Knight, A. J. Docherty, M. Lambert, L. Skelton, H. Jockusch, and J. W. Bartsch.** 2002. The metalloprotease disintegrin ADAM8. Processing by autocatalysis is required for proteolytic activity and cell adhesion. J. Biol. Chem. **277:**48210-9.

147. **Schneewind, O., D. Mihaylova-Petkov, and P. Model.** 1993. Cell wall sorting signals in surface proteins of gram-positive bacteria. Embo J. **12:**4803-11.

148. **Schubert, W. D., C. Urbanke, T. Ziehm, V. Beier, M. P. Machner, E. Domann, J. Wehland, T. Chakraborty, and D. W. Heinz.** 2002. Structure of internalin, a major invasion protein of *Listeria monocytogenes*, in complex with its human receptor E-cadherin. Cell **111:**825-36.

149. **Schuerch, D. W., E. M. Wilson-Kubalek, and R. K. Tweten.** 2005. Molecular basis of listeriolysin O pH dependence. Proc. Natl. Acad. Sci. USA **102:**12537-12542.

150. **Scott, J. R., and T. C. Barnett.** 2006. Surface proteins of gram-positive bacteria and how they get there. Annu. Rev. Microbiol. **60:**397-423.

151. **Serkina, A. V., A. B. Shevelev, and G. G. Chestukhina.** 2001. Structure and functions of bacterial proteinase precursors. Bioorg. Khim. **27:**323-346.

152. **Sevier, C. S., and C. A. Kaiser.** 2002. Formation and transfer of disulphide bonds in living cells. Nat. Rev. Mol. Cell Biol. **3:**836-47.

153. **Shinde, U., and M. Inouye.** 2000. Intramolecular chaperones: polypeptide extensions that modulate protein folding. Semin. Cell. Dev. Biol. **11:**35-44.

154. **Sieprawska-Lupa, M., P. Mydel, K. Krawczyk, K. Wojcik, M. Puklo, B. Lupa, P. Suder, J. Silberring, M. Reed, J. Pohl, W. Shafer, F. McAleese, T. Foster, J. Travis, and J. Potempa.** 2004. Degradation of human antimicrobial peptide LL-37 by *Staphylococcus aureus*-derived proteinases. Antimicrob. Agents Chemother. **48:**4673-9.

155. **Silhavy, T. J., D. Kahne, and S. Walker.** 2010. The bacterial cell envelope. Cold Spring Harb. Perspect. Biol. **2:**a000414.

156. **Singh, R., A. Jamieson, and P. Cresswell.** 2008. GILT is a critical host factor for *Listeria monocytogenes* infection. Nature **455:**1244-7.

157. **Slepkov, E. R., A. Pavinski Bitar, and H. Marquis.** 2010. Differentiation of propeptide residues regulating the compartmentalization, maturation and activity of the broad-range phospholipase C of *Listeria monocytogenes*. Biochem. J. **432:**557-63.

158. **Smith, G. A., H. Marquis, S. Jones, N. C. Johnston, D. A. Portnoy, and H. Goldfine.** 1995. The two distinct phospholipases C of *Listeria monocytogenes* have overlapping roles in escape from a vacuole and cell-to-cell spread. Infect. Immun. **63:**4231-7.

159. **Snyder, A., and H. Marquis.** 2003. Restricted translocation across the cell wall regulates secretion of the broad-range phospholipase C of *Listeria monocytogenes*. J. Bacteriol. **185:**5953-8.

160. **Stamm, A. M., W. E. Dismukes, B. P. Simmons, C. G. Cobbs, A. Elliott, P. Budrich, and J. Harmon.** 1982. Listeriosis in renal transplant recipients: report of an outbreak and review of 102 cases. Rev. Infect. Dis. **4:**665-82.

161. **Swoboda, J. G., J. Campbell, T. C. Meredith, and S. Walker.** 2010. Wall teichoic acid function, biosynthesis, and inhibition. Chembiochem **11:**35-45.

162. **Tan, K. S., B. Y. Wee, and K. P. Song.** 2001. Evidence for holin function of *tcdE* gene in the pathogenicity of *Clostridium difficile*. J. Med. Microbiol. **50:**613-9.

163. **Temple, M. E., and M. C. Nahata.** 2000. Treatment of listeriosis. Ann Pharmacother. **34:**656-61.

164. **Tilney, L. G., and D. A. Portnoy.** 1989. Actin filaments and the growth, movement, and spread of the intracellular bacterial parasite, *Listeria monocytogenes*. J. Cell Biol. **109:**1597-608.

165. **Tokuda, H., and S. Matsuyama.** 2004. Sorting of lipoproteins to the outer membrane in *E. coli*. Biochim. Biophys. Acta **1694:**IN1-9.

166. **Ton-That, H., G. Liu, S. K. Mazmanian, K. F. Faull, and O. Schneewind.** 1999. Purification and characterization of sortase, the transpeptidase that cleaves surface proteins of *Staphylococcus aureus* at the LPXTG motif. Proc. Natl. Acad. Sci. USA **96:**12424-9.

167. **Trivedi, M. V., J. S. Laurence, and T. J. Siahaan.** 2009. The role of thiols and disulfides on protein stability. Curr. Protein Pept. Sci. **10:**614-25.

168. **Van Wart, H. E., and H. Birkedal-Hansen.** 1990. The cysteine switch: a principle of regulation of metalloproteinase activity with potential applicability to the entire matrix metalloproteinase gene family. Proc. Natl. Acad. Sci. USA **87:**5578-82.

169. **Vazquez-Boland, J. A., C. Kocks, S. Dramsi, H. Ohayon, C. Geoffroy, J. Mengaud, and P. Cossart.** 1992. Nucleotide sequence of the lecithinase operon of

Listeria monocytogenes and possible role of lecithinase in cell-to-cell spread. Infect. Immun. **60:**219-230.

170. **Vazquez-Boland, J. A., M. Kuhn, P. Berche, T. Chakraborty, G. Dominguez-Bernal, W. Goebel, B. Gonzalez-Zorn, J. Wehland, and J. Kreft.** 2001. *Listeria* pathogenesis and molecular virulence determinants. Clin. Microbiol. Rev. **14:**584-640.

171. **Vitikainen, M., T. Pummi, U. Airaksinen, E. Wahlstrom, H. Wu, M. Sarvas, and V. P. Kontinen.** 2001. Quantitation of the capacity of the secretion apparatus and requirement for PrsA in growth and secretion of alpha-amylase in *Bacillus subtilis*. J. Bacteriol. **183:**1881-90.

172. **Walker, K. E., S. Moghaddame-Jafari, C. V. Lockatell, D. Johnson, and R. Belas.** 1999. ZapA, the IgA-degrading metalloprotease of *Proteus mirabilis*, is a virulence factor expressed specifically in swarmer cells. Mol. Microbiol. **32:**825-36.

173. **Walker, S. J., P. Archer, and J. G. Banks.** 1990. Growth of *Listeria monocytogenes* at refrigeration temperatures. J. Appl. Bacteriol. **68:**157-62.

174. **Ward, J. B.** 1973. The chain length of the glycans in bacterial cell walls. Biochem. J. **133:**395-8.

175. **Weaver, L. H., W. R. Kester, and B. W. Matthews.** 1977. A crystallographic study of the complex of phosphoramidon with thermolysin. A model for the presumed

catalytic transition state and for the binding of extended substances. J. Mol. Biol. **114:**119-32.

176. **Wei, Z., L. A. Zenewicz, and H. Goldfine.** 2005. *Listeria monocytogenes* phosphatidylinositol-specific phospholipase C has evolved for virulence by greatly reduced activity on GPI anchors. Proc. Natl. Acad. Sci. USA **102:**12927-31.

177. **Wetmore, D. R., S. L. Wong, and R. S. Roche.** 1994. The efficiency of processing and secretion of the thermolysin-like neutral protease from *Bacillus cereus* does not require the whole prosequence, but does depend on the nature of the amino acid sequence in the region of the cleavage site. Mol. Microbiol. **12:**747-759.

178. **Wiedmann, M., T. J. Arvik, R. J. Hurley, and K. J. Boor.** 1998. General stress transcription factor sigmaB and its role in acid tolerance and virulence of *Listeria monocytogenes*. J. Bacteriol. **180:**3650-3656.

179. **Wu, H. C., and M. Tokunaga.** 1986. Biogenesis of lipoproteins in bacteria. Curr. Top. Microbiol. Immunol. **125:**127-57.

180. **Yabuta, Y., H. Takagi, M. Inouye, and U. Shinde.** 2001. Folding pathway mediated by an intramolecular chaperone: propeptide release modulates activation precision of pro-subtilisin. J. Biol. Chem. **276:**44427-44434.

181. **Yeung, P. S., Y. Na, A. J. Kreuder, and H. Marquis.** 2007. Compartmentalization of the broad-range phospholipase C activity to the spreading vacuole is critical for *Listeria monocytogenes* virulence. Infect. Immun. **75:**44-51.

182. **Yeung, P. S., N. Zagorski, and H. Marquis.** 2005. The metalloprotease of *Listeria monocytogenes* controls cell wall translocation of the broad-range phospholipase C. J. Bacteriol. **187:**2601-8.

183. **Yiallouros, I., R. Kappelhoff, O. Schilling, F. Wegmann, M. W. Helms, A. Auge, G. Brachtendorf, E. G. Berkhoff, B. Beermann, H. J. Hinz, S. Konig, J. Peter-Katalinic, and W. Stocker.** 2002. Activation mechanism of pro-astacin: role of the pro-peptide, tryptic and autoproteolytic cleavage and importance of precise amino-terminal processing. J .Mol. Biol. **324:**237-46.

184. **Zemansky, J., B. C. Kline, J. J. Woodward, J. H. Leber, H. Marquis, and D. A. Portnoy.** 2009. Development of a mariner-based transposon and identification of *Listeria monocytogenes* determinants, including the peptidyl-prolyl isomerase PrsA2, that contribute to its hemolytic phenotype. J. Bacteriol. **191:**3950-64.

185. **Zuckert, W. R., H. Marquis, and H. Goldfine.** 1998. Modulation of enzymatic activity and biological function of *Listeria monocytogenes* broad-range phospholipase C by amino acid substitutions and by replacement with the *Bacillus cereus* ortholog. Infect. Immun. **66:**4823-31.

CHAPTER 2

THE PROPEPTIDE OF THE METALLOPROTEASE OF *LISTERIA MONOCYTOGENES* CONTROLS COMPARTMENTALIZATION OF THE ZYMOGEN DURING INTRACELLULAR INFECTION.*

* Adapted from Heather S. O'Neil, Brian M. Forster, Kari L. Roberts, Andrew J. Chambers, Alan Pavinski Bitar and Hélène Marquis. The propeptide of the metalloprotease of *Listeria monocytogenes* controls compartmentalization of the zymogen during intracellular infection. Journal of Bacteriology. 191:3594-3603. Copyright 2009. American Society for Microbiology.

ABSTRACT

The broad-range phospholipase C (PC-PLC) of the intracellular bacterial pathogen *Listeria monocytogenes* contributes to the bacterium's ability to escape vacuoles during its intracellular lifecycle. PC-PLC is produced as an inactive proprotein, whose maturation and secretion is dependent upon a decrease in pH and the metalloprotease (Mpl). Mpl is a thermolysin-like zinc metalloprotease that is produced as a zymogen containing an N-terminal propeptide. Maturation of Mpl occurs exclusively by intramolecular autocatalysis. In this study, we examined the role of the Mpl propeptide. A propeptide deletion mutant (MplΔpro) and two Mpl mutants, containing point mutations in the propeptide (Mpl H75V and H95L) were constructed for this purpose. In absence of the propeptide, mature Mpl is stably produced. Residues H75 and H95 contribute to the stability of the Mpl propeptide. All the Mpl propeptide mutants were able to mediate PC-PLC activation on egg yolk agar plates, although to a lesser extent than wild-type. However, during intracellular infection, none of these mutants were able to mediate PC-PLC maturation and secretion. In absence of the propeptide, Mpl was no longer retained in the periplasm of intracellular bacteria. Instead, Mpl was aberrantly secreted across the cell wall into the host cytosol. Taken together, these results show that the propeptide of Mpl is important for the proper compartmentalization of Mpl and that the localization of Mpl influences its ability to mediate PC-PLC activation during intracellular infection.

INTRODUCTION

Listeria monocytogenes is a Gram-positive, facultative intracellular bacterial pathogen that is the causative agent of the food borne disease listeriosis (22). *L. monocytogenes* is capable of invading both professional phagocytic and non-phagocytic cells, escaping from vacuoles formed upon entry into a cell and spreading from cell-to-cell while remaining in the intracellular compartment (32, 34). Cell-to-cell spread is mediated by ActA, a *Listeria* surface protein which polymerizes filamentous actin (7, 27). *L. monocytogenes* is able to invade the intestinal epithelial layer and translocate to the liver, spleen or mesenteric lymph nodes (34). Bacterial replication occurs mainly in hepatocytes. Uncontrolled bacterial growth will lead to *Listeria* gaining access to the bloodstream where it can migrate throughout the body. It preferentially targets the central nervous system, or the placenta in pregnant women.

One factor that mediates escape from double membrane vacuoles formed upon cell-to-cell spread is a broad-range phospholipase C (PC-PLC) (26, 33). PC-PLC, which is encoded by *plcB,* is produced as an inactive proenzyme, containing an N-terminal propeptide and a catalytic domain. Following translocation across the bacterial cytoplasmic membrane, PC-PLC accumulates in the periplasm, the space between the cytoplasmic membrane and the peptidoglycan cell wall (15, 29).

Upon a decrease in vacuolar pH, the metalloprotease of *L. monocytogenes* (Mpl) mediates the maturation and secretion of PC-PLC across the bacterial cell wall (15, 37). Mpl also mediates the pH-dependent degradation of ActA (21). Presumably, this degradation explains why

intracellular bacteria are not able to move immediately after escape from double membrane vacuoles.

Mpl is a secreted thermolysin-like zinc metalloprotease. Mpl is produced as a 55 kDa zymogen, containing a 176-amino-acid N-terminal propeptide and a 310-amino-acid protease domain. Recently, it was shown that activation of Mpl occurs by intramolecular autocatalysis (2).

Numerous secreted proteases are produced as inactive proproteins or zymogens. This is to ensure that the protein does not become active prematurely. These zymogens contain propeptides either at the N- and/or C-terminus of the mature protein. Most propeptides act as intramolecular chaperones, assisting in the proper folding of its cognate protease domain (25). The propeptide can either be covalently attached to the protein, or introduced in *trans* to assist in protein folding (13, 38). In subtilisin, the propeptide acts as a chaperone, altering the energy required to fold the molten globule state of the protein into its native state (8). The protein is then able to undergo autocatalysis. Following autocatalysis, the propeptide remains associated with the mature protein as an inactive, autoprocessed complex (36). Degradation or removal of the propeptide is necessary to generate a catalytically active protease (30). In the case of subtilisin, degradation of the propeptide is necessary to allow the protein to be secreted across the bacterial cell wall (19).

Some proproteins have propeptides that do not function as intramolecular chaperones (25). These propeptides can slow down folding and allow the protein to interact with other proteins

or chaperones (5, 9). An additional function these propeptides may have include targeting proteins to the proper cellular compartment (18, 31). The propeptide of PC-PLC is an example of such a propeptide (37). It slows the secretion of PC-PLC allowing for a pool of PC-PLC to accumulate in the periplasm. A propeptide deletion mutant of PC-PLC is rapidly secreted across the bacterial cell wall as an active enzyme, independent of pH and of Mpl.

Within the propeptides of thermolysin-like metalloproteases are two domains, a fungalysin-thermolysin propeptide (FTP) domain and a PepSY domain. Recent work has shown that the FTP domain from the propeptide of aureolysin, a thermolysin-like metalloprotease from the Gram-positive bacterium *Staphylococcus aureus*, has both chaperone function and modulates autocatalysis (17).

In this study, we sought to define the role of Mpl's propeptide. To do so, we constructed a propeptide deletion mutant (MplΔpro) and generated two point mutants, Mpl H75V and H95L. Our results show that that the propeptide of Mpl is not necessary for active Mpl to be stably produced. During intracellular infection, the propeptide is essential for Mpl activity. The propeptide serves to retain Mpl bacterium-associated in the periplasm. Taken together, these results suggest that the enzymatic activity of Mpl is dependent upon its localization during intracellular infection.

MATERIALS AND METHODS

Bacterial strains and growth conditions. *L. monocytogenes* strains and plasmids used in this study are listed in Tables 2.1 and 2.2, respectively. *L. monocytogenes* was grown in brain heart infusion media (BHI) or Luria-Bertani (LB) media supplemented with 50mM morpholinepropanesulfonic acid (MOPS), adjusted to pH 7.3, 0.2% (w/v) activated charcoal and 20 mM glucose (LB-MOPS-Glc). *E. coli* strains containing pKSV7-derived plasmids were grown in LB media supplemented with ampicillin (100 μg/mL). *E. coli* strains containing pAM401-derived plasmids were grown in LB supplemented with chloramphenicol (10 μg/mL). *L. monocytogenes* containing pKSV7-derived or pAM401-derived plasmids were grown in BHI supplemented with chloramphenicol (10 μg/mL).

Construction of internal in-frame deletion mutants. Internal in-frame deletion of the propeptide of Mpl was performed using Splicing by Overlapping Extension PCR (PCR SOEing) (10). PCR fragments amplifying the 3' end of the Mpl prodomain and 5' end of the catalytic domain were generated with primer pairs Marq344/Marq345 and Marq346/Marq347 (Table 2.3), respectively, using 10403S genomic DNA as the template. The respective 503-bp and 368-bp PCR products were used in a SOEing PCR with primers Marq344/Marq347. The 824-bp product was then digested with KpnI and EcoRI, and ligated into the shuttle vector pKSV7, thus generating pHSO849 (Table 2.2). Sequence integrity was verified by sequencing. pHSO849 was then electroporated into *L. monocytogenes* strains 10403S and NF-L943. *mpl* was replaced by *mpl*Δpro by allelic exchange (4), generating HEL-871 and HEL-927 (Table 2.1). Deletion of the *mpl* propeptide in the chromosome was verified by PCR using primers Marq 344/Marq 347.

Table 2.1. *L. monocytogenes* strains used in this study

Strain	Genotype & Relevant Features	Source/Ref
10403S	Wild-type (serotype 1/2a)	(1)
NF-L943	10403S *prfA* G155S; overexpresses PrfA-dependent genes	(24)
DP-L1935	Internal in-frame deletion of *plcB* in 10403S	(26)
DP-L2343	Deletion of *mpl* structural gene in 10403S	(23)
HEL-469	Internal in-frame deletion of *mpl* in NF-L943	(2)
HEL-780	*mpl* H95L in 10403S	This study
HEL-782	*mpl* H95L in NF-L943	This study
HEL-784	*mpl* H75V in 10403S	This study
HEL-786	*mpl* H75V in NF-L943	This study
HEL-798	*mpl*-Flag$_{C\text{-}cat}$ in NF-L943	(2)
HEL-871	Deletion of *mpl* propeptide (*mpl*Δpro) in 10403S	This study
HEL-903	10403S + pAM401	This study
HEL-904	HEL-871 + pAM401	This study
HEL-905	DP-L2343 + pAM401	This study
HEL-908	HEL-871 + pHSO909	This study
HEL-925	Internal in-frame deletion of *plcB* in NF-L943	This study
HEL-927	Deletion of *mpl* propeptide in NF-L943	This study
HEL-938	HEL-927 + pHSO909	This study
HEL-939	HEL-925 + pAM401	This study
HEL-940	NF-L943 + pAM401	This study
HEL-941	HEL-469 + pAM401	This study
HEL-942	HEL-927 + pAM401	This study
HEL-943	*mpl*Δpro -Flag$_{C\text{-}cat}$ in NF-L943	This study
HEL-996	*mpl* H75V, E350Q in NF-L943	This study
HEL-998	*mpl* H95L, E350Q in NF-L943	This study
HEL-1000	*mpl* H75V-Flag$_{C\text{-}cat}$ in NF-L943	This study

Table 2.2. Plasmids used in this study

Plasmid	Genotype & Relevant Features	Source/Ref
DP-1888	pKSV7 Δ*plcB* for internal in-frame deletion	(26)
pAB791	pKSV7 *mpl* E350Q	(2)
pAB796	pKSV7 *mpl* C-terminus plus $Flag_{C\text{-}cat}$	(2)
pAM401	Shuttle vector	(35)
pHSO849	pKSV7 *mpl*Δpro	This study
pHSO890	pAM401 with spac promoter	This study
pHSO909	pHSO890 with mpl signal sequence and propeptide	This study
pKR778	pKSV7 *mpl* H95L	This study
pKR779	pKSV7 *mpl* H75V	This study
pKSV7	Shuttle vector for allelic exchange	(28)
pLIV2	Inducible expression vector	(6)

Table 2.3. DNA oligonucleotide primers used in this study

Name	Sequence (5' – 3')[a]	Restriction Site
Marq310	CTACGCCAGAAGAGGATTGGAAG	
Marq313	TAACTGCAGCATATCCCAAAGTTTAAGC	PstI
Marq314	CGGTGTGACAAGGACCTTGATT	Eco0109I
Marq315	AATCAAGGTCCTTGTCACACCG	Eco0109I
Marq316	TAGAGCTCCACTGCGGAACTAAATTCTG	SacI
Marq317	CGAGCGTATACACCGTAACGCCTA	Bst1107I
Marq318	TAGGCGTTACGGTGTATACGCTCG	Bst1107I
Marq336	ACGGATCCAGAATTTAGTTCC	BamHI
Marq344	GCGGTACCAATAGAAATATCTCCATCTGG	KpnI
Marq345	CCATAGTCGGGCAAGATGTGCTTTTACCGT CATAGTGA	
Marq346	TCACTATGACGGTAAAAGCAGTAGAACGGG CTGATACC	
Marq347	GCGAATTCCCATAATGGACAAACGAATC	EcoRI
Marq395	GAGCATGCAGAGGAGTTTTATGAAAAGTAAA CTTATTTGTATC	SphI
Marq396	CTGCATGCCTCACTCGGAAAGCATATTTTGCTT	SphI
Marq398	GCGGATCCCTAACAGCACAAGAGCGGAAAG	BamHI
Marq399	GAGCATGCTCACCTCCTTAAGC	SphI

[a] Restriction site underlined

An internal in-frame deletion of *plcB*, the gene encoding for PC-PLC, was constructed in NF-L943 as described previously (26). Briefly, DP-1888 was electroporated into NF-L943 to delete *plcB* by allelic exchange to generate HEL-925. Lack of PC-PLC activity in HEL-925 was verified using LB-egg yolk agar plates, as described below.

Complementation of the Mpl propeptide in *trans*. MplΔpro strains were complemented by adding the Mpl propeptide in *trans* under the control of the spac promoter using pAM401, a multicopy plasmid. The spac promoter was amplified by PCR using primers Marq398/Marq399 and pLIV2 (Table 2.2) as the DNA template. The 172-bp product was then digested with BamHI and SphI and ligated into the multicopy plasmid pAM401, generating pHSO890 (Table 2.2). The signal sequence and propeptide of Mpl was then amplified by PCR using primers Marq395/Marq396 using genomic 10403S DNA as the template. The 622-bp product was then digested with SphI and ligated into pHSO890, generating pHSO909 (Table 2.2). Proper orientation of the signal sequence and propeptide of Mpl downstream of the spac promoter was verified by PCR using primers Marq395/Marq396. pHSO909 was sequenced and then electroporated into MplΔpro strains. Chloramphenicol-resistant colonies were selected, thus generating HEL-908 and HEL-938 (Table 2.1).

Construction of Mpl point mutants. Single point mutations in the propeptide of Mpl were constructed using PCR SOEing. To generate the H75V point mutation, PCR fragments were generated with primer pairs Marq313/Marq317 and Marq318/Marq316 (Table 2.3), respectively, using 10403S genomic DNA as the template. Primers Marq317/Marq318 introduces a Bst1107I restriction site to allow for screening of H75V. The respective 395-bp

and 631-bp PCR products were used in a SOEing PCR with primers Marq313/Marq316. The 1002-bp product was then digested with PstI and SacI, and ligated into the shuttle vector pKSV7, thus generating pKR779 (Table 2.2). To generate the H95L point mutation, PCR fragments were generated with primer pairs Marq313/Marq314 and Marq315/Marq316 (Table 2.3), respectively, using 10403S genomic DNA as the template. Primers Marq313/Marq314 introduces an Eco0109I restriction site to allow for screening of H95L. The respective 454-bp and 570-bp PCR products were used in a SOEing PCR with primers Marq313/Marq316. The 1002-bp product was then digested with PstI and SacI, and ligated into the shuttle vector pKSV7, thus generating pKR778 (Table 2.2). pKR779 and pKR778 was sequenced, then electroporated into *L. monocytogenes* 10403S or NF-L943 to introduce the *mpl* H75V and H95L mutations, respectively, into the chromosome by allelic exchange generating a series of strains listed in Table 2.1. Mutants were screened for chloramphenicol-sensitivity and for the presence of either the Bst1107I or the Eco0109I restriction site.

Construction of catalytic mutants of Mpl H75V and H95L were performed by generating the point mutation *mpl* E350Q as described previously (2). Briefly, pAB791 was electroporated into HEL-786 and HEL-782 to introduce the *mpl* E350Q mutation into the *Listeria* chromosome by allelic exchange, generating HEL-996 and HEL-998, respectively. Chloramphenicol-sensitive clones were screened for the mutation by restriction digest using BspHI.

Construction of Flag-tagged Mpl. A Flag tag (DYKDDDDK) was added to the C-terminus of MplΔpro and Mpl H75V as described previously (2), generating strains HEL-943 and

HEL-1000, respectively (Table 2.1). Briefly, pAB796 (Table 2.2) was electroporated into HEL-927 and HEL-786. The Flag tag was added to the C-terminus of Mpl (Mpl-$Flag_{C\text{-}cat}$) by allelic exchange. Chloramphenicol-sensitive colonies were screened for the presence of the Flag tag by PCR using primers Marq310/Marq336 (Table 2.3).

Western immunoblots. Western immunoblots of culture supernatants were performed as described previously (29). Briefly, NF-L943 background *L. monocytogenes* were grown in LB-MOPS-Glc to an OD_{600} = 1.0. Proteins from the equivalent of 1mL of OD_{600} = 1 culture supernatant were precipitated using 5% trichloroacetic acid and resuspended in 2X sample buffer (125 mM Tris-HCl [pH 6.8], 4% sodium dodecyl sulfate [SDS], 20% glycerol, 20 mM dithiothreitol). Proteins were resolved by SDS-PAGE, then transferred to a polyvinylidene difluoride membrane. To detect Mpl, rabbit serum against Mpl (a gift from Daniel Portnoy, University of California, Berkeley) was utilized, followed by alkaline phosphatase conjugated goat anti-rabbit IgG (24 ng/ml). To detect Flag, anti-Flag M2 (Sigma) was used at a concentration of 2 ng/ml, followed by alkaline phosphatase conjugated goat anti-mouse IgG (600 ng/ml). Nitroblue tetrazolium (0.33 mg/ml) and 5-bromo-4-chloro-3-indolyl phosphate (0.17 mg/ml) were used as substrates to detect the proteins.

Egg Yolk Agar Plate Assay. Detection of PC-PLC activity on LB egg yolk agar plates was performed as described previously (37). Briefly, NF-L943 background *L. monocytogenes* strains were spot inoculated onto LB egg yolk agar plates supplemented with 25 mM glucose 1-phosphate and 0.2% activated charcoal. Strains containing a pAM401-derived plasmid

were spot inoculated onto egg yolk plates supplemented with 10 μg/ml chloramphenicol. Plates were incubated at 37°C for 48 hours. PC-PLC activity is detected by a zone of opacity.

Metabolic labeling and immunoprecipitation assays. Metabolic labeling and immunoprecipitation of proteins from intracellular *L. monocytogenes* were performed as described previously (21, 29, 37). J774 mouse macrophage-like cells were infected with 10403S background *Listeria* as described previously. Prior to labeling, host protein synthesis and proteasomes were inhibited. Cell-to-cell spread was inhibited using cytochalasin D. To detect ActA or PC-PLC, infected cells were pulse-labeled with [^{35}S]-met/cys for five minutes, then chased in a nigericin-containing potassium buffer equilibrated to either pH 7.3 or pH 6.5. To detect PC-PLC, pulse-chased cells were lysed and the intracellular bacteria were separated from the host cell lysates by centrifugation. Bacteria were digested using purified Ply118, a *L. monocytogenes*-specific phage endolysin (11). PC-PLC was then immunoprecipitated from both the bacterial and host cell lysates. The immunoprecipitates were resolved on a 12% SDS-PAGE gel. To detect ActA, pulse-chased cells were lysed in pre-warmed 2X sample buffer, quickly frozen in dry ice and then boiled for five minutes. The lysates were then resolved on a 10% SDS-PAGE gel (21). To detect Mpl, infected cells were pulse-labeled for 30 minutes. The radiolabeled cells were immediately lysed and Mpl was immunoprecipitated from the cleared host cell lysates. Lysates were resolved on a 12% SDS-PAGE gel. Labeled proteins were detected by autoradiography.

To quantify the amount of Mpl secreted during an intracellular infection, three independent immunoprecipitations of Mpl were performed over the course of three consecutive days. The

immunoprecipitates from days 1 and 2 were frozen quickly in dry ice and stored at -80°C until they were ready to be resolved by SDS-PAGE. On the third day, the immunoprecipitates were resolved on a 12% SDS-PAGE gel and detected by phosphorimaging. Quantification of secreted Mpl zymogen and mature Mpl were performed using the ImageJ program (http://rsbweb.nih.gov/ij/). Band intensities were normalized to the number of met/cys residues in each Mpl species. Data was analyzed using a two-tailed paired *t*-test with a significance level (α) of 0.05.

Immunofluorescence Assay to detect Bacterium-Associated Mpl. 4 x 10^5 HeLa cells were seeded onto 18 x 18 mm sterile coverslips. HeLa cells were infected with NF-L943 background *L. monocytogenes* for approximately four hours. Infected cells were then fixed in a 1:1 (v/v) solution of ice cold methanol: acetone at room temperature for 2 minutes, then washed in phosphate-buffered saline, followed by Tris-buffered saline (TBS) supplemented with 0.1% Triton X-100 (TBS-TX). When indicated, mutanolysin (700U) (Sigma) was used for 15 minutes at 37°C to digest the bacterial cell wall. Coverslips were then blocked for 30 minutes in TBS-TX supplemented with 10% bovine serum albumin. To detect bacterium-associated Mpl-Flag, coverslips were reacted to mouse monoclonal anti-Flag M2 (1 μg/ml) for two hours at room temperature, followed by a donkey anti-mouse antibody conjugated to fluorescein isothiocyanate (FITC) (1.5 μg/ml) for 45 minutes at room temperature. To stain for bacteria, wheat-germ agglutinin (1 μg/ml) conjugated to Texas-Red was used for 30 minutes at room temperature. Coverslips were extensively washed between each incubation step using TBS-TX. Prior to mounting, coverslips were washed extensively with TBS then air dried. Coverslips were mounted onto glass slides using Prolong Gold antifade with 4',6-

diamidino-2-phenylindole (DAPI). Images were taken using an Olympus BX51 fluorescent microscope with Olympus DP70 digital camera.

RESULTS

The propeptide of Mpl is not necessary for stable Mpl to be produced. Propeptides of proenzymes can serve multiple functions. One such function is to act as an intramolecular chaperone to ensure proper folding of the catalytic domain and inhibit enzymatic activity. To determine the role of Mpl's propeptide, we constructed a mutant in which the propeptide of Mpl was deleted (MplΔpro). We first asked whether deleting the propeptide would affect Mpl production or stability. Bacteria expressing either wild-type Mpl or MplΔpro were grown in broth. Culture supernatants were collected and Mpl was detected by western immunoblot. Wild-type bacteria secrete four Mpl species, the Mpl zymogen, mature Mpl, a degradation product and the propeptide (2) (Figure 2.1A, lanes 1 and 5). As expected, when the propeptide was deleted, neither the zymogen nor the propeptide was detected (Figure 2.1A, lane 2). Equivalent amounts of mature Mpl were detected between the wild-type Mpl and MplΔpro, suggesting that the mature Mpl produced by the propeptide mutant is in fact stable.

Figure 2.1. Absence of the propeptide does not affect mature Mpl production. Detection of Mpl from culture supernatants of broth-grown *L. monocytogenes* using rabbit α-Mpl serum. **A.** The positions of the proform, mature form, degradation product, and propeptide of Mpl are indicated on the left. → indicates the presence of a novel Mpl proform degradation product in *mpl* H75V and *mpl* H95L. Numbers on the right indicate molecular markers (in kDa). Lanes: 1, HEL-940; 2, HEL-942; 3, HEL-938; 4, HEL-941; 5, NF-L943; 6, HEL-786; 7, HEL-782; 8, HEL-469. **B.** Detection of Mpl from catalytic mutants of *mpl* H75V and H95L. → indicates the presence of the Mpl proform degradation product. Numbers on the right indicate molecular markers (in kDa). Lanes: 1, NF-L943; 2, HEL-786; 3, HEL-996; 4, HEL-782; 5, HEL-998. **C.** Detection of Mpl-$Flag_{C\text{-}cat}$ constructs from culture supernatants. The positions of the proform, mature form, degradation product, and propeptide of Mpl-$Flag_{C\text{-}cat}$ constructs are indicated on the left. Asterisks (*) indicate the positions of Mpl species without a $Flag_{C\text{-}cat}$ tag. Numbers on the right indicate molecular markers (in kDa). Lanes: 1, NF-L943; 2, HEL-798; 3, HEL-943; 4, HEL-1000. Experiment shown in panel C was performed by Alan Bitar.

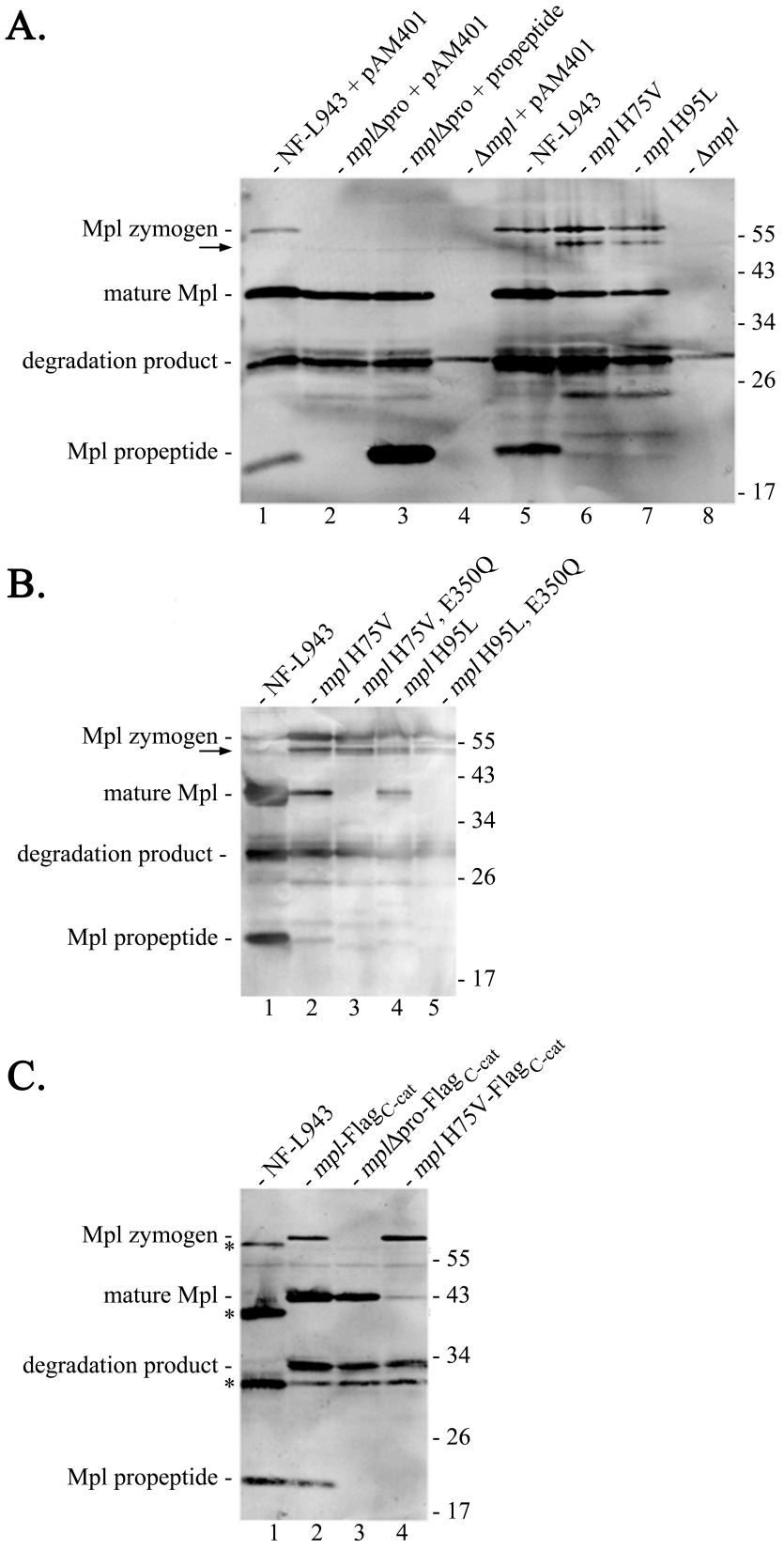
A.
- NF-L943 + pAM401
- mplΔpro + pAM401
- mplΔpro + propeptide
- Δmpl + pAM401
- NF-L943
- mpl H75V
- mpl H95L
- Δmpl
Mpl zymogen -
mature Mpl -
degradation product -
Mpl propeptide -
- 55
- 43
- 34
- 26
- 17
1 2 3 4 5 6 7 8
B.
- NF-L943
- mpl H75V
- mpl H75V, E350Q
- mpl H95L
- mpl H95L, E350Q
Mpl zymogen -
mature Mpl -
degradation product -
Mpl propeptide -
- 55
- 43
- 34
- 26
- 17
1 2 3 4 5
C.
- NF-L943
- mpl-Flag C-cat
- mplΔpro-Flag C-cat
- mpl H75V-Flag C-cat
Mpl zymogen -
mature Mpl -
degradation product -
Mpl propeptide -
*
*
*
- 55
- 43
- 34
- 26
- 17
1 2 3 4

To complement the *mpl*Δpro mutant, we introduced the Mpl propeptide in *trans*, on a multicopy plasmid. While the propeptide was produced in large quantities, we did not observe a difference in mature Mpl production between the *mpl*Δpro mutant and its complement (Figure 2.1A, lane 3). Taken together, these results show that the propeptide is dispensable for mature Mpl to be stably produced.

Mpl H75 and H95 contribute to the stability of the propeptide. Analysis of the propeptide of Mpl to other related metalloproteases identified two conserved histidine residues, H75 and H95 (refer to Figure 5.2 of chapter 5 for CLUSTALW alignment of Mpl to other metalloproteases). Both of these residues are part of the FTP domain in thermolysin-like metalloprotease propeptides. The FTP domain is important for autocatalysis in aureolysin, an Mpl ortholog from *S. aureus* (17). Therefore, we were interested in determining whether these amino acids contribute to Mpl autocatalysis. H75 and H95 were mutated to valine and leucine, respectively. Mpl production and stability was assessed by western immunoblot. Both the Mpl zymogen and mature form were detected (Figure 2.1A, lanes 6 and 7). The propeptide was not detected. We observed a 48 kDa Mpl species in both of these mutants (Figure 2.1A, →). This novel Mpl species may be due to cleavage in the propeptide since (i) the propeptide was not detected in these mutants, and (ii) the mature Mpl H75V and H95L bands migrated similarly to wild-type mature Mpl.

To determine if this cleavage was due to Mpl, we generated catalytic mutants of Mpl H75V and H95L. This was done by mutating the glutamic acid in the active site of Mpl for glutamine (E350Q) (2). Mpl production was again assessed by western immunoblot. As

expected, Mpl H75V and H95L catalytic mutants were not able to undergo autocatalysis and did not produce mature Mpl (Figure 2.1B, lanes 3 and 5). However, the prodegradation product was still present (Figure 2.1B, lanes 2 through 5, →). These results indicate that the cleavage in the propeptide is not due to Mpl. Mpl H75 and H95 are important for the stability of the propeptide.

The propeptide of Mpl contributes, but is not necessary for Mpl activity *in vitro*.

Activation of PC-PLC is mediated by Mpl (2, 14, 20). Therefore, we next questioned whether the Mpl propeptide is necessary to generate active mature Mpl *in vitro*. To investigate the activity of Mpl, we assessed PC-PLC activity in the Mpl propeptide mutants. PC-PLC activity *in vitro* is measured by egg yolk hydrolysis. *L. monocytogenes* strains were spot inoculated onto egg yolk plates. A zone of opacity around the colony is indicative of PC-PLC activity (Figure 2.2, panels 1 and 6). *L. monocytogenes* strains that contain isogenic deletions of either PC-PLC or Mpl do not show activity (Figure 2.2, panels 4, 5, 10, 14), confirming that this assay shows Mpl-mediated maturation of PC-PLC. A smaller zone of opacity was observed around the Mpl propeptide mutants, indicating that while these Mpl mutants were active, the propeptide does contribute to the activity of Mpl (Figure 2.2, panels 2, 7, 8 and 9). When the *mpl*Δpro mutant was complemented with the propeptide in *trans*, we did not detect a change in the zone of opacity around the mutant (Figure 2.2, compare panels 2 and 3). This result suggests that the propeptide added in *trans* cannot complement the activity defect we observe from MplΔpro. Taken together, these results indicate that the propeptide of Mpl contributes, but is not essential to generate active mature Mpl *in vitro*.

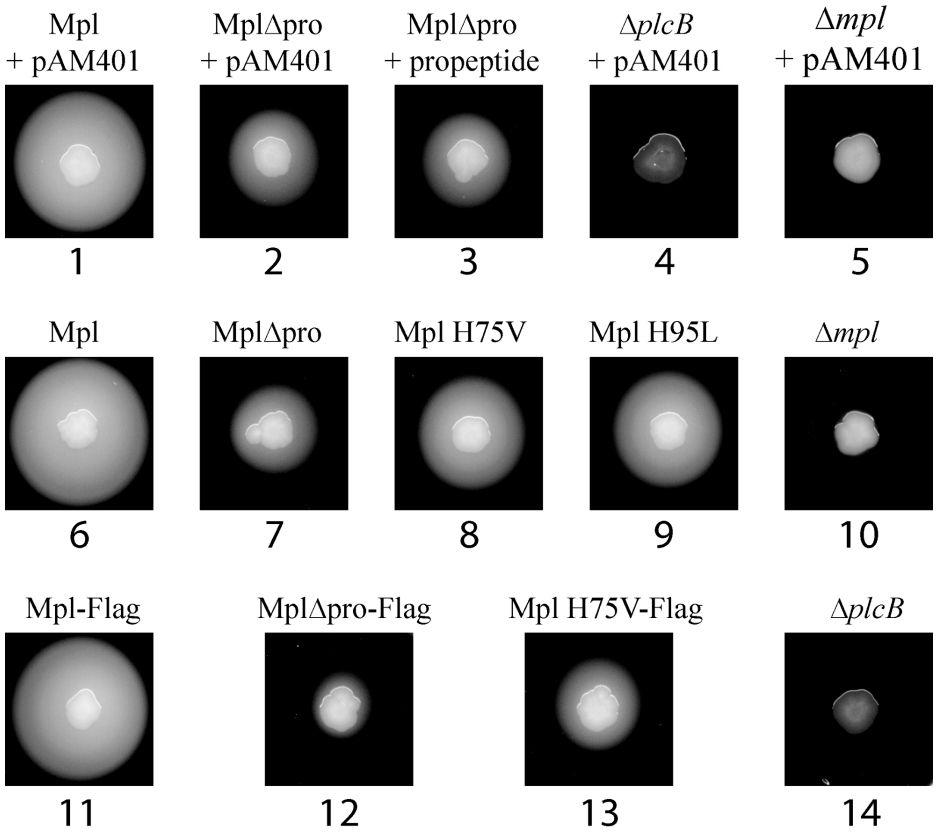

Figure 2.2. MplΔpro and Mpl point mutants are active *in vitro*. *L. monocytogenes* strains were spot inoculated onto LB egg yolk agar plates. Strains containing pAM401-derived plasmids were spot inoculated onto LB Egg yolk agar plates supplemented with chloramphenicol. PC-PLC activity is detected by a zone of opacity around the colony. Panels: 1, HEL-940; 2, HEL-942; 3, HEL-938; 4, HEL-939; 5, HEL-941; 6, NF-L943; 7, HEL-927; 8, HEL-786; 9, HEL-782; 10, HEL-469; 11, HEL-798; 12, HEL-943; 13, HEL-1000; 14, HEL-925. Experiment performed by Alan Bitar.

The propeptide of Mpl is necessary for intracellular activity. To determine whether the propeptide of Mpl is necessary for the intracellular activity of Mpl, bacterium-associated and secreted PC-PLC was immunoprecipitated from the bacterial and host cell lysates of infected J774 cells, respectively. As previously reported, when cells are infected with wild-type bacteria, the proform of PC-PLC is detected primarily bacterium-associated at pH 7.3 (Figure 2.3A, lanes 1 and 2). Upon a decrease in pH, mature PC-PLC is secreted (Figure 2.3A, lanes 3 and 4). This pH-dependent maturation and secretion of PC-PLC observed is mediated by Mpl since PC-PLC remains bacterium-associated in its proform in host cells infected with a Δ*mpl* mutant (Figure 2.3B, lanes 13 and 14). MplΔpro was unable to mediate the maturation and secretion of PC-PLC upon a decrease in pH (Figure 2.3B, lanes 5 through 8). Complementation of the propeptide in *trans* did not restore the wild-type phenotype (Figure 2.3B, lanes 9 through 12). When we immunoprecipitated PC-PLC from cells infected with the Mpl point mutants, PC-PLC remained bacterium-associated in its proform at acidic pH (Figure 2.3C and D). Maturation and secretion of PC-PLC was not observed. These results show that the propeptide of Mpl is necessary for the intracellular activity of Mpl on PC-PLC.

We further tested the intracellular activity of MplΔpro by observing the cleavage of ActA. During intracellular infection, ActA is proteolytically cleaved under acidic conditions in an Mpl-dependent manner (21). Therefore, we performed a metabolic labeling experiment to see if MplΔpro was able to mediate ActA degradation. Infected cells were pulse-labeled in the presence of host protein synthesis inhibitors, and labeled bacterial proteins were resolved by SDS-PAGE and visualized by autoradiography. ActA migrates on the gel as a distinctive triplet approximately 99 kDa in size.

Figure 2.3. Activity of Mpl on PC-PLC during intracellular infection is influenced by its propeptide. A. Immunoprecipitation of bacterium-associated (B) and secreted (S) PC-PLC at pH 7.3 or pH 6.5 was performed as described in Materials and Methods. Proform and mature PC-PLC are indicated on the left. Number on right indicates molecular marker (in kDa). Lanes. Lanes: 1 to 4, 10403S; 5 and 6, DP-L1935. **B.** MplΔpro is unable to mediate PC-PLC maturation and translocation across the bacterial cell wall upon a decrease in pH. Lanes: 1 to 4, HEL-903; 5 to 8, HEL-904; 9 to 12, HEL-908; 13 and 14, HEL-905. **C.** Mpl H75V is unable to mediate PC-PLC maturation and translocation across the bacterial cell wall upon a decrease in pH. Lanes: 1 to 4, 10403S; 5 to 8, HEL-784. **D.** Mpl H95L is unable to mediate PC-PLC maturation and translocation across the bacterial cell wall upon a decrease in pH. Lanes: 1 to 4, 10403S; 5 to 8, HEL-780. Experiments in (A), (B) and (C) were performed by Heather O'Neil and Kari Roberts.

A.

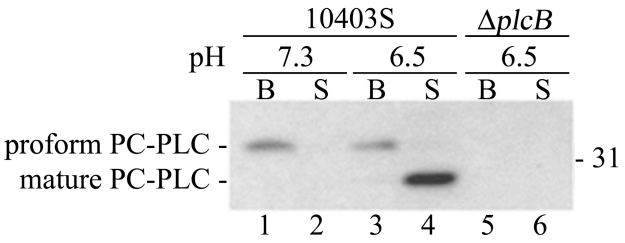
10403S
ΔplcB
pH
7.3
6.5
6.5
B S B S B S
proform PC-PLC -
mature PC-PLC -
- 31
1 2 3 4 5 6

B.

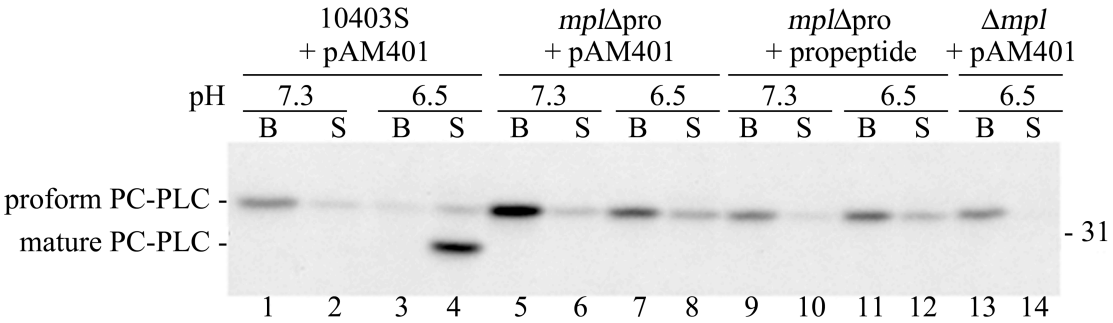
10403S + pAM401
mplΔpro + pAM401
mplΔpro + propeptide
Δmpl + pAM401
pH
7.3
6.5
7.3
6.5
7.3
6.5
6.5
B S B S B S B S B S B S B S
proform PC-PLC -
mature PC-PLC -
- 31
1 2 3 4 5 6 7 8 9 10 11 12 13 14

C.

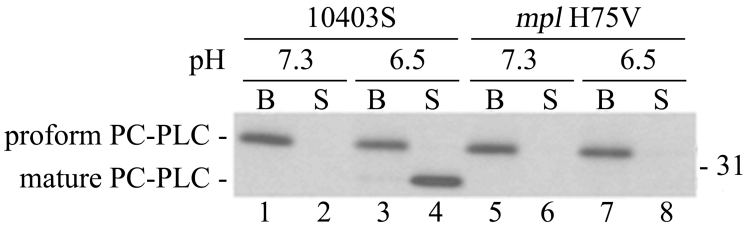
10403S
mpl H75V
pH
7.3
6.5
7.3
6.5
B S B S B S B S
proform PC-PLC -
mature PC-PLC -
- 31
1 2 3 4 5 6 7 8

D.

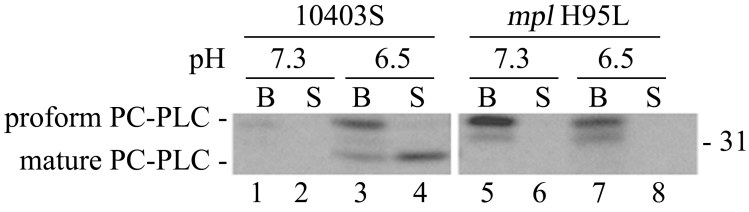
10403S
mpl H95L
pH
7.3
6.5
7.3
6.5
B S B S B S B S
proform PC-PLC -
mature PC-PLC -
- 31
1 2 3 4 5 6 7 8

This triplet is indicative of the different phosphorylated species of ActA (3). The ActA triplet was observed at pH 7.3 from the lysates of cells infected with wild-type, the *mpl*Δpro mutant and a Δ*mpl* mutant (Figure 2.4, lanes 1 through 3). At pH 6.5, cleavage of ActA was only observed from the lysates of cells infected with the wild-type (Figure 2.4, lanes 4 through 6). Taken together, these results show that the propeptide of Mpl is necessary for the intracellular activity of Mpl.

The propeptide of Mpl controls the proper compartmentalization of Mpl during intracellular infection. The results above show that the propeptide is indispensible for Mpl activity during infection. Given that the propeptide of PC-PLC serves to retain PC-PLC in the periplasm during infection (37), we next asked whether Mpl's propeptide serves a similar function. Due to technical difficulties, we were unable to immunoprecipitate Mpl from the lysates of intracellular bacteria in the same manner that bacterium-associated PC-PLC is detected (Figure 2.3). Therefore, we designed an immunofluorescence assay to observe Mpl-bacterium associated. This assay utilizes *L. monocytogenes* which has a Flag tag at the C-terminus of the catalytic domain of Mpl (Mpl-Flag$_{C\text{-}cat}$). Mpl-Flag$_{C\text{-}cat}$ was described in a previous publication (2). In this publication, this protein was identified as Mpl-Flag. Addition of the Flag tag to wild-type Mpl does not affect production (Figure 2.1C, lane 2) or activity on egg yolk agar plates (Figure 2.2, panel 11). We first asked the question of whether Mpl was surface accessible to antibodies. Infected HeLa cells were fixed and then treated in a potassium buffer with or without mutanolysin. Mutanolysin is an N-acetyl muramidase. Samples were then reacted to an anti-Flag M2 antibody. Bacteria were detected using wheat-germ agglutinin which binds to sialic acid and N-acetylglucosamine.

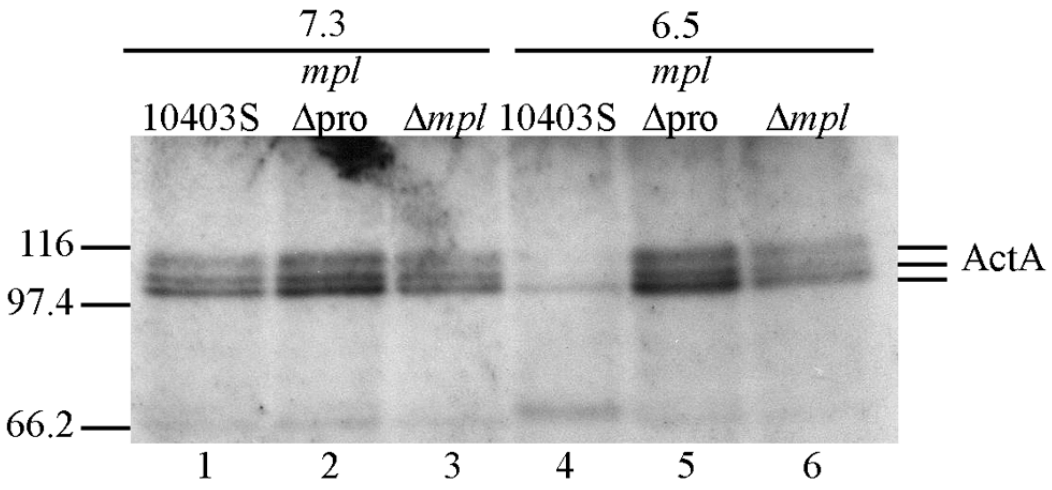

Figure 2.4. A decrease in pH does not affect the stability of ActA from cells infected with the *mpl*Δpro mutant. Infected J774 cells were pulse-labeled using [^{35}S] met/cys then chased in nigericin-containing buffer equilibrated to either pH 7.3 or pH 6.5, as indicated in the figure. Cells were then lysed in sample buffer. Lysates were resolved by SDS-PAGE and detected by autoradiography. ActA is indentified as a distinct triplet, as indicated on the right of the figure. Numbers on left indicate molecular mass markers (kDa). Lanes: 1 and 4, 10403S; 2 and 5, HEL-871; 3 and 6, DP-L2343. Experiment performed by Heather O'Neil.

Mpl was weakly detected in samples not treated with mutanolysin. However, following treatment, Mpl was more clearly observed from bacteria (Figure 2.5, panels A-D). No staining was observed from samples infected with *L. monocytogenes* that does not have a Flag tag on Mpl (Figure 2.5, panels I and J).

We next assessed whether MplΔpro or Mpl H75V is bacterium-associated during intracellular infection. The Flag tag was added to both of these Mpl mutants. Like wild-type Mpl, addition of $Flag_{C\text{-}cat}$ did not reduce the stability of these proteins (Figure 2.1C, lanes 3 and 4). However, the addition of $Flag_{C\text{-}cat}$ did reduce the activity of the Mpl propeptide mutants (Figure 2.2, panels 12 and 13). MplΔpro- $Flag_{C\text{-}cat}$ and Mpl H75V-$Flag_{C\text{-}cat}$ were not detected bacterium-associated in HeLa cells (Figure 2.5, panels E-H).

The lack of bacterium-associated Mpl staining suggested that MplΔpro and Mpl H75V were being aberrantly secreted into the host cytosol. We tested this hypothesis by immunoprecipitating Mpl from the host cell lysates of infected cells. Only the Mpl zymogen was detected from wild-type bacteria, *mpl* H75V and *mpl* H95L (Figure 2.6, lanes 1, 5, 7, 8). Interestingly, the 48 kDa Mpl degradation product observed from the two point mutants (Figure 2.1A and B) was not detected. A band corresponding to the mature form of Mpl was detected in the lysates of cells infected with bacteria expressing MplΔpro (Figure 2.6, lanes 2 and 6). Addition of the propeptide in *trans* did not influence the behavior of MplΔpro (Figure 2.6, lane 3). As a negative control, we immunoprecipitated Mpl from the host cell lysates of cells infected with a Δ*mpl* mutant. As expected, Mpl was not detected in these samples (Figure 2.6, lane 9).

Figure 2.5. MplΔpro and Mpl H75V are no longer bacterium-associated during intracellular infection. Bacterium-associated Mpl was detected by fluorescence microscopy. HeLa cells were infected with *L. monocytogenes* strains indicated on the left for approximately four hours, fixed and then digested with mutanolysin where indicated in the figure. *Listeria* was detected using wheat-germ agglutinin conjugated to Texas Red. Mpl-$Flag_{C\text{-}cat}$ was detected using anti-Flag M2 antibody, followed by a fluorescein isothiocyanate secondary antibody. Panels (A to D) HEL-798; (E and F) HEL-943; (G and H) HEL-1000; (I and J) NF-L943.

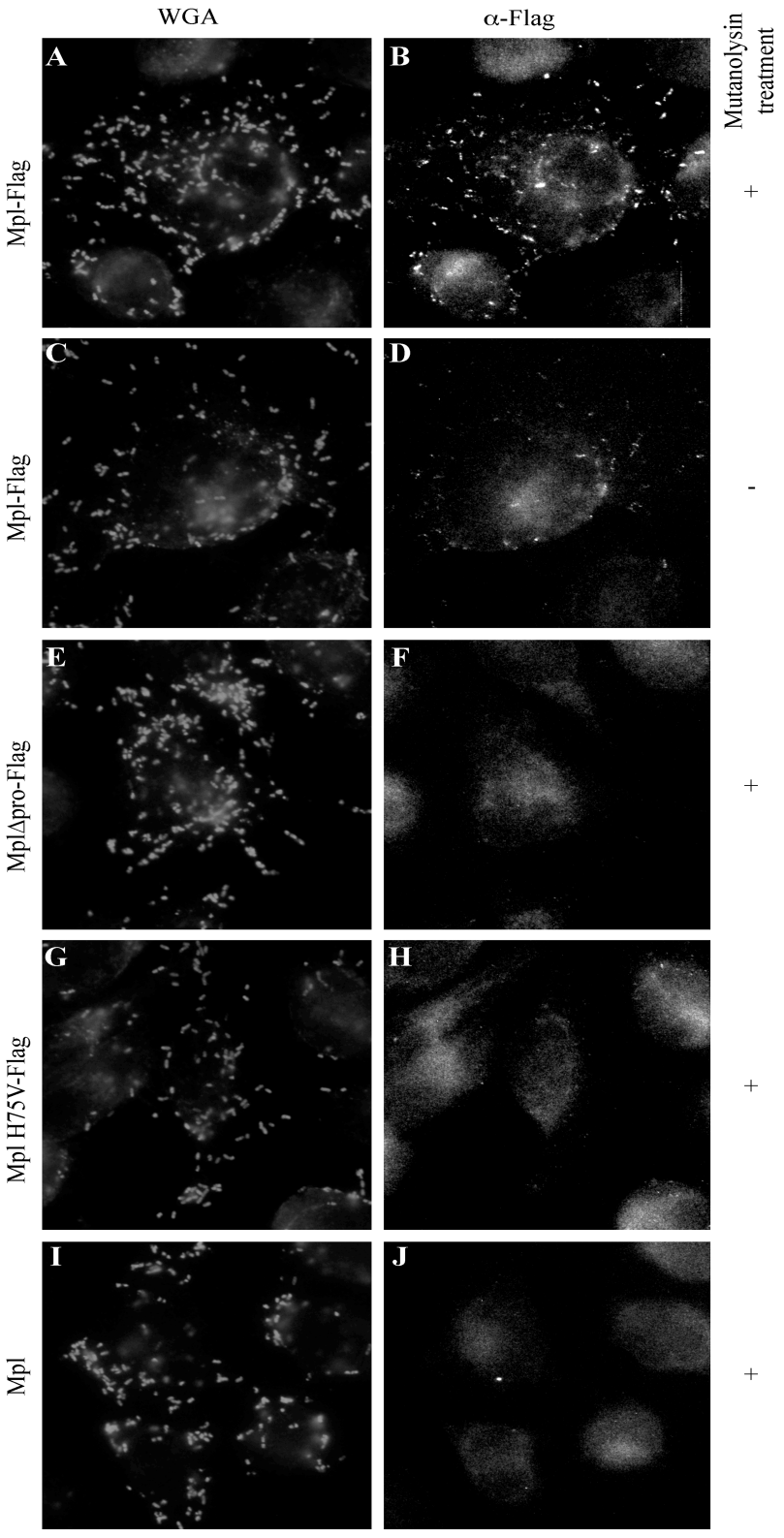
WGA
α-Flag
Mutanolysin treatment
A
B
Mpl-Flag
+
C
D
Mpl-Flag
-
E
F
MplΔpro-Flag
+
G
H
Mpl H75V-Flag
+
I
J
Mpl
+

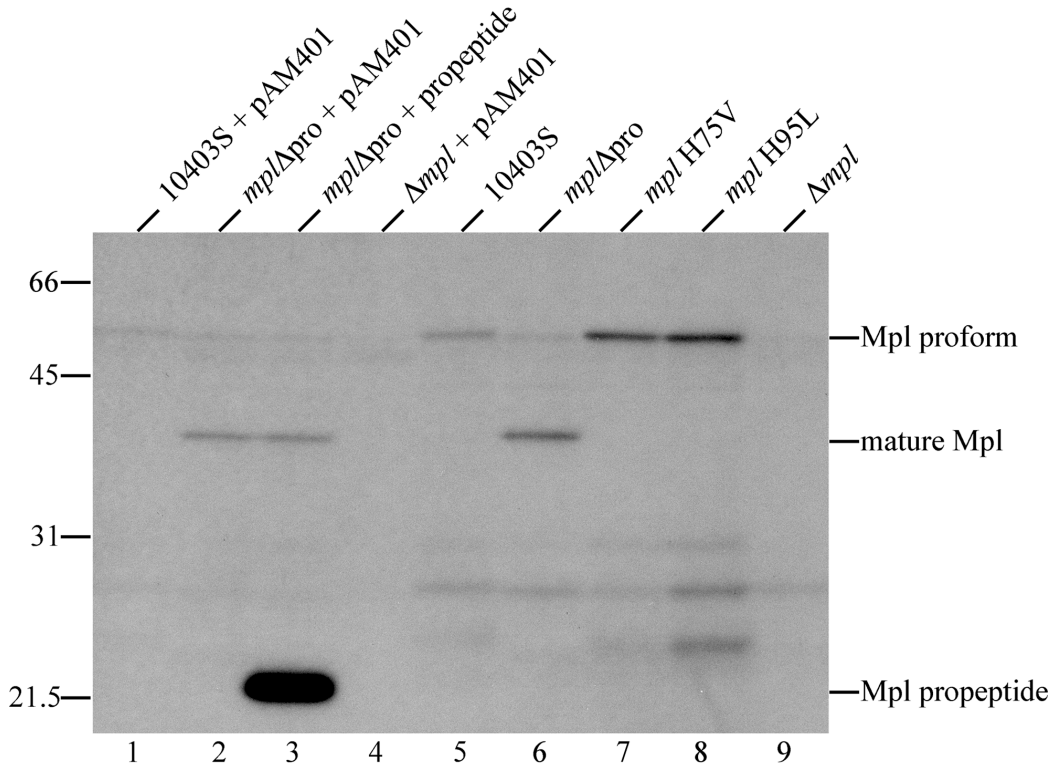

Figure 2.6. MplΔpro and Mpl point mutants are aberrantly secreted into the cytosol of infected host cells. Infected J774 cells were pulse-labeled with [^{35}S]-met/cys. Secreted Mpl was then immunoprecipitated from the host cell lysates of infected J774 cells, resolved by SDS-PAGE and detected by autoradiography. Mpl species are indicated on the right. Numbers on left indicate molecular markers (in kDa). Lanes: 1, HEL-903; 2, HEL-904; 3, HEL-908; 4, HEL-905; 5, 10403S; 6, HEL-871; 7, HEL-784; 8, HEL-780; 9, DP-L2343.

We observed that the intensities of the zymogen and mature Mpl bands detected on the autoradiograph varied between strains. We calculated the band intensities of the secreted zymogen and mature form of Mpl from three independent experiments using the program ImageJ (Table 2.4). We observed a significant increase in the amount of Mpl being secreted from the propeptide mutants, as compared to the wild-type. These results, taken together with our immunofluorescence data (Figure 2.5), suggest that the propeptide serves to retain Mpl bacterium-associated during infection.

DISCUSSION

L. monocytogenes is a facultative intracellular pathogen that can spread from cell-to cell without leaving the intracellular compartment (32). As a result of this movement, the bacterium becomes temporarily entrapped in a double membrane vacuole as it enters a neighboring cell. One factor that mediates escape from these vacuoles is PC-PLC (26). PC-PLC is produced as an inactive proenzyme that has an N-terminal propeptide (15, 29). This propeptide is necessary to keep PC-PLC bacterium-associated in the periplasm (37). Maturation and secretion of PC-PLC is dependent upon a drop in pH and Mpl (15). Mpl is produced as a zymogen that also has an N-terminal propeptide (16). Removal of this propeptide and subsequent activation of Mpl occurs by intramolecular autocatalysis (2). In this study, we were interested in determining the function of the Mpl propeptide. To do so, we constructed an Mpl deletion mutant (MplΔpro) and two point mutants (Mpl H75V and H95L). Our results indicated that the propeptide is dispensable for the catalytic domain of Mpl to fold into an active enzyme. Residues H75 and H95 are important for the stability of

Table 2.4. Quantitation of secreted Mpl during intracellular infection

Strain	Average Density ± Standard Deviation
Wild-type	77.1 ± 50.1
MplΔpro	234.5 ± 28.4*
Mpl H75V	252.9 ± 61.0*

[a] Data was analyzed using a two-tailed paired *t*-test compared to wild-type Mpl secretion with a significance level (α) of 0.05. * indicates $p = 0.02$.

the propeptide. During intracellular infection, the propeptide serves to retain Mpl in the periplasmic space, which is important for the enzymatic activity of Mpl.

Most thermolysin-like metalloproteases rely on their propeptide to act as an intramolecular chaperone (25). Our results indicate that this may not be the case for Mpl. The catalytic domain of Mpl can be stably produced in absence of the propeptide. There is a precedent for our observation. Active neutral protease, a thermolysin-like metalloprotease from *Bacillus stearothermophilus,* can be produced in the absence of its propeptide (12). Propeptides can also serve to inhibit enzymatic activity (25). Removal and/or degradation of the propeptide is necessary for enzymatic activity. Adding the propeptide in *trans* does not affect the behavior of MplΔpro. Following Mpl autocatalysis or when provided in *trans*, a full length propeptide is detected from broth-grown or intracellular bacteria. Taken together, these results suggest that the Mpl propeptide is not inhibitory and may not behave like other thermolysin-like metalloproteases.

While MplΔpro did demonstrate enzymatic activity on semi-solid agar, it had a lower level of activity. This may be indicative of a decrease in the kinetics of Mpl's folding rate. MplΔpro may be folding into a non-native, yet enzymatically active conformation. Perhaps Mpl's propeptide acts in a manner similar to PC-PLC's in slowing down protein folding to allow Mpl to fold into its native conformation properly (37). The propeptide may inhibit secretion of Mpl until the catalytic domain has enough time to fold properly and/or interact with folding factors located in the cell envelope. One such chaperone is PrsA2, the *L. monocytogenes* ortholog of PrsA, a peptidyl prolyl *cis-trans* isomerase from *Bacillus subtilis.* PrsA2 is

predicted to be anchored to the cell membrane. Interaction with this or other folding factors in the cell envelope could also explain why the propeptide of Mpl is necessary to keep Mpl bacterium-associated during infection.

The inability of MplΔpro to activate PC-PLC during intracellular infection could be due to the fact that the two proteins are now in two different compartments and therefore cannot interact with one another. PC-PLC is retained bacterium-associated and MplΔpro is rapidly secreted across the cell wall. Having both PC-PLC and Mpl accumulate in the periplasm increases the likelihood that the two proteins can interact with one another. PC-PLC is not as tightly retained in the periplasm when bacteria are grown *in vitro* (37). This could explain why the Mpl propeptide mutants demonstrated enzymatic activity on egg yolk agar plates, but did not demonstrate activity in infected cells. Perhaps MplΔpro is able to activate PC-PLC as both proteins are being secreted when the bacteria are grown on semi-solid media.

Although the immunofluorescence assay showed that intracellular bacteria generate a pool of bacterium-associated Mpl, the location of the Flag tag does not allow us to differentiate the zymogen from the mature form of Mpl. Since deletion of the propeptide results in the release of Mpl from the periplasmic space, we hypothesize that the Mpl species detected bacterium-associated is the zymogen, while mature Mpl is secreted. When we immunoprecipitated Mpl from infected host cells, we were only able to detect the zymogen. This is contrary to what is observed from bacteria grown in broth, where both the zymogen and processed form of Mpl are secreted. This result suggests that Mpl autocatalysis is a highly regulated step during intracellular infection. In addition, Mpl H75V and H95L did not secrete the 48 kDa

degradation product. Since this degradation occurs in an Mpl-independent manner, this result suggests that perhaps the protease responsible for this cleavage is not expressed when bacteria are intracellular. There may be additional factors that regulate Mpl autocatalysis during intracellular infection. Given that the maturation of PC-PLC requires a decrease in pH, perhaps autocatalysis and or secretion of Mpl is regulated by pH. Future work will focus on testing this hypothesis.

In conclusion, our study shows that Mpl's propeptide is not necessary for the production of a stable mature protein and is not inhibitory to the catalytic domain. The propeptide serves to retain Mpl bacterium-associated during intracellular infection. We therefore hypothesize that during intracellular infection, Mpl must remain bacterium-associated until it can fold into its native conformation and mediate the maturation and secretion of PC-PLC.

ACKNOWLEDGEMENTS

We thank Emily Slepkov for her assistance with the statistical analysis for the secreted Mpl quantitation experiment. This work was supported by Public Health Service grant A152154 from NIAID to H.M.

REFERENCES

1. **Bishop, D. K., and D. J. Hinrichs.** 1987. Adoptive transfer of immunity to *Listeria monocytogenes*. The influence of *in vitro* stimulation on lymphocyte subset requirements. J. Immunol. **139:**2005-2009.

2. **Bitar, A. P., M. Cao, and H. Marquis.** 2008. The metalloprotease of *Listeria monocytogenes* is activated by intramolecular autocatalysis. J. Bacteriol. **190:**107-11.

3. **Brundage, R. A., G. A. Smith, A. Camilli, J. A. Theriot, and D. A. Portnoy.** 1993. Expression and phosphorylation of the *Listeria monocytogenes* ActA protein in mammalian cells. Proc. Natl. Acad. Sci. USA **90:**11890-4.

4. **Camilli, A., L. G. Tilney, and D. A. Portnoy.** 1993. Dual roles of *plcA* in *Listeria monocytogenes* pathogenesis. Mol. Microbiol. **8:**143-57.

5. **Chaudhary, P. M., M. T. Eby, A. Jasmin, and L. Hood.** 1999. Activation of the c-Jun N-terminal kinase/stress-activated protein kinase pathway by overexpression of caspase-8 and its homologs. J. Biol. Chem. **274:**19211-9.

6. **Dancz, C. E., A. Haraga, D. A. Portnoy, and D. E. Higgins.** 2002. Inducible control of virulence gene expression in *Listeria monocytogenes*: temporal requirement of listeriolysin O during intracellular infection. J. Bacteriol. **184:**5935-5945.

7. **Domann, E., J. Wehland, M. Rohde, S. Pistor, M. Hartl, W. Goebel, M. Leimeister-Wachter, M. Wuenscher, and T. Chakraborty.** 1992. A novel bacterial virulence gene in Listeria monocytogenes required for host cell microfilament interaction with homology to the proline-rich region of vinculin. Embo. J. **11:**1981-90.

8. **Eder, J., M. Rheinnecker, and A. R. Fersht.** 1993. Folding of subtilisin BPN': characterization of a folding intermediate. Biochemistry **32:**18-26.

9. **Gray, T. E., J. Eder, M. Bycroft, A. G. Day, and A. R. Fersht.** 1993. Refolding of barnase mutants and pro-barnase in the presence and absence of GroEL. Embo J **12:**4145-50.

10. **Ho, S. N., H. D. Hunt, R. M. Horton, J. K. Pullen, and L. R. Pease.** 1989. Site-directed mutagenesis by overlap extension using the polymerase chain reaction. Gene **77:**51-59.

11. **Loessner, M. J., A. Schneider, and S. Scherer.** 1996. Modified *Listeria* bacteriophage lysin genes (*ply*) allow efficient overexpression and one-step purification of biochemically active fusion proteins. Appl. Environ. Microbiol. **62:**3057-60.

12. **Mansfeld, J., E. Petermann, P. Durrschmidt, and R. Ulbrich-Hofmann.** 2005. The propeptide is not required to produce catalytically active neutral protease from *Bacillus stearothermophilus*. Protein Expr. Purif. **39:**219-28.

13. **Marie-Claire, C., E. Ruffet, A. Beaumont, and B. P. Roques.** 1999. The prosequence of thermolysin acts as an intramolecular chaperone when expressed *in trans* with the mature sequence in *Escherichia coli*. J. Mol. Biol. **285:**1911-1915.

14. **Marquis, H., H. Goldfine, and D. A. Portnoy.** 1997. Proteolytic pathways of activation and degradation of a bacterial phospholipase C during intracellular infection by *Listeria monocytogenes*. J. Cell Biol. **137:**1381-92.

15. **Marquis, H., and E. J. Hager.** 2000. pH-regulated activation and release of a bacteria-associated phospholipase C during intracellular infection by *Listeria monocytogenes*. Mol. Microbiol. **35:**289-98.

16. **Mengaud, J., C. Geoffroy, and P. Cossart.** 1991. Identification of a new operon involved in *Listeria monocytogenes* virulence: its first gene encodes a protein homologous to bacterial metalloproteases. Infect. Immun. **59:**1043-1049.

17. **Nickerson, N. N., V. Joag, and M. J. McGavin.** 2008. Rapid autocatalytic activation of the M4 metalloprotease aureolysin is controlled by a conserved N-terminal fungalysin-thermolysin-propeptide domain. Mol. Microbiol. **69:**1530-43.

18. **Oda, M. N., S. V. Scott, A. Hefner-Gravink, A. D. Caffarelli, and D. J. Klionsky.** 1996. Identification of a cytoplasm to vacuole targeting determinant in aminopeptidase I. J. Cell Biol. **132:**999-1010.

19. **Power, S. D., R. M. Adams, and J. A. Wells.** 1986. Secretion and autoproteolytic maturation of subtilisin. Proc. Natl. Acad. Sci. USA **83:**3096-100.

20. **Raveneau, J., C. Geoffroy, J. L. Beretti, J. L. Gaillard, J. E. Alouf, and P. Berche.** 1992. Reduced virulence of a *Listeria monocytogenes* phospholipase-deficient mutant obtained by transposon insertion into the zinc metalloprotease gene. Infect. Immun. **60:**916-921.

21. **Robbins, J. R., A. I. Barth, H. Marquis, E. L. de Hostos, W. J. Nelson, and J. A. Theriot.** 1999. *Listeria monocytogenes* exploits normal host cell processes to spread from cell to cell. J. Cell Biol. **146:**1333-50.

22. **Schlech, W. F., 3rd.** 2000. Foodborne listeriosis. Clin. Infect. Dis. **31:**770-5.

23. **Shetron-Rama, L. M., H. Marquis, H. G. Bouwer, and N. E. Freitag.** 2002. Intracellular induction of *Listeria monocytogenes actA* expression. Infect. Immun. **70:**1087-96.

24. **Shetron-Rama, L. M., K. Mueller, J. M. Bravo, H. G. Bouwer, S. S. Way, and N. E. Freitag.** 2003. Isolation of *Listeria monocytogenes* mutants with high-level *in vitro* expression of host cytosol-induced gene products. Mol. Microbiol. **48:**1537-1551.

25. **Shinde, U., and M. Inouye.** 2000. Intramolecular chaperones: polypeptide extensions that modulate protein folding. Semin. Cell. Dev. Biol. **11:**35-44.

26. **Smith, G. A., H. Marquis, S. Jones, N. C. Johnston, D. A. Portnoy, and H. Goldfine.** 1995. The two distinct phospholipases C of *Listeria monocytogenes* have overlapping roles in escape from a vacuole and cell-to-cell spread. Infect. Immun. **63:**4231-7.

27. **Smith, G. A., D. A. Portnoy, and J. A. Theriot.** 1995. Asymmetric distribution of the *Listeria monocytogenes* ActA protein is required and sufficient to direct actin-based motility. Mol. Microbiol. **17:**945-951.

28. **Smith, K., and P. Youngman.** 1992. Use of a new integrational vector to investigate compartment-specific expression of the *Bacillus subtilis spoIIM* gene. Biochimie **74:**705-711.

29. **Snyder, A., and H. Marquis.** 2003. Restricted translocation across the cell wall regulates secretion of the broad-range phospholipase C of *Listeria monocytogenes*. J. Bacteriol. **185:**5953-8.

30. **Subbian, E., Y. Yabuta, and U. P. Shinde.** 2005. Folding pathway mediated by an intramolecular chaperone: intrinsically unstructured propeptide modulates stochastic activation of subtilisin. J. Mol. Biol. **347:**367-383.

31. **Takeshima, H., M. Sakaguchi, K. Mihara, K. Murakami, and T. Omura.** 1995. Intracellular targeting of lysosomal cathepsin D in COS cells. J. Biochem. **118:**981-988.

32. **Tilney, L. G., and D. A. Portnoy.** 1989. Actin filaments and the growth, movement, and spread of the intracellular bacterial parasite, *Listeria monocytogenes*. J. Cell Biol. **109:**1597-608.

33. **Vazquez-Boland, J. A., C. Kocks, S. Dramsi, H. Ohayon, C. Geoffroy, J. Mengaud, and P. Cossart.** 1992. Nucleotide sequence of the lecithinase operon of *Listeria monocytogenes* and possible role of lecithinase in cell-to-cell spread. Infect. Immun. **60:**219-230.

34. **Vazquez-Boland, J. A., M. Kuhn, P. Berche, T. Chakraborty, G. Dominguez-Bernal, W. Goebel, B. Gonzalez-Zorn, J. Wehland, and J. Kreft.** 2001. *Listeria* pathogenesis and molecular virulence determinants. Clin. Microbiol. Rev. **14:**584-640.

35. **Wirth, R., F. Y. An, and D. B. Clewell.** 1986. Highly efficient protoplast transformation system for *Streptococcus faecalis* and a new *Escherichia coli-S. faecalis* shuttle vector. J. Bacteriol. **165:**831-836.

36. **Yabuta, Y., H. Takagi, M. Inouye, and U. Shinde.** 2001. Folding pathway mediated by an intramolecular chaperone: propeptide release modulates activation precision of pro-subtilisin. J. Biol. Chem. **276:**44427-44434.

37. **Yeung, P. S., N. Zagorski, and H. Marquis.** 2005. The metalloprotease of *Listeria monocytogenes* controls cell wall translocation of the broad-range phospholipase C. J. Bacteriol. **187:**2601-8.

38. **Zhu, X. L., Y. Ohta, F. Jordan, and M. Inouye.** 1989. Pro-sequence of subtilisin can guide the refolding of denatured subtilisin in an intermolecular process. Nature **339:**483-484.

CHAPTER 3

THE METALLOPROTEASE OF *LISTERIA MONOCYTOGENES* IS REGULATED BY pH.*

* Brian M. Forster, Alan Pavinski Bitar, Emily R. Slepkov, Karthik J. Kota, Holger Sondermann and Hélène Marquis. The metalloprotease of *Listeria monocytogenes* is regulated by pH. Currently in submission to Journal of Bacteriology.

ABSTRACT

Listeria monocytogenes is an intracytosolic bacterial pathogen. Among the factors contributing to escape from vacuoles are a phosphatidylcholine phospholipase C (PC-PLC) and a metalloprotease (Mpl). Both enzymes are translocated across the bacterial membrane as inactive proproteins, whose propeptides serve in part to maintain them bacterium-associated. We have shown that PC-PLC maturation is regulated by Mpl and pH, and that Mpl maturation occurs by autocatalysis. In this study, we tested the hypothesis that Mpl activity is pH-regulated. To synchronize the effect of pH on bacteria, the cytosolic pH of infected cells was manipulated immediately after radiolabelling *de novo* synthesized bacterial proteins. Immunoprecipitation of secreted Mpl from host cell lysates revealed the presence of the propeptide and catalytic domain in samples treated at pH 6.5, but not at pH 7.3. The zymogen was present in small amount under all conditions. Since proteases often remain associated with their respective propeptide following autocatalysis, we aimed at determining whether pH regulates autocatalysis or secretion of the processed enzyme. For this purpose, we used an Mpl construct that contains a Flag tag at the N-terminus of its catalytic domain and antibodies that can distinguish N- and non N-terminal Flag. By fluorescence microscopy, we observed the Mpl zymogen bacterium-associated at physiological pH, but not following acidification. Mature Mpl was not detected bacterium-associated at either pH. Using purified proteins, we determined that processing of the PC-PLC propeptide by mature Mpl is also pH-sensitive. These results indicate that pH influences the activity of Mpl on itself and on PC-PLC.

INTRODUCTION

Listeria monocytogenes is a gram positive, facultative intracellular bacterial pathogen. It is the causative agent of the food-borne disease listeriosis, which has a high mortality rate (37). *L. monocytogenes* is able to invade host cells and spread from cell-to-cell using host actin (35). To escape the vacuoles formed upon initial entry into a cell or during cell-to-cell spread, *L. monocytogenes* relies on multiple virulence factors. These factors include listeriolysin O (7, 35), a phosphatidylinositol-specific phospholipase C (4) and a broad-range phospholipase C known as PC-PLC (phosphatidylcholine phospholipase C) (32). PC-PLC is synthesized as an inactive proenzyme and translocates across the cell membrane where it accumulates in the periplasm (21, 34). A decrease in pH and the metalloprotease of *L. monocytogenes* (Mpl) are required for PC-PLC maturation, which coincides with the rapid secretion of mature PC-PLC across the bacterial cell wall (21, 31).

Mpl is a member of the thermolysin family of metalloproteases, which contains a Zn^{2+} ion in the active site (11). Mpl is produced as a zymogen with an N-terminal propeptide (22). Similar to PC-PLC, Mpl translocates across the bacterial membrane and accumulates in the periplasm (24, 34). This compartmentalization of Mpl is dependent on the propeptide. Removal of the propeptide occurs exclusively by intramolecular autocatalysis (3).

Zymogen autocatalysis is a highly controlled step to prevent premature activation of a protease. There are several known mechanisms by which autocatalysis can be regulated. Autocatalysis can be triggered by the binding of specific molecules. This has been observed for the maturation of the *Vibrio cholerae* multifunctional autoprocessing RTX toxin, where

the binding of inositol hexakisphosphate in the host cytosol induces autocatalysis (27). Maturation of matrix metalloproteases is regulated by a cysteine switch mechanism, where the thiol group of a propeptide's cysteine residue interacts with the coordinated Zn^{2+} ion, thereby inhibiting protease activity (28, 36). In order for maturation to occur, the Zn^{2+}-thiol interaction must be disrupted either by thiol reduction or perturbation of the zymogen conformation. Intramolecular autocatalysis has also been shown to be regulated by pH for several proteases, with examples including the serine protease furin (1, 5) and members of the cathepsin family of cysteine proteases (15). GPR, an aspartic acid protease responsible for degrading spore proteins into amino acids during germination in *Bacillus* spp., also matures in a pH-dependent manner (14).

In this study, we investigated how Mpl activity is regulated during intracellular infection. Given that the maturation and secretion of PC-PLC requires both Mpl and a decrease in pH, we hypothesized that Mpl activity is pH-regulated and that Mpl autocatalysis is the pH-limiting step observed for PC-PLC maturation. Our results indicated that Mpl maturation and compartmentalization are regulated by pH. At physiological pH, the Mpl zymogen remains primarily bacterium-associated. Upon a decrease in pH, autocatalysis occurs, leading to secretion of the Mpl propeptide and catalytic domain across the bacterial cell wall. Moreover, proteolytic maturation of PC-PLC by mature Mpl occurs only at acidic pH.

MATERIALS AND METHODS

Bacterial strains and cell cultures. All *L. monocytogenes* strains and their relevant genotypes used in this study are listed in Table 3.1. *L. monocytogenes* strains were grown in brain heart infusion (BHI) media. For western immunoblots, *L. monocytogenes* was grown in Luria-Bertani (LB) broth supplemented with 50 mM morpholinepropanesulfonic acid (MOPS), adjusted to pH 7.3, 0.2% (w/v) activated charcoal and 20 mM glucose (LB-MOPS-Glc). *E. coli* DH5α and *L. monocytogenes* strains harboring pKSV7-derived plasmids were cultured in LB broth supplemented with ampicillin (100 μg/ml) or BHI supplemented with chloramphenicol (10 μg/ml), respectively. *E. coli* harboring a ppSUMO-derived plasmid was cultured in LB supplemented with kanamycin (30 μg/ml). J774 mouse macrophage-like cells were maintained in DMEM medium (Mediatech) with 7.5% (v/v) fetal bovine serum and 2mM L-glutamine. Human epithelial HeLa cells were maintained in RPMI-1640 (Mediatech) with 7.5% (v/v) fetal bovine serum and 2mM L-glutamine. All tissue culture cells were incubated in a 37°C, 5% CO_2 environment.

Construction of Flag-tagged Mpl. Splicing by Overlapping Extension PCR (SOEing PCR) (13) was used to add a Flag tag between the propeptide and the N-terminus of the Mpl catalytic domain (Mpl-$Flag_{N\text{-}cat}$). PCR fragments amplifying the 3' end of the Mpl propeptide and 5' end of the catalytic domain were generated with primer pairs Marq328/Marq487 and Marq488/Marq387 (Table 3.2), respectively, using 10403S genomic DNA as the template. The respective 560-bp and 384-bp PCR products were used in a SOEing PCR with primers Marq328/387. The 920-bp product was then digested with PstI and EcoRI, and ligated into the shuttle vector pKSV7 (33), thus generating pHM969 (Table 3.1).

Table 3.1. *L. monocytogenes* strains and plasmids used in this study

	Genotype & Relevant Features	Source/Ref
Strains		
10403S	Wild type (serotype 1/2a)	(2)
NF-L943	*prfA* G155S in 10403S background (overexpresses PrfA-dependent genes)	(30)
DP-L1935	Internal inframe deletion of *plcB* in 10403S background	(32)
DP-L2343	Deletion of *mpl* structural gene in 10403S background	(29)
HEL-469	Internal inframe deletion of *mpl* in NF-L943 background	(3)
HEL-583	*mpl* E350Q in 10403S background	(3)
HEL-587	*mpl* E350Q in NF-L943 background	(3)
HEL-798	*mpl*-Flag$_{C\text{-}cat}$ in NF-L943 background	(3)
HEL-800	*mpl* E350Q-Flag$_{C\text{-}cat}$ in NF-L943 background	(3)
HEL-971	*mpl*-Flag$_{C\text{-}cat}$, containing internal inframe deletions of *hly*, *plcB*, *inlAB* in NF-L943 background	This study
HEL-981	*mpl*-Flag$_{N\text{-}cat}$ in NF-L943 background	This study
HEL-982	*mpl* E350Q-Flag$_{C\text{-}cat}$, containing internal inframe *deletions of hly, plcB*, *inlAB* in NF-L943 background	This study
HEL-1084	*mpl* E350Q-Flag$_{N\text{-}pro}$ in NF-L943 background	This study
Plasmids		
pBMF1081	pKSV7 *mpl*-Flag at N-terminus of propeptide (*mpl*-Flag$_{N\text{-}pro}$)	This study
pHM802	ppSUMO *plcB*	This study
pHM969	pKSV7 *mpl*-Flag at N-terminus of catalytic domain (*mpl*-Flag$_{N\text{-}cat}$)	This study

Table 3.2. DNA oligonucleotide primers used in this study

Name	Sequence (5' – 3')[a]	Site
Marq288	GGAGCTCTACGTCCACTTGAACAA	SacI
Marq289	ATGCTGCAGAACGGTAATTGATGACC	PstI
Marq326	GTGGATCCTGTTGTGATGAATACTTAC	BamHI
Marq327	GTGCGGCCGCGAGTGGATAAGAATGTATTC	NotI
Marq328	GTGAATTCGATTCTGTCGGGGAAGAAAA	EcoRI
Marq387	GCACTGCAGCAATTCAAGCCATAATGGAC	PstI
Marq487	CTTGTCATCGTCATCCTTGTAATCCTCGGAAAGCA TATTTTG	Flag
Marq488	GATTACAAGGATGACGATGACAAGGTAGAACGGG CTGATA	Flag
Marq494	GTTTCTTTGGGAGTGACATGC	
Marg541	GATTACAAGGATGACGATGACAAGGATAGTGTCG GGGAAGAAAAAC	Flag
Marq542	CTTGTCATCGTCATCCTTGTAATCTGCTTTTAC CGTCATAGTGAAATG	Flag

[a] Restriction site / Flag tag are underlined

pHM969 was sequenced, and then electroporated into *L. monocytogenes* strain NF-L943 for allelic exchange (4), generating HEL-981 (Table 3.1). Allelic exchange was verified by sequencing chloramphenicol sensitive colonies.

Addition of a Flag tag to the N-terminus of the Mpl propeptide (Mpl-$Flag_{N\text{-}pro}$) was generated by SOEing PCR. Primer pairs Marq289/Marq542 and Marq541/Marq288 (Table 3.2) were used to amplify the upstream region and a portion of the Mpl prodomain, respectively, using 10403S genomic DNA as the template. In addition to introducing the Flag sequence, Marq541 and Marq542 introduces a silent serine mutation, resulting in an alteration of the HinfI restriction digest pattern. The 547-bp and 517-bp PCR products were used in a SOEing PCR using primers Marq288/Marq289. The 1040-bp product was digested with PstI and SacI, and ligated into pKSV7, thus generating pBMF1081 (Table 3.1). pBMF1081 was sequenced, then electroporated into HEL-587, a NF-L943 background *L. monocytogenes* strain expressing a catalytic mutant of Mpl (Mpl E350Q) (3), generating HEL-1084 (Table 3.1). Allelic exchange was verified by screening for chloramphenicol sensitivity and for an altered HinfI restriction pattern.

Construction of internal in-frame deletion mutants. Deletions of the genes encoding listeriolysin O (*hly*), PC-PLC (*plcB*) and Internalins A and B (*inlAB*) were made sequentially by allelic exchange in NF-L943 strains expressing Mpl-$Flag_{C\text{-}cat}$ (HEL-798) or Mpl E350Q-$Flag_{C\text{-}cat}$ (HEL-800) using plasmids pDP-2154 (16), pDP-1888 (32) and pHK2 (17), respectively, to generate HEL-971 and HEL-982 (Table 3.1). Chloramphenicol sensitive colonies were selected. The *hly* deletion was verified by loss of hemolysis on blood agar

plates (25). Deletion of *plcB* was verified by the loss of PC-PLC activity on egg yolk agar plates (39). Deletion of *inlAB* was confirmed by PCR using primers Marq41 (17) and Marq494 (Table 3.2). Deletion of *inlA* was further verified by western immunoblot (34).

Metabolic labeling and immunoprecipitation assays. Metabolic labeling of proteins synthesized by intracellular bacteria and immunoprecipitation assays were performed as described previously (24, 31). Briefly, infected J774 cells were pulse-labeled with [^{35}S]-met/cys, then chased in a potassium-based buffer at pH 7.3 or pH 6.5 supplemented with nigericin (10 μM) to mimic the cytosolic or vacuolar pH, respectively. Nigericin is a potassium ionophore that allows for the rapid equilibration of pH across biological membranes. Secreted Mpl was immunoprecipitated from cleared host cell lysates with rabbit immune serum against Mpl (24). Samples were resolved by SDS-PAGE and detected by autoradiography. For each experiment, the amount of sample loaded on the gel was normalized to the number of intracellular bacteria recovered in parallel dishes.

Western immunoblots. Western immunoblots for detecting Mpl constructs were performed as described previously (24). Briefly, *L. monocytogenes* strains were grown in LB-MOPS-Glc to a final OD_{600} ~1. Although the medium was buffered, its pH acidified over time due to bacterial metabolism. The equivalent of 1 ml of OD_{600} = 1 culture supernatant was precipitated with trichloroacetic acid, resolved by SDS-PAGE and transferred to a PVDF membrane by semi-dry electroblot. Rabbit immune serum against Mpl was used at a 1/1000 dilution, while mouse monoclonal anti-Flag M1 and M2 antibodies (Sigma-Aldrich) were used at a concentration of 9 ng/ml and 2 ng/ml, respectively. Alkaline phosphatase conjugated

goat anti-rabbit IgG (24 ng/ml) or goat anti-mouse IgG (600 ng/ml) (Jackson ImmunoResearch Laboratories, Inc.) were used as secondary antibodies, and nitroblue tetrazolium (0.33 mg/ml) and 5-bromo-4-chloro-3-indolyl phosphate (0.17 mg/ml) were used as substrates. All antibody incubations and washes for the anti-Flag M1 immunoblot were done in the presence of 1mM $CaCl_2$.

Immunofluorescent staining of Mpl. Bacterium-associated Mpl-Flag was detected by immunofluorescence, as described previously with modification (24). HeLa cells infected with *L. monocytogenes* were incubated in a potassium-based buffer equilibrated to either pH 7.3 or pH 6.5 supplemented with nigericin (10 μM). Cells were then fixed, and the bacterial cell wall was digested with purified phage endolysin Ply118 (19) at a final concentration of 150 μg/ml. To detect bacterium-associated Mpl-Flag, mouse monoclonal anti-Flag M1 (18 μg/ml) or M2 (1 μg/ml) was used followed by a donkey anti-mouse antibody conjugated to FITC (1.5 μg/ml). All antibody incubations and washes with anti-Flag M1 were done in the presence of 1mM $CaCl_2$. Bis-benzimide (Hoechst 33258) was used at a concentration of 1 μg/ml to detect bacteria and host nuclei.

PC-PLC purification. The proform of PC-PLC (proPC-PLC) was purified from *E. coli* BL21(DE3) cells. Primers Marq326/327 (Table 3.2) were used to amplify *plcB* (gene encoding PC-PLC) without its signal sequence by PCR, generating an 837-bp fragment. This fragment was digested with NotI and BamHI and ligated into ppSUMO (23), a pET28a derived vector thus generating pHM802 (Table 3.1). As a result, *plcB* was cloned in-frame with an N-terminal His_{6x} SUMO (small ubiquitin like modifier) tag. Sequence integrity was

verified by sequencing. BL21(DE3) cells transformed with pHM802 were grown in 4L of Terrific Broth at 37°C, 250 rpm to an OD_{600} ~ 0.5. The temperature was decreased to 18°C and isopropyl □-D-1-thiogalactopyranoside was added to a final concentration of 0.5 mM to induce protein expression. Cultures were grown overnight at 18°C. Cells were harvested by centrifugation (7.5k x *g*, 10 min., 4°C) and resuspended in 50 mL ice-cold Buffer A (25 mM Hepes, 500 mM NaCl, 10 mM imidazole, 25% (v/v) glycerol, pH 10) supplemented with a cocktail of protease inhibitors (Sigma-Aldrich P8849) and 5 mM tris(2-carboxyethyl)phosphine (TCEP). Cells were lysed by sonication and centrifuged (100k x *g*, 1.5 hrs, 4°C). Cleared supernatant was diluted five-fold in Buffer A to decrease the TCEP concentration to 1mM. His_{6x}-SUMO-proPC-PLC was purified by affinity chromatography using a 15 mL Ni^{2+}- nitrilotriacetic acid (NTA) column equilibrated in Buffer A. The column was washed with 10 column volumes of Buffer A. Affinity bound proteins were eluted in 8 x 3 ml fractions with Buffer B (25 mM Hepes, 500 mM NaCl, 500 mM imidazole, 25% glycerol, pH 10). Elutions were combined and passed through a buffer-exchange column equilibrated with Buffer C (25 mM Hepes, 50 mM NaCl, 25% glycerol, 0.5 M urea, pH 9.5) using an Econo-Pac 10DG column (BioRad). Purified His_{6x}-SUMO-proPC-PLC was treated with His_{6x}-ULP-1 protease at room temperature for 1 hour to cleave the His_{6x}-SUMO tag (23). His_{6x}-ULP-1 and His_{6x}-SUMO were removed by adding 1 mL Ni^{2+}-NTA resin per 10 mg of protein equilibrated in Buffer C, incubating for 30 minutes at room temperature, and pelleting the resin by centrifugation at 1000 x g for 1 min. Purified proPC-PLC was passed through a 0.22 μm filter and loaded onto a Sephacryl 100-HR size exclusion column, using an automated AKTApurifer TM FPLC and Fraction Collector Frac-950 (GE Health Care) column equilibrated in Buffer D (25 mM Hepes, 50 mM NaCl 50 mM arginine, 1 mM TCEP,

0.05% (w/v) sodium azide, final pH = 10.3). ProPC-PLC purification was verified by SDS-PAGE.

Mpl purification. Initial purification attempts indicated that LLO, PC-PLC and InlB co-purify with Mpl-Flag$_{C\text{-}cat}$. Therefore, we chose to purify Mpl- Flag$_{C\text{-}cat}$ and Mpl E350Q-Flag$_{C\text{-}cat}$ from *L. monocytogenes* strains that do not express these proteins: HEL-971 and HEL-982, respectively. *L. monocytogenes* was grown in 500 ml of LB-MOPS-Glc to final OD_{600} ~0.9. The bacterial supernatant was rapidly cooled down on ice and the following protease inhibitors were added: PMSF (to 100 μM), leupeptin (to 1 μM) and pepstatin A (to 1 μM). The culture was centrifuged (15k x *g*, 10 min., 4°C) and the supernatant was collected and filtered through a 0.22 μm PVDF membrane. Supernatant was reacted with 1 mL mouse anti-Flag M2 agarose resin (Sigma-Aldrich) equilibrated in 25 mM Hepes, 300 mM NaCl, 1 mM $CaCl_2$, 0.1% (w/v) 3-[(3-cholamidopropyl)dimethylammonio]-1-propanesulfonate (CHAPS), 10 μM $ZnSO_4$, pH 7.3. The resin was then washed five times with 10 column volumes of the same buffer. An additional wash of 5 column volumes of the same buffer without CHAPS was then performed. Bound proteins were eluted in 5 x 1 ml fractions with elution buffer (25 mM Hepes, 300 mM NaCl, 1 mM $CaCl_2$, 10 μM $ZnSO_4$, 5 mg/ml 3x Flag peptide, pH 7.3). Elutions were analyzed for the presence of Mpl by SDS-PAGE and by western immunoblot.

PC-PLC activation *in vitro* assay. Mpl was tested for its ability to mediate proPC-PLC maturation *in vitro*. Purified proPC-PLC (8.7 μg/ml) and/or Mpl (15.2 μg/ml) were mixed in reaction buffers equilibrated to either pH 6.0, 6.5 or 7.3 in a final volume of 250 μl. Each reaction buffer consisted of 35 mM 2-(N-morpholino)ethanesulfonic acid (Mes), 7.5 mM

Hepes, 65 mM NaCl, 3.7 mM $CaCl_2$, 2 μM $ZnSO_4$, 5 mM arginine, 0.1 mM TCEP and 0.005% (w/v) sodium azide. The reactions were incubated at 37°C for 4 hours. The proteins were then resolved by SDS-PAGE. Following electrophoresis, the gel was washed once in ddH_2O, twice in 25% isopropanol, three times in PBS (pH 7.1), overlaid with egg yolk soft agar (20), and incubated at 37°C for 4 hours. PC-PLC activity was detected by the formation of a zone of opacity in the overlay. Following the appearance of PC-PLC activity, the gel was removed and stained with Coomassie Brilliant Blue R-250 to detect PC-PLC.

RESULTS

Mature Mpl is secreted upon a decrease in pH during intracellular infection. The regulation of PC-PLC has been well documented using J774 mouse macrophage-like cells and has also been observed in human HeLa cells (21, 31, 34). Since PC-PLC maturation is dependent on both a decrease in vacuolar pH and Mpl (21), we infected J774 cells to test the hypothesis that Mpl autocatalysis is the pH-limiting step observed for PC-PLC maturation. To determine whether Mpl maturation is pH-dependent, we immunoprecipitated Mpl from the cleared lysates of radiolabeled infected cells incubated in a nigericin-containing potassium buffer equilibrated to either pH 7.3 or pH 6.5. These conditions mimic the pH *L. monocytogenes* would experience when in the cytosol of an infected cell (physiological pH) or when entrapped in a vacuole (acidic pH). A small amount of the Mpl zymogen was secreted into the cytosol of infected cells at either pH (Figure 3.1, lanes 1 and 2), whereas large amounts of the propeptide and mature Mpl were secreted exclusively upon a decrease in

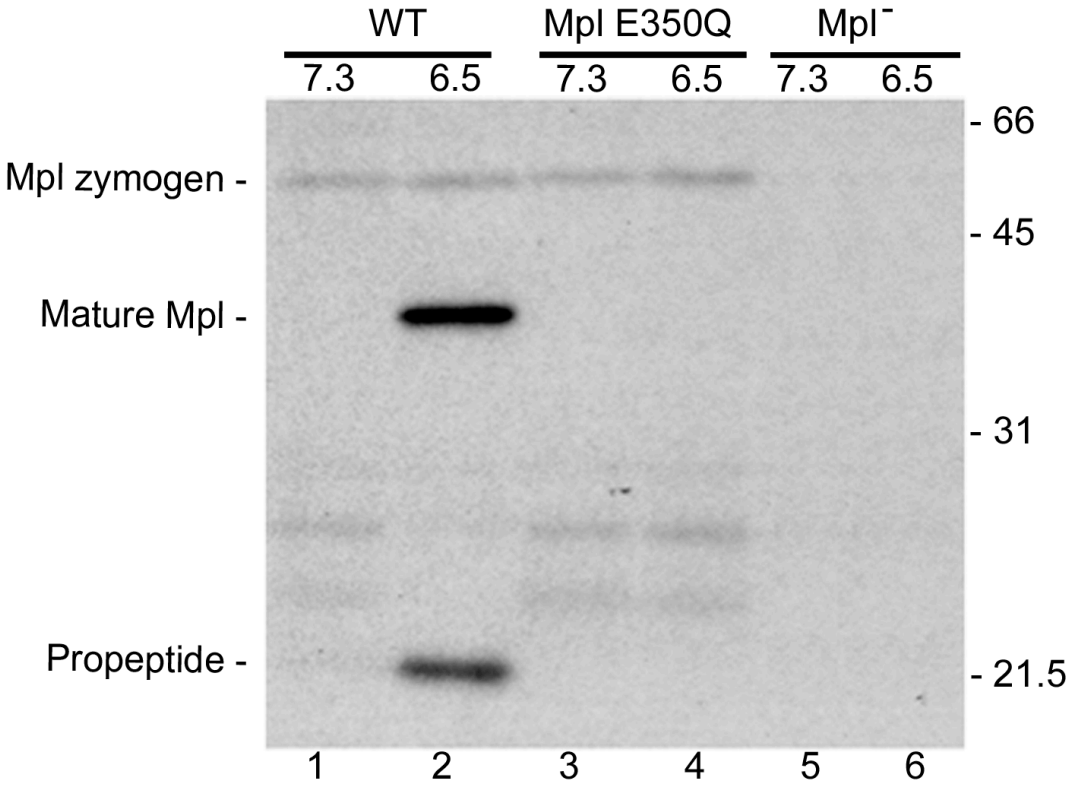

Figure 3.1. The propeptide and mature form of Mpl are secreted in the host cell cytosol upon a decrease in pH. J774 cells were infected with 10403S expressing wild-type (WT) Mpl, or isogenic mutants expressing Mpl E350Q or no Mpl (Mpl$^-$). Cells were pulse-labeled with [^{35}S]-met/cys, and chased in a nigericin-containing potassium buffer equilibrated to pH 7.3 or pH 6.5 (indicated above each lane). Secreted Mpl was immunoprecipitated from cleared host cell lysates. Numbers on right indicate molecular mass markers in kDa. Lanes: 1 and 2, 10403S; 3 and 4, HEL-583; Lanes 5 and 6, DP-L2343.

pH (Figure 3.1, lane 2). Cells were also infected with a *L. monocytogenes* strain expressing Mpl E350Q, an Mpl catalytic mutant that is unable to undergo autocatalysis (3). Mpl E350Q behaved like wild-type Mpl at physiological pH, but not at acidic pH, as no increase in protein secretion was observed at pH 6.5 (Figure 3.1, lanes 3 and 4). Lastly, the absence of protein bands in the immunoprecipitates from cells infected with an Mpl-minus strain confirmed that the antibody is specific to Mpl. Results from this experiment suggest that autocatalysis and an acidic pH are prerequisites for the efficient secretion of Mpl across the bacterial cell wall.

pH controls Mpl autocatalysis and compartmentalization during intracellular infection. Next, we aimed to determine what species of Mpl is bacterium-associated during intracellular infection. If autocatalysis and secretion of Mpl across the bacterial cell wall are pH-regulated, we would expect to detect only the Mpl zymogen and not the mature form bacterium-associated. However, if only secretion but not autocatalysis of Mpl is pH-regulated, we would expect to detect both the zymogen and mature forms of Mpl bacterium-associated. Immunoprecipitation of Mpl from bacterial lysates was not successful. Perhaps Mpl was degraded by proteases released from lyzed bacteria during processing of the bacterial pellet. Therefore, we devised a new approach to detect bacterium-associated Mpl. To differentiate the Mpl zymogen from mature Mpl, we made an Mpl construct that contains a Flag tag at the Mpl cleavage site (Mpl-$Flag_{N\text{-}cat}$) (Figure 3.2A), such that upon autocatalysis and removal of the propeptide, the Flag tag would be at the N-terminus of the catalytic domain. Mpl autocatalysis can then be monitored using two commercially available monoclonal antibodies, anti-Flag M1 and anti-Flag M2. M1 recognizes only a Flag tag at the free N-terminus of a tagged protein, while M2 recognizes an accessible Flag tag anywhere on the protein.

Figure 3.2. Anti-Flag antibodies allow for the differentiation of Mpl species. (A) Schematics of Mpl-Flag constructs used in this study and predicted patterns of reactivity with two different antibodies. Anti-Flag M1 recognizes a N-terminal Flag, while anti-Flag M2 recognizes any surface accessible Flag. **(B)** Detection of Mpl from culture supernatants. Strains were grown in LB-MOPS-Glc and the equivalent of 1.0 ml of OD_{600} = 1 supernatant was resolved by SDS-PAGE. Mpl and Mpl-Flag constructs were detected with either anti-Mpl, anti-Flag M1 or anti-Flag M2 antibodies. Numbers on right indicate molecular mass markers (in kDa). Positions of the Mpl zymogen, mature Mpl and propeptide are indicated on left. Lanes: 1,6 and 9, NF-L943; 2, HEL-587; 3,7 and 10, HEL-981; 4, 8 and 11, HEL-1084; 5, HEL-469.

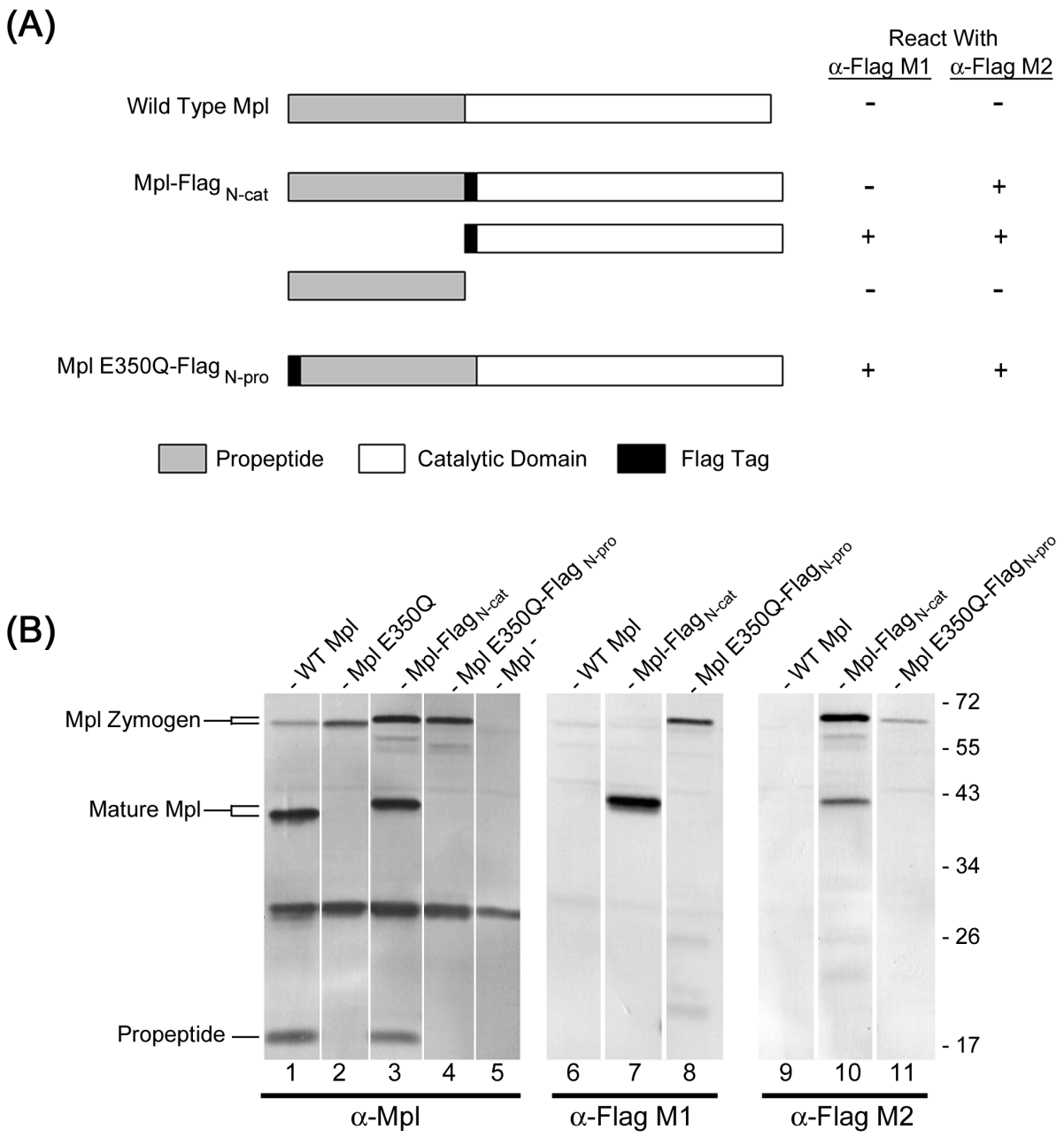
(A)
React With
α-Flag M1
α-Flag M2
Wild Type Mpl
Mpl-Flag N-cat
Mpl E350Q-Flag N-pro
Propeptide
Catalytic Domain
Flag Tag
(B)
- WT Mpl
- Mpl E350Q
- Mpl-Flag N-cat
- Mpl E350Q-Flag N-pro
- Mpl -
Mpl Zymogen
Mature Mpl
Propeptide
- 72
- 55
- 43
- 34
- 26
- 17
1 2 3 4 5 6 7 8 9 10 11
α-Mpl
α-Flag M1
α-Flag M2

Therefore, the M2 antibody should react with Mpl-Flag$_{N\text{-}cat}$ zymogen and mature form, whereas the M1 antibody should react exclusively with the mature form. The propeptide would not be detected by either antibody (Figure 3.2A). To confirm that the M1 and M2 antibodies were able to differentiate between the zymogen and mature form of Mpl-Flag$_{N\text{-}cat}$, supernatants from broth-grown *L. monocytogenes* strains expressing wild-type Mpl or Mpl-Flag$_{N\text{-}cat}$ were used for Western immunoblots with anti-Mpl serum, M1 or M2 antibodies. Three Mpl species were detected with the anti-Mpl serum: the zymogen, the mature form, and the propeptide. Neither M1 nor M2 antibodies were able to detect wild-type Mpl (Figure 3.2B, lanes 6 and 9), as it does not contain a Flag tag. However, M2 recognized the zymogen and the mature form of Mpl-Flag$_{N\text{-}cat}$, whereas M1 recognized the mature form only (Figure 3.2B, lanes 7 and 10).

Fluorescence microscopy was performed to determine which Mpl species is bacterium-associated during intracellular infection. Human HeLa cells were used for these experiments because mouse monoclonal antibodies bind to the immunoglobulin Fc receptor on mouse J774 cells, independent of the specificity of the antibody. Therefore, HeLa cells were infected with strains expressing wild-type Mpl or Mpl-Flag$_{N\text{-}cat}$. Four hours post-infection, infected cells were perfused for 5 minutes with a potassium buffer containing nigericin equilibrated to either pH 7.3 or pH 6.5. The cells were fixed, and stained for the detection of Mpl-Flag with M1 or M2. Bacteria and host cell nuclei were detected using bis-benzimide. Untagged wild-type Mpl was not detected bacterium-associated in infected cells (Figure 3.3, a-h).

Figure 3.3. The Mpl zymogen is bacterium-associated at physiological pH. Bacterium-associated Mpl was detected by fluorescence microscopy. Prior to fixing, infected HeLa cells were incubated in a nigericin-containing potassium buffer equilibrated to either pH 7.3 or pH 6.5. Host cell nuclei and bacteria were then stained with bis-benzimide (Hoechst 33258). Mpl-Flag was detected with anti-Flag M1 or anti-Flag M2 antibody followed by a FITC-conjugated secondary antibody. (a – h) NF-L943; (i – p) HEL-981; (q – x) HEL-1084.

Wild Type Mpl

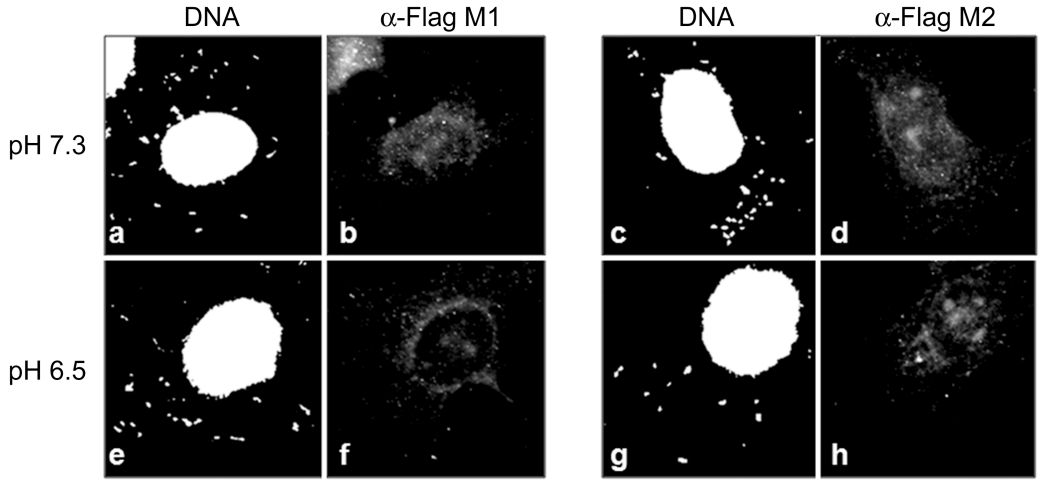

Mpl-Flag $_{N\text{-}cat}$

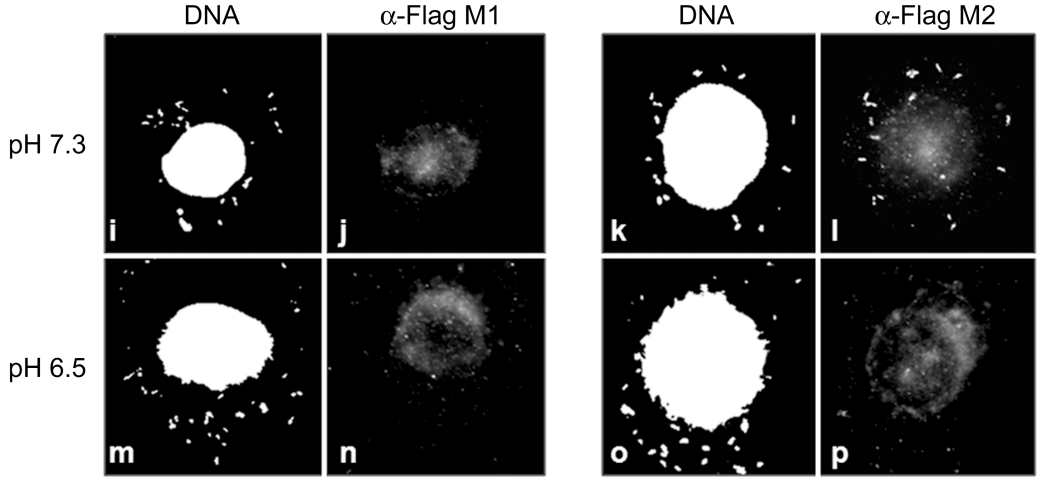

Mpl E350Q-Flag $_{N\text{-}pro}$

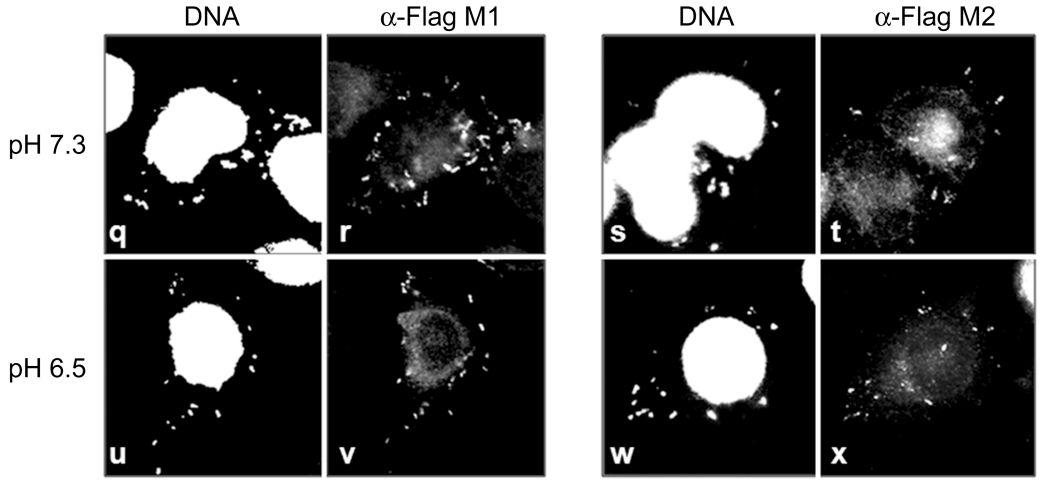

Mpl-Flag$_{N\text{-}cat}$ was detected by M2 (Figure 3, k and l), but not by M1 at pH 7.3 (Figure 3.3, i and j), suggesting that only the Mpl zymogen is bacterium-associated at pH 7.3. Upon a decrease in pH, Mpl-Flag$_{N\text{-}cat}$ was not detected by immunofluorescence (Figure 3.3, m-p). To ensure that M1 was capable of detecting bacterium-associated Mpl-Flag by fluorescence microscopy, we added a Flag tag to the N-terminus of the propeptide of Mpl E350Q (Mpl E350Q-Flag$_{N\text{-}pro}$) (Figure 3.2A). The program PrediSi (http://www.predisi.de/) (12) was used to make sure that addition of the Flag tag would not affect recognition and cleavage of the Mpl signal sequence. Supernatants from broth-grown *L. monocytogenes* expressing Mpl E350Q or Mpl E350Q-Flag$_{N\text{-}pro}$ were used to perform Western immunoblots. As expected for these catalytic mutants, the zymogen was the only Mpl species detected with the anti-Mpl serum (Figure 3.2B, lanes 2 and 4). Mpl E350Q-Flag$_{N\text{-}pro}$ was detected by the M1 antibody and weakly by the M2 antibody (Figure 3.2B, lanes 8 and 11). Mpl E350Q-Flag$_{N\text{-}pro}$ was detected bacterium-associated by the M1 and M2 antibodies in infected HeLa cells treated with buffer at pH 7.3 or pH 6.5 (Figure 3.3, q-x).

These results, taken together with the immunoprecipitation results (Figure 3.1), suggest that during intracellular infection Mpl autocatalysis and compartmentalization are controlled by pH. At physiological pH, the Mpl zymogen is bacterium-associated. As the intracellular pH acidifies, Mpl undergoes autocatalysis and is secreted across the bacterial cell wall.

Secretion of Mpl across the bacterial cell wall is PC-PLC independent. Previously, it was shown that the secretion of PC-PLC across the bacterial cell wall is dependent on both a decrease in pH and Mpl (39). Similarly, results from this study suggest that a decrease in pH

leads to secretion of Mpl across the bacterial cell wall. Next, we questioned whether PC-PLC influences the compartmentalization of Mpl. To address this point, cells were infected with either wild-type or a PC-PLC-minus strain of *L. monocytogenes* and treated as described above with buffers at physiological or acidic pH before immunoprecipitating Mpl from host cell lysates. The mature form of Mpl and the Mpl propeptide were secreted in cells treated with an acidic pH buffer, but not in cells maintained at physiological pH, and this phenomenon was independent of the presence of PC-PLC (Figure 3.4). This result indicated that the secretion of Mpl across the cell wall is not dependent on PC-PLC.

Mpl activity on PC-PLC is controlled by pH. The results reported above suggest that Mpl autocatalysis is regulated by pH. Next, we wished to determine whether Mpl activity on PC-PLC, a non-self substrate, is pH-regulated as well. For this purpose, wild-type Mpl, Mpl E350Q and proPC-PLC were purified as described in the Materials and Methods. Mpl proteins containing a Flag tag at the C-terminus of the catalytic domain ($Flag_{C\text{-}cat}$) (3) were purified from the supernatant of *L. monocytogenes* broth cultures. Since pH-dependent secretion of Mpl is not absolute, there is a gradual accumulation of the zymogen in the culture supernatant. The mature form is generated and secreted as the broth begins to acidify in late exponential phase as a consequence of bacterial metabolism. The proform of PC-PLC was produced in *E. coli* and purified from bacterial lysates. Examination of the protein samples on Coomassie stained gels indicated that the PC-PLC sample was devoid of contaminants and degradation products, while the Mpl-$Flag_{C\text{-}cat}$ and Mpl E350Q-$Flag_{C\text{-}cat}$ samples contained some degradation products (Figure 3.5 A and B).

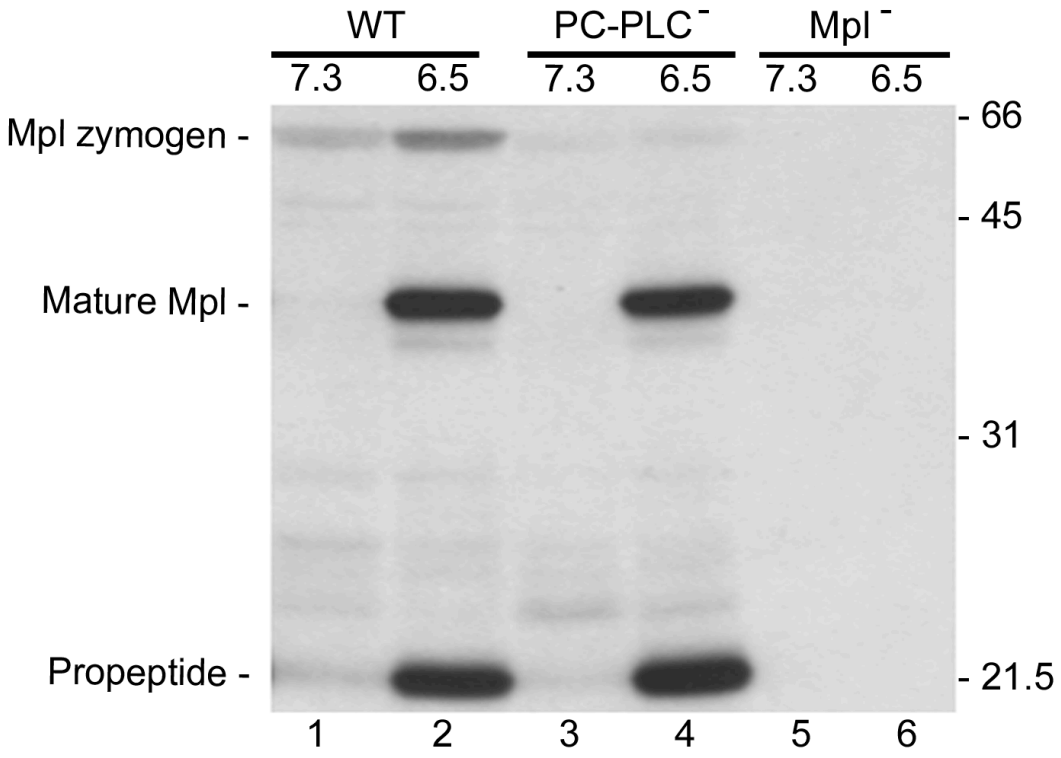

Figure 3.4. PC-PLC does not influence the secretion of mature Mpl. J774 cells were infected with 10403S expressing PC-PLC and Mpl (WT), or isogenic mutants with no PC-PLC (PC-PLC$^-$), or no Mpl (Mpl$^-$). Cells were pulse-labeled with [^{35}S]-met/cys, and chased in a nigericin-containing potassium buffer at pH 7.3 or pH 6.5 (indicated above each lane). Secreted Mpl was immunoprecipitated from cleared host cell lysates. Numbers on right indicate molecular mass markers in kDa. Lanes: 1 and 2, 10403S; 3 and 4, DP-L1935; Lanes 5 and 6, DP-L2343.

Figure 3.5. Mpl directly mediates the maturation of PC-PLC in a pH-dependent manner. (A) Stained protein gel of purified proPC-PLC fractions following size exclusion chromatography. **(B)** Stained protein gel of purified Mpl-Flag$_{C\text{-}cat}$ and Mpl E350Q-Flag$_{C\text{-}cat}$ following immunochromatography. The star (*) indicates GroEL which co-purified with Mpl-Flag$_{C\text{-}cat}$. **(C)** PC-PLC activation *in vitro* assay. Purified proPC-PLC and Mpl were mixed in a reaction buffer equilibrated to either pH 6.0, 6.5 or 7.3 (indicated above the lanes) and incubated at 37°C for 4 hours. Following incubation, the proteins were resolved by SDS-PAGE. PC-PLC activity was detected by the egg yolk soft agar overlay assay. A band of opacity in the agar indicates phospholipid hydrolysis (upper panel). Following the activity assay, the gel was stained with Coomassie Blue (lower panel). Numbers on right indicate molecular mass markers in kDa. Experiment in (A) was performed by Emily Slepkov. Experiment in (B) and (C) was performed by Alan Bitar.

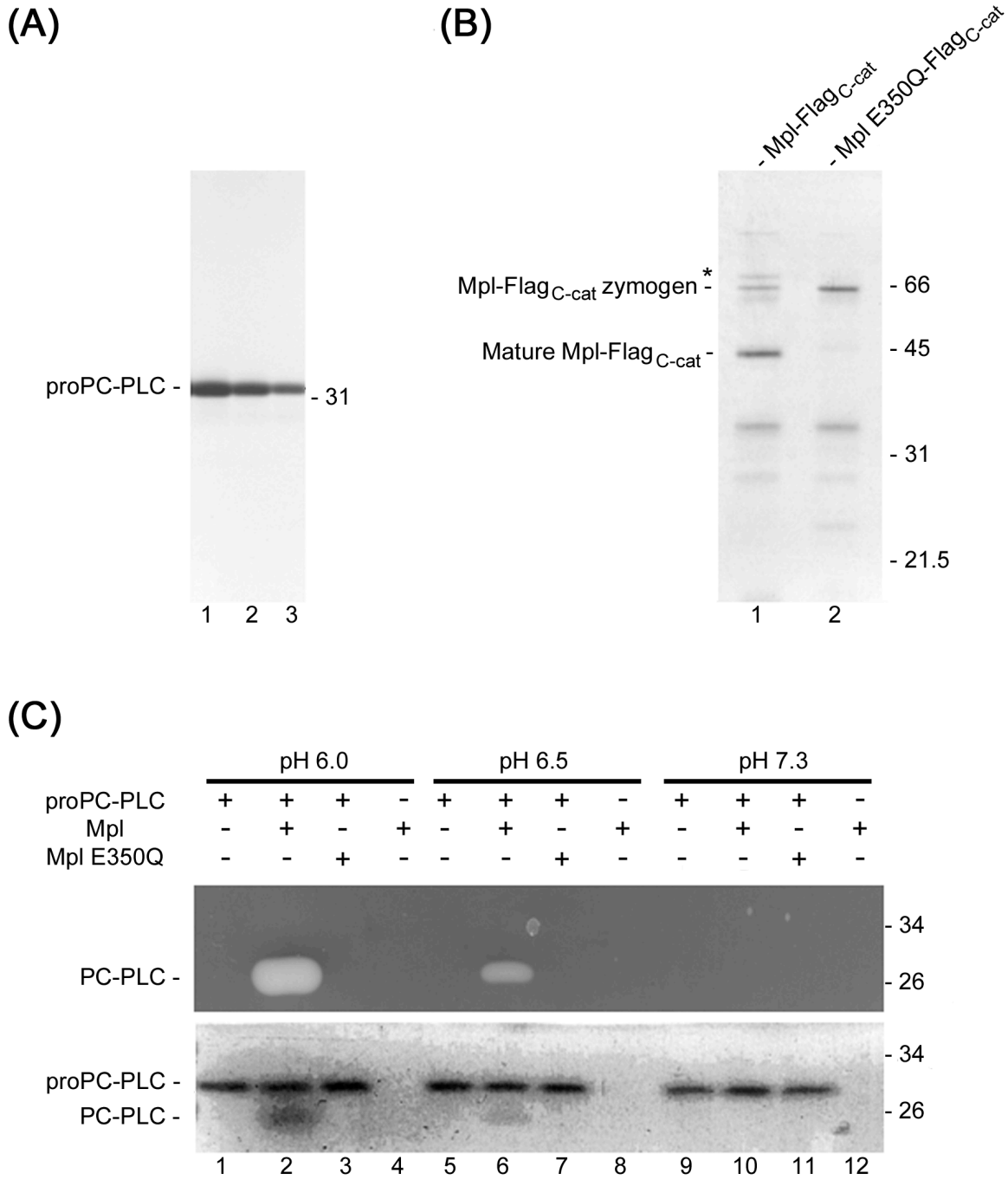
(A)
proPC-PLC -
- 31
1 2 3
(B)
- Mpl-Flag C-cat
- Mpl E350Q-Flag C-cat
Mpl-Flag C-cat zymogen *-
Mature Mpl-Flag C-cat -
- 66
- 45
- 31
- 21.5
1 2
(C)
pH 6.0
pH 6.5
pH 7.3
proPC-PLC + + + - + + + - + + + -
Mpl - + - + - + - + - + - +
Mpl E350Q - - + - - - + - - - + -
PC-PLC -
- 34
- 26
proPC-PLC -
PC-PLC -
- 34
- 26
1 2 3 4 5 6 7 8 9 10 11 12

There was a band greater than 66 kDa present in both Mpl purifications. In addition, the Mpl-Flag$_{C\text{-}cat}$ sample contained a band that was not present in the Mpl E350Q-Flag$_{C\text{-}cat}$ sample (Figure 3.5B, *). We identified this protein by matrix-assisted laser desorption/ionization-time of flight mass spectrometry to be the heat shock protein GroEL.

To determine whether Mpl can directly mediate the proteolytic maturation of PC-PLC, the purified Mpl-Flag$_{C\text{-}cat}$ preparation and proPC-PLC were incubated together for 4 hours at 37°C in a reaction buffer equilibrated to a final pH of 6.0, 6.5 or 7.3. The proteins were then resolved by SDS-PAGE and PC-PLC activity was detected by an egg yolk overlay assay. In this assay, PC-PLC activity is identified by the presence of a zone of opacity in the egg yolk overlay. PC-PLC activity was detected in samples containing purified Mpl-Flag$_{C\text{-}cat}$ and proPC-PLC incubated in buffers at pH 6.0 and pH 6.5, but not at pH 7.3 (Figure 3.5C, upper panel, lanes 2, 6 and 10). Controls included samples containing proPC-PLC (Figure 3.5C, lanes 1, 5, and 9), or Mpl-Flag$_{C\text{-}cat}$ (Figure 3.5C, lanes 4, 8, and 12), or proPC-PLC and Mpl E350Q-Flag$_{C\text{-}cat}$ (Figure 3.5C, lanes 3, 7, and 11). We did not use EDTA as a control to inhibit Mpl activity in this assay because PC-PLC is also a Zn^{2+}-dependent enzyme (9). None of the controls showed a zone of opacity. Once the enzymatic activity had developed in the overlay, the protein gel was recovered and stained with Coomassie Brilliant Blue R-250, which revealed the presence of proPC-PLC in the appropriate lanes (Figure 3.5C, lower panel, lanes 1-3, 5-7, and 9-11), and of mature PC-PLC exclusively in lanes where PC-PLC activity had been detected (Figure 3.5C, lower panel, lanes 2 and 6). These results show that Mpl directly mediates the proteolytic maturation of PC-PLC. Moreover, the activity of Mpl on a non-self substrate occurs at acidic pH, but not at physiological pH.

DISCUSSION

PC-PLC and Mpl are virulence factors of *L. monocytogenes* that accumulate as inactive proenzymes in the periplasm during growth in host cells (34). Upon cell-to-cell spread, bacteria in vacuoles experience a decrease in pH that triggers the rapid secretion of mature PC-PLC across the bacterial cell wall in an Mpl-dependent manner (21, 31). This mechanism of regulating PC-PLC activity is imperative to the virulence of *L. monocytogenes* as a propeptide-deletion mutant of PC-PLC is highly attenuated *in vivo* (38). In the present study, we tested the hypothesis that Mpl maturation is the pH-limiting step for PC-PLC maturation. Previously, we determined that Mpl maturation occurs by intramolecular autocatalysis (3). Herein, we observed that Mpl autocatalysis occurs upon a decrease in pH and correlates with the rapid secretion of mature Mpl and propeptide across the bacterial cell wall. Moreover, our data indicate that Mpl directly mediates the proteolytic maturation of PC-PLC and that this activity is also pH-regulated.

The Mpl zymogen remains mostly bacterium-associated at physiological pH while mature Mpl is found in host cells within minutes of a decrease in pH. This observation is in accordance with our previous result showing that when Mpl is synthesized in absence of its propeptide, it is secreted more efficiently across the bacterial cell wall (24). This phenomenon has also been observed for the serine protease subtilisin from *Bacillus subtilis*. Subtilisin precursor remains bacterium-associated while mature subtilisin is found in the supernatant (26). Our study provides further evidence that propeptides serve as a means of controlling the compartmentalization of bacterial proproteins, similarly to what has been observed for several eukaryotic proproteins (6, 10, 18).

There is evidence that following autocatalysis, the pro and catalytic domains of thermolysin-like metalloproteases remain associated as an autoprocessed complex that is void of enzymatic activity because the C-terminus of the propeptide remains in the active site. Degradation of the propeptide by its cognate catalytic domain is essential for full activation of the protease (8). We would argue that this mechanism of regulation does not apply to Mpl for two reasons. First, the propeptide of Mpl appears to be stable as it is detected in similar amounts as the mature form under conditions that lead to Mpl-mediated maturation of PC-PLC. Measuring the levels of detected Mpl from our immunoprecipitation assays revealed a ratio of 1:1.6 ± 0.4 (n= 17) for mature Mpl to propeptide, supporting our conclusion that the propeptide of Mpl is not degraded by its cognate catalytic domain. Second, mature Mpl-$Flag_{N\text{-}cat}$ was not detected bacterium-associated when using an antibody that specifically recognizes a free N-terminal Flag. Together, the results support a mechanism by which autocatalysis leads to full activation of Mpl.

Since Mpl autocatalysis is influenced by pH, we wished to determine if pH regulates Mpl activity on a non-self substrate. The obvious substrate would be PC-PLC. However, the evidence for the role of Mpl in mediating the maturation of PC-PLC is only circumstantial. To address whether Mpl directly activates PC-PLC, we performed an *in vitro* assay with purified proteins. The results indicated that Mpl directly mediates the proteolytic maturation of PC-PLC and, moreover, this activity is pH-regulated. Mature PC-PLC and PC-PLC activity were detected at pH 6.0, and to a lesser extent at pH 6.5, but not at pH 7.3 or when proPC-PLC was incubated alone or with the Mpl catalytic mutant. It is very unlikely that the heat shock protein GroEL, which contaminated the wild-type Mpl preparation, would have

affected the results, as GroEL is a chaperone with no known proteolytic activity. Therefore, our data indicate that Mpl directly mediates the proteolytic maturation of PC-PLC, and that Mpl activity on a non-self substrate is pH sensitive. Alternatively, pH may influence the conformation of mature Mpl and proPC-PLC enabling an interaction between these two proteins.

There are precedents to the observation that pH regulates the activity of a protease. For example, the serine protease furin undergoes autocatalysis once it reaches the acidic trans-Golgi network (1). The autocatalysis of furin is controlled by a histidine residue in its propeptide that acts as a pH sensor to acidic environments. Upon acidification, this histidine becomes protonated and disrupts a hydrophobic pocket allowing for autocatalysis (5). Members of the cathepsin family of cysteine proteases undergo autocatalysis in acidified lysosomes. Under acidic conditions, the propeptide of cathepsin L loses its tertiary conformation, resulting in a loss of affinity for the catalytic domain (15). Future studies will be focused on determining how pH influences the enzymatic activity of Mpl. Mpl activity may be controlled by amino acids acting as pH sensors. pH may also induce protein conformational changes in Mpl and/or in PC-PLC to allow Mpl and PC-PLC to interact.

In conclusion, our results indicate that pH regulates the enzymatic activity and compartmentalization of Mpl, and supports a model in which the proforms of PC-PLC and Mpl accumulate in the periplasm when the bacteria are in an environment at physiological pH, such as in the host cell cytosol. Upon cell-to-cell spread, bacteria become confined to double membrane vacuoles that acidify, leading to Mpl autocatalysis and proteolytic maturation of

PC-PLC by mature Mpl. The mature proteins are rapidly secreted across the bacterial cell wall into the vacuolar environment where PC-PLC can begin hydrolyzing vacuolar membrane phospholipids, contributing to lysis of the vacuole. As for Mpl, perhaps it targets additional substrates after accessing the vacuolar environment.

ACKNOWLEDGEMENTS

We thank Collin Parrish and Christopher Nelson for help with size exclusion purification of PC-PLC. This work was supported by Public Health Service grant A152154 from NIAID to H.M.

REFERENCES

1. **Anderson, E. D., S. S. Molloy, F. Jean, H. Fei, S. Shimamura, and G. Thomas.** 2002. The ordered and compartment-specfic autoproteolytic removal of the furin intramolecular chaperone is required for enzyme activation. J. Biol. Chem. **277:**12879-90.

2. **Bishop, D. K., and D. J. Hinrichs.** 1987. Adoptive transfer of immunity to *Listeria monocytogenes*. The influence of *in vitro* stimulation on lymphocyte subset requirements. J. Immunol. **139:**2005-2009.

3. **Bitar, A. P., M. Cao, and H. Marquis.** 2008. The metalloprotease of *Listeria monocytogenes* is activated by intramolecular autocatalysis. J. Bacteriol. **190:**107-11.

4. **Camilli, A., L. G. Tilney, and D. A. Portnoy.** 1993. Dual roles of *plcA* in *Listeria monocytogenes* pathogenesis. Mol. Microbiol. **8:**143-57.

5. **Feliciangeli, S. F., L. Thomas, G. K. Scott, E. Subbian, C. H. Hung, S. S. Molloy, F. Jean, U. Shinde, and G. Thomas.** 2006. Identification of a pH sensor in the furin propeptide that regulates enzyme activation. J. Biol. Chem. **281:**16108-16.

6. **Fortenberry, S. C., and J. M. Chirgwin.** 1995. The propeptide is nonessential for the expression of human cathepsin D. J. Biol. Chem. **270:**9778-9782.

7. **Gaillard, J. L., P. Berche, J. Mounier, S. Richard, and P. Sansonetti.** 1987. *In vitro* model of penetration and intracellular growth of *Listeria monocytogenes* in the human enterocyte-like cell line Caco-2. Infect. Immun. **55:**2822-2829.

8. **Gao, X., J. Wang, D. Q. Yu, F. Bian, B. B. Xie, X. L. Chen, B. C. Zhou, L. H. Lai, Z. X. Wang, J. W. Wu, and Y. Z. Zhang.** 2010. Structural basis for the autoprocessing of zinc metalloproteases in the thermolysin family. Proc. Natl. Acad. Sci. USA **107:**17569-74.

9. **Geoffroy, C., J. Raveneau, J. L. Beretti, A. Lecroisey, J. A. Vazquez-Boland, J. E. Alouf, and P. Berche.** 1991. Purification and characterization of an extracellular 29-

kilodalton phospholipase C from *Listeria monocytogenes*. Infect. Immun. **59:**2382-2388.

10. **Hansson, M., I. Olsson, and W. M. Nauseef.** 2006. Biosynthesis, processing, and sorting of human myeloperoxidase. Arch. Biochem. Biophys. **445:**214-224.

11. **Hase, C. C., and R. A. Finkelstein.** 1993. Bacterial extracellular zinc-containing metalloproteases. Microbiol. Rev. **57:**823-37.

12. **Hiller, K., A. Grote, M. Scheer, R. Munch, and D. Jahn.** 2004. PrediSi: prediction of signal peptides and their cleavage positions. Nucleic Acids Res. **32:**W375-9.

13. **Ho, S. N., H. D. Hunt, R. M. Horton, J. K. Pullen, and L. R. Pease.** 1989. Site-directed mutagenesis by overlap extension using the polymerase chain reaction. Gene **77:**51-59.

14. **Illades-Aguiar, B., and P. Setlow.** 1994. Autoprocessing of the protease that degrades small, acid-soluble proteins of spores of *Bacillus* species is triggered by low pH, dehydration, and dipicolinic acid. J. Bacteriol. **176:**7032-7.

15. **Jerala, R., E. Zerovnik, J. Kidric, and V. Turk.** 1998. pH-induced conformational transitions of the propeptide of human cathepsin L. A role for a molten globule state in zymogen activation. J. Biol. Chem. **273:**11498-504.

16. **Jones, S., and D. A. Portnoy.** 1994. Characterization of *Listeria monocytogenes* pathogenesis in a strain expressing perfringolysin O in place of listeriolysin O. Infect. Immun. **62:**5608-5613.

17. **Kim, H., H. Marquis, and K. J. Boor.** 2005. SigmaB contributes to *Listeria monocytogenes* invasion by controlling expression of *inlA* and *inlB*. Microbiology **151:**3215-22.

18. **Koo, B. H., J. M. Longpre, R. P. Somerville, J. P. Alexander, R. Leduc, and S. S. Apte.** 2007. Regulation of ADAMTS9 secretion and enzymatic activity by its propeptide. J. Biol. Chem. **282:**16146-16154.

19. **Loessner, M. J., A. Schneider, and S. Scherer.** 1996. Modified *Listeria* bacteriophage lysin genes (*ply*) allow efficient overexpression and one-step purification of biochemically active fusion proteins. Appl. Environ. Microbiol. **62:**3057-60.

20. **Marquis, H., H. Goldfine, and D. A. Portnoy.** 1997. Proteolytic pathways of activation and degradation of a bacterial phospholipase C during intracellular infection by *Listeria monocytogenes*. J. Cell Biol. **137:**1381-92.

21. **Marquis, H., and E. J. Hager.** 2000. pH-regulated activation and release of a bacteria-associated phospholipase C during intracellular infection by *Listeria monocytogenes*. Mol. Microbiol. **35:**289-98.

22. **Mengaud, J., C. Geoffroy, and P. Cossart.** 1991. Identification of a new operon involved in *Listeria monocytogenes* virulence: its first gene encodes a protein homologous to bacterial metalloproteases. Infect. Immun. **59:**1043-1049.

23. **Navarro, M. V., N. De, N. Bae, Q. Wang, and H. Sondermann.** 2009. Structural analysis of the GGDEF-EAL domain-containing c-di-GMP receptor FimX. Structure **17:**1104-16.

24. **O'Neil, H. S., B. M. Forster, K. L. Roberts, A. J. Chambers, A. P. Bitar, and H. Marquis.** 2009. The propeptide of the metalloprotease of *Listeria monocytogenes* controls compartmentalization of the zymogen during intracellular infection. J. Bacteriol. **191:**3594-603.

25. **Portnoy, D. A., P. S. Jacks, and D. J. Hinrichs.** 1988. Role of hemolysin for the intracellular growth of *Listeria monocytogenes*. J. Exp. Med. **167:**1459-71.

26. **Power, S. D., R. M. Adams, and J. A. Wells.** 1986. Secretion and autoproteolytic maturation of subtilisin. Proc. Natl. Acad. Sci. USA **83:**3096-100.

27. **Prochazkova, K., and K. J. Satchell.** 2008. Structure-function analysis of inositol hexakisphosphate-induced autoprocessing of the *Vibrio cholerae* multifunctional autoprocessing RTX toxin. J Biol Chem **283:**23656-64.

28. **Ra, H. J., and W. C. Parks.** 2007. Control of matrix metalloproteinase catalytic activity. Matrix Biol. **26:**587-96.

29. **Shetron-Rama, L. M., H. Marquis, H. G. Bouwer, and N. E. Freitag.** 2002. Intracellular induction of *Listeria monocytogenes actA* expression. Infect. Immun. **70:**1087-96.

30. **Shetron-Rama, L. M., K. Mueller, J. M. Bravo, H. G. Bouwer, S. S. Way, and N. E. Freitag.** 2003. Isolation of *Listeria monocytogenes* mutants with high-level *in vitro* expression of host cytosol-induced gene products. Mol. Microbiol. **48:**1537-1551.

31. **Slepkov, E. R., A. Pavinski Bitar, and H. Marquis.** 2010. Differentiation of propeptide residues regulating the compartmentalization, maturation and activity of the broad-range phospholipase C of *Listeria monocytogenes*. Biochem. J. **432:**557-63.

32. **Smith, G. A., H. Marquis, S. Jones, N. C. Johnston, D. A. Portnoy, and H. Goldfine.** 1995. The two distinct phospholipases C of *Listeria monocytogenes* have overlapping roles in escape from a vacuole and cell-to-cell spread. Infect. Immun. **63:**4231-7.

33. **Smith, K., and P. Youngman.** 1992. Use of a new integrational vector to investigate compartment-specific expression of the *Bacillus subtilis spoIIM* gene. Biochimie **74:**705-711.

34. **Snyder, A., and H. Marquis.** 2003. Restricted translocation across the cell wall regulates secretion of the broad-range phospholipase C of *Listeria monocytogenes*. J. Bacteriol. **185:**5953-8.

35. **Tilney, L. G., and D. A. Portnoy.** 1989. Actin filaments and the growth, movement, and spread of the intracellular bacterial parasite, *Listeria monocytogenes*. J. Cell Biol. **109:**1597-608.

36. **Van Wart, H. E., and H. Birkedal-Hansen.** 1990. The cysteine switch: a principle of regulation of metalloproteinase activity with potential applicability to the entire matrix metalloproteinase gene family. Proc. Natl. Acad. Sci. USA **87:**5578-82.

37. **Vazquez-Boland, J. A., M. Kuhn, P. Berche, T. Chakraborty, G. Dominguez-Bernal, W. Goebel, B. Gonzalez-Zorn, J. Wehland, and J. Kreft.** 2001. *Listeria* pathogenesis and molecular virulence determinants. Clin. Microbiol. Rev. **14:**584-640.

38. **Yeung, P. S., Y. Na, A. J. Kreuder, and H. Marquis.** 2007. Compartmentalization of the broad-range phospholipase C activity to the spreading vacuole is critical for *Listeria monocytogenes* virulence. Infect. Immun. **75:**44-51.

39. **Yeung, P. S., N. Zagorski, and H. Marquis.** 2005. The metalloprotease of *Listeria monocytogenes* controls cell wall translocation of the broad-range phospholipase C. J. Bacteriol. **187:**2601-8.

CHAPTER 4

THE POST-TRANSLOCATION CHAPERONE PRSA2 REGULATES THE MATURATION AND SECRETION OF *LISTERIA MONOCYTOGENES* PROPROTEIN VIRULENCE FACTORS*

* Brian M. Forster, Jason Zemansky, Daniel A. Portnoy and Hélène Marquis. The post-translocation chaperone PrsA2 regulates the maturation and secretion of *Listeria monocytogenes* proprotein virulence factors. Currently in submission to Journal of Bacteriology.

ABSTRACT

PrsA2 is a conserved post-translocation chaperone and a peptidyl prolyl *cis-trans* isomerase that contributes to the virulence of the gram-positive intracellular pathogen *Listeria monocytogenes.* One of the phenotypes associated with a *prsA2* mutant is decreased activity of the broad-range phospholipase C (PC-PLC). PC-PLC is made as a proenzyme whose maturation is mediated by a metalloprotease (Mpl). The proforms of PC-PLC and Mpl accumulate in the periplasm until a decrease in pH triggers their maturation and rapid secretion into the host cell. In this study, we examined the mechanism by which PrsA2 regulates the activity of PC-PLC. We observed that in the absence of PrsA2, the proenzymes are secreted at physiological pH and do not mature upon a decrease in pH. The sensitivity of the *prsA2* mutant to cell wall hydrolases was modified. However, no apparent changes in cell wall porosity were detected. Interestingly, synthesis of PC-PLC in the absence of its propeptide lead to the secretion of a fully active enzyme in the cytosol of host cells independent of PrsA2, indicating that neither the propeptide of PC-PLC nor PrsA2 is required for native folding of the catalytic domain, although both influence secretion of the enzyme. Taken together, these results suggest that PrsA2 regulates compartmentalization of Mpl and PC-PLC by influencing cell wall properties and perhaps by interacting with the PC-PLC propeptide. Moreover, the ability of these proproteins to respond to a decrease in pH during intracellular growth depends on their localization in the periplasm.

INTRODUCTION

Bacterial proteins that are secreted through the cell envelope rely on various folding factors. These folding factors, located outside the cell membrane, include disulfide bond oxidoreductases, peptidyl prolyl *cis-trans* isomerases (PPIases) and chaperones (10). In general, chaperones assist proteins folding into their native conformations by inhibiting improper protein-protein interactions and altering the activation energy necessary for proper folding (11). PPIases serve as chaperones in addition to their isomerase activity and contribute to cell envelope integrity (10). PrsA, a parvulin-type PPIase of the gram-positive bacterium *Bacillus subtilis*, contributes to the folding of penicillin binding proteins (PBPs) (17). PBPs catalyze the crosslinking of glycan chains with short peptides forming peptidoglycan, and transglycosylase reactions during cell wall biosynthesis (14). Peptidoglycan of the *B. subtilis prsA* mutant shows a crosslinking defect, causing changes in cell morphology and a decrease in viability (42). PrsA2, a PrsA ortholog from the Gram-positive pathogen *Listeria monocytogenes,* is not essential for viability during extracellular growth, but the mutant leaks cytoplasmic proteins, suggesting that it is important for cell envelope homeostasis (1, 3, 45).

L. monocytogenes is a facultative intracellular pathogen and the causative agent of the food-borne disease listeriosis (41). Following entry into a host cell, membrane-bound bacteria rapidly escape vacuoles to access the host cytosol where they multiply (40). *L. monocytogenes* uses an actin-based mechanism of motility to spread from cell-to-cell without exiting to the extracellular milieu. During cell-to-cell spread, bacteria become entrapped in double membrane vacuoles from which they must escape to perpetuate their intracellular

growth cycle. Escape from vacuoles is mediated by a pore-forming hemolysin called listeriolysin O (LLO) (13) and two phosopholipases of type C (9, 36). PrsA2 contributes to LLO folding and activity, and to the activity of the broad-range phospholipase C (2, 45). Accordingly, the intracellular growth and cell-to-cell spread of *L. monocytogenes* are affected in the absence of PrsA2. In addition, *L. monocytogenes* is highly attenuated *in vivo* in absence of PrsA2. Interestingly, the PPIase activity of PrsA2 is not required for PC-PLC activity, but it is needed for optimal LLO activity and virulence (3).

PC-PLC and the metalloprotease of *L. monocytogenes* (Mpl) are synthesized as proenzymes, containing N-terminal propeptides. During intracytosolic growth, bacteria accumulate these two proteins in the periplasmic space between the cell membrane and cell wall (26, 29, 38). Upon cell-to-cell spread, bacteria in vacuoles experience a decrease in pH, which initiates Mpl intramolecular autocatalysis, leading to PC-PLC maturation ((6), chapter 3 results). Concomitant to maturation, both proteins are rapidly secreted across the bacterial cell wall. The secretion of PC-PLC in response to pH is dependent on Mpl, but the secretion of Mpl is not dependent on PC-PLC ((44), chapter 3 results).

In this study, we investigated the mechanism by which PrsA2 affects the activity of PC-PLC. Our results indicated that PrsA2 is required to maintain the proforms of Mpl and PC-PLC bacterium-associated during infection, possibly due to its influence on cell wall composition. Interestingly, the secreted proenzymes did not undergo maturation upon a decrease in intracellular pH, indicating that Mpl autocatalysis is spatially controlled in addition to being controlled by pH. Also, phospholipase activity was independent of PrsA2 when PC-PLC was

produced in the absence of its propeptide. Therefore, it appears that the PC-PLC maturation defect observed in the absence of PrsA2 results from the premature secretion of the Mpl zymogen possibly due to changes in the biochemical properties of the cell wall, and the inability of the zymogen to undergo autocatalysis post-secretion.

MATERIALS AND METHODS

Bacterial Strains. All *L. monocytogenes* strains used in this study are listed in Table 4.1. *L. monocytogenes* strains were grown in brain heart infusion (BHI) media or Luria-Bertani (LB) broth supplemented with 50 mM morpholinepropanesulfonic acid (MOPS) adjusted to pH 7.3, 0.2% (w/v) activated charcoal and 25 mM glucose 1-phosphate (LB-MOPS-G1P). *E. coli* with pKSV7-derived plasmids were cultured in LB supplemented with ampicillin (100 μg/ml). *E. coli* containing pPL2-derived plasmids were cultured in LB supplemented with chloramphenicol (25 μg/ml). *L. monocytogenes* strains harboring pPL2-derived or pKSV7-derived plasmids were cultured in BHI supplemented with chloramphenicol (10 μg/ml).

Transduction of *prsA2*::*Himar1*. Transductions were performed as described previously (16, 45). Briefly, U153 phage grown on donor strain 10403S *prsA2::Himar1* (DP-L5596) was used to infect recipient *Listeria* strains (Table 4.1). Transductants were selected at 37°C on semi-solid medium supplemented with lincomycin (25 μg/ml) and erythromycin (2 μg/ml).

Construction of *prsA2* promoter-*gus* fusion plasmid. SOEing PCR was used to fuse the promoter of *prsA2* to *gus* (gene encoding β-glucuronidase, Gus).

Table 4.1. ***L. monocytogenes*** **strains and plasmids used in this study**

	Genotype & Relevant Features	Source/Ref
Strains		
10403S	Wild-type (serotype 1/2a)	(5)
NF-L943	*prfA* G155S in 10403S background (overexpresses PrfA-dependent genes)	(34)
DP-L1075	10403S *prfA*::Tn*917*-LTV3	(12)
DP-L1935	Internal inframe deletion of *plcB* in 10403S background	(36)
DP-L2296	Internal inframe deletion of *mpl* in 10403S background	(25)
DP-L2343	Deletion of *mpl* structural gene in 10403S background	(33)
DP-L5596	10403S *prsA2::Himar1*	(45)
DP-L5601	Internal inframe deletion of $prsA2_{(29\text{-}291)}$ in 10403S background (Δ*prsA2*)	(45)
DP-L5603	DP-L5601 + pJZ065 integrated at $tRNA^{Arg}$ site	(45)
DP-L5749	10403S + pBHE573	(32)
DP-L5750	10403S expressing PSA bacteriophage holin/lysin + pBHE573	(32)
DP-L5751	DP-L5601 + pBHE573	This study
DP-L5755	10403S + pJZ095 integrated at $tRNA^{Arg}$ site	This study
EJ-L12	10403S Δ*inlA*	(4)
HEL-335	10403S *plcB*Δpro	(44)
HEL-981	NF-L943 *mpl*-Flag $_{N\text{-}cat}$	Chapter 3
HEL-1216	DP-L2296 *prsA2::Himar1*	This study
HEL-1230	NF-L943 *mpl*-Flag $_{N\text{-}cat}$, *prsA2::Himar1*	This study
HEL-1232	NF-L943 *mpl*-Flag $_{N\text{-}cat}$, *prsA2::Himar1* + pJZ065 integrated at $tRNA^{Arg}$ site	This study
HEL-1405	HEL-335 *prsA2::Himar1*	This study
NF-L1166	10403S *actA-gus-neo-plcB, prfA* L140F	(28)
Plasmids		
pBHE573	Firefly lucifersase with cytomegalovirus promoter	(32)
pKSV7	Shuttle vector for allelic exchange	(37)
pJZ065	116-bp upstream, *prsA2* open reading frame without *prfA* box (PrsA2 #2) cloned into pPL2	(45)
pJZ095	*prsA2* promoter-*gus* cloned into pPL2 ($P_{(PrsA2)}$-*gus*)	This study
pPL2	Site-specific shuttle integration vector	(21)

The promoter of *prsA2* and the *gus* structural gene were amplified by PCR using primer pairs JZ-241 (45) / BK-011 and BK-012 / BK-013, respectively, and NF-L1166 (kindly provided by Nancy Freitag) genomic DNA as the template (Tables 4.1 and 4.2). The respective 307-bp and 1851-bp PCR products were used in a SOEing PCR with primers JZ-241 and BK-013. The 2108-bp product was digested with EagI and SalI, and ligated into the shuttle integration vector pPL2, thus generating pJZ095 (Table 4.1).

Conjugation experiments. All pPL2-derived plasmids (Table 4.1) were introduced into *Listeria* by conjugation as described previously (30). Chloramphenicol-resistant conjugants were screened for plasmid integration at the *attB* site of the $tRNA^{Arg}$ gene by PCR using primers NC16 and PL95 (21).

Metabolic labeling and immunoprecipitation assays. The specific detection of metabolically labeled PC-PLC or Mpl synthesized by intracellular bacteria was performed as described previously (29, 35, 38). Secreted PC-PLC and Mpl were immunoprecipitated from cleared host cell lysates, whereas bacterium-associated PC-PLC was immunoprecipitated from the lysate of intracellular bacteria. For pulse-chase experiments, radiolabeled infected cells were chased in tissue culture media containing unlabeled methionine (5 mM), cysteine (1 mM) and chloramphenicol (20 μg/ml) for the times indicated in the text. To detect PC-PLC or Mpl as a function of pH, radiolabeled infected cells were chased in a potassium-based buffer adjusted to either pH 7.3 or pH 6.5 and supplemented with nigericin (10 μM). Immunoprecipitates were resolved by SDS-PAGE and detected by autoradiography or phosphorimaging.

Table 4.2. DNA oligonucleotide primers used in this study

Name	Sequence (5' – 3')[a]	Site
BK-011	GTTTCTACAGGACGGACCATTAAATAAAACACAC TCCTTAGTTGTTGGAA	
BK-012	TTCCAACAACTAAGGAGTGTGTTTTATTTAATGGTC CGTCCTGTAGAAAC	
BK-013	TTTGTCGACTCATTGTTTGCCTCCCTGCTG	SalI

[a] Restriction site underlined

To determine the half-life of PC-PLC, the intensities of protein bands detected by phosphorimaging from pulse-chase experiments were quantified using ImageJ (rsbweb.nih.gov/ij/). A regression curve was generated and was used to calculate half-life.

Immunofluorescent staining of Mpl. Bacterium-associated Mpl-Flag$_{N\text{-}cat}$ was detected by immunofluorescence, as described previously with modification (29). Briefly, HeLa cells infected with *L. monocytogenes* were fixed, and then treated with purified *L. monocytogenes*-specific phage endolysin Ply118. To detect bacterium-associated Mpl-Flag, mouse monoclonal anti-Flag M2 (Sigma) was used followed by a donkey anti-mouse antibody conjugated to FITC. Bis-benzimide (Hoechst 33258) was used to detect *Listeria*.

Expression of *prsA2*. Levels of *prsA2* expression were measured using a quantitative Gus assay as described previously (34). *L. monocytogenes* strains containing pJZ095 were grown in BHI for 8 hours. At each hour, optical density measurements (OD_{600}) were taken and bacterial pellets were resuspended in 100 mM potassium phosphate, pH 7.0, 100 mM NaCl, 0.1% Triton X-100. Gus substrate (4-methylumbelliferyl-β-D-glucuronide , 4-MUGIcU), was added to lysates at a concentration of 0.4 mg/mL for one hour at room temperature. Fluorescence measurements were taken after adding 200mM sodium carbonate to each sample. Fluorescence measurements (λ_{excite} = 360nm, $\lambda_{emission}$ = 460nm) were made using a Horiba-FluoroMax-3 fluorometer and normalized to OD_{600} readings. Normalized fluorescence measurements were converted to concentrations of Gus using a standard curve of fluorescence intensity to concentrations of 4-methylumbelliferone.

Preparation of cell wall fractions. Bacterial cell wall fractions were isolated as described previously (38). Briefly, bacteria were grown in LB-MOPS-G1P to an OD_{600} of ~ 1.2. Bacterial cells were suspended in protoplast buffer supplemented with Ply118 to a calculated OD_{600} = 12. Protoplast formation was monitored by microscopy. The protoplasts were pelleted by centrifugation at 18k x *g* for 5 minutes at 4°C and the cell wall proteins were recovered in the supernatant. The proteins were precipitated using 5% trichloroacetic acid, resolved by SDS-PAGE and detected with Coomassie Brilliant Blue R-250. Purity of the cell wall fraction was verified by performing western immunoblots for InlA, a cell wall protein, and PrfA, a cytoplasmic protein as described previously (38).

Cell wall hydrolysis assays. Bacteria were grown in BHI at 37°C, 200 rpm to an OD_{600} of ~ 0.5, pelleted and suspended in 20mM Tris-HCl pH 8.0 to a calculated OD_{600} of 1.0. Chicken egg white lysozyme (Sigma) or Ply118 was added to a final concentration of 50 μg/mL. OD_{600} measurements were taken every minute for 30 minutes at 37°C using a BioTek PowerWave XS microplate spectrophotometer. Three experimental replicates were performed.

Bacteriolysis luciferase assay. The luciferase assay to test for bacterial lysis in infected cells was performed as described previously (32). Briefly, bone marrow-derived macrophages from IFNAR -/- mice were infected with *L. monocytogenes* strains expressing firefly luciferase under the control of a cytomegalovirus promoter (pBHE573, Table 4.1). Six hours post-infection, luciferase reagent (Sigma) was added to infected host cell lysates and luciferase activity was measured.

Detection of phospholipase activity. PC-PLC activity was detected on LB egg yolk agar plates, as described previously (44). Bacteria were spot inoculated onto plates and incubated for 48 hours at 37°C.

Plaquing Assay. Cell-to-cell spread efficiency of intracellular bacteria was measured using the plaquing assay, as described previously (39). The infected monolayers of mouse L2 fibroblast cells were stained with neutral red and plaque areas were calculated. Plaque area is reported as a percentage of wild-type plaque size. Three independent experiments were performed.

Statistical analysis. Cell wall hydrolysis assay results were analyzed using a two-tailed paired *t*-test to determine if the *prsA2* mutant was more sensitive to cell wall hydrolases compared to the wild-type strain. Plaque assay results were analyzed using a one-way analysis of variance (ANOVA) with a Tukey-Kramer multiple comparisons test to determine whether the plaque sizes between each of the strains tested were significantly different. A significance level (α) of 0.05 was set for both tests.

RESULTS

PC-PLC and Mpl are no longer found bacterium-associated in the absence of PrsA2. Previous studies have reported that PC-PLC secretion and activity are reduced in the absence of PrsA2 (2, 45). PC-PLC and Mpl are translocated across the bacterial membrane as inactive

proenzymes and accumulate in the periplasm (38). Upon a decrease in pH, which is normally experienced when bacteria are in vacuoles, Mpl undergoes autocatalysis and mediates the maturation of PC-PLC ((6), chapter 3 results). This maturation process is followed by the rapid secretion of these two enzymes across the bacterial cell wall ((26, 38), chapter 3 results). We questioned the role of PrsA2 in regulating the compartmentalization of PC-PLC and Mpl. Infected cells were pulse-labeled and bacterium-associated PC-PLC was immunoprecipitated from lysates of intracellular bacteria. The proform of PC-PLC was detected from the wild-type but not from the *prsA2*$^{-}$ bacterium-lysate (Figure 4.1A). Using an immunofluorescence assay, we observed Mpl bacterium-associated in cells infected with wild-type bacteria, but not in cells infected with the *prsA2* mutant (Figure 4.1B). Complementation of the mutant restored the wild-type phenotype for PC-PLC and Mpl. This result indicated that PrsA2 is necessary for the accumulation of PC-PLC and Mpl within bacteria, suggesting that these proteins are degraded rapidly post-translocation or secreted prematurely in the absence of PrsA2.

PC-PLC and Mpl are prematurely secreted from bacteria in the absence of PrsA2. The rate of protein secretion across the bacterial cell wall could be influenced by the biophysical and biochemical properties of the cell wall, protein structure, protein-protein interactions, and ionic interactions. Considering that PrsA2 is likely to act as a chaperone and therefore assisting in the folding of proteins post-translocation, we hypothesized that the absence of PrsA2 could influence the rate of PC-PLC and Mpl secretion. Therefore, we assessed whether PC-PLC and Mpl were secreted prematurely in the absence of PrsA2.

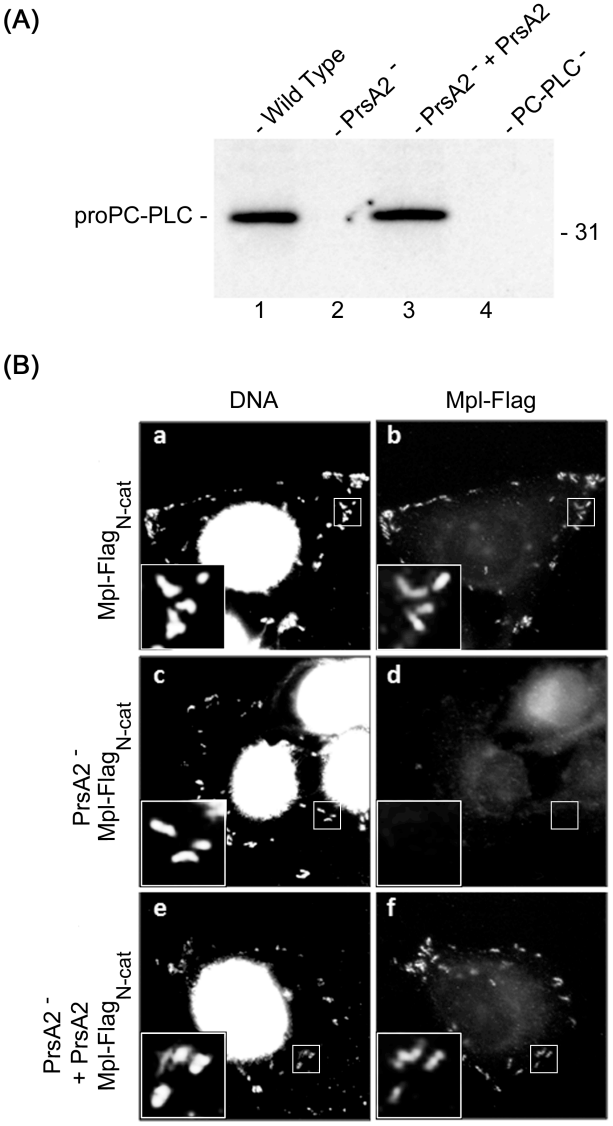

Figure 4.1. PC-PLC and Mpl are not bacterium-associated in the absence of PrsA2. (A) Bacterium-associated PC-PLC was immunoprecipitated from intracellular bacterial cell lysates. Lanes: 1, 10403S; 2, DP-L5601; 3, DP-L5603; 4, DP-L1935. Position of the 31 kDa protein standard is indicated on the right. **(B)** Infected HeLa cells were fixed and stained for fluorescence microscopy. Bis-Benzamide was used to detect host cell nuclei and bacterial chromosome, and anti-Flag M2 antibody was used to detect Mpl-Flag. (a-b) HEL-981, (c-d) HEL-1230, (e-f) HEL-1232.

Infected cells were pulse-labeled, then chased for 1, 2, or 5 minutes post-infection. PC-PLC was immunoprecipitated from the secreted bacterial fraction in lysates of infected cells and from lysates of intracellular bacteria. The results showed that the proform of PC-PLC was found exclusively in the secreted fraction of the *prsA2* mutant immediately after the pulse, but remained bacterium-associated for the entire time of the chase with the wild-type strain (Figure 4.2A). Mpl was also immunoprecipitated from the secreted bacterial fraction in lysates of infected cells. Similar to PC-PLC, Mpl zymogen was secreted rapidly from the *prsA2* mutant, but not from wild-type bacteria (Figure 4.2B). Although we were unable to isolate Mpl from intracellular bacterial lysates, these results indicated that wild-type bacteria maintain a pool of Mpl whereas the *prsA2* mutant does not (Figure 4.1B).

Mpl controls the secretion of PC-PLC across the cell wall. In the absence of Mpl, PC-PLC remains bacterium-associated upon a decrease in pH. The ability of Mpl to facilitate the secretion of PC-PLC is independent of its role in mediating the maturation of PC-PLC, suggesting that perhaps Mpl serves to transport PC-PLC across the cell wall (44). We therefore questioned if the secretion of PC-PLC from the *prsA2* mutant was dependent on Mpl. Infected cells were pulse labeled and PC-PLC was immunoprecipitated from bacteria that lacked either Mpl and/or PrsA2. As previously reported, PC-PLC remained bacterium-associated at physiological pH in the presence or absence of Mpl (Figure 4.3, lanes 1 and 5). However, in the absence of PrsA2, PC-PLC was secreted independently of Mpl (Figure 4.3, lanes 4 and 8). Together, these results indicated that, at physiological pH, PrsA2 is required (i) to prevent the premature secretion of PC-PLC and Mpl across the bacterial cell wall, and (ii) to enable Mpl to control PC-PLC secretion.

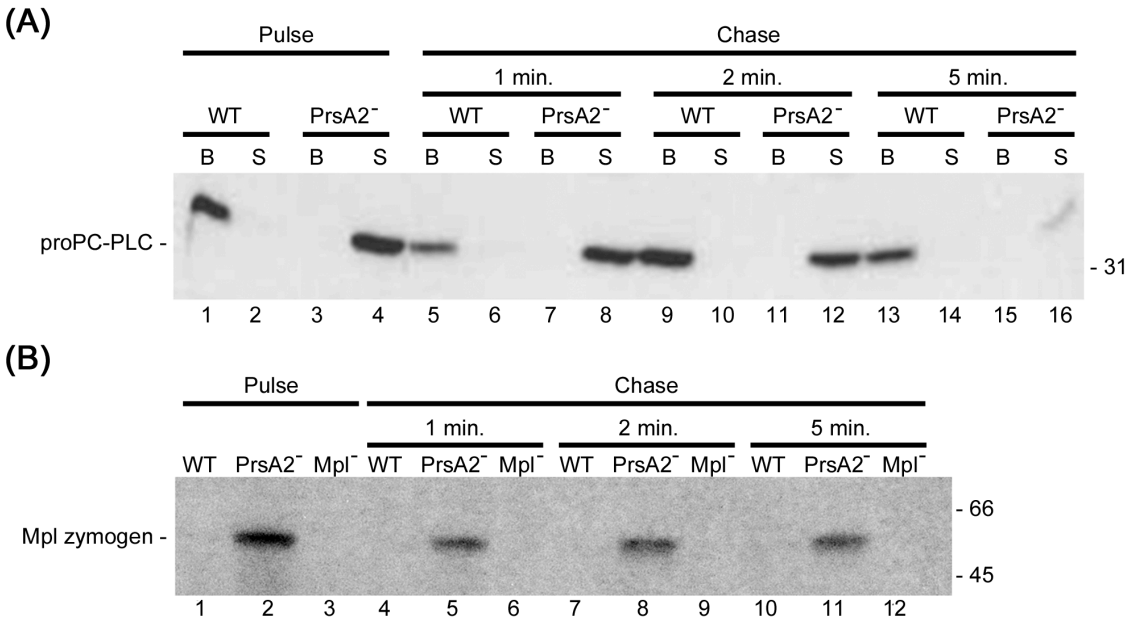

Figure 4.2. PC-PLC and Mpl are prematurely secreted into the host cytosol in the absence of PrsA2. Infected J774 cells were pulse labeled, and then chased with cold met/cys and chloramphenicol for either 1, 2 or 5 minutes as indicated in the figure. **(A)** Bacterium-associated (B) and secreted (S) PC-PLC were immunoprecipitated from bacteria and host cell lysates, respectively. Lanes: 1,2,5,6,9,10,13,14: 10403S; 3,4,7,8,11,12,15,16: DP-L5601. **(B)** Secreted Mpl was immunoprecipitated from the host cell lysates. Lanes: 1,4,7,10: 10403S; 2,5,8,11: DP-L5601; 3,6,9,12: DP-L2343. Numbers on the right indicate molecular mass markers (in kDa).

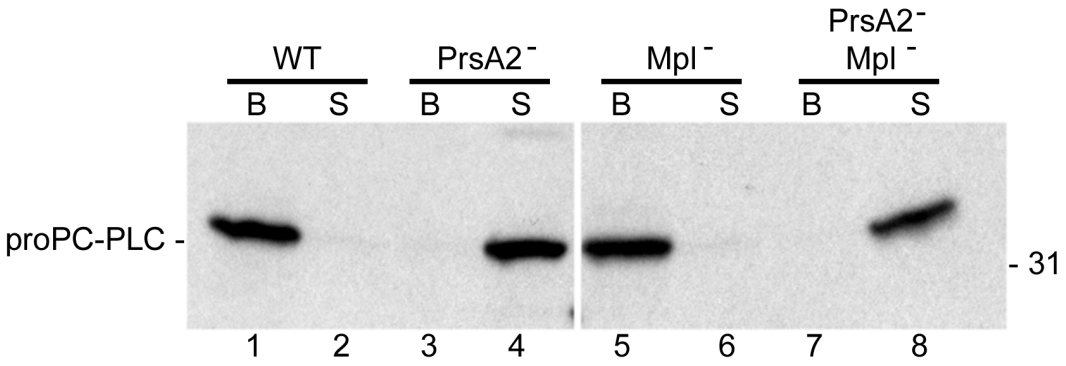

Figure 4.3. PC-PLC is secreted into the host cytosol independent of Mpl in the absence of PrsA2. Infected J774 cells were pulse-labeled. Bacterium-associated (B) and secreted (S) PC-PLC were immunoprecipitated from bacteria and host cell lysates, respectively. Lanes: 1 and 2, 10403S; 3 and 4, DP-L5596; 5 and 6, DP-L2343; 7 and 8, HEL-1216. Number on the right indicates molecular mass marker (in kDa).

Maturation of PC-PLC and Mpl does not occur in the absence of PrsA2 during intracellular infection. We previously hypothesized that the maturation of PC-PLC by Mpl in response to a decrease in pH occurs prior to secretion through the cell wall because secretion of PC-PLC synthesized in the absence of its propeptide is very rapid as opposed to secretion of the proform (44). To test this hypothesis, we assessed whether a decrease in pH would lead to PC-PLC maturation in cells infected with the *prsA2* mutant. Infected cells were pulse-labeled with [^{35}S]-methionine/cysteine and chased under conditions that maintain the host cell cytosol at physiological pH or mimic the acidified vacuolar pH to induce PC-PLC maturation. Secreted PC-PLC was immunoprecipitated from host cell lysates and detected by autoradiography. As previously reported, mature PC-PLC was detected in the host cell lysate following a decrease in intracellular pH in cells infected with wild-type bacteria (Figure 4.4). However, pH-mediated maturation of PC-PLC did not occur in cells infected with the *prsA2* mutant.

The absence of PC-PLC maturation in response to a decrease in pH could be due to a failure by Mpl to either undergo autocatalysis or to process PC-PLC post-secretion. To answer this question, we performed the same experiments as described above, except that secreted Mpl, and not PC-PLC, was immunoprecipitated. As previously observed, mature Mpl was detected in the host cell lysate following a decrease in intracellular pH in cells infected with wild-type bacteria (Figure 4.4). However, Mpl maturation did not occur in response to a decrease in pH in cells infected with the *prsA2* mutant. Together, these results suggested that the effect of pH on Mpl autocatalysis and Mpl-mediated maturation of PC-PLC is spatially controlled, and that PrsA2 is required to maintain the proproteins in the periplasm where maturation occurs.

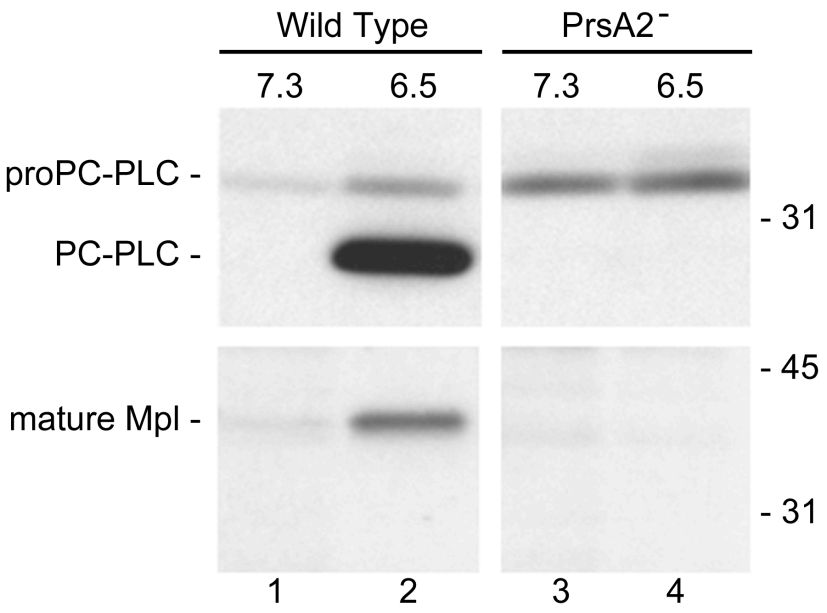

Figure 4.4. pH-dependent PC-PLC maturation and Mpl autocatalysis do not occur in the absence of PrsA2. Infected J774 cells were pulse labeled, and then chased in a nigericin-containing potassium buffer equilibrated to pH 7.3 or pH 6.5. Secreted PC-PLC (top panels) and Mpl (bottom panels) were immunoprecipitated from the host cell lysates. Lanes: 1 and 2: 10403S; 3 and 4: DP-L5601. Numbers on the right indicate molecular mass marker in kDa.

Cell wall permeability does not appear to be increased in the absence of PrsA2. Since the *B. subtilis* ortholog of PrsA2 is important for peptidoglycan crosslinking (17) and the *L. monocytogenes prsA2* mutant secretes larger amounts of proteins than wild-type bacteria (1, 45), we suspected that perhaps the cell wall of the PrsA2 mutant was more porous than that of wild-type bacteria. To assess differences in cell wall porosity, we opted to examine the profile of proteins that are present within the cell wall or are retained in the periplasm of *L. monocytogenes*. Before performing this experiment, we determined the temporal regulation of *prsA2* expression in broth culture to assess when a defect in *prsA2* expression was most likely to affect cell wall integrity. A *prsA*2 promoter and *gus* structural gene transcriptional fusion was constructed, and levels of Gus were measured (Figure 4.5). Gus was detected early during exponential growth phase, peaked in late log phase, and dropped during stationary phase suggesting that PrsA2 was most important during the exponential phase of bacterial growth.

Cell wall porosity was assessed using bacteria in the exponential phase of growth. Protoplasts were generated using a purified cell wall hydrolase and the solubilized cell wall fraction was resolved by SDS-PAGE. This cell wall fraction is expected to contain cell wall anchored proteins as well as translocated proteins that had not yet been secreted across the cell wall. If the *prsA2* mutant cell wall were more porous, we would expect to detect fewer proteins in this fraction. Although we observed minor differences, overall the protein pattern was very similar between the wild-type strain, the *prsA2* mutant and the complemented mutant strain (Figure 4.6A). This result suggested that there is no gross difference in cell wall porosity between wild-type *L. monocytogenes* and the *prsA2* mutant.

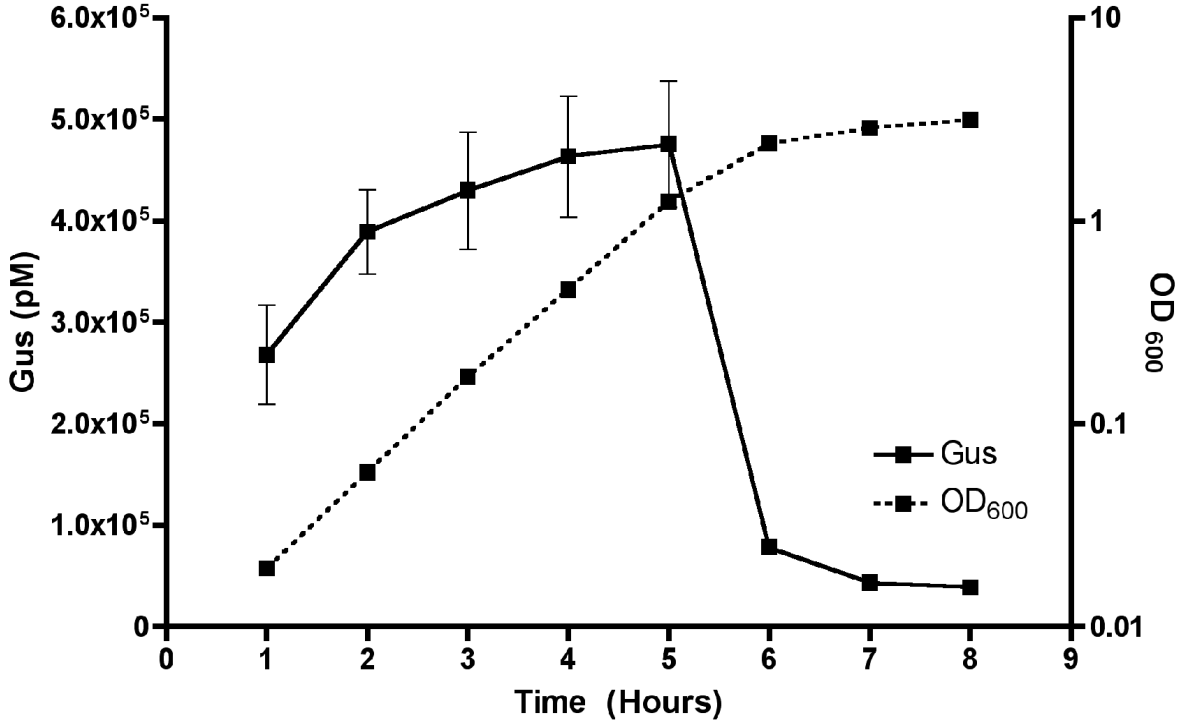

Figure 4.5. *prsA2* is expressed during exponential growth in broth culture. 10403S carrying pJZ095 (DP-L5755) was grown for 8 hours in BHI. Each hour, OD_{600} measurements were taken (dashed line) and the Gus levels from 1 mL of culture was measured. Gus levels were normalized to the OD_{600} measurements of the culture at each time point (solid line). Error bars represent the standard error of the mean. Data were collected from duplicate samples from three independent experiments. Experiment performed by Jason Zemansky.

Figure 4.6. Protein profiles of *L. monocytogenes* wild-type and *prsA2* mutant cell wall fractions. (A) Proteins that localize in the cell wall and periplasmic space were isolated as described in Materials and Methods. Equivalent amounts of culture OD units were loaded per lane. Proteins were resolved by SDS-PAGE and detected by Coomassie Brilliant Blue staining. The heavy band just above the 31 kDa marker corresponds to Ply118. Lanes: 1, 10403S; 2, DP-L5601; 3, DP-L5603. Numbers on the right indicate molecular mass markers in kDa. **(B)** Detection of InlA and PrfA from cell wall (C) and protoplast (P) fractions by Western immunoblot. Lanes: 1-2, 10403S; 3-4, DP-L5601; 5-6, DP-L5603; 7-8, EJL-12; 9-10, DP-L1075. Numbers on the right indicate molecular mass markers in kDa.

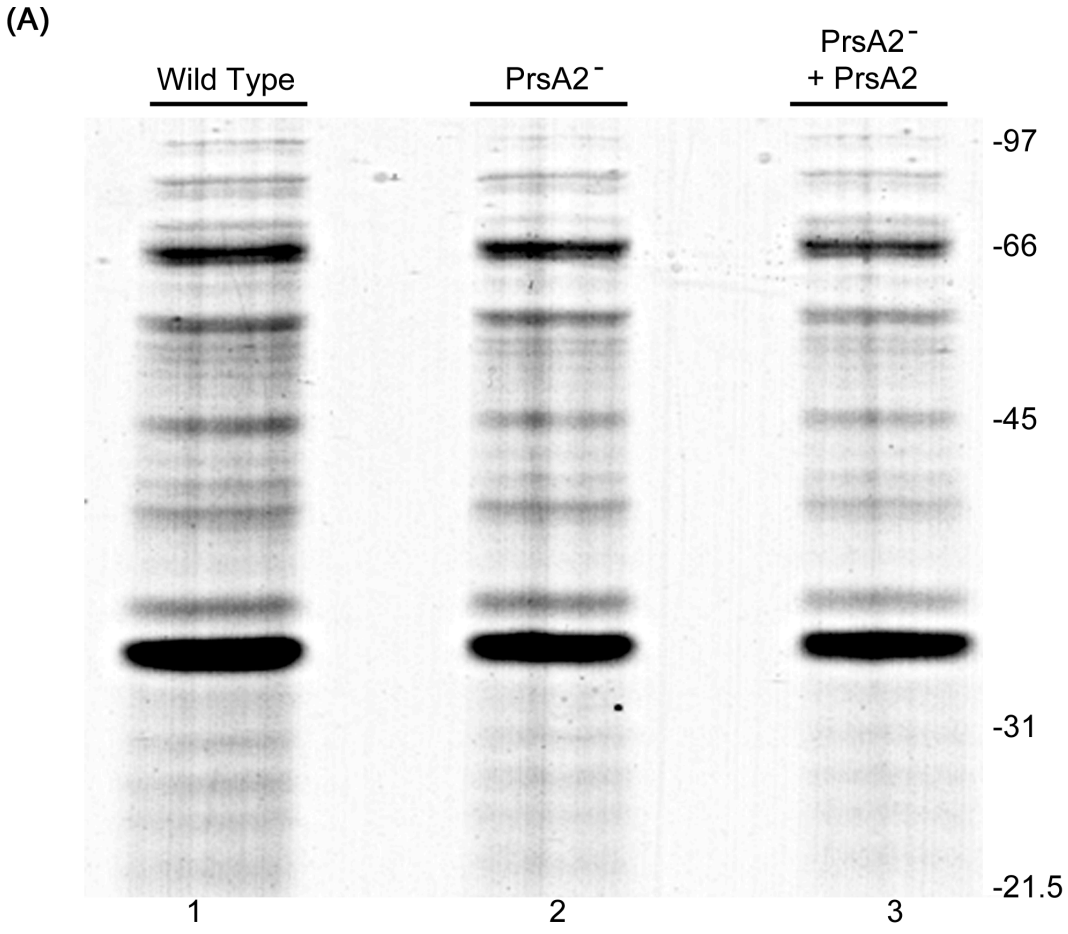
(A)
Wild Type
PrsA2⁻
PrsA2⁻ + PrsA2
-97
-66
-45
-31
-21.5
1
2
3
(B)
Wild Type
PrsA2⁻
PrsA2⁻ + PrsA2
InlA⁻
PrfA⁻
C P C P C P C P C P
InlA -
PrfA -
-97
-72
-26
1 2 3 4 5 6 7 8 9 10

To verify the purity of the cell wall fractions, we performed western immunoblots of both the cell wall and protoplast fractions to detect InlA, a cell wall anchored protein, and PrfA, a cytoplasmic protein (38). PrfA was detected only in the protoplast fractions, indicating that the cell wall fractions were devoid of cytoplasmic proteins (Figure 4.6B).

Susceptibility of *L. monocytogenes* to cell wall hydrolases is modified in the absence of PrsA2. To further investigate potential differences in the biochemical properties of the cell wall from wild-type and *prsA2* mutant bacteria, we assessed the susceptibility of the cell wall to lysozyme and to a *L. monocytogenes*-specific cell wall hydrolase. Lysozyme cleaves the β(1,4) linkage between the N-acetylglucosamine and N-acetylmuramic acid residues of peptidoglycan. Independent of its enzymatic activity, lysozyme has also been shown to induce cell lysis through the activation of autolysins (20). To determine if the *prsA2* mutant was more susceptible to lysozyme-mediated lysis, the optical density of exponential phase wild-type and *prsA2* bacteria incubated with or without lysozyme was measured as a function of time (Figure 4.7A). In the presence of lysozyme, PrsA2-deficient bacteria exhibited a slight but significant increase in the rate of lysis as compared to wild-type bacteria, beginning at t = 10 minutes ($p < 0.05$). The same assay was performed with purified Ply118, a *L. monocytogenes*-specific phage endolysin that cleaves the peptidoglycan peptide backbone between the L-alanine and D-glutamate residues (23). PrsA2-deficient bacteria were slightly more sensitive to Ply118 during the first ten minutes of incubation (Figure 4.7B). However, as incubation progressed, the mutant showed more resistance to Ply118 than wild-type bacteria. This difference was significant beginning at t = 25 minutes ($p < 0.05$) (Figure 4.7B).

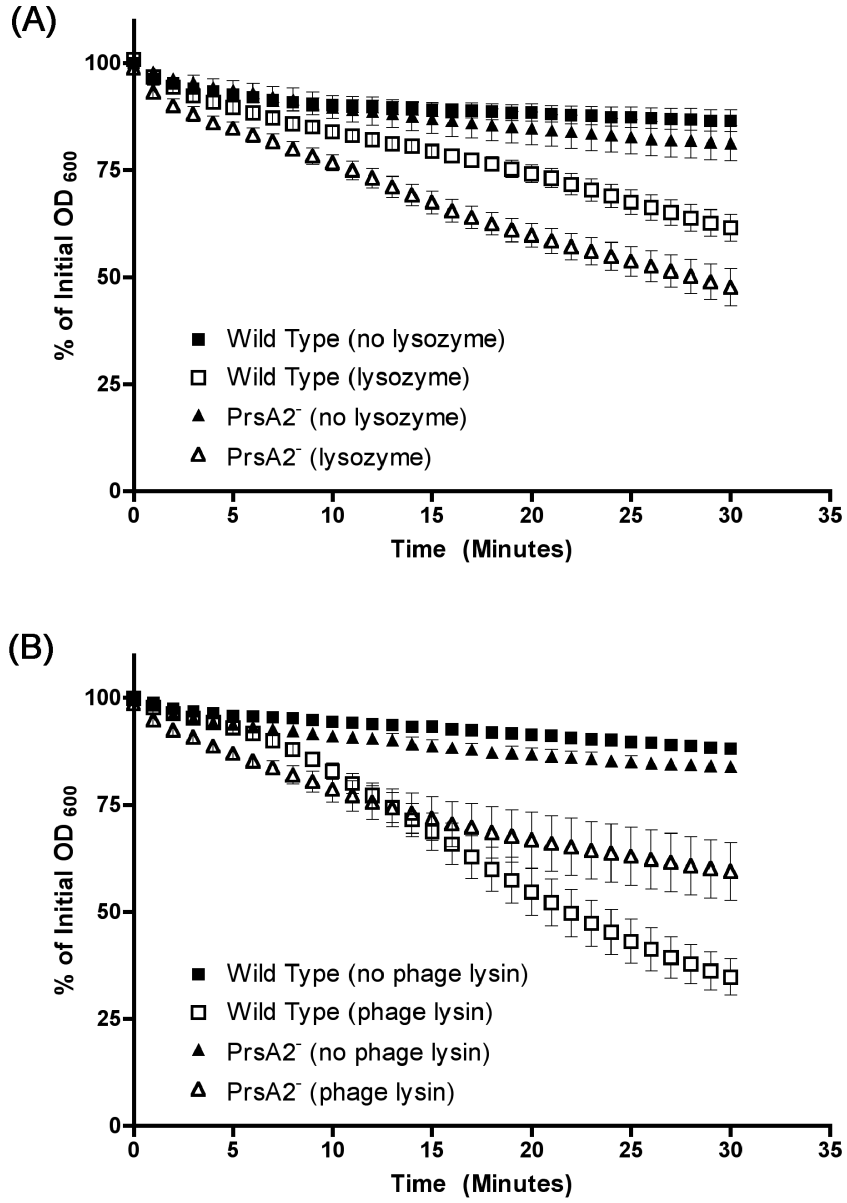

Figure 4.7. Deletion of *prsA2* affects the cell wall of *L. monocytogenes*. Sensitivity of mid-log phase bacteria to lysis in the presence (open icons) or absence (filled icons) of lysozyme **(A)** or phage endolysin Ply118 **(B)** was monitored by spectrometry. OD_{600} measurements were normalized to the initial optical density prior to incubation. Error bars represent the standard error of the mean from three independent experiments. Strains tested include 10403S (squares) and DP-L5601 (triangles).

Taken together, these results indicated that there are biochemical differences, albeit minor, in the peptidoglycan cell wall between wild-type and PrsA2-deficient bacteria

The absence of PrsA2 does not increase the susceptibility of *L. monocytogenes* to intracellular lysis. Next, we investigated whether differential susceptibility of wild-type and *prsA2* mutant bacteria to cell wall hydrolases would predispose the *prsA2* mutant to lysis during intracellular growth. Host cells were infected with bacteria carrying the gene coding for luciferase on a plasmid (32). The luciferase-coding gene is under the control of a cytomegalovirus promoter whose expression is dependent on host cell transcription factors, thus on bacterial lysis. No significant differences were observed between wild-type and *prsA2* mutant infected host cells (Figure 4.8). As a positive control for this assay, we infected cells with bacteria expressing PSA bacteriophage holin and lysin. This bacterial strain underwent autolysis and the infected host cells generated high levels of luciferase activity. This result indicated that intracellular bacteria lacking PrsA2 are not predisposed to intracellular lysis to a larger extent than wild-type bacteria.

PC-PLC is less stable when produced in the absence of PrsA2. The rapid secretion of PC-PLC and Mpl across the bacterial cell wall in the absence of PrsA2 could result from modifications in protein structure. To assess if PrsA2 assists in the folding of PC-PLC and Mpl, the stability of the proteins secreted in the cytosol of infected cells was assessed. Pulse-labeled bacterial proteins from infected cells were chased for incremental periods of time. Secreted PC-PLC and Mpl were immunoprecipitated from the host cell lysate, fractionated by SDS-PAGE, and detected by phosphorimaging.

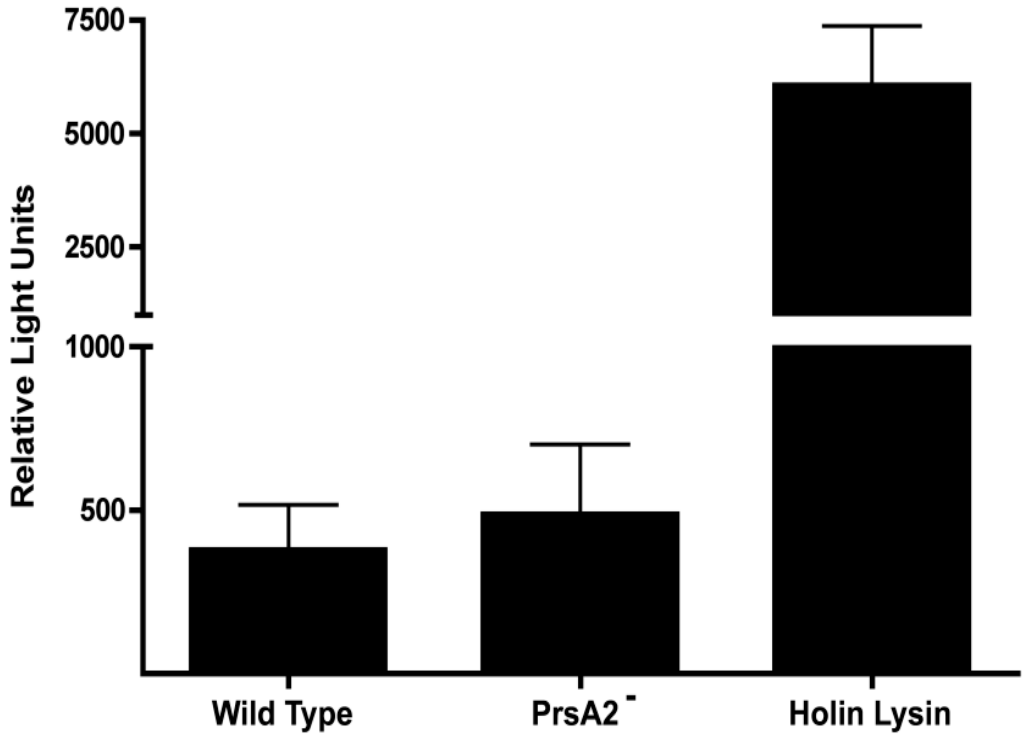

Figure 4.8. The *prsA*2 mutant does not show an increased sensitivity to lysis during intracellular growth. Intracellular bacterial lysis was measured using the luciferase reporter plasmid pBHE573 in infected macrophage cells. Error bars represent the standard deviation from three independent experiments. Strains tested include wild-type (DP-L5749), PrsA2$^-$ (DP-L5751), and a 10403S strain expressing holin/lysin (DP-L5750). Experiment performed by Jason Zemansky and Chelsea Witte.

Because wild-type bacteria secrete lower amounts of proproteins than the *prsA2* mutant, the wild-type sample gels were exposed for two to three times as long as the *prsA2* sample gels. Intensities of protein bands were quantified using ImageJ and protein half-lives were calculated. The half-lives of proPC-PLC made by the *prsA2* mutant and wild-type strain were 5 minutes and greater than 10 minutes, respectively (Figures 4.9 and 4.2 upper panel). In contrast, Mpl was very stable in the absence or presence of PrsA2 (Figure 4.2 lower panel). These results suggested that the secreted proform of PC-PLC, but not the Mpl zymogen, is folded differently in the absence of PrsA2, and thus more sensible to proteolysis.

Deletion of the propeptide rescues PC-PLC activity defect in the absence of PrsA2. PC-PLC synthesized in the absence of its propeptide is rapidly secreted across the bacterial cell wall as an active enzyme, and this phenomenon is independent of pH and of Mpl (44). We questioned whether PrsA2 contributes to folding of PC-PLC catalytic domain by examining phospholipase activity generated by a propeptide deletion mutant. Wild-type and mutant bacteria were spotted on egg yolk agar, where a zone of opacity around the colony is indicative of PC-PLC activity. As previously reported, the *prsA2* mutant generated less activity than the wild-type strain and the propeptide deletion mutant generated a higher level of phospholipase activity than the wild-type strain (44-45) (Figure 4.10A, panels 1,2,4). Interestingly, the level of phospholipase activity generated by the propeptide deletion mutant was independent of PrsA2 (Figure 4.10A, panel 5).

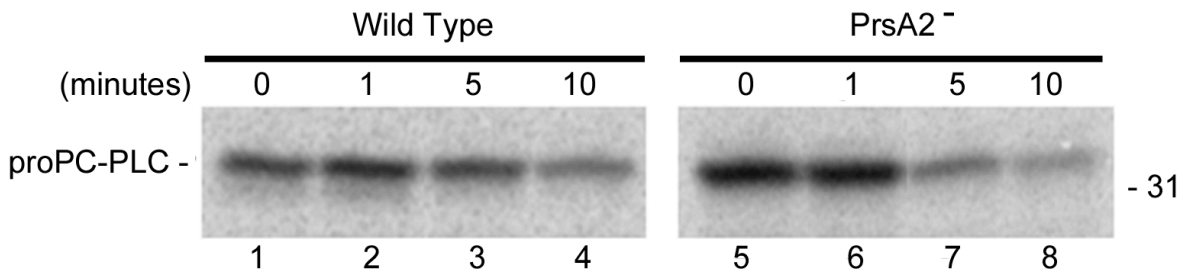

Figure 4.9. PC-PLC is less stable when produced in the absence of PrsA2. Infected J774 cells were pulse-labeled for 5 minutes and chased for the times indicated in the figure. Secreted PC-PLC was then immunoprecipitated as described in the text and detected by phosphorimaging. Number on the right indicates molecular mass marker in kDa. Lanes: 1-4: 10403S; 5-8: DP-L5601.

Figure 4.10. Deletion of the PC-PLC propeptide restores phospholipase activity in PrsA2-deficient bacteria. (A) Detection of PC-PLC activity on LB egg yolk agar plates. A zone of opacity indicates PC-PLC activity. Panels: 1, 10403S; 2, DP-L5596; 3, DP-L1935; 4, HEL-335; 5, HEL-1405. **(B)** Plaque assay to measure cell-to-cell spread. Plaque area is reported as percentage of wild-type plaque area. Error bars represent the standard deviation from independent experiments. Strains tested include wild-type (10403S), PrsA2$^-$ (DP-L5596), PC-PLC$^-$ (DP-L1935), PC-PLCΔpro (HEL-335) and PC-PLCΔpro with PrsA2$^-$ (HEL-1405). Statistical significance was tested using ANOVA with Tukey-Kramer multiple comparisons test. All comparisons were significantly different ($p \leq 0.05$) except between DP-L1935 and HEL-1405.

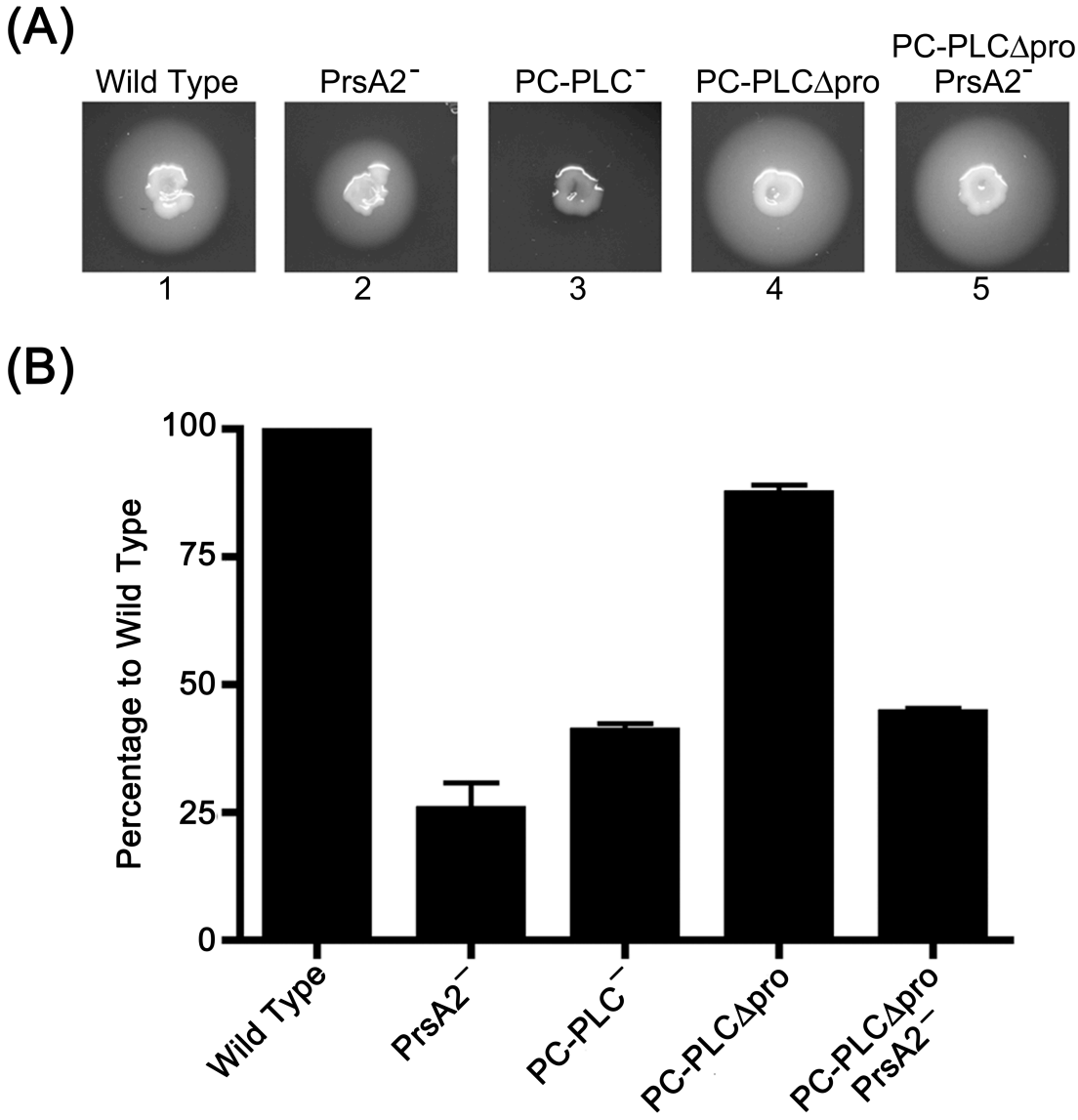
(A)
Wild Type
PrsA2⁻
PC-PLC⁻
PC-PLCΔpro
PC-PLCΔpro PrsA2⁻
1
2
3
4
5
(B)
Percentage to Wild Type
100
75
50
25
0
Wild Type
PrsA2⁻
PC-PLC⁻
PC-PLCΔpro
PC-PLCΔpro PrsA2⁻

We next wished to determine whether deleting the propeptide of PC-PLC in the *prsA2* mutant would restore the cell-to-cell spread defect of the *prsA2* mutant in infected cells. To address this question, we used a plaque assay in which the size of the plaques is proportional to the efficiency of bacteria cell-to-cell spread (Figure 10B). As previously reported, the *prsA2* mutant makes a small plaque (25.5% of wild-type), whereas the Δpro*plcB* mutant makes a plaque that is close in size to a wild-type plaque (87.3% of wild-type) (2, 43, 45). The *plcB* deletion mutant generated a larger plaque than the *prsA2* mutant (40.8% vs. 25.5% of wild-type), indicating that the plaquing defect observed in the *prsA2* mutant is not due to its effect on PC-PLC alone. PrsA2 also contributes to LLO activity, another factor that contributes to efficient cell-to-cell spread (2, 45). When the propeptide of PC-PLC was deleted in the *prsA2* mutant, the plaque size increased from 25.5% to 44.5% of wild-type. This result suggests that deleting the propeptide resulted in PC-PLC activity, allowing for the plaque defect to be partially recovered. These results, taken together with the egg yolk assay results (Figure 10A), indicate that PrsA2 does not contribute to folding of the PC-PLC catalytic domain.

DISCUSSION

L. monocytogenes relies on numerous virulence factors to facilitate its intracellular lifestyle. Two of these factors, PC-PLC and Mpl, contribute to vacuolar lysis. Both proteins are produced as proenzymes that are translocated across the bacterial membrane and retained in the periplasm until a decrease in vacuolar pH triggers Mpl autocatalysis followed by Mpl-mediated maturation of PC-PLC (26, 29, 38). This maturation process correlates with the detection of Mpl and PC-PLC in the host cell. PrsA2, a PPIase and post-translocation

chaperone, was identified as contributing to the activity of PC-PLC (2-3, 45). In this study, we assessed the mechanism by which PrsA2 controls PC-PLC activity. Our data showed that, in the absence of PrsA2, the proforms of PC-PLC and Mpl are prematurely secreted across the cell wall and that a decrease in intracellular pH did not lead to maturation of either protein. This phenomenon does not appear to result from a change in cell wall porosity, although there is biochemical evidence that the cell wall of the PrsA2 mutant is slightly modified compared to wild-type bacteria. The stability of the secreted proform of PC-PLC was compromised in the absence of PrsA2, whereas the secreted Mpl zymogen was very stable. However, the PC-PLC activity defect observed in the absence of PrsA2 was rescued by deleting the propeptide of PC-PLC. We conclude that the PC-PLC activity defect observed in the absence of PrsA2 results from the premature secretion of the Mpl zymogen due to changes in the biochemical properties of the cell wall and the inability of the zymogen to undergo autocatalysis post-secretion.

The ability of Mpl to localize in the periplasm during intracellular growth is imperative to its function (29). This fact was emphasized in this study by the observation that, in the absence of PrsA2, Mpl was prematurely secreted and did not undergo maturation upon a decrease in pH. This phenomenon is probably not due to a change in Mpl conformation, as the prematurely secreted enzyme was very stable. This was not surprising, as Mpl folding is unlikely to be assisted by PrsA2 considering that the individual propeptides of metalloproteases have been shown to act as folding chaperones (8, 24). Arguably, if Mpl autocatalysis occurs before being secreted across the cell wall, Mpl-mediated maturation of PC-PLC is likely to occur within the periplasmic space as the confined area within the cell

envelope would favor these two proteins encountering. Control of Mpl-mediated activation of PC-PLC is less stringent when the proteins are secreted by bacteria grown on complex medium, as some PC-PLC activity was detected around the colonies formed by the *prsA2* mutant. However, it is difficult to compare extracellular and intracellular conditions. The pH conditions of a vacuole cannot be recapitulated when *L. monocytogenes* is grown on complex medium. Consequently, the Mpl zymogen may be exposed to acidic conditions during translocation across the bacterial membrane, enabling immediate autocatalysis. However, the fact that some level of PC-PLC was detected on complex medium in the absence of PrsA2 argues that PrsA2 is not required for Mpl folding. We conclude that Mpl autocatalysis is controlled by factors and/or conditions that prevail within the cell envelope, and that a decrease in pH is not sufficient to trigger Mpl autocatalysis.

Results from the present study indicated that the cell wall of the PrsA2 mutant was modified as assessed by an increased sensitivity to lysozyme and a modified sensitivity to a *L. monocytogenes*-specific cell wall hydrolase. It appears that biochemical differences exist in the glycan chains of peptidoglycan between the wild-type and the *prsA2* mutant, as both lysozyme and Ply118 recognize the sugar moieties of peptidoglycan (22, 27). The resistance of *L. monocytogenes* to lysozyme is conferred by PgdA, an enzyme that deacetylates N-acetylglucosamine residues of peptidoglycan (18). Absence of PrsA2 may alter the activity of PgdA, thus making peptidoglycan more sensitive to lysozyme (7). Alternatively, lysozyme activity may be affected by cell wall charges. Levels of D-alanylation of teichoic and lipoteichoic acids modulate the levels of negative charges in the cell wall (31). Lysozyme is positively charged, and bacteria unable to D-alanylate teichoic acid are more susceptible to

lysozyme (15, 19). The absence of PrsA2 may affect cell wall charges and levels of cations bound to the cell wall, which could modulate the rate of folding and secretion of the Mpl zymogen. Similarly, these differences could influence the folding and secretion of proform PC-PLC. Alternatively, these changes in cell wall properties could influence other proteins that contribute to maintain the Mpl zymogen and the proform of PC-PLC bacterium-associated.

The mechanism that controls the compartmentalization of PC-PLC is unknown. The proform of PC-PLC is secreted across the cell wall at a rate that is slower than the rate of translocation across the cytoplasmic membrane, enabling the protein to accumulate in the periplasm (38) . However, when PC-PLC is synthesized without its propeptide or in the absence of PrsA2, the protein is rapidly secreted across the cell wall. Synthesis of PC-PLC in the absence of its propeptide generates an active enzyme independent of PrsA2. Therefore, neither the propeptide of PC-PLC nor PrsA2 is required for native folding of the catalytic domain, but both influence secretion of the enzyme. However, the secreted proform of PC-PLC is more stable in the presence of PrsA2, suggesting a role for PrsA2 in folding of proPC-PLC. Recent work has shown that the N-terminus of PrsA2 is necessary for PC-PLC activity (3). Perhaps the propeptide of PC-PLC serves to slow down protein folding and to interact with the N-terminus of PrsA2. The interaction with PrsA2 would be released only once the proprotein has reached its native conformation, which would explain the slow rate of protein secretion, and the difference in protein stability observed between the slow and fast-secreted forms of proPC-PLC.

In conclusion, during intracytosolic growth, *L. monocytogenes* requires PrsA2 to maintain the Mpl zymogen and the proform of PC-PLC in close proximity within the bacterial cell envelope. This condition is imperative to rapidly generate and deliver active PC-PLC in vacuoles formed upon cell-to-cell spread. We hypothesize that PrsA2 regulates the compartmentalization and activity of these proenzymes by influencing cell wall properties and by interacting with the PC-PLC propeptide. This mechanism of regulating in a spatial and temporal manner the secretion of active virulence factors is similar, in principle, to the mechanisms used by Gram-negative bacteria to deliver type III and IV secretion system effectors into eukaryotic cells.

ACKNOWLEDGEMENTS

We would like to thank Nancy Freitag for providing us with strain NF-L1166. We additionally thank David Drubin and Georjana Barnes from the University of California at Berkeley for use of the Horiba FluoroMax-3 fluorometer. We also thank members of the Portnoy laboratory for their assistance with this project, especially Ben Kline for constructing pJZ095 and Chelsea Witte for her assistance with the bacterial lysis luciferase assay.

This research was supported by National Institutes of Health Grants AI27655 and AI063302 (D.A.P.) and AI52154 (H.M.). D.A.P. has a consulting relationship with and financial interest in Aduro Biotech.

REFERENCES

1. **Alonzo, F., 3rd, and N. E. Freitag.** 2010. *Listeria monocytogenes* PrsA2 is required for virulence factor secretion and bacterial viability within the host cell cytosol. Infect. Immun. **78:**4944-57.

2. **Alonzo, F., 3rd, G. C. Port, M. Cao, and N. E. Freitag.** 2009. The posttranslocation chaperone PrsA2 contributes to multiple facets of *Listeria monocytogenes* pathogenesis. Infect. Immun. **77:**2612-23.

3. **Alonzo, F., 3rd, B. Xayarath, J. C. Whisstock, and N. E. Freitag.** 2011. Functional analysis of the *Listeria monocytogenes* secretion chaperone PrsA2 and its multiple contributions to bacterial virulence. Mol. Microbiol. **80:**no. doi: 10.1111/j.1365-2958.2011.07665.x.

4. **Bakardjiev, A. I., B. A. Stacy, S. J. Fisher, and D. A. Portnoy.** 2004. Listeriosis in the pregnant guinea pig: a model of vertical transmission. Infect. Immun. **72:**489-497.

5. **Bishop, D. K., and D. J. Hinrichs.** 1987. Adoptive transfer of immunity to *Listeria monocytogenes*. The influence of *in vitro* stimulation on lymphocyte subset requirements. J. Immunol. **139:**2005-2009.

6. **Bitar, A. P., M. Cao, and H. Marquis.** 2008. The metalloprotease of *Listeria monocytogenes* is activated by intramolecular autocatalysis. J. Bacteriol. **190:**107-11.

7. **Boneca, I. G., O. Dussurget, D. Cabanes, M. A. Nahori, S. Sousa, M. Lecuit, E. Psylinakis, V. Bouriotis, J. P. Hugot, M. Giovannini, A. Coyle, J. Bertin, A. Namane, J. C. Rousselle, N. Cayet, M. C. Prevost, V. Balloy, M. Chignard, D. J. Philpott, P. Cossart, and S. E. Girardin.** 2007. A critical role for peptidoglycan N-deacetylation in *Listeria* evasion from the host innate immune system. Proc. Natl. Acad. Sci. USA **104:**997-1002.

8. **Braun, P., J. Tommassen, and A. Filloux.** 1996. Role of the propeptide in folding and secretion of elastase of *Pseudomonas aeruginosa*. Mol. Microbiol. **19:**297-306.

9. **Camilli, A., L. G. Tilney, and D. A. Portnoy.** 1993. Dual roles of *plcA* in *Listeria monocytogenes* pathogenesis. Mol. Microbiol. **8:**143-57.

10. **Duguay, A. R., and T. J. Silhavy.** 2004. Quality control in the bacterial periplasm. Biochim. Biophys. Acta **1694:**121-34.

11. **Ellis, R. J., and S. M. van der Vies.** 1991. Molecular chaperones. Annu. Rev. Biochem. **60:**321-47.

12. **Freitag, N. E., L. Rong, and D. A. Portnoy.** 1993. Regulation of the *prfA* transcriptional activator of *Listeria monocytogenes*: multiple promoter elements contribute to intracellular growth and cell-to-cell spread. Infect. Immun. **61:**2537-2544.

13. **Gaillard, J. L., P. Berche, J. Mounier, S. Richard, and P. Sansonetti.** 1987. *In vitro* model of penetration and intracellular growth of *Listeria monocytogenes* in the human enterocyte-like cell line Caco-2. Infect. Immun. **55:**2822-2829.

14. **Goffin, C., and J. M. Ghuysen.** 1998. Multimodular penicillin-binding proteins: an enigmatic family of orthologs and paralogs. Microbiol. Mol. Biol. Rev. **62:**1079-93.

15. **Herbert, S., A. Bera, C. Nerz, D. Kraus, A. Peschel, C. Goerke, M. Meehl, A. Cheung, and F. Gotz.** 2007. Molecular basis of resistance to muramidase and cationic antimicrobial peptide activity of lysozyme in *Staphylococci*. PLoS Pathog. **3:**e102.

16. **Hodgson, D. A.** 2000. Generalized transduction of serotype 1/2 and serotype 4b strains of *Listeria monocytogenes*. Mol. Microbiol. **35:**312-323.

17. **Hyyrylainen, H. L., B. C. Marciniak, K. Dahncke, M. Pietiainen, P. Courtin, M. Vitikainen, R. Seppala, A. Otto, D. Becher, M. P. Chapot-Chartier, O. P. Kuipers, and V. P. Kontinen.** 2010. Penicillin-binding protein folding is dependent on the PrsA peptidyl-prolyl *cis-trans* isomerase in *Bacillus subtilis*. Mol. Microbiol. **77:**108-27.

18. **Kamisango, K., I. Saiki, Y. Tanio, H. Okumura, Y. Araki, I. Sekikawa, I. Azuma, and Y. Yamamura.** 1982. Structures and biological activities of peptidoglycans of *Listeria monocytogenes* and *Propionibacterium acnes*. J. Biochem. **92:**23-33.

19. **Kristian, S. A., V. Datta, C. Weidenmaier, R. Kansal, I. Fedtke, A. Peschel, R. L. Gallo, and V. Nizet.** 2005. D-alanylation of teichoic acids promotes Group A *Streptococcus* antimicrobial peptide resistance, neutrophil survival, and epithelial cell invasion. J. Bacteriol. **187:**6719-25.

20. **Laible, N. J., and G. R. Germaine.** 1985. Bactericidal activity of human lysozyme, muramidase-inactive lysozyme, and cationic polypeptides against *Streptococcus sanguis* and *Streptococcus faecalis*: inhibition by chitin oligosaccharides. Infect. Immun. **48:**720-8.

21. **Lauer, P., M. Y. Chow, M. J. Loessner, D. A. Portnoy, and R. Calendar.** 2002. Construction, characterization, and use of two *Listeria monocytogenes* site-specific phage integration vectors. J. Bacteriol. **184:**4177-4186.

22. **Loessner, M. J., K. Kramer, F. Ebel, and S. Scherer.** 2002. C-terminal domains of *Listeria monocytogenes* bacteriophage murein hydrolases determine specific recognition and high-affinity binding to bacterial cell wall carbohydrates. Mol. Microbiol. **44:**335-49.

23. **Loessner, M. J., A. Schneider, and S. Scherer.** 1996. Modified *Listeria* bacteriophage lysin genes (*ply*) allow efficient overexpression and one-step purification of biochemically active fusion proteins. Appl. Environ. Microbiol. **62:**3057-60.

24. **Marie-Claire, C., E. Ruffet, A. Beaumont, and B. P. Roques.** 1999. The prosequence of thermolysin acts as an intramolecular chaperone when expressed *in trans* with the mature sequence in *Escherichia coli*. J. Mol. Biol. **285:**1911-1915.

25. **Marquis, H., V. Doshi, and D. A. Portnoy.** 1995. The broad-range phospholipase C and a metalloprotease mediate listeriolysin O-independent escape of *Listeria monocytogenes* from a primary vacuole in human epithelial cells. Infect. Immun. **63:**4531-4.

26. **Marquis, H., and E. J. Hager.** 2000. pH-regulated activation and release of a bacteria-associated phospholipase C during intracellular infection by *Listeria monocytogenes*. Mol. Microbiol. **35:**289-98.

27. **Masschalck, B., and C. W. Michiels.** 2003. Antimicrobial properties of lysozyme in relation to foodborne vegetative bacteria. Crit. Rev. Microbiol. **29:**191-214.

28. **Miner, M. D., G. C. Port, and N. E. Freitag.** 2008. Functional impact of mutational activation on the *Listeria monocytogenes* central virulence regulator PrfA. Microbiology **154:**3579-89.

29. **O'Neil, H. S., B. M. Forster, K. L. Roberts, A. J. Chambers, A. P. Bitar, and H. Marquis.** 2009. The propeptide of the metalloprotease of *Listeria monocytogenes* controls compartmentalization of the zymogen during intracellular infection. J. Bacteriol. **191:**3594-603.

30. **O'Neil, H. S., and H. Marquis.** 2006. *Listeria monocytogenes* flagella are used for motility, not as adhesins, to increase host cell invasion. Infect. Immun. **74:**6675-81.

31. **Perego, M., P. Glaser, A. Minutello, M. A. Strauch, K. Leopold, and W. Fischer.** 1995. Incorporation of D-alanine into lipoteichoic acid and wall teichoic acid in *Bacillus subtilis*. Identification of genes and regulation. J. Biol. Chem. **270:**15598-606.

32. **Sauer, J. D., C. E. Witte, J. Zemansky, B. Hanson, P. Lauer, and D. A. Portnoy.** 2010. *Listeria monocytogenes* triggers AIM2-mediated pyroptosis upon infrequent bacteriolysis in the macrophage cytosol. Cell Host Microbe **7:**412-419.

33. **Shetron-Rama, L. M., H. Marquis, H. G. Bouwer, and N. E. Freitag.** 2002. Intracellular induction of *Listeria monocytogenes actA* expression. Infect. Immun. **70:**1087-96.

34. **Shetron-Rama, L. M., K. Mueller, J. M. Bravo, H. G. Bouwer, S. S. Way, and N. E. Freitag.** 2003. Isolation of *Listeria monocytogenes* mutants with high-level *in vitro* expression of host cytosol-induced gene products. Mol. Microbiol. **48:**1537-1551.

35. **Slepkov, E. R., A. Pavinski Bitar, and H. Marquis.** 2010. Differentiation of propeptide residues regulating the compartmentalization, maturation and activity of the broad-range phospholipase C of *Listeria monocytogenes*. Biochem. J. **432:**557-63.

36. **Smith, G. A., H. Marquis, S. Jones, N. C. Johnston, D. A. Portnoy, and H. Goldfine.** 1995. The two distinct phospholipases C of *Listeria monocytogenes* have overlapping roles in escape from a vacuole and cell-to-cell spread. Infect. Immun. **63:**4231-7.

37. **Smith, K., and P. Youngman.** 1992. Use of a new integrational vector to investigate compartment-specific expression of the *Bacillus subtilis spoIIM* gene. Biochimie **74:**705-711.

38. **Snyder, A., and H. Marquis.** 2003. Restricted translocation across the cell wall regulates secretion of the broad-range phospholipase C of *Listeria monocytogenes*. J. Bacteriol. **185:**5953-8.

39. **Sun, A. N., A. Camilli, and D. A. Portnoy.** 1990. Isolation of *Listeria monocytogenes* small-plaque mutants defective for intracellular growth and cell-to-cell spread. Infect. Immun. **58:**3770-8.

40. **Tilney, L. G., and D. A. Portnoy.** 1989. Actin filaments and the growth, movement, and spread of the intracellular bacterial parasite, *Listeria monocytogenes*. J. Cell Biol. **109:**1597-608.

41. **Vazquez-Boland, J. A., M. Kuhn, P. Berche, T. Chakraborty, G. Dominguez-Bernal, W. Goebel, B. Gonzalez-Zorn, J. Wehland, and J. Kreft.** 2001. *Listeria* pathogenesis and molecular virulence determinants. Clin. Microbiol. Rev. **14:**584-640.

42. **Vitikainen, M., I. Lappalainen, R. Seppala, H. Antelmann, H. Boer, S. Taira, H. Savilahti, M. Hecker, M. Vihinen, M. Sarvas, and V. P. Kontinen.** 2004. Structure-function analysis of PrsA reveals roles for the parvulin-like and flanking N- and C-terminal domains in protein folding and secretion in *Bacillus subtilis*. J. Biol. Chem. **279:**19302-14.

43. **Yeung, P. S., Y. Na, A. J. Kreuder, and H. Marquis.** 2007. Compartmentalization of the broad-range phospholipase C activity to the spreading vacuole is critical for *Listeria monocytogenes* virulence. Infect. Immun. **75:**44-51.

44. **Yeung, P. S., N. Zagorski, and H. Marquis.** 2005. The metalloprotease of *Listeria monocytogenes* controls cell wall translocation of the broad-range phospholipase C. J. Bacteriol. **187:**2601-8.

45. **Zemansky, J., B. C. Kline, J. J. Woodward, J. H. Leber, H. Marquis, and D. A. Portnoy.** 2009. Development of a mariner-based transposon and identification of *Listeria monocytogenes* determinants, including the peptidyl-prolyl isomerase PrsA2, that contribute to its hemolytic phenotype. J. Bacteriol. **191:**3950-64.

CHAPTER 5

IDENTIFICATION OF AMINO ACIDS INFLUENCING THE SECRETION OF THE METALLOPROTEASE OF *LISTERIA MONOCYTOGENES* AND ITS ABILITY TO PROCESS THE BROAD-RANGE PHOSPHOLIPASE C

ABSTRACT

Mpl is a thermolysin-like metalloprotease produced by the Gram-positive, facultative intracellular bacterial pathogen *Listeria monocytogenes*. During intracellular infection, Mpl and a broad-range phospholipase C (PC-PLC) are synthesized as proproteins that translocate across the bacterial cell membrane and accumulate in the periplasmic space. Upon a decrease in pH, Mpl undergoes intramolecular autocatalysis and activates PC-PLC. The mature proteins are then rapidly secreted across the cell wall and aid *L. monocytogenes* to escape from vacuoles formed upon cell-to-cell spread. In this study, we were interested in determining which amino acids outside of Mpl's active site contribute to its intracellular behavior. Using a homology model of mature Mpl, we targeted amino acids that had predicted pK_a values in the physiological pH range (6.0-7.4). Single point mutations in Mpl were made at these residues and intracellular activity was assessed. Our results identified two amino acids in the N-terminus of the catalytic domain, H226 and H241 that influence Mpl secretion and its ability to process PC-PLC. These two residues are located approximately seven Å apart in two random coil loops on the same side as the active site pocket. Interestingly, a positive charge is required at position 226, whereas a positive charge at position 241 has detrimental effects on Mpl. We conclude that H226 and H241 influence the interaction of Mpl with the cell envelope and with PC-PLC.

INTRODUCTION

Metalloproteases are important factors for bacterial pathogens (25). They can target host factors to assist in colonization, invasion, dissemination and cell damage. These proteases

can also assist in the activation of other virulence factors. One such metalloprotease is the metalloprotease of the Gram-positive bacterium *Listeria monocytogenes* (Mpl) (24), a facultative intracellular pathogen which causes the food-borne disease listeriosis (37).

L. monocytogenes is capable of invading both professional and non-professional phagocytic cells. Once in a host cell, bacteria escape from vacuoles, multiply in the host cytosol and spread from cell-to-cell using an actin mechanism of motility to avoid host defenses (36). Two virulence factors that contribute to the escape from vacuoles formed during cell-to-cell spread are Mpl and a broad-range phospholipase C (PC-PLC). Both Mpl and PC-PLC are secreted as proproteins with an N-terminal propeptide covalently attached to their catalytic domain (21, 26, 34). Translocation of the proproteins is faster than the rate of secretion across the bacterial cell wall, generating a pool of bacterium-associated PC-PLC and Mpl in the periplasm. Two factors influence the compartmentalization of the proproteins: the propeptides and the peptidyl-prolyl *cis-trans* isomerase PrsA2 ((26, 38) , chapter 4). Upon a decrease in pH, Mpl undergoes intramolecular autocatalysis and activates PC-PLC ((6), chapter 3). The mature proteins are then rapidly secreted across the cell wall, allowing PC-PLC to hydrolyze the vacuolar membrane. Independent of processing PC-PLC, Mpl also facilitates the secretion of PC-PLC (38).

Mpl is a member of the thermolysin family of zincin metalloproteases (16). The model protease in this family is thermolysin from the Gram-positive bacterium *Bacillus thermoproteolyticus*. The crystal structure for the catalytic domain of thermolysin and other related metalloproteases have been resolved (2, 14, 23). The catalytic domain of thermolysin

contains two structural subdomains. The N-terminal subdomain is composed mainly of beta strands. The C-terminal subdomain is composed predominantly of alpha helices. Entrance to the active site is between these two subdomains. The active site of Mpl contains a conserved HEXXH(19X)E motif where the histidines (H349, H353), the second glutamic acid (E373) and a water molecule coordinate the Zn^{2+} ion (2, 18) (Figure 5.1). The most energetically favorable mechanism of catalysis suggests that the substrate entering the active site displaces the water molecule, bringing it closer to the first glutamic acid in the motif (7, 22, 28). The glutamic acid deprotonates the water, promoting nucleophillic attack of the carbonyl carbon of the P1 residue by the water molecule. This transition state is stabilized by a histidine residue 83 residues downstream from the motif (3). The glutamic acid then transfers the proton to the amide nitrogen on the P1' residue, resulting in hydrolysis of the peptide bond. In Mpl, these residues correspond to E350 and H437, respectively (Figure 5.1). Mpl also binds four Ca^{2+} ions. The binding of these calcium ions contributes to thermal stability of the protein by preventing major conformational changes (9, 11).

Mpl activity is affected by pH (chapter 3). Proteins sensitive to pH can rely on specific amino acids that act as pH sensors (35). To be involved in pH sensing, the amino acid must contain a titratable group on its side chain or reside at the amino or carboxyl terminus of the amino acid backbone. Depending on the side group pK_a, these amino acids can become protonated or deprotonated upon a change in pH. Amino acids acting as pH sensors can affect protein conformation (10, 13), protein stability (29), and zymogen autocatalysis (12).

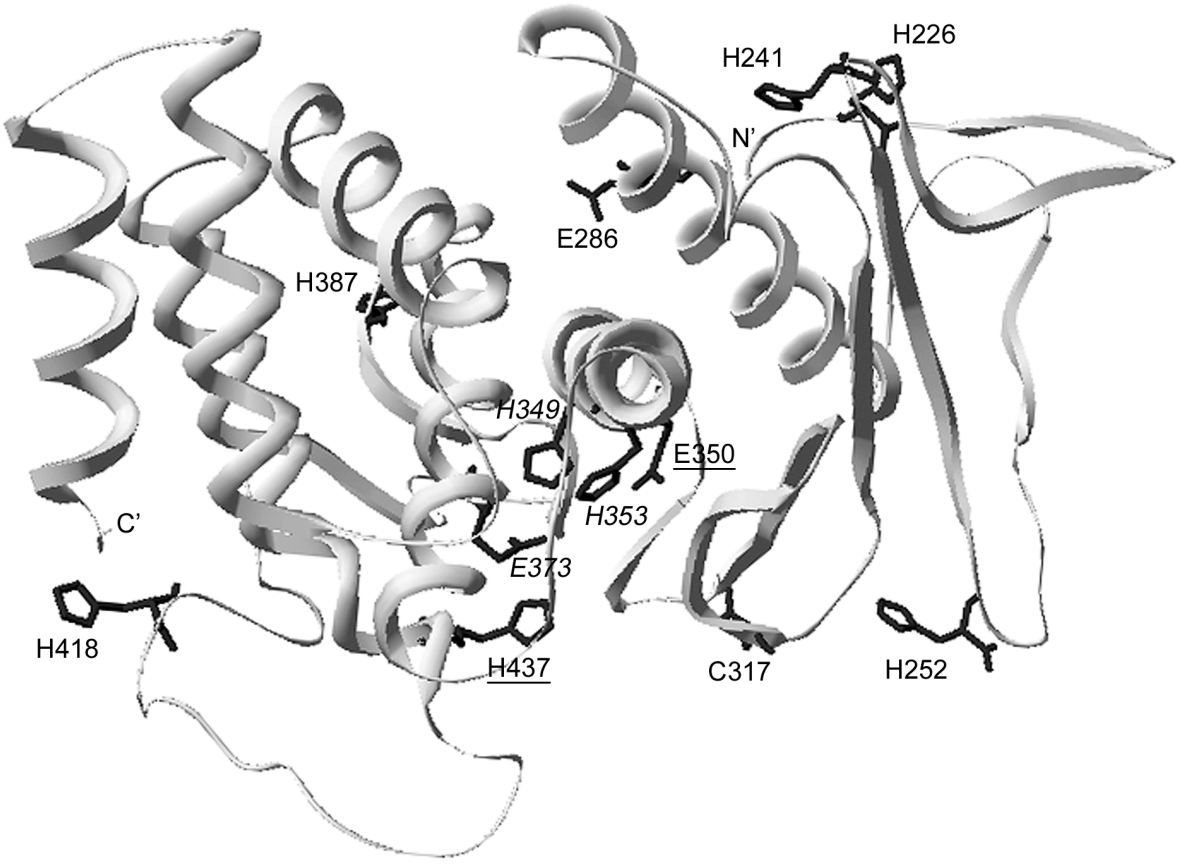

Figure 5.1. Ribbon model of Mpl showing the catalytic domain amino acids investigated in this study. A homology model of Mpl was constructed using SWISS-MODEL using aureolysin from *Staphylococcus aureus* (PDB ID: 1BQB) as the template. The N-terminus (N'), C-terminus (C') and amino acids targeted for mutation in this study are indicated throughout the structure. Active site amino acids are underlined. Amino acids involved in the coordination of the Zn^{2+} ion are italicized.

In this study, we wished to determine which amino acids not present in the active site contribute to the intracellular activity of Mpl. Our results determined that H226 and H241 influence Mpl secretion and its ability to process PC-PLC. These two residues are located approximately seven Å apart in two random coil loops on the same side as the active site pocket. Interestingly, a positive charge is required at position 226. On the contrary, a positive charge at residue 241 has detrimental effects on Mpl.

MATERIALS AND METHODS

Bacterial strains and growth conditions. All *L. monocytogenes* strains used in this study are listed in Table 5.1. Each strain is a derivative of the *L. monocytogenes* strain NF-L943. NF-L943 is a derivative of the clinical isolate 10403S (5) that contains a point mutation in *prfA* (G155S) resulting in the constitutive expression of PrfA-regulated genes, including *plcB* (gene encoding PC-PLC) and *mpl*. All *Listeria* strains were maintained in brain heart infusion (BHI) media. *Escherichia coli* strains containing pPL2-derived plasmids were cultured in Luria-Bertani (LB) media supplemented with chloramphenicol (25 μg/ml). *E. coli* strains harboring pKSV7-derived plasmids were cultured in LB supplemented with ampicillin (100 μg/ml). *L. monocytogenes* strains harboring either pKSV7 or pPL2-derived plasmids were cultured in BHI supplemented with chloramphenicol (10 μg/ml).

Complementation of Mpl. Wild-type Mpl containing a Flag tag at the N-terminus of the catalytic domain (Mpl-$Flag_{N\text{-}cat}$) was amplified from strain HEL-981 (Table 5.1) using primers Marq 413 and 416 (Table 5.2). The 1898-bp product was digested using SalI and

Table 5.1. *L. monocytogenes* strains used in this study

Strain	Genotype & Relevant Features	Source/Ref
NF-L943	*L. monocytogenes prfA* G155S	(31)
HEL-469	Internal in-frame deletion of *mpl* in NF-L943 background	(6)
HEL-883	NF-L943 *mpl* H141A	This study
HEL-981	NF-L943 *mpl*-$Flag_{N\text{-}cat}$	Chapter 3
HEL-986	NF-L943 *mpl* H207G	This study
HEL-987	NF-L943 *mpl* H226T	This study
HEL-1004	NF-L943 *mpl* H226F	This study
HEL-1007	NF-L943 *mpl* H226R	This study
HEL-1195	NF-L943 *mpl* H226F-$Flag_{N\text{-}cat}$	This study
HEL-1214	NF-L943 *mpl* H226E	This study
HEL-1220	NF-L943 *mpl* H387D	This study
HEL-1225	NF-L943 *mpl* H241R	This study
HEL-1235	NF-L943 *mpl* H226R-$Flag_{N\text{-}cat}$	This study
HEL-1272	HEL-469 $tRNA^{Arg}$::pPL2 (*mpl*-$Flag_{N\text{-}cat}$)	This study
HEL-1302	HEL-469 $tRNA^{Arg}$::pPL2 (empty)	This study
HEL-1305	HEL-469 $tRNA^{Arg}$::pPL2 (*mpl* H252N-$Flag_{N\text{-}cat}$)	This study
HEL-1307	HEL-469 $tRNA^{Arg}$::pPL2 (*mpl* E286Q-$Flag_{N\text{-}cat}$)	This study
HEL-1312	HEL-469 $tRNA^{Arg}$::pPL2 (*mpl* C317Y-$Flag_{N\text{-}cat}$)	This study
HEL-1316	HEL-469 $tRNA^{Arg}$::pPL2 (*mpl* H418N-$Flag_{N\text{-}cat}$)	This study
HEL-1342	HEL-469 $tRNA^{Arg}$::pPL2 (*mpl* C317D-$Flag_{N\text{-}cat}$)	This study
HEL-1344	HEL-469 $tRNA^{Arg}$::pPL2 (*mpl* C317V-$Flag_{N\text{-}cat}$)	This study
HEL-1346	HEL-469 $tRNA^{Arg}$::pPL2 (*mpl* C317R-$Flag_{N\text{-}cat}$)	This study
HEL-1348	HEL-469 $tRNA^{Arg}$::pPL2 (*mpl* C317S-$Flag_{N\text{-}cat}$)	This study

Table 5.2. Plasmids[a,b] and oligonucleotide primers[c] used to construct plasmids used in this study

Plasmids	Genotype[c]	Primer Pairs	SOEing Primers	Restriction
pBMF880	pKSV7 *mpl* H141A	316/363, 364/365	316/365	EcoRI, SacI
pBMF984	pKSV7 *mpl* H207G	328/490, 489/491	328/489	EcoRI, PstI
pBMF985	pKSV7 *mpl* H226T	328/492, 489/493	328/489	EcoRI, PstI
pBMF1001	pKSV7 *mpl* H226F	328/499, 489/500	328/489	EcoRI, PstI
pBMF1002	pKSV7 *mpl* H226R	328/501, 489/502	328/489	EcoRI, PstI
pBMF1194	pKSV7 *mpl* H226F-$Flag_{N\text{-}cat}$	328/499, 489/500	328/489	EcoRI, PstI
pBMF1213	pKSV7 *mpl* H226E	328/616, 489/615	328/489	EcoRI, PstI
pBMF1219	pKSV7 *mpl* H387D	237/629, 242/630	237/242	PstI, SstI
pBMF1224	pKSV7 *mpl* H241R	328/636, 489/628	328/489	EcoRI, PstI
pBMF1234	pKSV7 *mpl* H226R-$Flag_{N\text{-}cat}$	328/487, 387/488	328/387	EcoRI, PstI
pBMF1267	pPL2 *mpl*-$Flag_{N\text{-}cat}$	413/416		SalI, EcoRV
pBMF1285	pPL2 *mpl* H252N-$Flag_{N\text{-}cat}$	416/662, 659/663	416/659	BlpI, EcoRV
pBMF1287	pPL2 *mpl* E286Q-$Flag_{N\text{-}cat}$	416/664, 659/665	416/659	BlpI, EcoRV
pBMF1291	pPL2 *mpl* C317Y-$Flag_{N\text{-}cat}$	416/668, 659/669	416/659	BlpI, EcoRV
pBMF1297	pPL2 *mpl* H418N-$Flag_{N\text{-}cat}$	416/672, 659/673	416/659	BlpI, EcoRV
pBMF1334	pPL2 *mpl* C317D-$Flag_{N\text{-}cat}$	416/684, 659/685	416/659	BlpI, EcoRV
pBMF1336	pPL2 *mpl* C317V-$Flag_{N\text{-}cat}$	416/686, 659/687	416/659	BlpI, EcoRV
pBMF1338	pPL2 *mpl* C317R-$Flag_{N\text{-}cat}$	416/682, 659/683	416/659	BlpI, EcoRV
pBMF1340	pPL2 *mpl* C317S-$Flag_{N\text{-}cat}$	416/680, 659/681	416/659	BlpI, EcoRV

[a] = Plasmids pBMF985 through pBMF1213 also carry a silent mutation at *mpl* V227. Plasmid pBMF1224 also carries a silent mutation at *mpl* G243.

[b] = All plasmids that do not have $Flag_{N\text{-}cat}$ were constructed using wild-type 10403S genomic DNA. Plasmids with the exception of pBMF1234 that carry $Flag_{N\text{-}cat}$ were generated from HEL-981. pBMF1234 was generated using HEL-1007 as the DNA template.

[c] = Primer sequences are listed in Table 5.3.

EcoRV, then cloned into the shuttle integration vector pPL2 (19) generating pBMF1267. Sequence integrity of pBMF1267 was verified by sequencing. pBMF1267 was then introduced into the genome of HEL-469 (NF-L943 Δ*mpl*, Table 5.1) by conjugation (27), generating HEL-1272. Cloramphenicol-resistant colonies were screened for integration of pPL2 at the $tRNA^{Arg}$ site using PCR primers PL95 and NC16 (19).

Generation of Mpl point mutants. Site-directed mutagenesis with overlap extension PCR (SOEing PCR) (17) was used to construct single point mutations in the Mpl sequence. To generate Mpl point mutants, two approaches were used. Mutations in histidine residues 141, 207, 226, 241 and 387 were generated in the *Listeria* chromosome by allelic exchange (8) using the shuttle vector pKSV7 (33). Mpl mutants were generated by SOEing PCR using genomic DNA from *L. monocytogenes* and a selection of primers listed in Table 5.3. SOEing PCR products were digested with restriction enzymes and ligated into pKSV7, thus creating a series of plasmids (Table 5.2). Each plasmid was sequenced, then electroporated into NF-L943 to generate a series of strains listed in Table 5.1. Allelic exchange was verified by screening chloramphenicol-sensitive clones for the acquisition or lost of a restriction site within the *mpl* gene as designed with the SOEing primers.

Mutations in Mpl amino acids H252, E286, C317 and H418 relied on cloning Mpl into pPL2, then introducing the plasmid into the chromosome of strain HEL-469. Point mutations were constructed by SOEing PCR using the primers listed in Table 4.3 with HEL-981 as the DNA template. SOEing PCR products were then digested with BlpI and EcoRV and cloned into pBMF1267, thus generating a series of plasmids (Table 5.2). Each plasmid was sequenced

Table 5.3. DNA oligonucleotides primer used in this study

Name	Sequence (5' – 3')
Marq 237	CTGCTGCAGGATTGTTCAAGTGGACG
Marq 242	GGAGCTCGGCCTTCATTTTCACTAAT
Marq 316	TAGAGCTCCACTGCGGAACTAAATTCTG
Marq 328	GTGAATTCGATTCTGTCGGGGAAGAAAA
Marq 363	AGAGTGAAGCTGCAGTGAAAAGTTATGTCG
Marq 364	CGACATAACTTTTCACTGCAGCTTCACTCT
Marq 365	ATGAATTCTACTGCAAAACGTATAATTT
Marq 387	GCACTGCAGCAATTCAAGCCATAATGGAC
Marq 413	CGAGTCGACAGAAGAATTAACAAATGTAAAAG
Marq 416	GCAGATATCGCCTTCATTTTCACTAATTTAT
Marq 487	CTTGTCATCGTCATCCTTGTAATCCTCGGAAAGCATATTTTG
Marq 488	GATTACAAGGATGACGATGACAAGGTAGAACGGGCTGATA
Marq 489	GATAACTGCAGGCGTTAGTTCATGACCA
Marq 490	CTGATACCGGTAAAGATTTTCAAG
Marq 491	CTTGAAAATCTTTACCGGTATCAG
Marq 492	GCCACTAACTGTAATGAAAATTAATG
Marq 493	CATTAATTTTCATTACAGTTAGTGGC
Marq 499	CATTAATTTTCATTACAAATAGTGGC
Marq 500	GCCACTATTTGTAATGAAAATTAATG
Marq 501	CATTAATTTTCATTACACGTAGTGGC
Marq 502	GCCACTACGTGTAATGAAAATTAATG
Marq 615	GCCACTAGAAGTAATGAAAATTAATG
Marq 616	CATTAATTTTCATTACTTCTAGTGGC
Marq 628	GAACTAGGAAAGGCCTCATAAGAAC
Marq 629	ATCCTCACCAATCAACCAGTCATTTG
Marq 630	CAAATGACTGGTTGATTGGTGAGGAT
Marq 636	GTTCTTATGAGGCCTTTCCTAGTTCTATCCACTAAGTAAAATAGG
Marq 659	ATTTTTGCTGAGCCGGAAGTTGCGAGTTG
Marq 662	GAACTTTTGATTTAAAAAATAATACCGACACTTCGT
Marq 663	ACGAAGTGTCGGTATTATTTTTTAAATCAAAAGTTC
Marq 664	CTCATTTTTACGCAAGTCAAGTGTACGAATACTATA
Marq 665	TATAGTATTCGTACACTTGACTTGCGTAAAAATGAG
Marq 668	CATTATGGCTTGAATTACAATAATGCCTTTTGGGAT
Marq 669	ATCCCAAAAGGCATTATTGTAATTCAAGCCATAATG
Marq 670	GACAAATATAATCAAGCGGCTATGAAGGATTAC
Marq 671	GCGATTCGTAATCCTTCATAGCCGCTTGATTAT
Marq 672	ATATAATCAAGCGGCTAATATGAAGGATTACGAATC
Marq 673	GATTCGTAATCCTTCATATTAGCCGCTTGATTATA
Marq 680	CATTATGGCTTGAATTCGAATAATGCCTTTTGGGAT
Marq 681	ATCCCAAAAGGCATTATTCGAATTCAAGCCATAATG
Marq 682	CATTATGGCTTGAATCGCAATAATGCCTTTTGGGAT
Marq 683	ATCCCAAAAGGCATTATTGCGATTCAAGCCATAATG
Marq 684	CATTATGGCTTGAATGACAATAATGCCTTTTGGGAT
Marq 685	ATCCCAAAAGGCATTATTGTCATTCAAGCCATAATG
Marq 686	CATTATGGCTTGAATGTAAATAATGCCTTTTGGGAT
Marq 687	ATCCCAAAAGGCATTATTTACATTCAAGCCATAATG

and then introduced into the genome of HEL-469 by conjugation, thus generating a series of strains (Table 5.1).

Metabolic Labeling & Immunoprecipitation Assays. Metabolic labeling and immunoprecipitation of PC-PLC and Mpl was performed as described previously (26, 32). *Listeria*-infected J774 mouse macrophage-like cells were pulse labeled using [^{35}S]-methionine/cysteine. Radiolabeled cells were incubated in a nigericin-supplemented, potassium buffer equilibrated to either physiological or acidic pH. Chloramphenicol (20 μg/ml) and tetracycline (50 μg/ml) were present during this chase to inhibit further bacterial protein synthesis. Host cell lysates were then separated from intracellular bacteria by centrifugation. Secreted PC-PLC and Mpl were immunoprecipitated from the cleared host cell lysates. Immunoprecipitates were resolved on a 12% SDS polyacrylamide gel and detected by autoradiography.

Quantification of Mpl intracellular activity. The intracellular activity of Mpl at acidic pH was quantified by measuring (i) the secretion of mature Mpl, and (ii) PC-PLC maturation. Levels of detected Mpl and PC-PLC species from the immunoprecipitation assays were measured using ImageJ (http://rsbweb.nih.gov/ij/). Band intensities were normalized to the number of methionine and cysteine residues in each protein species. Evaluation of mature Mpl secretion was determined by determining the relative ratio of catalytic and propeptide domains secreted between each Mpl species and wild-type Mpl. Efficacy of PC-PLC maturation was determined as described previously by calculating the ratio of mature PC-PLC to the sum of pro and mature PC-PLC (32).

Immunofluorescence Assays. Detection of bacterium-associated Mpl was detected by immunofluorescence as described in chapter 3. Briefly, HeLa cells were infected with *L. monocytogenes* strains expressing Mpl-$Flag_{N\text{-}cat}$ mutants. Four hours post-infection, infected cells were incubated in nigericin-supplemented potassium buffer equilibrated to either pH 7.3 or pH 6.5. HeLa cells were fixed and the cell walls of intracellular bacteria were partially digested using purified Ply118, a *L. monocytogenes*-specific phage endolysin (20). Mpl-$Flag_{N\text{-}cat}$ was detected using either anti-Flag M1 or M2 antibodies (Sigma), followed by a secondary antibody conjugated to fluorescein isothiocyanate. *Listeria* was detected using Bis-benzimide (Hoechst 33258).

RESULTS

Identification of candidate amino acids important for Mpl activity. Mpl is produced as a secreted 55kDa zymogen, with its propeptide composed of amino acid residues 25 through 200 and its catalytic domain composed of amino acid residues 201 through 510. Since Mpl activity has been observed to be influenced by pH (chapter 3), we sought to identify residues that would have a titratable side group with a predicted pK_a in the physiological pH range (6.0 - 7.4) and contribute to the intracellular activity of Mpl. We excluded residues that were part of the active site. One amino acid that can act as a pH sensor residue is histidine. Histidine's imidazole ring has a pK_a of approximately 6.0. Upon protonation, the imidazole ring loses its hydrophobic character, and can participate in intra- and intermolecular hydrogen bonding. Although histidine's imidazole ring is the only amino acid whose side group pK_a is in this

range, other amino acid side group pK_a's can be influenced by neighboring amino acids in the protein's tertiary structure. Currently, a crystal structure of Mpl has not been resolved. Therefore, we constructed homology models of the catalytic domain of Mpl based off the crystal structure of aureolysin from the Gram-positive bacterium *Staphylococcus aureus* (PDB # 1BQB, 46% sequence identity) (Figure 5.1) and thermolysin from *B. thermoproteolyticus* (PDB # 2TMN, 45.2% sequence identity) using SWISS-MODEL (1, 15, 30). The homology models constructed were similar to a previously published homology model of Mpl (9). We used an *in silico* approach to determined the titratable amino acid side group pK_a values. We submitted our Mpl homology models to PROPKA 3.0 (http://propka.ki.ku.dk/), an online interface that determines pK_a values for solvent exposed titratable side groups. PROPKA calculates pK_a values based on the environment where the amino acid is located in the tertiary structure. Environmental factors that influence pK_a values include whether the residue (i) is buried or solvent exposed, (ii) participates in any hydrogen bonding or (iii) has electrostatic interactions with neighboring amino acids. Amino acids with pK_a values in the physiological pH range that were identified included H226, H241, H252, E286, C317 and H387 (Figure 5.1).

Our homology model only covered amino acid residues 223 through 510. Since a crystal structure of a thermolysin-like metalloprotease propeptide or zymogen is unavailable for a homology model to be constructed, we were unable to determine if any non-histidine amino acids would have predicted pK_a values in the physiological pH range in the propeptide or the first 22 amino acids of the catalytic domain. Therefore, we additionally focused our study on residues H141 in the propeptide and residue H207 in the catalytic domain. To determine what

mutations to construct in these residues, we performed a CLUSTALW alignment using the ConSeq server (http://conseq.bioinfo.tau.ac.il/) (4). We aligned the primary sequence of Mpl to other metalloproteases found in both Gram-positive and Gram-negative bacteria (Figure 5.2). Single point mutations were made to change the targeted amino acids to either closely structured residues or residues that were found in other metalloproteases. Mutations were made using either allelic exchange (8) or by cloning the *mpl* promoter region and ORF sequence containing the desired mutation into the shuttle vector pPL2. The pPL2-derived plasmid was then introduced into the chromosome of a *Listeria* strain containing an isogenic deletion of Mpl.

To assess the role of the selected amino acids on the activity of Mpl, we looked at pH-dependent Mpl autocatalysis and maturation of PC-PLC during intracellular infection. Infected cells were pulse-labeled with [^{35}S]-met and chased in nigericin-containing buffer at physiological or acidic pH. Nigericin is a potassium ionophore that allows for the equilibration of pH across all biological membranes. Therefore, the chase mimics the conditions intracellular bacteria would experience in the cytosol of host cells (physiological pH) or in vacuoles (acidic pH). After the chase, Mpl and PC-PLC were immunoprecipitated from host cell lysates. At physiological pH, both proteins remain largely bacterium-associated in their proform (Figure 5.3, lane 1). Under acidic conditions, the catalytic domain and propeptide of Mpl are secreted into the host cytosol (Figure 5.3, lane 2), as well as the mature form of PC-PLC. The intracellular behavior of wild-type and mutant Mpl species at acidic pH was evaluated by measuring the relative ratio of secreted mature form to propeptide (Table 4.4). For wild-type Mpl, the actual ratio was 1:1.7±0.3 (n=10), suggesting that the

Figure 5.2. CLUSTALW alignment of Mpl to other metalloproteases. The primary sequence of Mpl was aligned to other bacterial metalloproteases using a BLOSUM protein matrix. Alignment includes elastase (*Staphylococcus epidermidis*); aureolysin (*Staphylococcus aureus*); bacillolysin (*Bacillus subtilis* subsp. *amylosacchariticus*); thermolysin (*Bacillus thermoproteolyticus*) and vibriolysin (*Vibrio cholerae*). Numbers on left indicate amino acid positions. Amino acids targeted in this study are boxed. Underlined amino acids represent the HEXXH consensus sequence in zincin metalloproteases. * indicates catalytic residues.

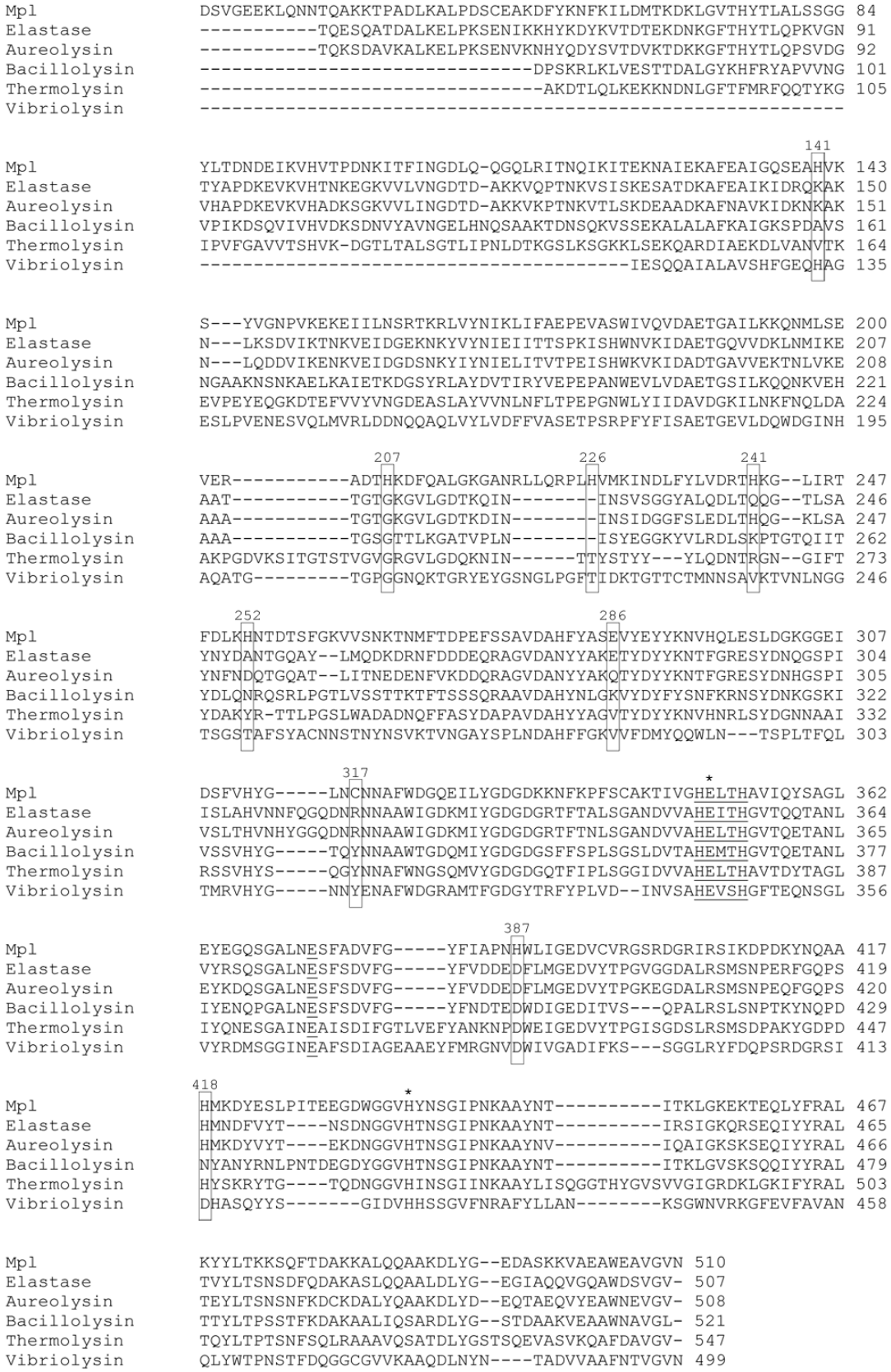
Mpl DSVGEEKLQNNTQAKKTPADLKALPDSCEAKDFYKNFKILDMTKDKLGVTHYTLALSSGG 84
Elastase ----------TQESQATDALKELPKSENIKKHYKDYKVTDTEKDNKGFTHYTLQPKVGN 91
Aureolysin ----------TQKSDAVKALKELPKSENVKNHYQDYSVTDVKTDKKGFTHYTLQPSVDG 92
Bacillolysin ---------------------------------DPSKRLKLVESTTDALGYKHFRYAPVVNG 101
Thermolysin ---------------------------------AKDTLQLKEKKNDNLGFTFMRFQQTYKG 105
Vibriolysin --
141
Mpl YLTDNDEIKVHVTPDNKITFINGDLQ-QGQLRITNQIKITEKNAIEKAFEAIGQSEAHVK 143
Elastase TYAPDKEVKVHTNKEGKVVLVNGDTD-AKKVQPTNKVSISKESATDKAFEAIKIDRQKAK 150
Aureolysin VHAPDKEVKVHADKSGKVVLINGDTD-AKKVKPTNKVTLSKDEAADKAFNAVKIDKNKAK 151
Bacillolysin VPIKDSQVIVHVDKSDNVYAVNGELHNQSAAKTDNSQKVSSEKALALAFKAIGKSPDAVS 161
Thermolysin IPVFGAVVTSHVK-DGTLTALSGTLIPNLDTKGSLKSGKKLSEKQARDIAEKDLVANVTK 164
Vibriolysin --IESQQAIALAVSHFGEQHAG 135
Mpl S---YVGNPVKEKEIILNSRTKRLVYNIKLIFAEPEVASWIVQVDAETGAILKKQNMLSE 200
Elastase N---LKSDVIKTNKVEIDGEKNKYVYNIEIITTSPKISHWNVKIDAETGQVVDKLNMIKE 207
Aureolysin N---LQDDVIKENKVEIDGDSNKYIYNIELITVTPEISHWKVKIDADTGAVVEKTNLVKE 208
Bacillolysin NGAAKNSNKAELKAIETKDGSYRLAYDVTIRYVEPEPANWEVLVDAETGSILKQQNKVEH 221
Thermolysin EVPEYEQGKDTEFVVYVNGDEASLAYVVNLNFLTPEPGNWLYIIDAVDGKILNKFNQLDA 224
Vibriolysin ESLPVENESVQLMVRLDDNQQAQLVYLVDFFVASETPSRPFYFISAETGEVLDQWDGINH 195
207
226
241
Mpl VER----------ADTHKDFQALGKGANRLLQRPLHVMKINDLFYLVDRTHKG--LIRT 247
Elastase AAT----------TGTGKGVLGDTKQIN--------INSVSGGYALQDLTQQG--TLSA 246
Aureolysin AAA----------TGTGKGVLGDTKDIN--------INSIDGGFSLEDLTHQG--KLSA 247
Bacillolysin AAA----------TGSGTTLKGATVPLN--------ISYEGGKYVLRDLSKPTGTQIIT 262
Thermolysin AKPGDVKSITGTSTVGVGRGVLGDQKNIN------TTYSTYY---YLQDNTRGN--GIFT 273
Vibriolysin AQATG---------TGPGGNQKTGRYEYGSNGLPGFTIDKTGTTCTMNNSAVKTVNLNGG 246
252
286
Mpl FDLKHNTDTSFGKVVSNKTNMFTDPEFSSAVDAHFYASEVYEYYKNVHQLESLDGKGGEI 307
Elastase YNYDANTGQAY--LMQDKDRNFDDDEQRAGVDANYYAKETYDYYKNTFGRESYDNQGSPI 304
Aureolysin YNFNDQTGQAT--LITNEDENFVKDDQRAGVDANYYAKQTYDYYKNTFGRESYDNHGSPI 305
Bacillolysin YDLQNRQSRLPGTLVSSTTKTFTSSSQRAAVDAHYNLGKVYDYFYSNFKRNSYDNKGSKI 322
Thermolysin YDAKYR-TTLPGSLWADADNQFFASYDAPAVDAHYYAGVTYDYYKNVHNRLSYDGNNAAI 332
Vibriolysin TSGSTAFSYACNNSTNYNSVKTVNGAYSPLNDAHFFGKVVFDMYQQWLN---TSPLTFQL 303
317
*
Mpl DSFVHYG-----LNCNNAFWDGQEILYGDGDKKNFKPFSCAKTIVGHELTHAVIQYSAGL 362
Elastase ISLAHVNNFQGQDNRNNAAWIGDKMIYGDGDGRTFTALSGANDVVAHEITHGVTQQTANL 364
Aureolysin VSLTHVNHYGGQDNRNNAAWIGDKMIYGDGDGRTFTNLSGANDVVAHELTHGVTQETANL 365
Bacillolysin VSSVHYG-----TQYNNAAWTGDQMIYGDGDGSFFSPLSGSLDVTAHEMTHGVTQETANL 377
Thermolysin RSSVHYS-----QGYNNAFWNGSQMVYGDGDGQTFIPLSGGIDVVAHELTHAVTDYTAGL 387
Vibriolysin TMRVHYG-----NNYENAFWDGRAMTFGDGYTRFYPLVD--INVSAHEVSHGFTEQNSGL 356
387
Mpl EYEGQSGALNESFADVFG-----YFIAPNHWLIGEDVCVRGSRDGRIRSIKDPDKYNQAA 417
Elastase VYRSQSGALNESFSDVFG-----YFVDDEDFLMGEDVYTPGVGGDALRSMSNPERFGQPS 419
Aureolysin EYKDQSGALNESFSDVFG-----YFVDDEDFLMGEDVYTPGKEGDALRSMSNPEQFGQPS 420
Bacillolysin IYENQPGALNESFSDVFG-----YFNDTEDWDIGEDITVS---QPALRSLSNPTKYNQPD 429
Thermolysin IYQNESGAINEAISDIFGTLVEFYANKNPDWEIGEDVYTPGISGDSLRSMSDPAKYGDPD 447
Vibriolysin VYRDMSGGINEAFSDIAGEAAEYFMRGNVDWIVGADIFKS---SGGLRYFDQPSRDGRSI 413
418
*
Mpl HMKDYESLPITEEGDWGGVHYNSGIPNKAAYNT----------ITKLGKEKTEQLYFRAL 467
Elastase HMNDFVYT----NSDNGGVHTNSGIPNKAAYNT----------IRSIGKQRSEQIYYRAL 465
Aureolysin HMKDYVYT----EKDNGGVHTNSGIPNKAAYNV----------IQAIGKSKSEQIYYRAL 466
Bacillolysin NYANYRNLPNTDEGDYGGVHTNSGIPNKAAYNT----------ITKLGVSKSQQIYYRAL 479
Thermolysin HYSKRYTG----TQDNGGVHINSGIINKAAYLISQGGTHYGVSVVGIGRDKLGKIFYRAL 503
Vibriolysin DHASQYYS-------GIDVHHSSGVFNRAFYLLAN--------KSGWNVRKGFEVFAVAN 458
Mpl KYYLTKKSQFTDAKKALQQAAKDLYG--EDASKKVAEAWEAVGVN 510
Elastase TVYLTSNSDFQDAKASLQQAALDLYG--EGIAQQVGQAWDSVGV- 507
Aureolysin TEYLTSNSNFKDCKDALYQAAKDLYD--EQTAEQVYEAWNEVGV- 508
Bacillolysin TTYLTPSSTFKDAKAALIQSARDLYG--STDAAKVEAAWNAVGL- 521
Thermolysin TQYLTPTSNFSQLRAAAVQSATDLYGSTSQEVASVKQAFDAVGV- 547
Vibriolysin QLYWTPNSTFDQGGCGVVKAAQDLNYN----TADVVAAFNTVGVN 499

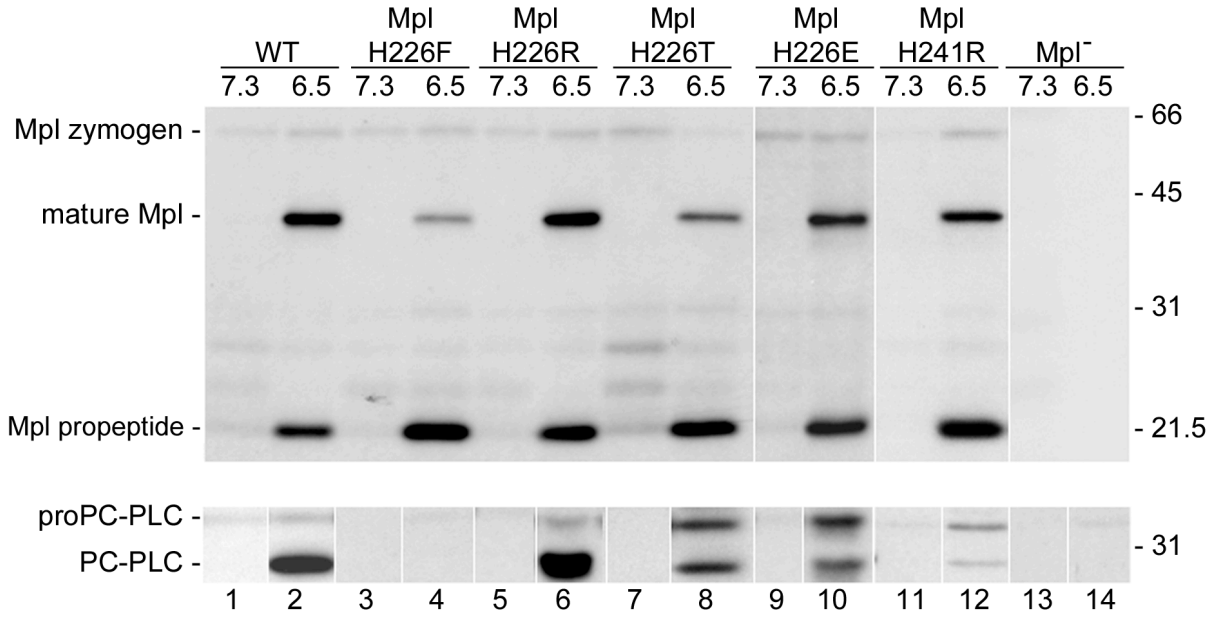

Figure 5.3. Intracellular activity of Mpl H226 and H241 mutants. Infected J774 cells were radiolabeled and chased in a potassium buffer equilibrated to either pH 7.3 or pH 6.5 and supplemented with nigericin. The intracellular activity of wild-type Mpl (WT) and Mpl mutants was assessed by immunoprecipitating Mpl (top panels) and PC-PLC (bottom panels) from cleared host lysates. Numbers on right indicate molecular mass markers (in kDa). Lanes: 1 and 2, 10403S; 3 and 4, HEL-1004; 5 and 6, HEL-1007; 7 and 8, HEL-987; 9 and 10, HEL-1214; 11 and 12, HEL-1225; 13 and 14, HEL-469.

propeptide is either secreted more efficiently or is more stable than the catalytic domain. The efficacy of Mpl-mediated maturation of PC-PLC was quantified by determining the ratio of mature form to mature and proform secreted at acidic pH. As previously reported, the ratio of PC-PLC maturation by wild-type Mpl at acidic pH was 0.92 (32). With the exception of residues H226 and H241 as described below, the mutations in Mpl generated in this study did not significantly alter Mpl activity.

A positive charge is necessary at residue 226 for the efficient secretion of Mpl catalytic domain and processing of PC-PLC. Aligning the primary structure of Mpl to other metalloproteases revealed that at position H226, other metalloproteases have threonine in this position (Figure 5.2). Mpl H226T was able to undergo pH-dependent autocatalysis (Figure 5.3, lanes 7 and 8), but exhibited a 2-fold defect in the secretion of mature Mpl as determined by the relative ratio of mature form to propeptide (Table 5.4). In addition, Mpl H226T did not process PC-PLC efficiently as determined by an increased level of proform being secreted (Table 5.4 and Figure 5.3, compare lanes 2 and 8). To further understand how H226 contributes to the intracellular activity of Mpl, we generated additional point mutants. Since threonine has a polar uncharged side group, we generated H226F, H226R, and H226E to assess the effect of a hydrophobic, basic or acidic side groups at that position, respectively. All Mpl H226 mutants demonstrated pH-dependent autocatalysis (Figure 5.3, lanes 3-10). However, while similar levels of Mpl propeptide were detected amongst the H226 mutants, there were varying amounts of catalytic domain being secreted. Mpl H226R behaved similar to wild-type Mpl, whereas Mpl H226E behaved like Mpl H226T.

Table 5.4. Secretion of mature Mpl and efficacy of PC-PLC maturation by *L. monocytogenes* strains expressing mutated Mpl species

Mpl	Relative ratio ± SEM of Mpl catalytic and propeptide domains secreted at acidic pH (n)	Ratio ± SEM of PC-PLC maturation at acidic pH (n)
wild-type	1.00 ± 0.07 (10)	0.92 ± 0.01 (6)
H226F	0.09 ± 0.02 (5)	Not detected
H226T	0.46 ± 0.07 (4)	0.56 (1)
H226R	0.95 ± 0.13 (4)	0.95 (1)
H226E	0.52 ± 0.06 (4)	0.49 (1)
H241R	0.51 (1)	0.37 ± 0.10 (2)
Mpl^-	Not detected	Not detected

Mpl H226E had a 2-fold decrease in the amount of secreted catalytic domain and in the efficiency of PC-PLC processing. Mpl H226F had a pronounced defect. Mpl H226F had more than a 10-fold decrease in the amount of secreted catalytic domain and no PC-PLC was secreted in response to a decrease in pH.

The phenotype of the Mpl H226F mutant suggested that either the catalytic domain is rapidly degraded following autocatalysis or that it remains bacterium-associated. To address this question, we performed an immunofluorescence assay with antibodies that can distinguish the mature form of Mpl from the zymogen. For this assay we utilized an Mpl species that has a Flag tag at the N-terminus of the catalytic domain ($Flag_{N\text{-}cat}$). Monoclonal antibody M1 recognizes N-terminal Flag and will detect Mpl that has undergone autocatalysis, hence the mature form. Monoclonal antibody M2 recognizes a Flag tag anywhere in the protein and therefore will recognize either the zymogen or mature form of Mpl. Wild-type Mpl, Mpl H226F and Mpl H226R were tagged with $Flag_{N\text{-}cat}$. As previously reported, wild-type Mpl-$Flag_{N\text{-}cat}$ was detected associated with bacterial staining at pH 7.3 only when M2 was utilized, (Figure 5.4A, panels 1 -4) (chapter 3). This demonstrates that the zymogen is bacterium-associated under these conditions. Neither antibody could detect Mpl-$Flag_{N\text{-}cat}$ in cells treated at acidic pH, indicating that the protein had been secreted (Figure 5.4A, panels 5 -8). Similarly, Mpl H226F-$Flag_{N\text{-}cat}$ was detected bacterium associated by the M2 antibody at pH 7.3 (Figure 5.4B, panels 1 -4). However, contrary to wild-type, Mpl H226F remained bacterium-associated following a drop in intracellular pH, and the protein was detected by both antibodies (Figure 5.4B, panels 5-8).

Figure 5.4. A positive charge at residue 226 is necessary for the efficient secretion of Mpl. Infected HeLa cells were incubated in a potassium buffer supplemented with nigericin and equilibrated to either pH 7.3 or pH 6.5. Mpl-$Flag_{N\text{-}cat}$ was detected using either α-Flag M1 or M2 antibodies. Bacteria and host nuclei were detected using bis-benzamide (Hoechst 33258). (A) HEL-981; (B) HEL-1195; (C) HEL-1235.

(A) Mpl-Flag$_{N\text{-}cat}$

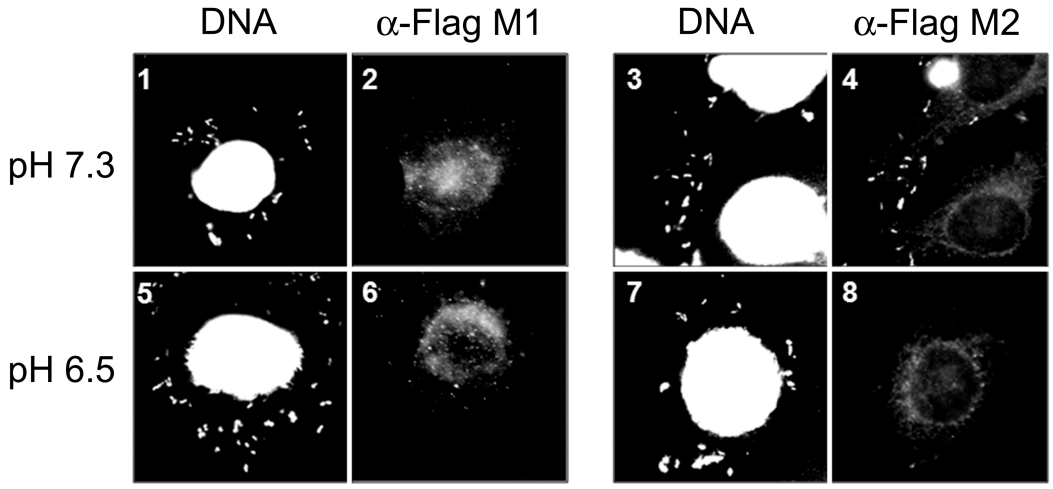

(B) Mpl H226F-Flag$_{N\text{-}cat}$

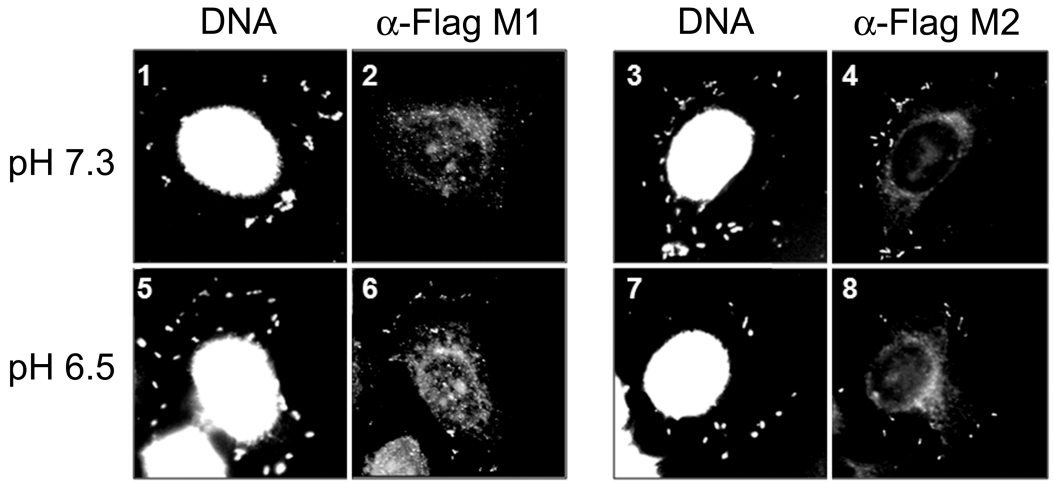

(C) Mpl H226R-Flag$_{N\text{-}cat}$

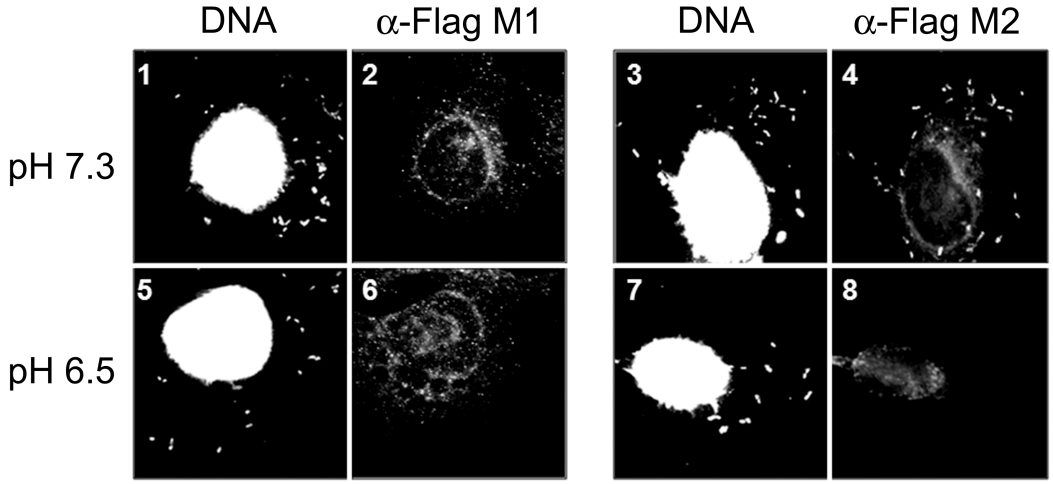

These results suggested that upon a decrease in pH, Mpl H226F undergoes autocatalysis, but the catalytic domain remains bacterium-associated, whereas the propeptide is secreted. The phenotype of Mpl H226R-Flag$_{N\text{-}cat}$ was the same as wild type Mpl-Flag$_{N\text{-}cat}$ (Figure 5.4C). Taken together, these results suggested that a positive charge on the side group of H226 is necessary for secretion of Mpl catalytic domain and for enzymatic activity on a non-self substrate.

A positive residue is detrimental at position 241 for efficient processing of PC-PLC. The CLUSTALW alignment revealed that metalloproteases do not have a conserved amino acid at position 241 (Figure 5.2). However, we noted that both thermolysin and bacillolysin had a positively charged amino acid at this location. Therefore, we chose to mutate H241 to arginine. Mpl H241R was able to undergo autocatalysis at acidic pH (Figure 5.3, lanes 11 and 12). This mutant had a 2-fold decrease in the amount of secreted catalytic domain and was defective in processing PC-PLC (Table 5.4). In addition, low levels of PC-PLC were detected from host cells infected with this mutant (Figure 5.3, lanes 11 and 12). Taken together, these results indicate that H241 also contributes to Mpl activity and that a positive residue is detrimental at this location.

DISCUSSION

During its intracellular lifecycle, *L. monocytogenes* relies on PC-PLC to aid in escape from double-membrane vacuoles formed during cell-to-cell spread. PC-PLC is produced as an inactive proprotein that is translocated across the cell wall and accumulates in the periplasmic

space. Maturation and secretion of PC-PLC across the bacterial cell wall is dependent upon Mpl (38). Mpl is a thermolysin-like metalloprotease that is produced as a zymogen. Upon a decrease in vacuolar pH, Mpl undergoes intramolecular autocatalysis and cleaves the propeptide of PC-PLC ((6), chapter 3). In this study, we generated a series of Mpl point mutants to identify amino acid residues outside of the active site that contribute to Mpl's functions. None of the mutants tested affected Mpl's ability to undergo pH-dependent autocatalysis, which is indicative that the mutants were properly folded and catalytically active. However, we identified two amino acids, H226 and H241, that regulate Mpl secretion and its ability to generate active PC-PLC. These two residues are located approximately seven Å apart in two random coil loops on the same side as the active site pocket. Interestingly, a positive charge is required at position 226, whereas a positive charge at residue 241 has detrimental effects on Mpl.

Residues H226 and H241 are important for the secretion of Mpl. Although we showed mature Mpl H226F to be bacterium-associated at acidic pH, we have not yet determined whether Mpl H241 is also bacterium-associated. Our data suggests that a hydrophobic residue may be preferred at position 241 along with a positive charge at residue 226. The retention of these Mpl mutants may be due to mature Mpl associating with other cell envelope proteins. One such candidate is PrsA2. Previous results have suggested that PrsA2 may serve as an anchor for PC-PLC and the Mpl zymogen (chapter 4). Perhaps upon autocatalysis, the mature Mpl mutants are unable to dissociate from PrsA2 and pass through the cell wall. Similarly, the Mpl mutants may be participating in an improper protein-protein interaction within the cell envelope. If H226 is deprotonated at physiological pH, then this amino acid

may act as a pH sensor for Mpl secretion following autocatalysis. pH sensors have been identified in regulating protein folding and secretion from Type III secretion effectors from Gram-negative bacteria (10, 39). However, the crystal structure of Mpl has not been resolved and therefore the pK_a of H226 has not yet been determined.

Several negatively charged and hydrophobic residues on PC-PLC's propeptide are necessary for Mpl-mediated maturation of PC-PLC (32). Results from this study suggest that a positive charge at position 226 and possibly a hydrophobic residue at position 241 are preferred for Mpl-mediated activation of PC-PLC. Taken together, these results indicate that there may be an electrostatic interaction between the propeptide of PC-PLC and Mpl. Perhaps upon autocatalysis, mature Mpl is able to displace the propeptide of PC-PLC from PrsA2. Free PC-PLC can then be cleaved by mature Mpl. This model would explain why Mpl is still necessary for PC-PLC to be efficiently secreted, independent of propeptide removal (38). Perhaps following autocatalysis, the change in charge at the N-terminus of mature Mpl prevents the protein from interacting efficiently with the propeptide of PC-PLC. If this hypothesis is true, then we would expect to find PC-PLC bacterium-associated in its proform under acidic conditions in these *mpl* mutants. Future work will be focused on testing this hypothesis.

In conclusion, our data demonstrates that the mere event of Mpl autocatalysis does not lead to processing of PC-PLC. Both H226 and H241 influence the interaction of Mpl with the cell envelope and with PC-PLC. Mutations in these residues could be used as a tool for us to

better understand the contribution of charge to Mpl-mediated processing and secretion of PC-PLC.

REFERENCES

1. **Arnold, K., L. Bordoli, J. Kopp, and T. Schwede.** 2006. The SWISS-MODEL workspace: a web-based environment for protein structure homology modelling. Bioinformatics **22:**195-201.

2. **Banbula, A., J. Potempa, J. Travis, C. Fernandez-Catalan, K. Mann, R. Huber, W. Bode, and F. Medrano.** 1998. Amino-acid sequence and three-dimensional structure of the Staphylococcus aureus metalloproteinase at 1.72 A resolution. Structure **6:**1185-93.

3. **Beaumont, A., M. J. O'Donohue, N. Paredes, N. Rousselet, M. Assicot, C. Bohuon, M. C. Fournie-Zaluski, and B. P. Roques.** 1995. The role of histidine 231 in thermolysin-like enzymes. A site-directed mutagenesis study. J. Biol. Chem. **270:**16803-8.

4. **Berezin, C., F. Glaser, J. Rosenberg, I. Paz, T. Pupko, P. Fariselli, R. Casadio, and N. Ben-Tal.** 2004. ConSeq: the identification of functionally and structurally important residues in protein sequences. Bioinformatics **20:**1322-4.

5. **Bishop, D. K., and D. J. Hinrichs.** 1987. Adoptive transfer of immunity to *Listeria monocytogenes*. The influence of *in vitro* stimulation on lymphocyte subset requirements. J. Immunol. **139:**2005-2009.

6. **Bitar, A. P., M. Cao, and H. Marquis.** 2008. The metalloprotease of *Listeria monocytogenes* is activated by intramolecular autocatalysis. J. Bacteriol. **190:**107-11.

7. **Blumberger, J., G. Lamoureux, and M. L. Klein.** 2007. Peptide Hydrolysis in Thermolysin: Ab Initio QM/MM Investigation of the Glu143-Assisted Water Addition Mechanism. J. Chem. Theory Comput. **3:**1837-1850.

8. **Camilli, A., L. G. Tilney, and D. A. Portnoy.** 1993. Dual roles of *plcA* in *Listeria monocytogenes* pathogenesis. Mol. Microbiol. **8:**143-57.

9. **Coffey, A., B. van den Burg, R. Veltman, and T. Abee.** 2000. Characteristics of the biologically active 35-kDa metalloprotease virulence factor from *Listeria monocytogenes*. J. Appl. Microbiol. **88:**132-41.

10. **Dawson, J. E., J. Seckute, S. De, S. A. Schueler, A. B. Oswald, and L. K. Nicholson.** 2009. Elucidation of a pH-folding switch in the *Pseudomonas syringae* effector protein AvrPto. Proc. Natl. Acad. Sci. USA **106:**8543-8.

11. **Feder, J., L. R. Garrett, and B. S. Wildi.** 1971. Studies on the role of calcium in thermolysin. Biochemistry **10:**4552-6.

12. **Feliciangeli, S. F., L. Thomas, G. K. Scott, E. Subbian, C. H. Hung, S. S. Molloy, F. Jean, U. Shinde, and G. Thomas.** 2006. Identification of a pH sensor in the furin propeptide that regulates enzyme activation. J. Biol. Chem. **281:**16108-16.

13. **Fritz, R., K. Stiasny, and F. X. Heinz.** 2008. Identification of specific histidines as pH sensors in flavivirus membrane fusion. J. Cell Biol. **183:**353-61.

14. **Gao, X., J. Wang, D. Q. Yu, F. Bian, B. B. Xie, X. L. Chen, B. C. Zhou, L. H. Lai, Z. X. Wang, J. W. Wu, and Y. Z. Zhang.** 2010. Structural basis for the autoprocessing of zinc metalloproteases in the thermolysin family. Proc. Natl. Acad. Sci. USA **107:**17569-74.

15. **Guex, N., and M. C. Peitsch.** 1997. SWISS-MODEL and the Swiss-PdbViewer: an environment for comparative protein modeling. Electrophoresis **18:**2714-23.

16. **Hase, C. C., and R. A. Finkelstein.** 1993. Bacterial extracellular zinc-containing metalloproteases. Microbiol. Rev. **57:**823-37.

17. **Ho, S. N., H. D. Hunt, R. M. Horton, J. K. Pullen, and L. R. Pease.** 1989. Site-directed mutagenesis by overlap extension using the polymerase chain reaction. Gene **77:**51-59.

18. **Holmes, M. A., and B. W. Matthews.** 1982. Structure of thermolysin refined at 1.6 A resolution. J. Mol. Biol. **160:**623-639.

19. **Lauer, P., M. Y. Chow, M. J. Loessner, D. A. Portnoy, and R. Calendar.** 2002. Construction, characterization, and use of two *Listeria monocytogenes* site-specific phage integration vectors. J. Bacteriol. **184:**4177-4186.

20. **Loessner, M. J., A. Schneider, and S. Scherer.** 1996. Modified *Listeria* bacteriophage lysin genes (*ply*) allow efficient overexpression and one-step purification of biochemically active fusion proteins. Appl. Environ. Microbiol. **62:**3057-60.

21. **Marquis, H., and E. J. Hager.** 2000. pH-regulated activation and release of a bacteria-associated phospholipase C during intracellular infection by *Listeria monocytogenes*. Mol. Microbiol. **35:**289-98.

22. **Matthews, B. W.** 1988. Structual Basis of the Action of Thermolysin and Related Zinc Peptidases. Acc. Chem. Res **21:**333-340.

23. **Matthews, B. W., J. N. Jansonius, P. M. Colman, B. P. Schoenborn, and D. Dupourque.** 1972. Three-dimensional structure of thermolysin. Nat. New Biol. **238:**37-41.

24. **Mengaud, J., C. Geoffroy, and P. Cossart.** 1991. Identification of a new operon involved in *Listeria monocytogenes* virulence: its first gene encodes a protein homologous to bacterial metalloproteases. Infect. Immun. **59:**1043-1049.

25. **Miyoshi, S., and S. Shinoda.** 2000. Microbial metalloproteases and pathogenesis. Microbes Infect. **2:**91-8.

26. **O'Neil, H. S., B. M. Forster, K. L. Roberts, A. J. Chambers, A. P. Bitar, and H. Marquis.** 2009. The propeptide of the metalloprotease of *Listeria monocytogenes* controls compartmentalization of the zymogen during intracellular infection. J. Bacteriol. **191:**3594-603.

27. **O'Neil, H. S., and H. Marquis.** 2006. *Listeria monocytogenes* flagella are used for motility, not as adhesins, to increase host cell invasion. Infect. Immun. **74:**6675-81.

28. **Pelmenschikov, V., M. R. Blomberg, and P. E. Siegbahn.** 2002. A theoretical study of the mechanism for peptide hydrolysis by thermolysin. J. Biol. Inorg. Chem. **7:**284-98.

29. **Schuerch, D. W., E. M. Wilson-Kubalek, and R. K. Tweten.** 2005. Molecular basis of listeriolysin O pH dependence. Proc. Natl. Acad. Sci. USA **102:**12537-12542.

30. **Schwede, T., J. Kopp, N. Guex, and M. C. Peitsch.** 2003. SWISS-MODEL: An automated protein homology-modeling server. Nucleic Acids Res. **31:**3381-5.

31. **Shetron-Rama, L. M., K. Mueller, J. M. Bravo, H. G. Bouwer, S. S. Way, and N. E. Freitag.** 2003. Isolation of *Listeria monocytogenes* mutants with high-level *in vitro* expression of host cytosol-induced gene products. Mol. Microbiol. **48:**1537-1551.

32. **Slepkov, E. R., A. Pavinski Bitar, and H. Marquis.** 2010. Differentiation of propeptide residues regulating the compartmentalization, maturation and activity of the broad-range phospholipase C of *Listeria monocytogenes*. Biochem. J. **432:**557-63.

33. **Smith, K., and P. Youngman.** 1992. Use of a new integrational vector to investigate compartment-specific expression of the *Bacillus subtilis spoIIM* gene. Biochimie **74:**705-711.

34. **Snyder, A., and H. Marquis.** 2003. Restricted translocation across the cell wall regulates secretion of the broad-range phospholipase C of *Listeria monocytogenes*. J. Bacteriol. **185:**5953-8.

35. **Srivastava, J., D. L. Barber, and M. P. Jacobson.** 2007. Intracellular pH sensors: design principles and functional significance. Physiology (Bethesda) **22:**30-9.

36. **Tilney, L. G., and D. A. Portnoy.** 1989. Actin filaments and the growth, movement, and spread of the intracellular bacterial parasite, *Listeria monocytogenes*. J. Cell Biol. **109:**1597-608.

37. **Vazquez-Boland, J. A., M. Kuhn, P. Berche, T. Chakraborty, G. Dominguez-Bernal, W. Goebel, B. Gonzalez-Zorn, J. Wehland, and J. Kreft.** 2001. *Listeria* pathogenesis and molecular virulence determinants. Clin. Microbiol. Rev. **14:**584-640.

38. **Yeung, P. S., N. Zagorski, and H. Marquis.** 2005. The metalloprotease of *Listeria monocytogenes* controls cell wall translocation of the broad-range phospholipase C. J. Bacteriol. **187:**2601-8.

39. **Yu, X. J., K. McGourty, M. Liu, K. E. Unsworth, and D. W. Holden.** 2010. pH sensing by intracellular Salmonella induces effector translocation. Science **328:**1040-3.

CHAPTER 6

CONCLUSIONS AND FUTURE DIRECTIONS

Part I. Brief summary of results

During intracellular infection, *L. monocytogenes* synthesizes two proteins, PC-PLC and Mpl. These virulence factors contribute to escape from vacuoles formed during cell-to-cell spread. Both PC-PLC and Mpl are produced as proproteins that must undergo maturation in order to become active. In this study, we sought to determine the regulation of Mpl. Our data, along with previously published data (3, 5-9, 11) supports the model shown in Figure 6.1. When the bacterium is in the host cytosol at physiological pH, both the proform of PC-PLC and Mpl zymogen accumulate in the bacterial periplasm. The retention of these proteins is due to their propeptides and PrsA2. If these proproteins are secreted across the cell wall, they are unable to undergo maturation. As the bacteria spreads from cell-to-cell and is entrapped in a secondary vacuole, the decrease in vacuolar pH triggers Mpl autocatalysis and processing of PC-PLC. The mature proteins and the propeptide of Mpl are then secreted across the cell wall. Specific histidine residues within the N-terminus of Mpl were identified as contributing to Mpl secretion and PC-PLC activation.

Part II. Future directions

1. Compartmentalization

Peptidoglycan has been reported to be permeable to proteins up to approximately 50 kDa in size (4). While this observation could explain why the Mpl zymogen remains in the periplasm, it does not explain why the proform of PC-PLC remains bacterium-associated.

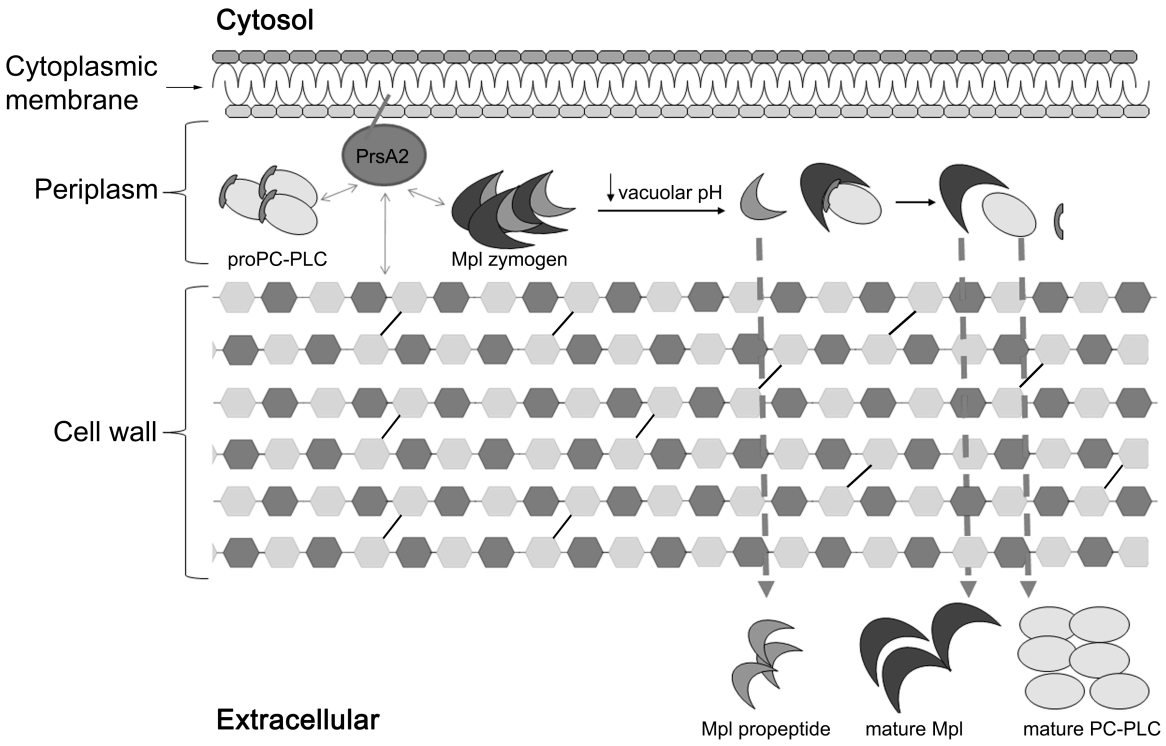

Figure 6.1. Proposed model for *L. monocytogenes* proprotein localization and maturation during intracellular infection. Refer to text for details. Doubleheaded gray arrows indicate potential interactions between PC-PLC, Mpl, PrsA2 and the cell wall. Dashed arrows indicate secretion across the cell wall.

Neither PC-PLC nor Mpl are lipid anchored or contain cell wall binding motifs that would facilitate these proteins being retained (9). The N-terminus of PrsA2 is necessary for PC-PLC activity (1). Based on these observations, we hypothesize that PC-PLC and/or Mpl are kept in a protein complex and that PrsA2 serves as an anchor. To test this hypothesis, we could introduce a cysteine to serine mutation in the LXXC motif of PrsA2 to prevent PrsA2 from being anchored to the cell membrane. If PrsA2 is serving as an anchor, we would then expect to see aberrant secretion of the proproteins.

PC-PLC and Mpl may directly interact with PrsA2. Similarly, PC-PLC and Mpl may interact with PrsA2 through another cell envelope protein that directly binds to PrsA2. To determine candidate cell envelope proteins, we could perform a screen using affinity chromatography. Cell wall fractionations of broth-grown bacteria could be prepared as described in chapter 4 and passed through resin bound with PrsA2. The proteins that are retained from the column could then be identified. Candidate proteins could then be further tested using either yeast-two hybrid assays or by constructing deletion mutants in *L. monocytogenes* and screening for mutants that demonstrate a phenotype similar to the *prsA2* deletion mutant.

Mature Mpl H226F remains bacterium-associated at acidic pH. This result suggests that following autocatalysis, Mpl is either unable to be released from the complex or is participating in an improper protein-protein interaction. The fact that Mpl H226F undergoes autocatalysis suggests that the protein is properly folded. On egg yolk agar plates, Mpl H226F generates less active PC-PLC compared to wild-type Mpl (Figure 6.2A, panels 1 and 3). We therefore tested whether mature Mpl H226F was complexing with PC-PLC.

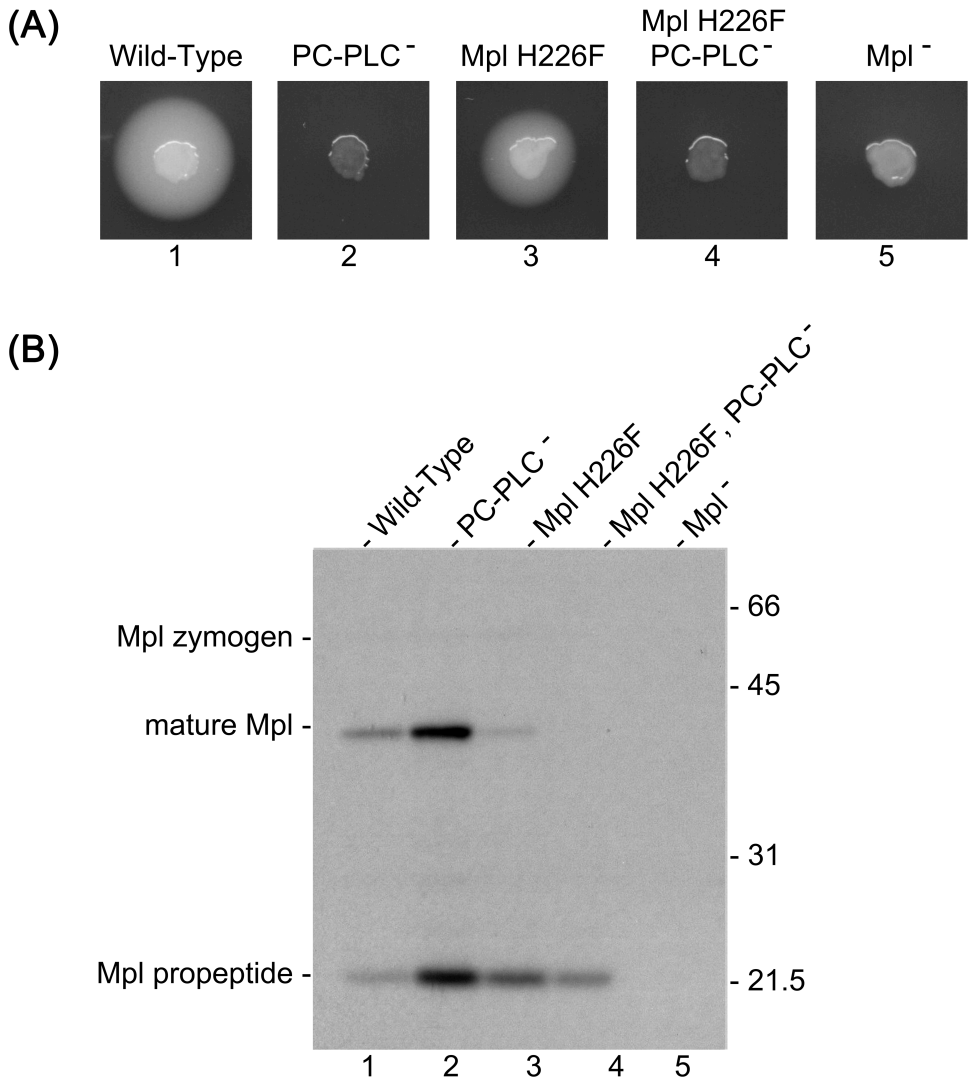

Figure 6.2. PC-PLC does not inhibit secretion of mature Mpl H226F. (A) Detection of PC-PLC activity on egg yolk agar plates. A zone of opacity indicates PC-PLC activity. Panels: 1, NF-L943; 2, HEL-925; 3, HEL-1004; 4, HEL-1005; 5, HEL-469. **(B)** Infected J774 cells were pulse-labeled and then chased in a nigericin-containing potassium buffer equilibrated to pH 6.5. Secreted Mpl was immunoprecipitated from host cell lysates. Lanes: 1, NF-L943; 2, HEL-925; 3, HEL-1004; 4, HEL-1005; 5, HEL-469.

We introduced an internal in-frame deletion of *plcB* in *mpl* H226F (HEL-1229) as described in chapter 2. As expected, PC-PLC activity was not detectable from this mutant (Figure 6.2A, panel 4). When we immunoprecipitated Mpl from the cytosol of infected host cells at acidic pH, we were unable to restore mature Mpl secretion (Figure 6.2B). This result suggests that PC-PLC is not inhibiting mature Mpl from being secreted. It is possible that mature Mpl H226F remains complexed with PrsA2. To test this hypothesis, we could assess Mpl H226F secretion in the *prsA2* mutant. If Mpl H226F is complexed to PrsA2, then deletion of PrsA2 should restore Mpl secretion. If Mpl H226F is involved in another type of protein-protein interaction, then deletion of PrsA2 should not restore Mpl H226F secretion.

Results from chapter 5 showed Mpl H241R also had a secretion defect. We have not yet determined whether Mpl H241R is retained bacterium-associated at acidic pH or is unstable. Future work will focus on addressing this question by performing the bacterium-associated Mpl immunofluorescence assay. In addition, our results suggest that histidine in its hydrophobic state may be preferred at residue 241. We will test this hypothesis by generating an Mpl point mutant with a hydrophobic residue at this position and assessing Mpl activity.

2. Mpl enzymatic activity

The results from chapter 5 demonstrated that proproteins that are secreted are not able to undergo autocatalysis upon a decrease in pH. This result suggests that pH alone does not result in Mpl autocatalysis. Additional components in the periplasm may be necessary. The divalent metal cations that are present in the cell envelope may be necessary (2). Upon a decrease in pH, the functional groups in the cell wall would become protonated, releasing the

divalent cations. Perhaps the rate limiting step in Mpl autocatalysis is the concentration of free cations.

To test this hypothesis, we will repeat the Mpl immunoprecipitation assay using infected J774 cells. After pulse labeling the cells, we could perform a chase in media equilibrated to pH 7.3 and containing ATP, Zn^{2+} and Ca^{2+} in excess. The presence of extracellular ATP depolarizes J774 cells to promote ion transport across the cell membrane and increase levels of intracellular calcium (10). If cations are triggering Mpl autocatalysis, then we should be able to circumvent the need to drop the pH.

Previous results suggested that a negative charge and hydrophobic residues within the N-terminus of the PC-PLC's propeptide are necessary for efficient Mpl-mediated maturation of PC-PLC (7). Results from chapter 5 suggest that a positive charge and a hydrophobic residue on the catalytic domain of Mpl are preferred for Mpl-mediated activation of PC-PLC. Taken together, these results indicate that there may be an electrostatic interaction between the propeptide of PC-PLC and Mpl. Perhaps upon autocatalysis, mature Mpl is able to displace the propeptide of PC-PLC from the anchor. PC-PLC can then be cleaved by mature Mpl. This model would explain why Mpl is still necessary for PC-PLC to be efficiently secreted, independent of propeptide removal (11). If our model is correct, we should be able to immunoprecipitate bacterium-associated proPC-PLC from cells infected with the *mpl* H226 or H241 mutants. It is also possible that we will detect mature PC-PLC bacterium-associated. In terms of our model, this result could indicate that the Mpl mutants are able to process the

propeptide and that mature PC-PLC remains complexed with bacterium-associated mature Mpl.

H226 and H241 are approximately seven Å apart in two random coil loops on the same side as the active site pocket of Mpl. Perhaps these histidine residues interact with the negative and hydrophobic residues of PC-PLC to promote release from the anchor. The changes in charge may alter the conformation of Mpl and inhibit its ability to displace and cleave the propeptide of PC-PLC. For Mpl H226T and H226E, such changes may only affect Mpl-mediated cleavage of the propeptide, not release from the anchor. These mutations could be used to test our hypothesis that charges on the propeptide of PC-PLC and Mpl are critical for Mpl-mediated release and processing of PC-PLC. The Mpl H226 and H241 mutants could be used in combination with PC-PLC propeptide mutants that have a defect in Mpl-mediated activation of PC-PLC (7). We could generate combinations of hydrophobic and positive charge on residues 226 and 241 and test their ability to mediate activation of PC-PLC from these propeptide mutants.

The results from the PC-PLC activation *in vitro* assay described in chapter 3 showed mature Mpl is active only under acidic conditions. Perhaps the pH is necessary for the proteins to undergo conformational changes to allow for interaction to occur. To begin testing this hypothesis, we performed fluorescence spectroscopy on the purified proform of PC-PLC. This method serves to measure intrinsic fluorescence. PC-PLC was incubated in buffer equilibrated to either pH 7.3 or pH 6.5. The protein was then excited at a wavelength of 290 nm. An emission scan of PC-PLC was taken on the range of 310 nm to 440 nm (Figure 6.3).

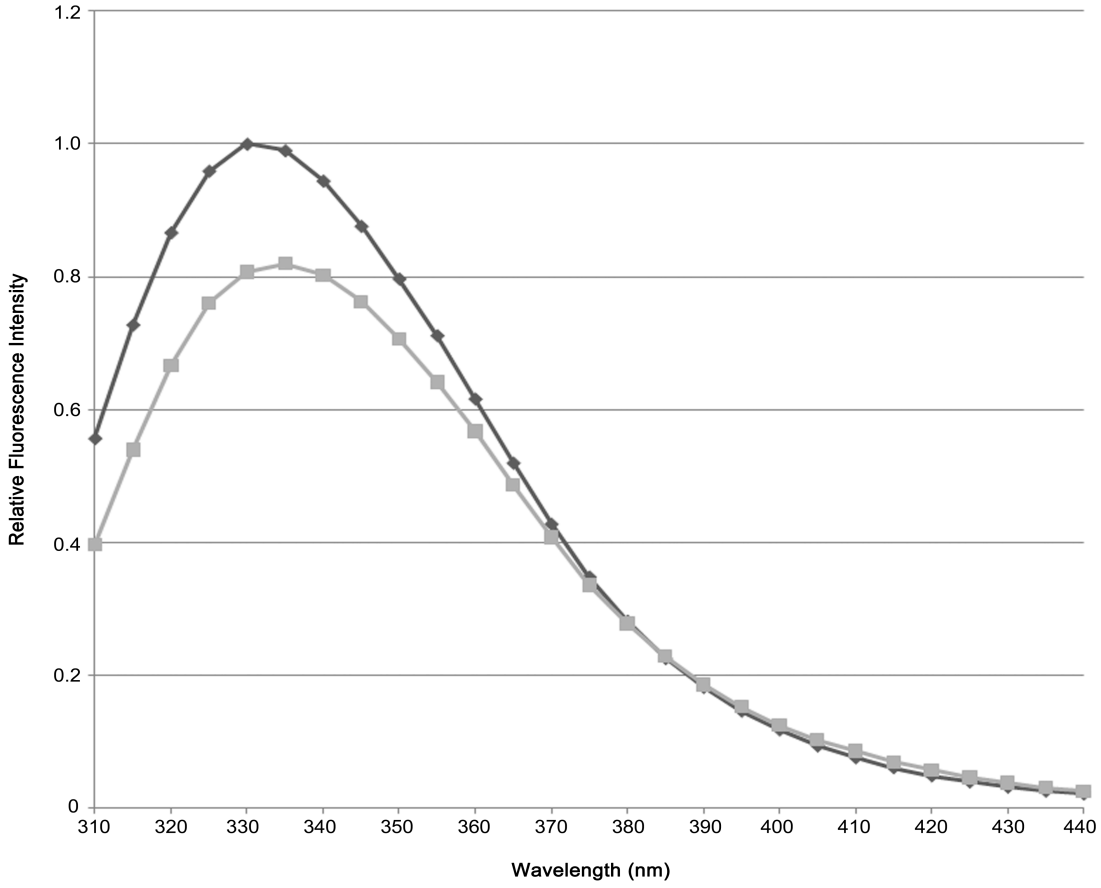

Figure 6.3. Fluorescence emission spectra of purified proform PC-PLC. Purified PC-PLC was incubated in either buffer equilibrated to either pH 7.3 (dark gray) or pH 6.5 (light gray) and excited at 290 nm. Emission spectra were measured from 310 nm to 440 nm. The change in maximum emission wavelength and intensity is indicative of protein conformation change.

The wavelength of maximum emission for PC-PLC was 330 nm at pH 7.3 and 335 nm at pH 6.5. Additionally, the fluorescence of PC-PLC at acidic pH was partially quenched from 310 to 350 nm. These results suggest that the proform of PC-PLC does undergo a change in conformation upon a decrease in pH. Arguably, a change in PC-PLC conformation may be required for Mpl to bind and process the propeptide. Perhaps a change in the conformation of mature Mpl is also necessary to mediate PC-PLC activation. This could be tested in the future. Alternatively, we can perform circular dichroism experiments to look at changes in secondary structure at different pHs.

In order for us to perform these spectroscopy experiments, we will need to further purify Mpl. The Mpl purification discussed in chapter 3 had additional proteins present. Our lab has currently been working on trying to improve the purification of Mpl. We have begun to try to purify Mpl E350Q-$Flag_{C\text{-}cat}$ by overexpressing it on a multi-copy plasmid in *L. monocytogenes* and passing the culture supernatant through an anion-exchange column prior to the Flag M2 resin. Work on this is still ongoing.

In summary, our results show that the Mpl zymogen is retained in the periplasm of *L. monocytogenes*. While in the periplasm, Mpl is able to undergo autocatalysis at acidic pH and mediate the secretion and maturation of PC-PLC. These results suggest *L. monocytogenes* uses an interesting mechanism of post-translational regulation for these proteins. Perhaps similar mechanisms are used in other Gram-positive bacterial pathogens.

REFERENCES

1. **Alonzo, F., 3rd, B. Xayarath, J. C. Whisstock, and N. E. Freitag.** 2011. Functional analysis of the *Listeria monocytogenes* secretion chaperone PrsA2 and its multiple contributions to bacterial virulence. Mol. Microbiol. **80:**no. doi: 10.1111/j.1365-2958.2011.07665.x.

2. **Beveridge, T. J., and R. G. Murray.** 1980. Sites of metal deposition in the cell wall of *Bacillus subtilis*. J. Bacteriol. **141:**876-87.

3. **Bitar, A. P., M. Cao, and H. Marquis.** 2008. The metalloprotease of *Listeria monocytogenes* is activated by intramolecular autocatalysis. J. Bacteriol. **190:**107-11.

4. **Demchick, P., and A. L. Koch.** 1996. The permeability of the wall fabric of *Escherichia coli* and *Bacillus subtilis*. J. Bacteriol. **178:**768-73.

5. **Marquis, H., H. Goldfine, and D. A. Portnoy.** 1997. Proteolytic pathways of activation and degradation of a bacterial phospholipase C during intracellular infection by *Listeria monocytogenes*. J. Cell Biol. **137:**1381-92.

6. **Marquis, H., and E. J. Hager.** 2000. pH-regulated activation and release of a bacteria-associated phospholipase C during intracellular infection by *Listeria monocytogenes*. Mol. Microbiol. **35:**289-98.

7. **Slepkov, E. R., A. Pavinski Bitar, and H. Marquis.** 2010. Differentiation of propeptide residues regulating the compartmentalization, maturation and activity of the broad-range phospholipase C of *Listeria monocytogenes*. Biochem. J. **432:**557-63.

8. **Smith, G. A., H. Marquis, S. Jones, N. C. Johnston, D. A. Portnoy, and H. Goldfine.** 1995. The two distinct phospholipases C of *Listeria monocytogenes* have overlapping roles in escape from a vacuole and cell-to-cell spread. Infect. Immun. **63:**4231-7.

9. **Snyder, A., and H. Marquis.** 2003. Restricted translocation across the cell wall regulates secretion of the broad-range phospholipase C of *Listeria monocytogenes*. J. Bacteriol. **185:**5953-8.

10. **Sung, S. S., J. D. Young, A. M. Origlio, J. M. Heiple, H. R. Kaback, and S. C. Silverstein.** 1985. Extracellular ATP perturbs transmembrane ion fluxes, elevates cytosolic [Ca2+], and inhibits phagocytosis in mouse macrophages. J. Biol. Chem. **260:**13442-9.

11. **Yeung, P. S., N. Zagorski, and H. Marquis.** 2005. The metalloprotease of *Listeria monocytogenes* controls cell wall translocation of the broad-range phospholipase C. J. Bacteriol. **187:**2601-8.